Inter-American Development Bank

Water Resource Investigations

Port-au-Prince Metropolitan Region
Republic of Haiti

Water and Sanitation Division

Authors:
James K. Adamson
Javan Miner
Pierre-Yves Rochat

Editors:
Sergio Perez Monforte
Maria Rodriguez

TECHNICAL NOTE Nº
IDB-TN-2446

March 2022

Water Resource Investigations

Port-au-Prince Metropolitan Region
Republic of Haiti

Authors:
James K. Adamson
Javan Miner
Pierre-Yves Rochat

Editors:
Sergio Perez Monforte
Maria Rodriguez

Inter-American Development Bank
Water and Sanitation Division

March 2022

Cataloging-in-Publication data provided by the
Inter-American Development Bank
Felipe Herrera Library
Adamson, James K.
Water resource investigations : Port-au-Prince metropolitan region, Republic of Haiti / James K. Adamson, Javan Miner, Pierre-Yves Rochat; Sergio Pérez Monforte, María Rodríguez.
p. cm. — (IDB Technical Note; 2446)
Includes bibliographic references.
1. Water resources development-Haiti. 2. Watershed management-Haiti. 3. Water supply-Environmental aspects-Haiti. I. Miner, Javan. II. Rochat, Pierre-Yves. III. Pérez Monforte, Sergio, editor. IV. Rodríguez, María, editor. V. Inter-American Development Bank. Water and Sanitation Division. VI. Title. VII. Series.
IDB-TN-2446

Keywords: Water resource, hydrology, source monitoring, source protection, groundwater flow model

JEL Codes: L95, Q25

http://www.iadb.org

WATER RESOURCE INVESTIGATIONS

Port-au-Prince Metropolitan Region

Republic of Haiti

AUTHORS:
James K. Adamson, PG
Javan Miner, EIT
Pierre-Yves Rochat

EDITORS:
Sergio Perez Monforte
Maria Rodriguez

March 2022

WATER RESOURCE INVESTIGATIONS

Port-au-Prince Metropolitan Region

Republic of Haiti

With support from: Northwater International & Rezodlo, S.A, DINEPA, OREPA-Ouest and CTE-RMPP

IDB Inter-American Development Bank

Spanish Cooperation

PEPSICO FOUNDATION We Feed Potential

Schweizerische Eidgenossenschaft
Confédération suisse
Confederazione Svizzera
Confederaziun svizra

Swiss Agency for Development and Cooperation SDC

DINEPA Direction Nationale de l'Eau Potable et de l'Assainissement

Federal Ministry
Republic of Austria
Finance

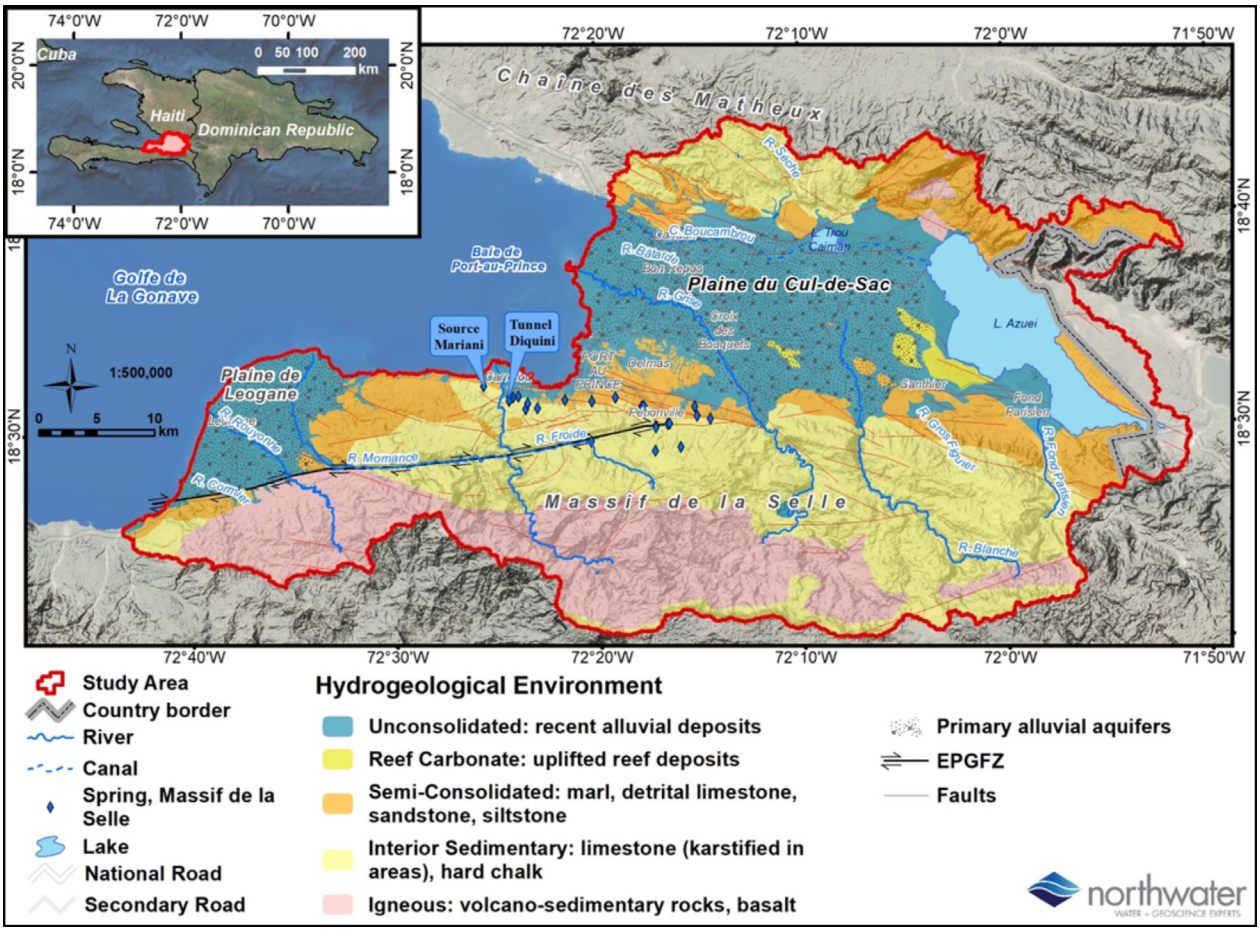

Water Resource Investigations - Study Area.

Table of Contents

PREFACE AND SUMMARIES

Hydrogeological Investigation of Tunnel Diquini: Characterization of Hydrology and Guidance for Source Monitoring and Protection.

Hydrogeological Investigation of Source Mariani: Characterization of Hydrology and Guidance for Source Monitoring and Protection.

Plaine du Cul-de-Sac Groundwater Flow Model.

Preface and Summaries

This work is financed with support from the AquaFund. The AquaFund is the IDB's thematic fund for water and sanitation, and has been the main financing mechanism to support the Bank's investments in the sector since its creation in 2008. The AquaFund has contributed to the achievement of the Millennium Development Goals for water and sanitation in Latin America and the Caribbean and will play a crucial role in supporting the region's governments in achieving the new Sustainable Development Goals. It has done so by facilitating investments to increase the provision of water and sanitation, water resources management, solid waste management, and wastewater treatment, while contributing to the sustainability and accessibility of these services for low-income populations. It also supports the Bank's client countries in addressing the emerging challenges of climate change, rapid degradation of freshwater ecosystems, and increasing water insecurity. The AquaFund is financed through the IDB's own resources and resources from donor partners, namely the Government of Austria, the Spanish Agency for International Development Cooperation AECID, the PepsiCo Foundation, and the Swiss Agency for Development and Cooperation SDC and the State Secretariat for Economic Affairs SECO.

Background and context. The metropolitan area of Port-au-Prince has an estimated population of 2.8 million and projected to increase to 3.5 million by 2030 (CIA 2020). With an estimated water demand of 365,000 m³/day, protecting existing supplies and securing additional water supply is an urgent priority for the region. Since the 1980s, there has been insufficient investment in advancing knowledge of the primary resources that Port-au-Prince greatly relies on.

The Port-au-Prince water supplies include:

- Massif de la Selle aquifer system, a karst carbonate bedrock aquifer system that feeds fifteen springs and one well that supply the network. The average supply from these sources is approximately 120,000 m³/day.
- The Plaine du Cul-de-Sac aquifer is an unconsolidated alluvial aquifer. There are 26 municipal wells that take ~37,000 m³/day based on 2015-2018 data. Municipal pumping can potentially be increased by ~45,000 m³/day through new proposed wells and rehabilitation of inactive wells.

Based on this information, there is a significant gap between water supply and demand. This has prompted the urgent need to protect existing resources and secure additional water supplies.

In 2018 – 2019, Northwater International and Rezodlo SA were contracted to perform three water resource investigations in the Port-au-Prince region. The Government of Haiti supported the research both in the field and with historical data compilation.

The investigations included:

1. Characterization of Tunnel Diquini
2. Characterization of Source Mariani
3. Groundwater Flow Model for the Plaine du Cul-de-Sac aquifer

Tunnel Diquini is a ~1.5 km long tunnel constructed in 1940 that collects groundwater from fractures and a fault in the Massif de la Selle carbonate aquifer system. It is the single largest water source for the Port-au-Prince municipal water system, accounting for approximately 26% of the supply.

Source Mariani is the second largest naturally flowing source that serves the Port-au-Prince municipal water system. The spring is a primary discharge of the Massif de la Selle carbonate aquifer system, the same aquifer complex as Tunnel Diquini. Due to its distal location from Port-au-Prince and low elevation, it requires a pumping system. When in operation, the spring accounts for approximately 17% of the Port-au-Prince water supply.

The Plaine du Cul-de-Sac aquifer is one of Haiti's most productive and largest aquifers (~360 km² aerial extent). This multi-layer unconsolidated alluvial aquifer has a thickness of more than 200 m, and supports municipal,

private and agricultural wells. The Port-au-Prince municipal system includes ~ 26 wells that serve the lower-lying areas of the metropolitan region. Historical peak aquifer-wide abstraction was estimated to be nearly 300,000 m³/day in the 1970s and 1980s as a result of the sugar cane industry, thus suffering declines in the water tables and increases in salinity. Current abstraction is significantly lower than historical peaks due to unreliable power and lack of commercial agriculture. A groundwater flow modeling exercise was performed to establish a preliminary estimate of renewable quantities of groundwater, and to improve the understanding of recharge origins and the interaction between groundwater and surface water. These parameters are important to guide water supply planning and development for Port-au-Prince and, at the same time, to manage and protect these resources.

The objective of this research is to improve the understanding of Port-au-Prince's critical water resources and to guide informed planning and investments to secure sustainable water supplies to satisfy the growing demand from the region. These studies guide further research and reveal important monitoring needs to strengthen resource characterization and data-driven decision-making and resource management. These investigations are preliminary in nature and limited due to the scarcity of data.

I. Tunnel Diquini Summary

Tunnel Diquini is the largest single source of water for the municipal water system of Port-au-Prince. Based on records from 2014-2018, the tunnel supplies an average of 29,449 m³/day to the metropolitan Port-au-Prince water system. The tunnel accounts for ~26% of total municipal production, and 37% of all gravity-fed spring flow that the metropolitan area obtains. An inspection was performed to characterize the hydrology of the tunnel waters and to better understand the origin of its flow and its relationship with groundwater and surface water systems. This knowledge is important to guide future studies and monitoring of the tunnel and to aid the Centre Technique d'Exploitation de la Région Métropolitaine de Port-Au-Prince (CTE-RMPP) in water use planning and management.
The investigation was accomplished by using a combination of literature review, satellite and topographic imagery analysis, and field reconnaissance. A brief field mission to the tunnel was conducted on April 15, 2018, including: (i) physical and chemical sampling, (ii) stable isotope sampling, (iii) chlorofluorocarbon (CFC) and sulfur hexafluoride (SF6) sampling, (iv) flow rate measurement and (v) visual inspection of tunnel geology.

Note: Additional data collection and research since the Tunnel Diquini study was conducted warrants revisiting and updating some of the interrogations and findings of the report. This summary presents data primarily based on the original report, with the exception of an increased range of recharge rate and a decreased catchment area based on updated research.

Photo 1. Limestone exposed in the main tunnel.

Photo 2. The tunnel portal facing into the tunnel.

Flow Characteristics

1. Recharge to the Massif de la Selle carbonate aquifer system and tunnel appears to be largely affected by high intensity and high-volume rainfall events such as hurricanes and tropical storms. It appears to be a 3-to-7-year cycle of recharge trends partially influenced by El Niño and La Niña events.

2. Tunnel discharge varies seasonally with recorded flows ranging from 11,085 to 73,265 m^3/d, with a geometric mean for all known recorded flows of 27,987 m^3/d (1980-2018 dataset).

3. Decreases in tunnel flow result from extended periods of normal precipitation and consecutive years without high intensity rainfall periods such as tropical storms and hurricanes.

a. The recharge dynamics and flow regression can influence flow trends over periods of several years. Tunnel flows do not appear to have been decreasing over the long-term.

b. Limited historical data from 1959 suggests that dry season low-flow conditions were comparable or perhaps lower than current low-flow conditions and strongly influenced by major recharge and drought events.

c. The response time of the aquifer to major recharge events such as hurricanes may be shortening, possibly due to land cover and climatic changes.

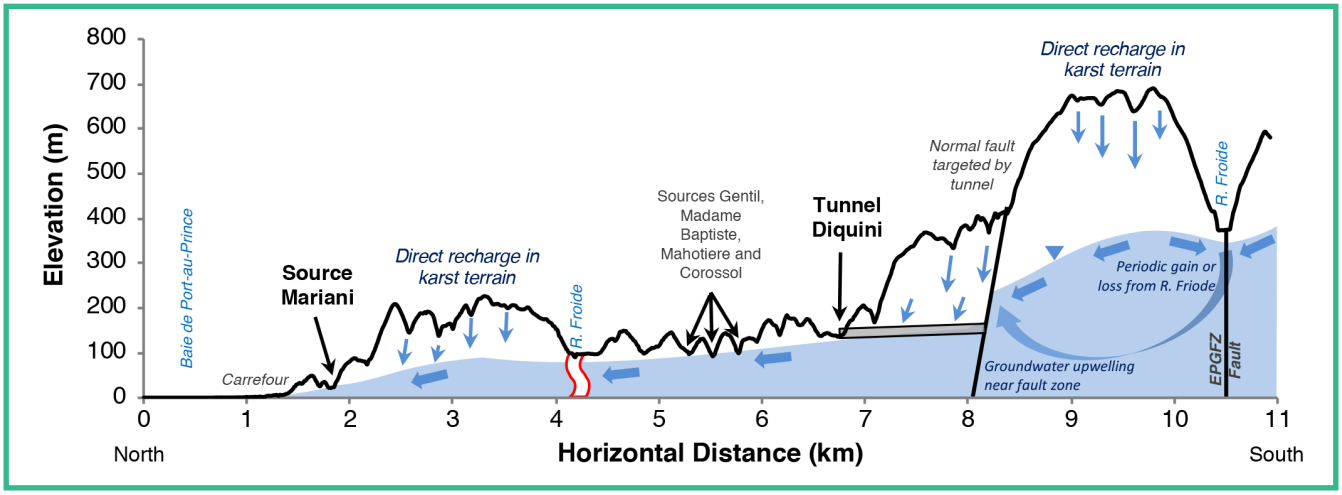

Figure 1. Conceptual cross section of Diquini Tunnel groundwater flow.

Groundwater / Surface Water Interaction

1. Based on water chemistry and tracers, the tunnel and Riviere Froide are connected to the same regional karst limestone aquifer and gain flow from it. The Riviere Froide may recharge the aquifer at various spatial and temporal extents, and this could result in a possible link between the tunnel and river system.

2. Based on geology and structure, Tunnel Diquini does not appear to have a hydraulic connection to the Riviere Momance, which is located farther to the south in the mountains and flows westerly to the Plaine de Leogane.

a. The EPG fault zone and a perpendicular fault appear to direct groundwater in the Momance basin either into the Riviere Momance or into the lower reaches of the Riviere Froide, below where recharge to the tunnel would likely occur.

Spatial Distribution of Groundwater Recharge

1. The long-term mean annual recharge rate in the karst terrain is estimated greater than 40% of annual precipitation. Recharge rates can be higher in years with tropical storms and hurricanes, and less than 15% in years with normal or low precipitation.

2. Recharge rates are higher during high intensity precipitation events, and lower during periods of average and low precipitation.

3. Aquifer storage of the 'spring shed' of the tunnel is estimated between 265 and 327 Mm^3.

4. The aquifer is well mixed and has an average groundwater age of 26 to 32 years based on a single sampling event.

5. Recharge area of the tunnel flow appears to in the range of 12.4 km^2.

a. Recharge area is dependent on the rate and duration of Riviere Froide leakage to the regional carbonate aquifer.

b. The average recharge elevation is estimated at 650m, indicating that a portion of tunnel flow may originate from river leakage from the Riviere Froide to the regional carbonate aquifer.

Aquifer Vulnerability

1. Due to the high permeability and high infiltration rates typical in karst limestone environments, the tunnel waters are vulnerable to contamination. For example, fecal coliform, E. coli, and salmonella contamination was reported by Eptisa in March 2014.

2. Urbanization and land use changes in the hills south of the tunnel portal may have negative impacts to tunnel water quality and flow. The lack of centralized waste management and sanitation in karst environments increases the risk of aquifer contamination. Increase of impervious surfaces and loss of soil decreases recharge to the aquifer that contributes to tunnel flows.

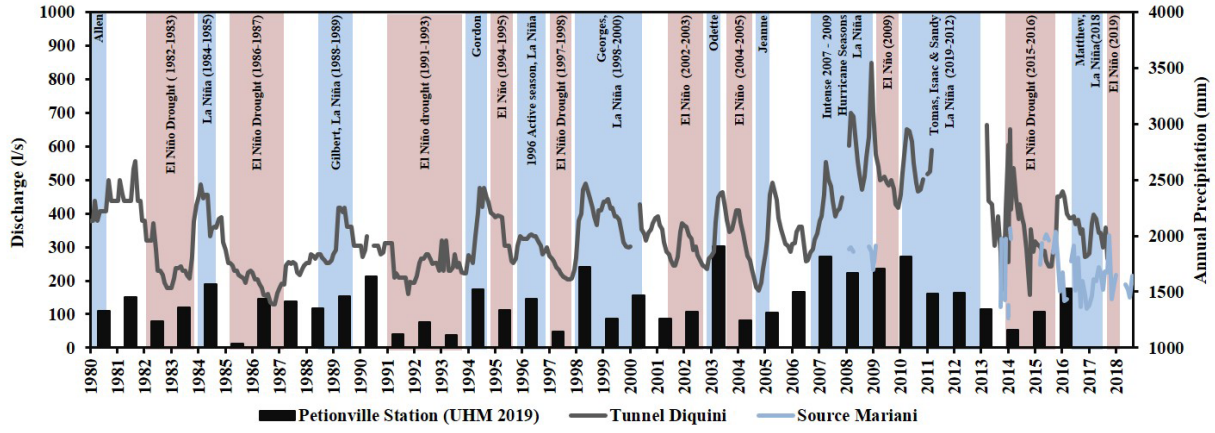

Figure 2. Tunnel Diquini and Source Mariani discharge with ENSO climate events, 1980 - 2018.

II. Source Mariani Summary

Source Mariani is currently the most distal source of water that supplies the CTE-RMPP water system. It is the largest naturally flowing spring and second largest single water source that supplies the Port-au-Prince municipal water system. When the pumping station is in operation, an average of ~19,000 m³/day is available to supply ~17% of total municipal production, and 24% of all spring flow supplying metropolitan Port-au-Prince region (based on CTE-RMPP data 2014-2018). The spring discharges from limestones that drain a portion of the Massif de La Selle carbonate aquifer system, west of the Riviere Froide and north of the Riviere Momance. The objective of this evaluation is to better understand the spring flow characteristics and the origin of the waters to guide future study of the Massif de la Selle aquifer system and to aid CTE-RMPP in water use planning, development, monitoring and protection.

This investigation was accomplished using a combination of literature and data review, satellite and topographic imagery analysis, and field reconnaissance. A brief field mission to the spring was conducted in April 2019, including: (i) physical and chemical sampling, (ii) stable isotope sampling, (iii) chlorofluorocarbon (CFC) and sulfur hexafluoride (SF6) sampling, and (iv) visual observation of local geology. At a follow-up visit to the spring was conducted in January 2020 to verify more recent flow monitoring data received from CTE-RMPP, two nearby springs were subsequently document that represent ~25% of the overall flow from the Mariani spring system.

Photo 3. The Source Mariani catchment.

Photo 4. Source Mariani pumping station.

Water Budget

1. The long-term mean annual recharge rate in the karst terrain is estimated greater than 30% of annual precipitation. Recharge rates can be higher in years with tropical storms and hurricanes, and less than 15% in years with normal or low precipitation.

1. Aquifer storage of the 'spring shed' is estimated between 155 and 259 Mm^3.

2. The limestone karst aquifer that feeds the spring is well mixed and has an average groundwater age of between 21 and 35 years based on a single sampling event.

Photo 5. Limestone outcrop near Source Mariani.

Spatial Distribution of Groundwater Recharge

1. The groundwater recharge area that contributes to the spring flow appears to be approximately 13.3 km^2 but may be larger.

a. This uncertainty in the recharge area is largely due to the complexity of groundwater flow in karst environments and limited datasets regarding tracers and hydrochemistry.

2. The average recharge elevation is estimated at 580 m above mean sea level with a corresponding temperature of 22.7 C. This suggests the possibility that some spring flow may originate from distal zones in the regional carbonate aquifer such as within the Riviere Momance basin.

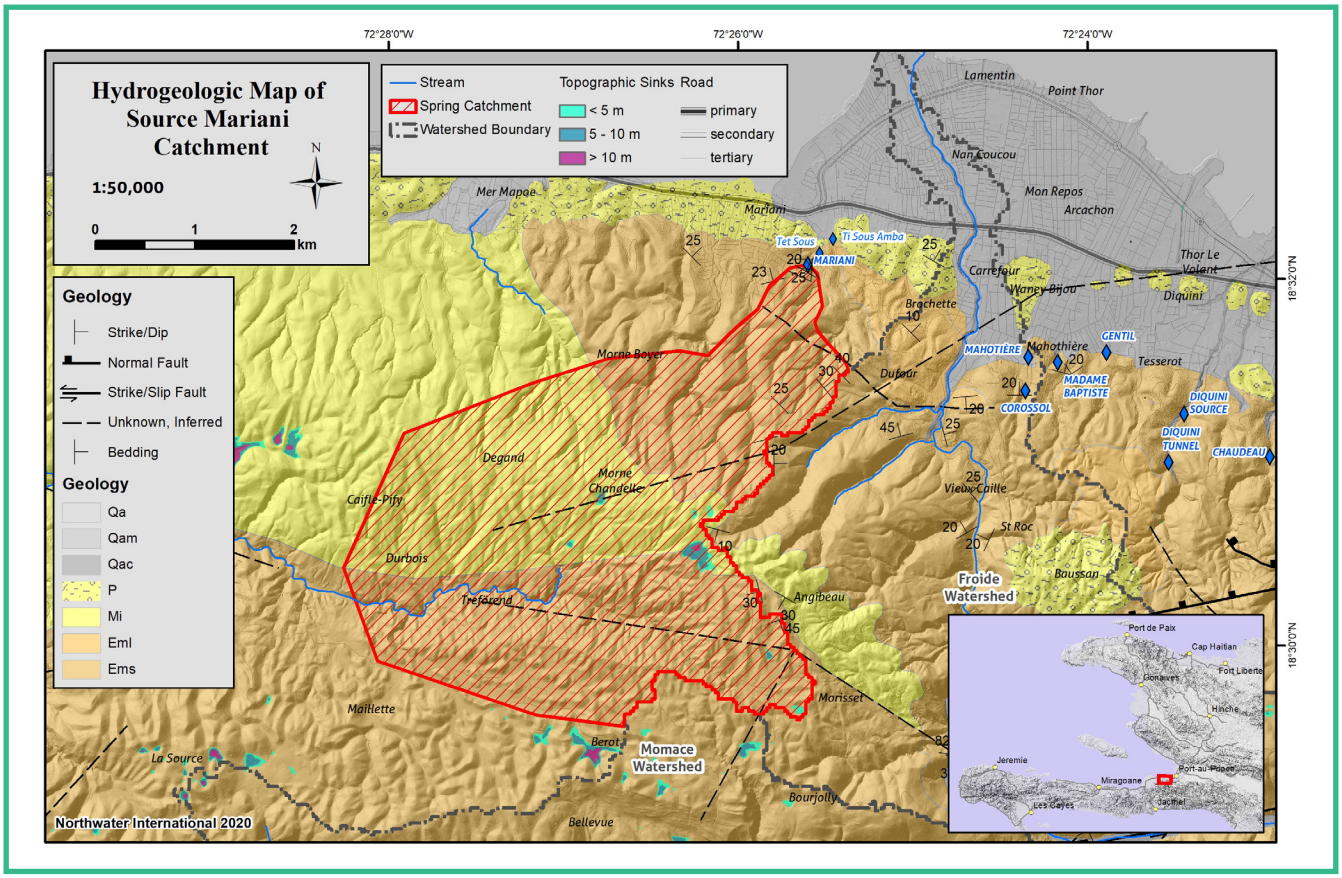

Figure 3. Geologic Map of Interpreted Catchment Area of Source Mariani

Flow Characteristics

1. Recharge to Massif de la Selle aquifer system appears to be largely affected by high intensity and high-volume rainfall events such as hurricanes and tropical storms. There appears to be a 3-to-7-year cycle of recharge trends partially influenced by El Niño and La Niña events.

2. Spring discharge displays mild seasonal variability, with monthly average flows typically ranging between 14,500 and 25,000 m³/d with an average of 19,500 m³/d.

a. Instantaneous (daily) flows display greater variability, ranging from 7,600 to 30,700 m³/d.

b. Based on the spring catchment infrastructure as observed in 2019, spring flow is measured from a single water meter. Since this method does not account for overflow, some high spring flows could be underreported.

3. The spring flow is most vulnerable to extended periods of average or below average precipitation and to consecutive years without high intensity rainfall periods such as tropical storms and hurricanes.

a. This recharge characteristic and resulting flow regression that extends from 2014 to 2019, may foster perceptions that the spring flow has been decreasing over the long-term or that acute impacts have occurred.

b. Historical flow data from 1925 and 1933 has similar flow rates as the present.

4. The cyclic and multi-annual recharge characteristics are important for water managers to understand in order to balance water use allocations from the different water sources of CTE-RMPP.

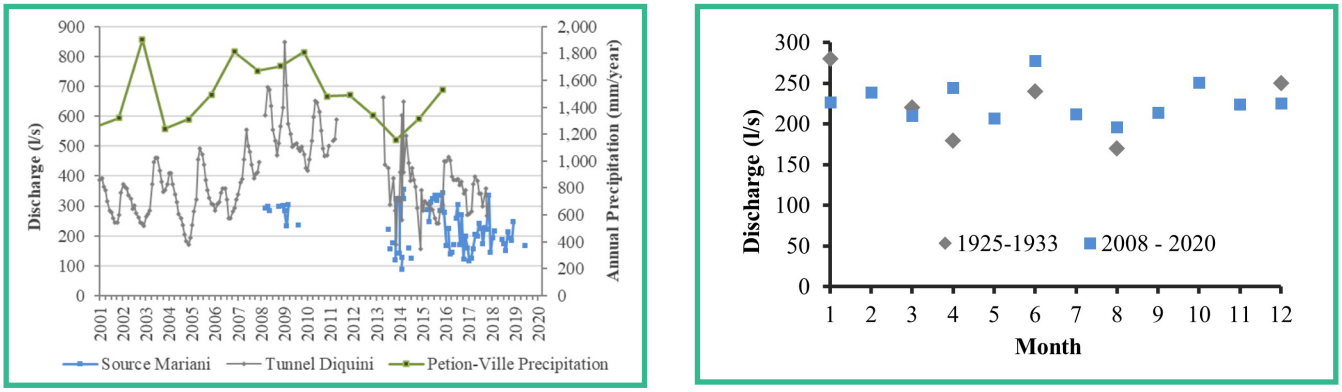

Figure 4. (i) Source Mariani and Tunnel Diquini flow compared with annual precipitation, (ii) average monthly flow of Source Mariani by month.

Groundwater / Surface Water Interaction

1. Source Mariani flows from the regional Massif de la Selle carbonate aquifer system.

a. Source Mariani is the lowest elevation terrestrial outlet known for the aquifer and appears to emanate from a topographic exposure of the main aquifer lithology rather than as a contact spring. This may act to sustain flows even when higher elevation springs exhibit reduced flows.

b. Source Mariani essentially serves as a drain for the western portion of the Massif de la Selle aquifer.

2. Source Mariani does not appear to have a significant hydraulic connection to the Riviere Momance or Riviere Froide. This is supported by the isotope and tracer sampling and analysis of recharge catchment size.

Aquifer Vulnerability

1. Due to the high permeability and rapid infiltration rates typical in karst limestone environments, the spring vulnerable to contamination. For example, fecal coliform, E. coli, and salmonella contamination was reported by Eptisa in March 2014.

2. Urbanization and land use changes in the hills south of the spring may result in negative impacts to water quality and flow. The lack of centralized waste management and sanitation in karst environments increases the risk of aquifer contamination. Increase of impervious surfaces and loss of soil decreases recharge to the aquifer that contributes to spring flow.

III. Plaine du Cul-de-Sac Summary

The Plaine du Cul-de-Sac (PCS) aquifer is one of the largest aquifers in Haiti and currently provides at least 25% of the water supply for Port-au-Prince from 26 municipal wells. The aquifer is also an important water supply for private, agricultural and industrial wells. A numerical groundwater flow model was developed to better understand the hydraulic parameters and behavior of the PCS aquifer and support water supply development planning for the Port-au-Prince metropolitan region. The model effort was preceded with data mining and research to support the model construction and calibration.

The primary goal of the modeling exercise was to better understand i) the sustainable and renewable quantities of groundwater available from the aquifer, ii) the complex recharge dynamics, and iii) surface water/ groundwater interactions between lakes and river systems. MODFLOW[1] 2005 code was selected for modeling the PCS aquifer. ViewLog software from Earthfx Inc. was applied to build the model, this software directly integrates with the borehole database for building, developing and refining the model. Groundwater Vistas Advanced, version. 6 was used to run the model simulations and scenarios.

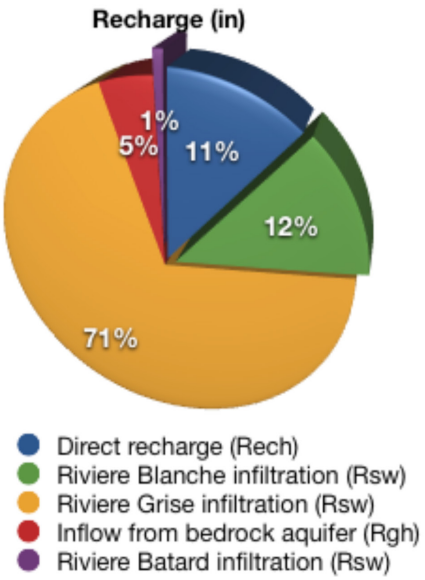

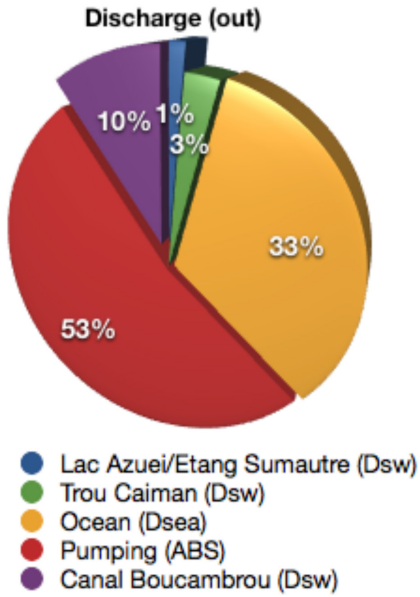

Calibrated Baseline Groundwater Flow Model Details

1. Aquifer extent of 363 km²

2. Maximum thickness greater than 200 meters.

3. Multi-layer aquifer system, silty sand, and sandy gravel layers.

4. Current pumping simulation: 71,600 m³/day from 141 wells, 26 of which are municipal wells.

Groundwater Flow

The groundwater flow shows similar trends as has been illustrated in previous reports. The hydraulic gradient is steepest in the southern limits of the aquifer where the Riviere Grise and Riviere Blanche enter the plain and recharge the aquifer. A groundwater divide bisects the aquifer in the east-central portion where groundwater flows either westward towards the ocean or north and eastward into Trou Caiman, Canal Boucambrou, and Lac Azuei.

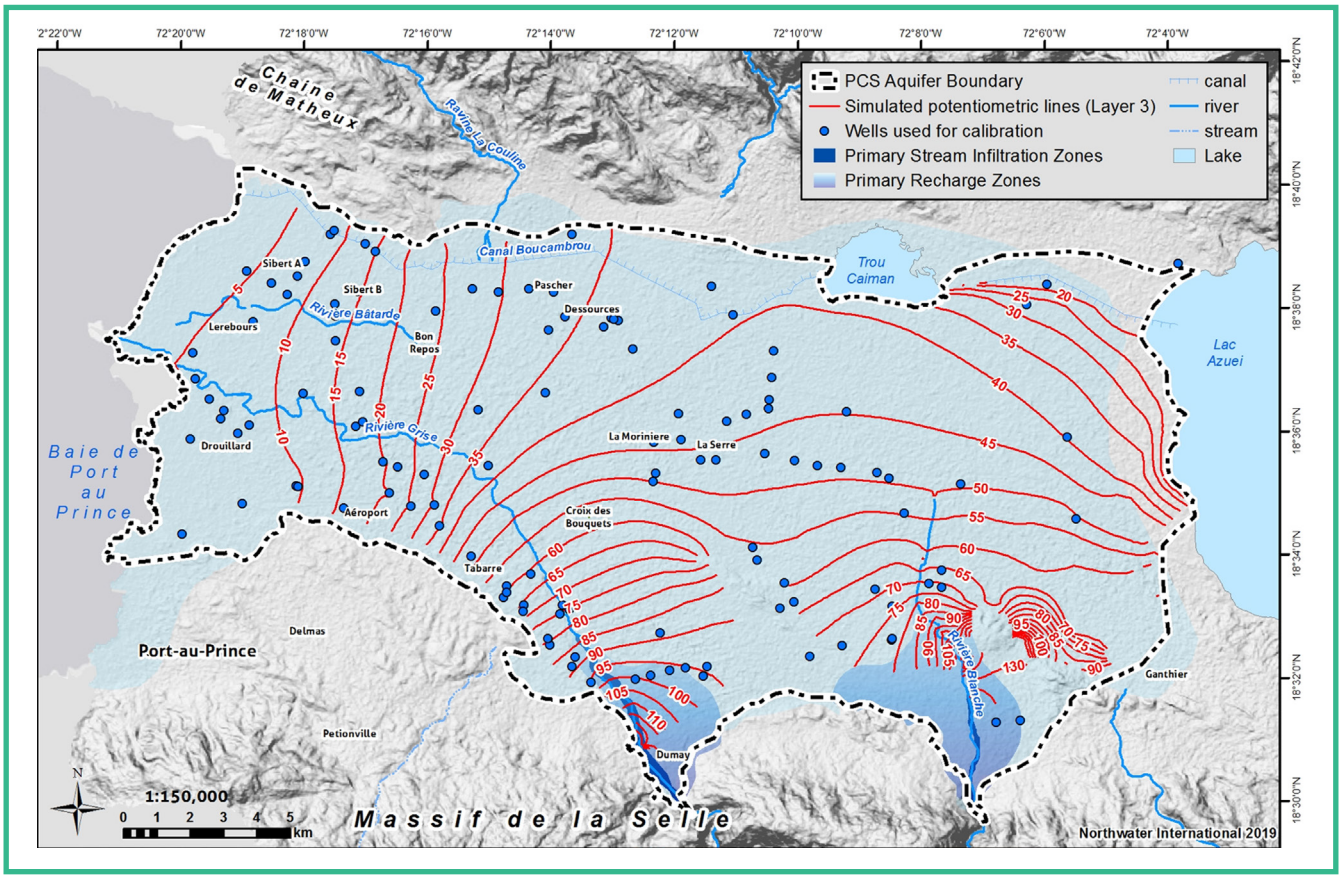

Figure 5. Simulated groundwater piezometry under steady-state conditions.

[1] MODFLOW is the United States Geological Survey (USGS) three-dimensional finite-difference groundwater model.

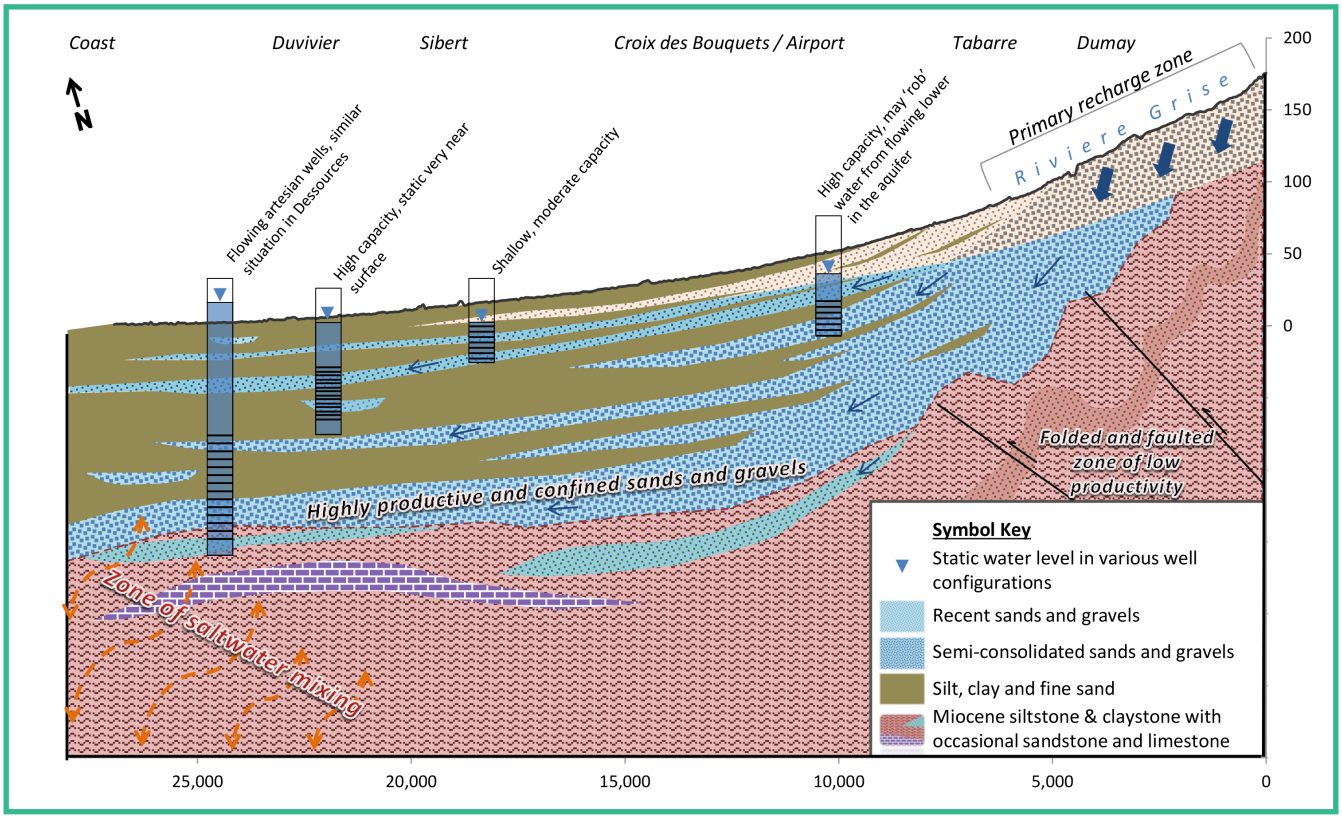

Figure 6. Conceptual hydrogeologic cross section of the Plaine du Cul-de-Sac aquifer.

Takeaways and Insights

Based on the steady-state model and initial model run the following observations are noted regarding the water balance:

- Renewable recharge inputs to the aquifer are on the order of 135,000 m³/day. If current pumping is 71,600 m³/day, this would imply a 0.53, groundwater development ratio.

- 83% of the aquifer inputs are from infiltration of the Riviere Grise and the Riviere Blanche, consistent with historical findings.

- Canal Boucambrou appears to be a drain from the PCS aquifer. This relationship needs to be examined through investigation and monitoring.

- Lac Azuei does not appear to receive a significant proportion of its water budget from the PCS aquifer, and in fact the simulation suggests 21 L/s (1,838 m³/day). Lac Azuei appears influenced by stream infiltration of the Riviere Blanche. Groundwater that discharges to the eastern portion of Canal Boucambrou may flow into Lac Azuei. The relationship between the aquifer, Lac Azeui and Canal Boucambrou be further investigated through studies and monitoring.

• Based on the steady state simulation and assumed pumping schemes, saltwater intrusion does not appear to be a major factor at present for the primary aquifer layer. Dry season stress periods may enhance the risk, and the shallow layer is most susceptible. The coastal area of the aquifer has few wells; further, there was limited data to calibrate the model along the coast..

• Trou Caiman appears to receive water from the PCS aquifer, at a range that the model simulation suggests of 45 L/s (3,890 m^3/day).

Model Scenario Results Summary

Model scenarios suggest that impacts should be anticipated from both climate change and increased pumping.

• Rehabilitation of existing wells and addition of new municipal wells may drawdown the water table, thus affecting nearby wells. This may also create a stronger gradient between the Riviere Grise and the aquifer.

• Pessimistic climate change scenarios appear to have a regional impact on the aquifer, since this is largely sensitive due to a decrease in river flows that in turn reduce the volume of the river water available to infiltrate into the aquifer.

• The modeling exercise indicates that the Riviere Grise and the Riviere Blanche are critical components of the aquifer and its ability to sustain groundwater abstraction and flows to surface water bodies. The recharge from the river drives the hydraulic gradient, replenishes the aquifer when there is pumping or climate change stress, and it mitigates saltwater intrusion risk in coastal areas. Aquifer impacts from schemes related to river diversions and/or dams need to be understood and mitigated.

IV. Conclusions

Summary

The three investigations were effective in advancing preliminary understandings of Tunnel Diquini, Source Mariani and the PCS aquifer.

The investigations shared common challenges, as all were limited due to the scarcity of data and knowledge to perform detailed hydrogeological studies. Uncovered data was often poorly documented. Significant efforts were necessary to synthesize, verify and utilize the few datasets that were available to support these studies. The 40-year record of flow collected and maintained for Tunnel Diquini should be strongly commended.

A key finding from these studies is the importance of the Massif de la Selle carbonate aquifer system. It is arguably Haiti's most important aquifer system, as it is responsible for the provision of a significant proportion of water supply to Port-au-Prince due to its large springs and the added benefit of gravity. The rivers originating in the Massif supply the bulk of recharge to the Plaine du Cul-de-Sac, and perhaps the Plaine de Leogane aquifer as well. High intensity precipitation events and ENSO cycles appear critical for recharging both the bedrock and alluvial aquifers. RMPP resource quantities are especially vulnerable during El Nino periods and consecutive years without pulses of recharge from tropical storms and hurricanes. The water quality of the aquifer systems is also a concern due to changing land use and inadequate waste management and sanitation. Potential impacts on the aquifer from schemes related to river diversions and/or dams need to be understood and mitigated given that there is a strong connection between the aquifers and rivers.

Scientific characterizations of the aquifer systems in Haiti are poorly developed, largely due to the lack of monitoring and data availability. This study and future studies will continue to be limited without time-series/temporal datasets on spring flows, river flows, groundwater abstraction, water quality, environmental isotopes and meteorological parameters. Establishing and strengthening hydrological and hydrogeological monitoring programs with systematic procedures for data management and dissemination is an important recommendation that spans not just the three study areas, but the country as a whole.

Tunnel Diquini and Source Mariani

These studies provide a preliminary basis to inform planning and decision-making regarding the use, sustainability, and protection of the sources, so they continue to be an important source of water supply in the future.

Considering the regional importance of these water supplies, additional investments are warranted and fall into three categories:

1. Strengthening of flow, precipitation, and water quality monitoring programs are outlined for both sources and nearby rivers to address important data gaps and to strengthen the understanding of the springs and the associated aquifer system. For example, monitoring is required to better understand connectivity between Riviere Froide, the aquifer, and the Tunnel Diquini.

2. Water source protection and enhancement –recharge protection areas should be delineated and protected to preserve the quantity and quality of the waters. Public education, land use planning, zoning, and controlled development in these areas is necessary especially as Haiti's population has grown and waste management and sanitation practices are lacking.

3. Further study of both sources is necessary. The delineation of recharge areas and understanding of interactions with river systems requires more detailed geological mapping and isotope/tracer studies.

Monitoring is important to advance the understanding and characterization of the tunnel and the Massif de la Selle regional

aquifer that supports it. Using the data and findings in this study, the potential exists for source protection and enhancement programs in key zones of the tunnel watershed. Additional studies are necessary to better understand the interaction between the tunnel and the nearby Riviere Froide. If any hydraulic or significant watershed changes are proposed for the Riviere Froide, we recommend comprehensive studies to evaluate and quantify the tunnel's impacts.

Plaine du Cul-de-Sac

The steady-state groundwater flow model presented serves as a good tool to support the next steps of groundwater development and management in a regional context. The model is structured to support steady-state simulations of various groundwater abstraction, environmental and climate change scenarios. The resulting model suggest a renewable groundwater resources' use on the order of 130,000 m³/day, thus further validating the importance of the Riviere Grise and Riviere Blanche streamflow infiltrations the recharge and groundwater flow dynamics of the aquifer system.

Although a significant volume of data was compiled to support model development and calibration, the quality and reliability of data is variable. Further, a limited quantity of time-series or temporal data was available for river/stream stages and water levels in wells. The development of transient and stress period models instead of should be considered, but must be supported with additional data mining, and a focused monitoring campaign of surface water flows and groundwater levels.

Scientific characterization needs to be strengthened in the northeast, east and southeast portions of the aquifer to better understand lithology and the surface and groundwater interactions related to Lac Azuei, Canal Boucambrou and Trou Caiman. These will support model refinement and result in a greater level of confidence for these zones of the aquifer.

Saltwater intrusion risk in the coastal areas should also be further investigated with monitoring.

The importance of temporal monitoring of water levels and water quality in wells is important to support groundwater flow modeling and simulations. Temporal monitoring of flow and stage along multiple reaches of the Riviere Grise, Riviere Blanche and Canal Boucambrou is also important considering the three systems' relevance in the aquifer's dynamics. Well pumping estimates and monitoring also present a significant data gap that could be addressed through future activities, in the same manner that the estimation of current aquifer-wide abstraction was based on limited data.

HYDROGEOLOGICAL INVESTIGATION OF TUNNEL DIQUINI

Characterization of Hydrology and Guidance for Source Monitoring and Protection

Department Ouest, Republic of Haiti

Final Report
October 2018

Note: Additional data collection and research since this study was completed warrants revisiting and updating some of the analysis and findings of this report.

Prepared for:
Inter-American Development Bank & DINEPA

Prepared by:
Northwater International and Rezodlo S.A.

Keywords
Tunnel Diquini, Plaine du Cul-de-Sac; Groundwater; Haiti; Port au Prince; hydrogeology; water supply; Massif de la Selle

Latitude, Longitude
18.517N, 72.393W

Citation
Northwater International and Rezodlo. 2018. Hydrogeological Characterization of Tunnel Diquini: Port-au-Prince, Haiti, Inter-American Development Bank, Technical Report, HA-T1239-P001

Original report in English, French translation available.

Authors
James K. Adamson, PG
Javan Miner, EIT
Pierre-Yves Rochat

Table of Contents

EXECUTIVE SUMMARY **20**

SECTION 1.0 – INTRODUCTION AND PHYSICAL SETTING 21

SECTION 1.1 – GEOLOGY 22

SECTION 2.0 – METHODS AND RESULTS **24**

SECTION 2.1 – HYDROLOGY 25
SECTION 2.2 – WATER QUALITY AND HYDROCHEMISTRY 27
SECTION 2.3 – STABLE ISOTOPE AND TRACER 29
SECTION 2.4 – GROUNDWATER AGE 30
SECTION 2.5 – AQUIFER STORAGE 30
SECTION 2.6 – GROUNDWATER RECHARGE 30

SECTION 3.0 – DISCUSSION **32**

SECTION 4.0 – RECOMMENDATIONS FOR CONTINUED ACTIVITIES **33**

A – STRENGTHENING ONGOING MONITORING EFFORTS 33
B – WATER SOURCE PROTECTION, ENHANCEMENT AND RIVER MONITORING 34
C – FURTHER HYDROGEOLOGICAL CHARACTERIZATION 35

SECTION 5.0 – CONCLUSIONS **37**

REFERENCES **38**

EXECUTIVE SUMMARY

Tunnel Diquini is the largest single source of water for the municipal water system of Port-au-Prince, with an average supply of 29,449 m³/day to its metropolitan water system, based on records from 2014-2018. The tunnel accounts for ~26% of all the municipal production of water, and for 37% of all the gravity-fed spring flow that supplies the metropolitan area. An investigation was performed to analyze the hydrology of the tunnel's waters and better understand the origin of the flow and its relationship with the groundwater and surface water systems. Knowing this is important to guide future studies and monitoring the tunnel, and also to aid the water use planning and management by Centre Technique d'Exploitation de la Région Métropolitaine de Port-Au-Prince (CTE-RMPP).

The research was undertaken using a combination of literature review, satellite and topographic imagery analysis, and field reconnaissance. A brief field mission inside the tunnel was conducted on April 15, 2018, including: (i) physical and chemical sampling, (ii) stable isotope sampling, (iii) chlorofluorocarbon (CFC) and sulfur hexafluoride (SF6) sampling, (iv) flow rate measurement, and (v) visual inspection of tunnel geology.

Based on the study, the key results and conclusions are summarized below:

Spatial Distribution of Groundwater Recharge

1. The groundwater recharge area that contributes to the tunnel flow appears to range between 22 and 55 km².

a. This recharge area depends on the rate and duration of Riviere Froide leakage to the regional carbonate aquifer.

b. The average recharge elevation is estimated at 650 m. above mean sea level, indicating the possibility that some of the tunnel flow may originate from river leakage from the Riviere Froide to the regional carbonate aquifer.

Groundwater Budget

1. The long-term average annual recharge rate in the karst terrain is estimated at 26% of annual precipitation. During high intensity rainfall periods, the recharge rates are substantially above 26%, while during normal or low precipitation periods the recharge could be lower than 10%.

2. Aquifer storage relative to the tunnel is estimated between 265 and 327 million m³.

3. The limestone karst aquifer that feeds the tunnel is well mixed and has an average groundwater age of 26 to 32 years based on a single sampling event.

Flow Characteristics

1. Recharge to the regional aquifer and particularly to the tunnel appears to be largely affected by high intensity and high-volume rainfall events such as hurricanes and tropical storms. There appears to be a 3-to-7-year cycle of recharge trends partially influenced by El Niño and La Niña events.

2. Tunnel discharge is seasonally variable, with recorded flows ranging from 11,085 to 73,265 m³/d, and a geometric mean for all known recorded flows of 27,987 m³/d.

3. The tunnel flow is most vulnerable to extended periods of normal precipitation and consecutive years without high intensity rainfall periods such as tropical storms and hurricanes.

a. This recharge characteristic, combined with the resulting flow regression that can extend over periods of years, may foster perceptions that the tunnel flow has been decreasing over the long-term or that some events have had an acute impact on it.

b. Limited historical data from 1959 suggests that dry season low-flow conditions

are comparable or perhaps lower than current low-flow conditions and strongly influenced by major recharge or drought events.

c. The response time of the aquifer to major recharge events such as hurricanes may be shortening, possibly due to land cover and climatic changes.

Connection to Regional Groundwater and Surface Water

1. Both the tunnel and Riviere Froide are connected to the same regional karst limestone aquifer, from where they both receive flow. The Riviere Froide may recharge the aquifer at various spatial and temporal extents, and this could result in a possible link between the tunnel and river system.

a. Further study and monitoring is required to better understand the complex hydraulic links between the Riviere Froide, the regional aquifer and the tunnel.

2. Tunnel Diquini does not appear to have a hydraulic connection to the Riviere Momance. This is supported by the nature of geological structure and faulting.

a. The EPG fault zone and a perpendicular fault appear to direct groundwater in the Momance basin either into the Riviere Momance or into the lower reaches of the Riviere Froide, below where recharge to the tunnel would likely occur.

Aquifer Vulnerability

1. Due to the high permeability and rapid infiltration rates typical in karst limestone environments, the tunnel waters have high vulnerability to contamination.

2. Urbanization and land use changes in the hills south of the tunnel portal are considered the greatest risk to the tunnel water quality and flow. The lack of centralized waste management and sanitation, combined with the karst hydrogeology, significantly increases the risk of direct contamination of the aquifer and tunnel waters. Increase of impervious surfaces and loss of soil associated with urbanization increases runoff and decreases recharge to the aquifer that contributes to tunnel flows.

a. Land use planning, zoning, and managed development of the area south of the tunnel portal is necessary in order to protect the tunnel water from future water quality and flow impacts.

Conclusions and Recommendations

This study provides a preliminary basis to inform planning and decision-making with regards to the sustainability and protection of Tunnel Diquini so that it continues to be an important water supply in the future. If further work is planned in the tunnel watershed or more information is needed concerning the tunnel, recommendations are provided at the end of the report about water source protection, compiling historical data, and monitoring of climate, flow and water quality.

SECTION 1.0 - INTRODUCTION and Physical Setting

This study is part of a coordinated effort to better understand the existing and potential water supplies to serve the metropolitan area of Port-au-Prince. The intent of this study is to determine the hydrology of the tunnel waters and better understand the origin of its flow and its relationship with groundwater and surface water systems. Specifically, it is important to better understand whether significant recharge of the tunnel occurs from either the Momance or Froide rivers.

Tunnel Diquini was completed in 1940 by the J.G. White Engineering Corporation. It is

currently the largest single water source of the Port-au-Prince municipal water system. Tunnel flow accounts for approximately 24% of total municipal production, and 38% of all gravity-fed spring flow that supply the metropolitan region. Although design and construction documents for the tunnel were not available, it has been assumed that its primary target was an east-west trending normal fault, approximately 1.5 km south of the tunnel's portal. It is believed that this fault drains a sizeable portion of the Massif de La Selle carbonate aquifer system in this area.

The tunnel is reportedly 1.5-km in length along its main shaft. It appears to have an alignment approximately southward, although several minor changes in bearing were noted over the first several hundred meters from its entrance. At least one secondary tunnel branches from the main tunnel toward the southeast. The main tunnel is approximately 2.4 m wide with rectangular cross-section. Although minor roof collapse had occurred in several places, no constrictions to flow were observed. Below the normal fault, additional flow enters the tunnel from its sidewall, and roof seeps in fractures, merging with the main channel flowing toward the portal. The tunnel floor is rough, with fractured limestone bedding planes protruding into the water course. At the portal, the final length is concrete lined as the flow is channeled into a large pipe to supply the municipal system. The entire tunnel length is reportedly inspected annually by Mr. Mackenson Louis of CTE-RMPP.

The tunnel watershed ranges from the portal elevation at 140 meters to over 1,800 meters in the upper reaches of the Riviere Froide watershed. Average annual rainfall ranges from 1,400 mm/year near the portal to 2,100 mm/year in the upper reaches of the watershed. Land cover in the watershed is variable, with steeper slopes tending to be covered with scrub and flatter areas used for subsistence agriculture. Woodring (1924) described the watershed above Source Diquini as primarily scrub vegetation, indicating the possibility that land cover has not changed considerably in this watershed over the last 100 years. Given this land use history, it is possible that the hydrology of the area of study had largely adjusted to deforestation by the early years of the tunnel.

Section 1.1 - Geology

The geology of the tunnel area is primarily composed of carbonates that range from lower-Miocene to Paleocene age. Most of the tunnel appears to be bored through upper to middle Eocene-age limestones that are hard and well bedded with low bedding attitude. In the area of the tunnel portal, beds of limestone were observed to be near horizontal. To the south of the portal, the Eocene limestones are dissected by fault-controlled valleys, and primarily consist of detrital limestones and chalky limestones of lower to upper Miocene age. The entire length of the tunnel is within the hanging wall fault block (stratigraphically offset by the normal fault that traverses east-west 1.5 km south of the portal). The northern wall of this fault is downthrown, and it likely impounds groundwater and fosters preferential groundwater flow paths along the fault trace through the higher permeability limestones. This is believed to be the primary target and main source of groundwater to the tunnel. Figure 1 displays the geology around the tunnel and associated watersheds based on country-wide geologic mapping (CERCG, 1989) and faults based on mapping by Pubellier (2000) and Cox et al (2011). Figure 2 displays a generalized geologic cross-section along the tunnel alignment southward to the Riviere Froide drainage at the Enriquillo-Plantain-Garden Fault.

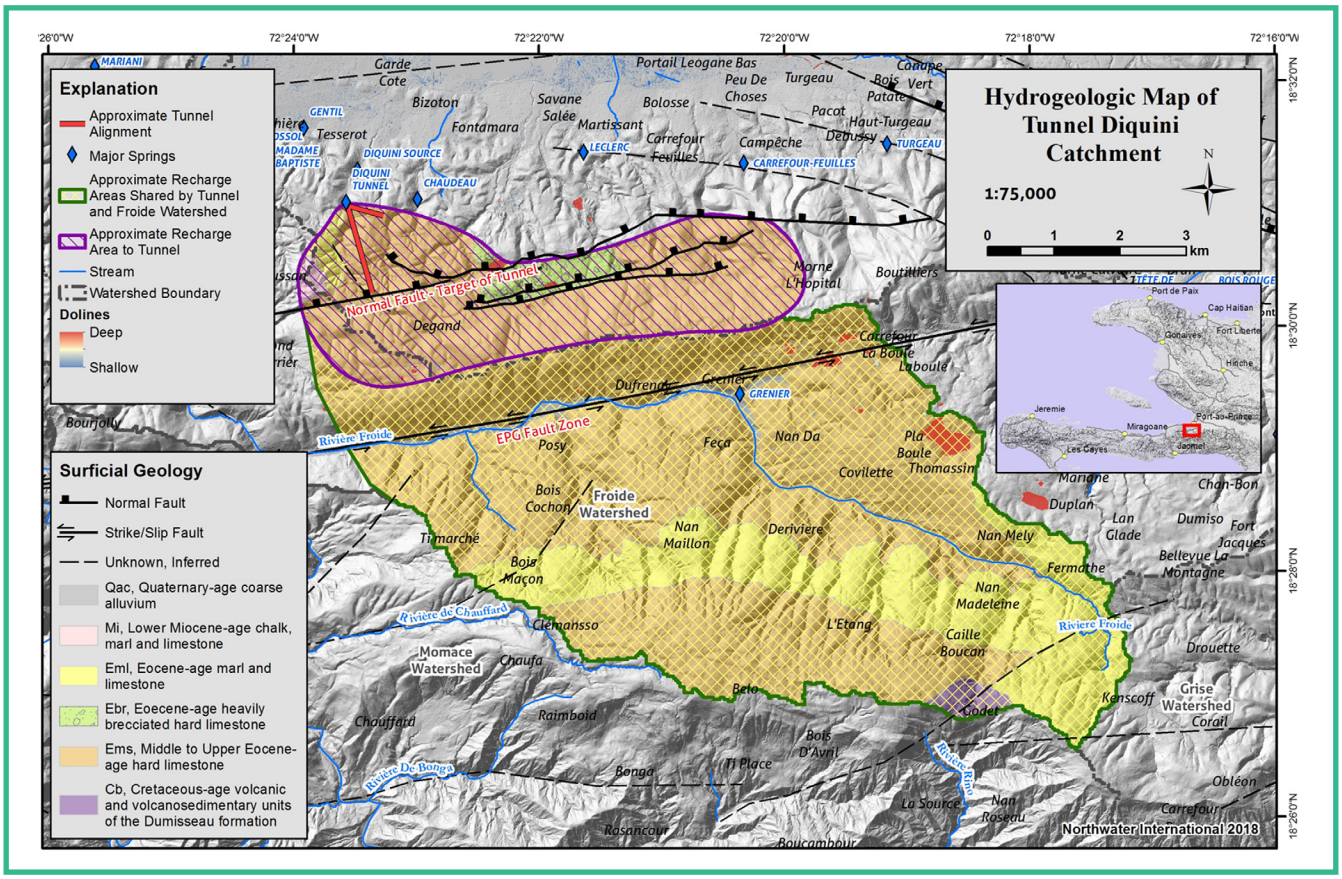

Figure 1 - Geologic map of tunnel and associated watersheds with interpreted recharge zones.

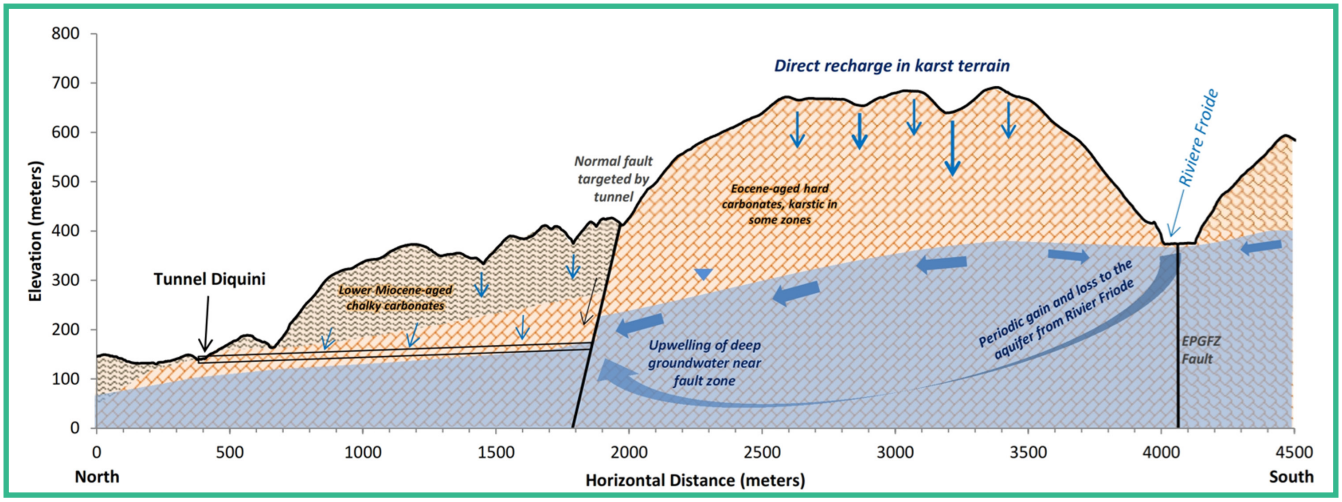

Figure 2 - Generalized cross section of tunnel geology and hydrology.

Section 2.0 - Methods and Results

A brief field mission in the tunnel was conducted on April 15, 2018, including: (i) physical and chemical sampling, (ii) stable isotope sampling, (iii) chlorofluorocarbon (CFC) and sulfur hexafluoride (SF6) sampling, (iv) flow rate measurement, and (v) visual inspection of the tunnel's portal geology. All activities at the tunnel were performed under the supervision of the caretaker of the tunnel, Mr. Mackenson Louis.

The tunnel flow was measured at the tunnel's portal just prior to the point where the flow leaves the open-rock channel with a Marsh-McBirney Flo-Mate 2000 portable electromagnetic velocity meter. The open-channel width was approximately 2.44 meters with an average water depth of 0.215 meters. The calculated flow rate was 1,300 m^3/h, or 361 L/s, corresponding to a stage-height of 15.5 centimeters on the staff gauge affixed to the east side of the tunnel portal (this staff gauge does not extend to the channel bottom).

The field team was escorted approximately 300 meters into the tunnel for geological inspection. The limestone appeared to be well-bedded, moderate to hard, and with a near-horizontal bedding attitude. Numerous seeps entered the tunnel from fractures and cavities daylighting the walls and ceiling along the 300 meters length inspected. Many of these seeps were less than 1 L/s, although several were estimated to flow at more than 5 L/s and one was estimated at 20 L/s. At approximately 150 meters from the tunnel portal, a secondary smaller tunnel enters the main tunnel from the east. This branch produces significantly cooler water than the main tunnel flow. This smaller tunnel was barricaded with cobble that surrounded a concrete pipe. Mr. Mackenson Louis reported that each November/December he walks the full length of the tunnel to inspect it. His father (now deceased) was the original caretaker of the tunnel since it was constructed. Based on their observations, they believe that the tunnel's flow rate has been decreasing over the last several decades.

Water was sampled several meters into the tunnel, as sampling farther into the tunnel was not feasible. Mr. Mackenson Louis believed that our sampling event was representative of a lower flow condition for the tunnel. A 12V sampling pump with flexible tygon tubing was used to collect low-flow samples where the tunnel flow was considered laminar. Samples for physical, chemical, and stable isotope analysis were collected by filling prepared sample bottles provided by the laboratories of analysis (First Environmental and Isotech). Chlorofluorocarbons (CFCs) and Sulfur Hexafluoride (SF6) were collected to age-date the groundwater discharging from the tunnel. Samples for CFC-11, CFC-12 and CFC-113 were collected using the glass bottle method with copper tubing as described by USGS and Reston Chlorofluorocarbon Laboratory. Samples for SF6 were collected using 1-Liter plastic-coated safety amber glass bottles with polyseal cone-lined caps, also applying methodologies developed by USGS and University of Utah Noble Gas Lab. All sampling bottles and excess air tubes for CFC's and SF6 were provided by the Dissolved and Noble Gas Lab at the University of Utah. Samples for excess air analysis were also collected in ¼-inch copper tubes with clamps; these samples support correction of the SF6 data. Upon completion of sampling, all samples were wrapped in insulating materials and transported to the US for shipment to the analysis labs.

Photo 1. View inside tunnel portal.

Photo 2. Secondary adit approximately 150 m from portal, noticeably colder flow.

Photo 3. View of limestone geology looking toward tunnel portal.

Photo 4. Example of near horizontal bedding.

Photo 5. Example of seep in east tunnel wall.

Section 2.1 - Hydrology

Tunnel discharge varies significantly based on the intensity and duration of recharge events and the transit time through the aquifer. A discontinuous tunnel flow dataset was compiled from various sources spanning between 1980 and 2018. The data was primarily provided by Engineer Pierre Colon Geffrard of CTE-RMPP. Flow measurements were provided as average monthly flow data from 1980 to 2010, single monthly flow measurements estimated using a spinner velocity-meter from 2010 to 2014 and monthly flow measurements using an electromagnetic velocity-meter from 2014 to 2018. The project team was informed that a CTE-RMPP technician continues to measure flow rate at the tunnel each month. One older flow

Photo 6. Sampling for CFC's and SF6.

Photo 7. Existing staff gauge.

measurement that was located for the tunnel, from August 1959 (Waite, 1960) recorded 217 L/s. Based on the available data, tunnel flow rates are seasonally and annually variable and range from 128 L/s to 848 L/s with a geometric mean of 324 L/s.

Recharge to the regional aquifer and to the tunnel in particular appear to be largely affected by high intensity and high-volume rainfall events such as hurricanes and tropical storms, something that is typical of karst aquifers. There appears to be a 3-to-7-year cycle of recharge trends partially influenced by El Niño and La Niña events. Conversely, extended periods of declining flow rates occur during drought and El Niño years. Figure 3 shows flow data from 1980 to 2018 along with recorded hurricanes and droughts. A lag time of several months or longer is visible between the rainfall event and an increase in discharge; however, the response time of the aquifer to major recharge events may be shortening. Decadal climatic variations may also be illustrated by the flow data, showing a downward trend in flow rate from 1980 to 1990, a slight upward trend from 1990 to 2000, a potentially strong upward trend from 2000 to 2010, and a decreasing trend from 2010 to 2018. Trends from 2010 to 2018 may be misleading due to the difference in monthly average vs. single-event flow measurements.

There was insufficient data available to establish clear long-term trends in the tunnel's discharge since its construction. The common understanding is that the tunnel flow rates have been decreasing through time, however this trend is not apparent in the 1980 to 2018 flow data. A decreasing trend is also not present when comparing the August 1959 flow rate (217 L/s) to average August flow rates between 1980 and 2010 (324 L/s) or 2011 and 2018 (404 L/s). While the trend is not clear for Tunnel Diquini, Source Diquini, shows a 44% decrease in flow over ninety

years. The average recorded flow of Source Diquini between 1923 and 1938 was 62 L/s, and the 2014 monitoring period recorded an average of 34.4 L/s. However, Source Diquini's decreased flows may be related to changes in hydrology related to dewatering near the tunnel. Further study of these long-term and cyclic flow dynamics of the tunnel and other major Port-au-Prince springs would provide valuable insights for water management and planning.

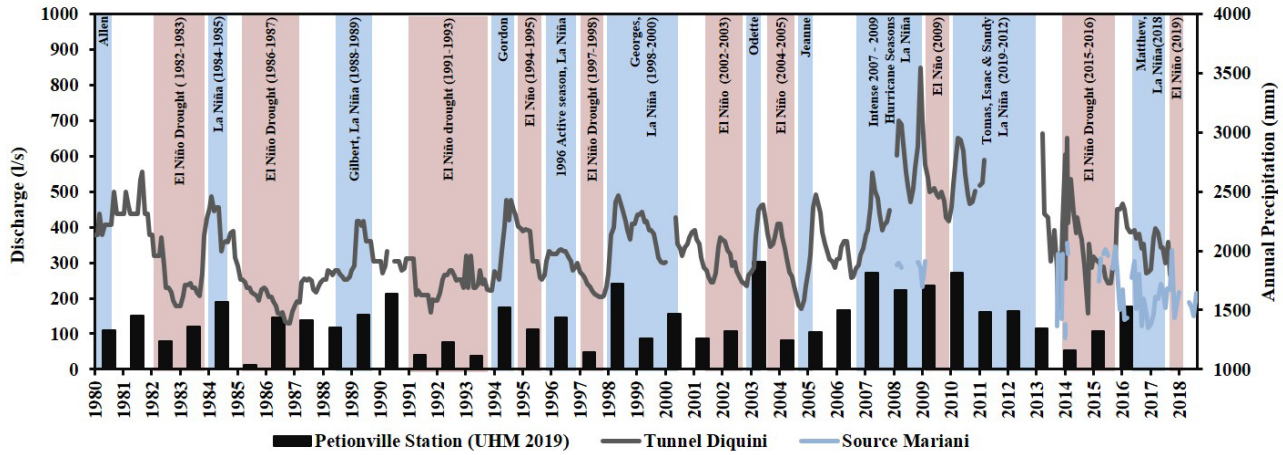

Figure 3. Tunnel Diquini discharge with major meteorological events, 1980 - 2018.

Section 2.2 - Water Quality and Hydrochemistry

Tunnel Diquini is considered to have excellent physical and chemical quality as a drinking water source, with a fairly dilute groundwater (214 mg/L total dissolved solids). The groundwater is a CaHCO3 type water typical of a limestone aquifer (Figure 4). Nitrate was the only potential parameter of concern from the sampling event (8.64 mg/L as NO3). Past analysis from 2014, and monitoring between 2006 and 2013 also reported elevated nitrate concentrations, although nitrates were still below the USEPA (10 mg/l as NO3-N), WHO (50 mg/l as NO3) and DINEPA (50 mg/l as NO3) potable water guidelines (Table 1). Biological sampling and analysis were not performed as a part of this study. The total organic carbon (TOC) measurement of 0.4 mg/L

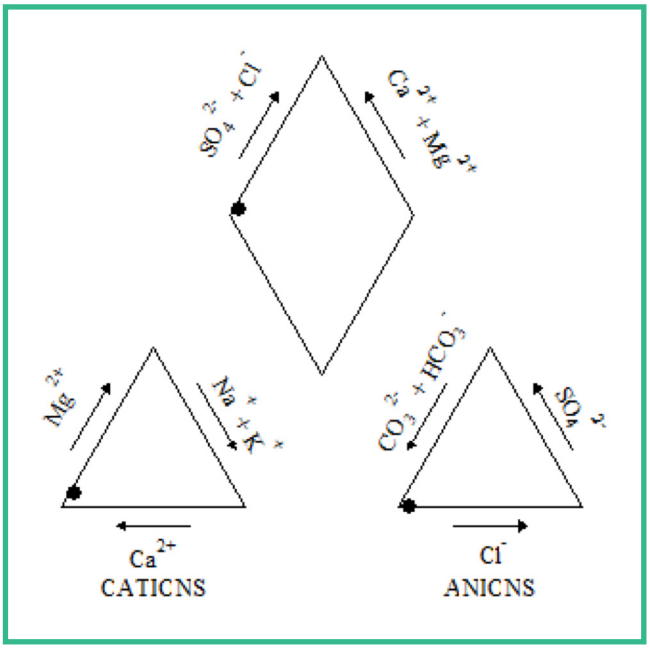

Figure 4. Piper diagram of Tunnel Diquini water, April 2018.

is a typical concentration in groundwater, particularly in the tropical climate zone. There was also a measurable amount of barium in the groundwater at 0.116 mg/L. Barium occurs in the open ocean at a concentration of 0.05 mg/L and is a group-two element as calcium. Barium substitutes for calcium during limestone formation, and, when the limestone dissolves, barium ends in the groundwater. Other trace metals were below detection limits, indicating a low likelihood of current industrial or commercial contamination.

Due to the karst-conduit and rapid recharge nature of the aquifer, the tunnel is susceptible to surficial contamination within the recharge areas, especially near the tunnel portal. Further study concerning the aquifer and tunnel hydrology would help locate the primary recharge areas and locations where the aquifer is most susceptible due to increased conduit flow and concentrated recharge. Table 1 provides the water quality and hydrochemistry data available from previous studies and the sampling event from April 15, 2018.

Parameter	Units	DINEPA Standard	WHO Guidelines	USEPA MCL	USEPA Secondary MCL	Tunnel Diquini 18.517 -72.393		
Date Collected						13-Jan-14	4-Nov-14	15-Apr-18
Alkalinity, Total (CaCO3)	mg/L	500	--	--	--	200	200	230
Bicarbonate (CaCO3)	mg/L	--	--	--	--	0	0	< 5
Chloride	mg/L	250	250	--	250	11.99	15.5	6.2
Conductivity	umhos/cm	--	--	--	--	390	387	382
Fluoride	mg/L	2	1.5	4	--			0.27
Ammonia (N)	mg/L	--	--	--	--	0	0.013	< 0.01
Nitrite (NO2)	mg/L	3	3	1	--		0.023	0.033
Nitrate (NO3)	mg/L	50	50	10	--	16.82	12.4	8.64
pH @ 25°C	Units	--	--	--	--	7.29	7.6	7.42
Sulfate	mg/L	250	500	--	250	4	5	< 15
Silica (SiO2)	mg/L	--	--	--	--			12.9
TOC	mg/L	--	--	--	--			0.4
Antimony	mg/L	--	0.02	0.006	--			< 0.006
Arsenic	mg/L	--	0.01	0.01	--			< 0.01
Barium	mg/L	--	0.7	2	--			0.116
Beryllium	mg/L	--	--	0.004	--			< 0.004
Cadmium	mg/L	--	0.003	0.005	--			< 0.005
Calcium	mg/L	100	--	--	--	78.47	76.6	74.4
Chromium	mg/L	--	0.05	0.1	--			< 0.005
Copper	mg/L	1	2	1.3	--			< 0.005
Iron	mg/L	0.2	--	--	0.3			< 0.05
Lead	mg/L	0.01	0.01	0.015	--			< 0.005
Magnesium	mg/L	100	--	--	--	2.91	4.86	4.1
Manganese	mg/L	--	0.5	--	0.05			< 0.005
Potassium	mg/L	--	--	--	--	0.6	0.7	< 0.5
Silver	mg/L	--	--	--	0.1			< 0.005
Sodium	mg/L	--	--	--	--	3.18	2.07	3.1
Thallium	mg/L	--	--	0.002	--			< 0.01
Zinc	mg/L	3	--	--	5			< 0.01
Total Hardness (CaCO3)	mg/L	300	--	--	--			202
Mercury	mg/L	--	0.0005	0.002	--			< 0.0005
Total Dissolved Solids	mg/L	600	1000	--	500		186.3	214

Note: 2014 sampling based on EPTISA database (2016)

Table 1. Hydrochemical analyses of Tunnel Diquini waters.

Section 2.3 - Stable Isotope and Tracer

Stable isotopes of oxygen ($\delta^{18}O$) and hydrogen (δD) were sampled to aid in evaluating recharge dynamics. Gonfiantini and Simonot (1988) observed a linear trajectory of $\delta^{18}O$ versus elevation from samples collected south of Port au Prince. They found that there is a -0.9 per mil change for every 1000 meters of elevation gain for water points on the plain, and estimated a slope of -1.4 per mil change for every 1000 meters of elevation for the springs south of Port-au-Prince. This linear trajectory can be applied to Tunnel Diquini, as it was one of the originally sampled points in 1987 and has similar characteristics to springs in the area.

The stable isotope composition of the sample collected in April this 2018 was $\delta^{18}O$ = -3.28 per mil and δD = -14.4 per mil, while Gonfiantini and Simonot (1988) measured the groundwater discharging from the tunnel in 1980s and their results were $\delta^{18}O$ = -3.36 per mil and δD = -14 per mil. These results are essentially the same, since the analytical uncertainty in the measurement is ±0.1 $\delta^{18}O$, and ±1 δD. Applying the $\delta^{18}O$ value to the -0.9 and -1.4 per mil/1000 meter regression slopes, the likely minimum recharge elevation is 200 meters above sea level and the average recharge elevation is 650 meters above sea level. The aquifer water has had essentially the same isotopic composition over the past 31 years. That implies that the aquifer is well mixed before it emerges from the tunnel.

The stable isotope values recorded for this study and by Gonfiantini and Simonot (1988) plot above the Global Meteoric Water Line, which typically indicates that the groundwater has been subject to limited evaporation fractionation. However, the 1988 study and the analysis for this study indicate greater complexity in drawing conclusions from the value of $\delta^{18}O$. Gonfiantini and Simonot (1988) observed that water from the Riviere Grise and Riviere Blanche followed a similar trend to the carbonate springs, with an average $\delta^{18}O$ of -3.66 for the Grise and -4.23 for the Blanche. Based on the mean elevations of the Grise, Blanche and Froide, and their geographic and topographic similarities, an assumption can be made that the river water in the Riviere Froide may have an isotopic composition displaying the same relationship between $\delta^{18}O$ and elevation. Such a calculation indicates that the Froide may have a baseflow $\delta^{18}O$ of around -3.34. This $\delta^{18}O$ result is nearly identical to that of Tunnel Diquini (-3.36 or -3.28).

However, based on topography, the average elevation of the Riviere Froide watershed is roughly 150 m higher than the tunnel watershed. This apparent elevation difference is likely due to the evaporative fractionation of $\delta^{18}O$ during surface flow in the river channel. When these pieces are put together, this indicates two possibilities for how the tunnel and Rivière Froide are related: i) both derive their discharge from roughly the same regional carbonate aquifer zone; or ii) stream losses in the Froide infiltrate the normal fault and end up discharging into the tunnel. In any case, the hydrologic dynamics of the two are likely linked. Further study including isotopic sampling and flow rate measurements at various locations and hydrologic conditions on the Froide are necessary to further evaluate these possibilities. A better understanding of this link is a key aspect of future studies to better define the tunnel.

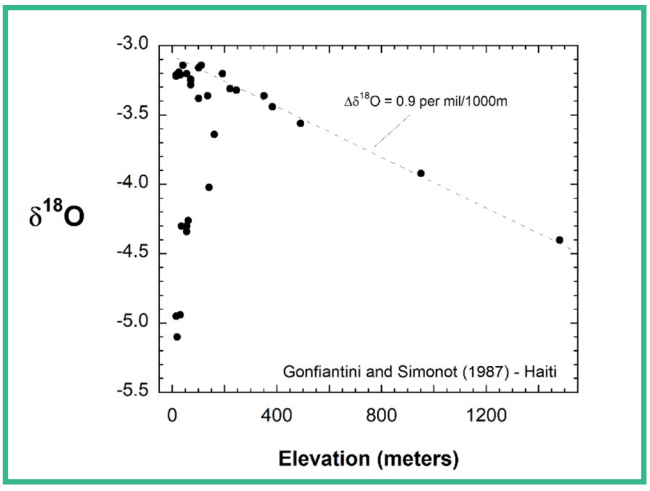

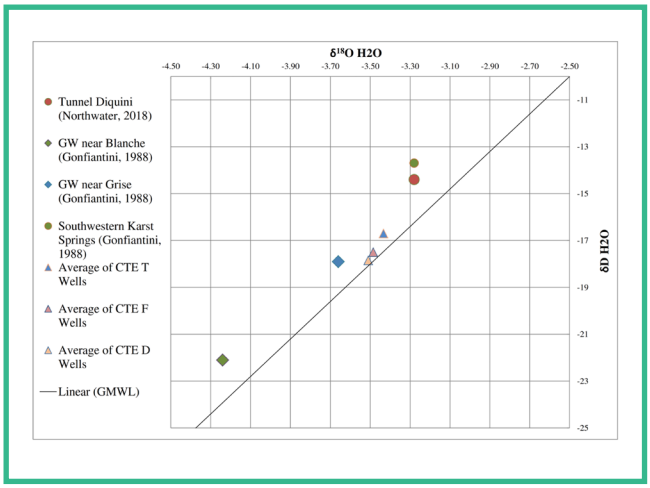

Figure 5 - Stable isotope data plotted with Global Meteoric Water Line (GMWL).

Section 2.4 - Groundwater Age

Chlorofluorocarbons (CFCs) and Sulfur Hexafluoride (SF6) were collected to age-date the groundwater. These estimates are based on CFCs and SF6 accumulating in air during the 20th century, measuring their solubility in water and extrapolating back to the atmosphere (see Appendix B). Both methods require assumption or measurement of other parameters. For CFCs the primary adjustable parameter is the recharge temperature, which affects solubility of the CFCs. For SF6 the primary adjustable parameters are excess air, recharge temperature, and recharge elevation. For both analyses, the recharge temperature was set at 25˚C, and for SF6 the recharge elevation was set at 500 meters, and the excess air at 2 cc/l, which is a common value for most groundwater. The CFC calculated recharge age date was 1986, indicating the water is 32 years old. The calculated recharge date for the SF6 was 1992, indicating the water is 26 years old. It is not uncommon for these two age-dating methods to be in slight disagreement (the older the water the more discrepancy there typically is). Taking these results together, we can assume a groundwater age for the tunnel during an average flow regime of 29 years. Further sampling of CFC's and SF6 during higher flow and lower flow events could further help illuminate the recharge dynamics of the aquifer.

Section 2.5 - Aquifer Storage

With the available data, a planning level estimate of storage in the aquifer can be made. Recognizing that the isotope data from 1988 and 2018 indicate that the aquifer is well mixed, meaning dispersion is high in the aquifer porous structure, then the annual output of the spring multiplied by the age of the groundwater equates to a qualitative storage estimate. Using the calculated annual discharge from 1980 to 2000 of 9.36 million m^3/year, this method estimates between 243 and 300 million m^3 of storage. This evaluation is very approximate; refinements are likely possible with further analysis of discharge, sampling data, and tracer tests.

Section 2.6 - Groundwater Recharge

The groundwater recharge rates associated with the tunnel discharge were estimated using the chloride mass balance method and a custom GIS-based direct recharge model developed by Miner and Adamson (2017). Forty-one chloride measurements for the tunnel waters and 13 rainfall chloride samples were available for the mass balance (Table 2). The geometric mean rainfall chloride is 2.5 mg/l and the tunnel geometric mean is 9.8 mg/L, yielding an average annual recharge rate of 26%, or 434 mm of the roughly 1,700 mm/year, which falls in the probable recharge area. Combining this recharge rate with the average annual tunnel discharge, indicates that the recharge area of the tunnel aquifer could be approximately 22 km^2.

The GIS-based recharge model developed by Miner and Adamson was calibrated to

historical average annual baseflow in the Riviere's Grise, Blanche and Momance that flank the tunnel, and Riviere Froide to the east and west. Average modeled recharge in the Riviere Froide watershed was 206 mm/year, less than half that has been indicated by the chloride mass-balance. This would equate to a roughly 55 km² drainage area. One possible reason for this discrepancy could be the scarcity of rainfall chloride measurements, especially at the elevations where primary recharge is occurring. A second potential reason could be that the tunnel is receiving baseflow from the Riviere Froide, so the chloride levels of the tunnel reflect the chloride and recharge dynamics of the larger aquifer that supplies the Riviere Froide. In any case, it is likely that the spatial extent of the tunnel recharge area ranges between 22 km² and 55 km². This large potential range points to the need of more comprehensive and diagnostic studies to better delineate the tunnel recharge area and flow pathways, and also to characterize the nature of the Riviere Froide along the reaches south of the tunnel.

Site	Type	Date	Lat (dd)	Long (dd)	Elevation	Cl (mg/L)
Tunnel Diquini	Spring	4/15/2018	18.517	-72.393	140	6.2
Tunnel Diquini	Spring	1/13/2014	18.517	-72.393	140	12
Tunnel Diquini	Spring	11/4/2014	18.517	-72.393	140	15.5
Tunnel Diquini[3]	Spring	2006 - 2013	18.517	-72.393	140	9.7
Momance River	River	8/1/2018	18.475	-72.407	305	6
Froide River	River	8/1/2018	18.487	-72.412	280	6.2
Thomassin 36	Rainfall	10/6/2018	18.482	-72.317	1025	1.24
Thomassin 36	Rainfall	10/2/2018	18.482	-72.317	1025	0.71
Thomassin 36	Rainfall	9/28/2018	18.482	-72.317	1025	1.78
Anse-a-Galet	Rainfall	8/26/2018	18.834	-72.868	20	4.04
Anse-a-Galet	Rainfall	8/14/2018	18.834	-72.868	20	3.4
Anse-a-Galet	Rainfall	8/10/2018	18.834	-72.868	20	8.86
Anse-a-Galet	Rainfall	8/5/2018	18.834	-72.868	20	10.5
Bas de Delmas	Rainfall	8/1/2018	18.563	-72.340	5	2
Petionville	Rainfall	8/1/2018	18.511	-72.290	380	7.1
Petionville	Rainfall	8/2/2018	18.511	-72.290	380	13.6
Petionville	Rainfall	8/2/2018	18.511	-72.290	380	9.89
Laboule	Rainfall	10/19/2016	18.495	-72.315	850	< 0.7
Laboule[1]	Rainfall	10/4/2016	18.495	-72.315	850	< 0.7
Laboule	Rainfall	10/24/2016	18.495	-72.315	850	< 0.7
Clercine 12	Rainfall	10/30/2016	18.575	-72.277	42	< 0.7
Cabaret #1	Rainfall	9/16/2015	18.736	-72.418	45	1.32
Cabaret #4	Rainfall	3/6/2016	18.736	-72.418	45	3.91
Cabaret #2	Rainfall	2/2/2016	18.736	-72.418	45	14
Lafito	Rainfall	2/11/2016	18.697	-72.349	29	22
Anse-a-Galet	Rainfall	10/17/2015	18.834	-72.868	20	0.8
					Geometric Mean for Rainfall [2]	2.7
					Geometric Mean for Tunnel Diquini	10.5

[1] Sample taken during Hurricane Matthew
[2] Assumes chloride values for Laboule and Clercine 12 are approximately 0.5 mg/L
[3] Note CTE-RMPP records contain 38 chloride samples; the geometric mean of these is presented.

Table 2. Rainfall and tunnel water chloride values.

Section 3.0 - Discussion

Based on the study, the key results are outlined and discussed below:

Spatial Distribution of Groundwater Recharge

1. The groundwater recharge area that contributes to the tunnel flow appears to range between 22 and 55 km².

a. This recharge area depends on the rate and duration of Riviere Froide leakage to the regional carbonate aquifer.

b. The average recharge elevation is estimated at 650 m above mean sea level, indicating the possibility that some tunnel flow may originate from river leakage from the Riviere Froide to the regional carbonate aquifer.

Groundwater Budget

1. The long-term average annual recharge rate in the karst terrain is estimated at 26% of annual precipitation. During high intensity rainfall periods, the recharge rates are substantially higher than 26%, while during normal or low precipitation periods the recharge could be lower than 10%.

2. Aquifer storage relative to the tunnel is estimated between 265 and 327 million m³.

3. The limestone karst aquifer that feeds the tunnel is well-mixed and has an average groundwater age of 26 to 32 years, based on a single sampling event.

Flow Characteristics

1. Recharge to the regional aquifer and to the tunnel in particular appears to be largely affected by high intensity and high-volume rainfall events such as hurricanes and tropical storms. There appears to be a 3-to-7-year cycle of recharge trends partially influenced by El Niño and La Niña events.

2. Tunnel discharge is seasonally variable with recorded flows ranging from 11,085 to 73,265 m³/d, with a geometric mean for all known recorded flows of 27,987 m³/d.

3. The tunnel flow is most vulnerable to extended periods of normal precipitation and consecutive years without high intensity rainfall periods such as tropical storms and hurricanes.

a. This recharge characteristic, combined with resulting flow regression that can extend over periods of years, may foster perceptions that the tunnel flow has been decreasing over the long-term or that acute impacts have occurred.

b. Limited historical data from 1959 suggests that dry season low-flow conditions are comparable or perhaps lower than current low-flow conditions and are strongly influenced by major recharge or drought events.

c. The response time of the aquifer to major recharge events such as hurricanes may be shortening, possibly due to land cover and climatic changes.

Connection to Regional Groundwater and Surface Water

1. Both the tunnel and Riviere Froide are connected to the same regional karst limestone aquifer, and both receive flow from the aquifer. The Riviere Froide may recharge the aquifer at various spatial and temporal extents, and this could result in a possible link between the tunnel and river system.

a. Further study and monitoring is required to better understand the complex hydraulic links between the Riviere Froide, the regional aquifer, and the tunnel.

2. Tunnel Diquini does not appear to have a hydraulic connection to the Riviere Momance. This is supported by the nature of the geological structure and faulting.

a. The EPG fault zone and a perpendicular fault appear to direct groundwater in the Momance basin either into

the Riviere Momance or into the lower reaches of the Riviere Froide, below where recharge to the tunnel would likely occur.

Aquifer Vulnerability

1. Due to the high permeability and rapid infiltration rates typical in karst limestone environments, the tunnel waters have high vulnerability to contamination.

2. Urbanization and land use changes in the hills south of the tunnel portal are considered the greatest risk to the tunnel water quality and flow. The lack of centralized waste management and sanitation combined with the karst hydrogeology significantly increases the risk of direct contamination of the aquifer and tunnel waters. Increase of impervious surfaces and loss of soil associated with urbanization increases runoff and decreases recharge to the aquifer that contributes to tunnel flows.

a. Land use planning, zoning, and managed development of the area south of the tunnel portal is necessary to protect the tunnel water from future water quality and flow impacts.

Section 4.0 - Recommendations for Continued Activities

Due to Tunnel Diquini's importance as the largest single water supply to Port-au-Prince, additional work may be warranted to guide water source protection and enhancement, water use planning, and future water supply development in the Massif de la Selle aquifer. Based on the findings of this study, this section provides recommendations in three categories for (i) improvements to ongoing monitoring efforts, (ii) water source protection and enhancement, and (iii) options for additional study. Any future activities would be greatly aided by increased availability of temporal datasets for climate, discharge, hydrochemistry, and stable isotopes. Table 3 and Table 4 summarize the recommendations by category, and the narrative provides supplemental detail.

A - Strengthening Ongoing Monitoring Efforts

Historical monitoring data collected by CTE-RMPP provided key insights into the tunnel dynamics. It is our understanding that current monitoring efforts, when performed, include (i) monthly flow measurement at the tunnel portal and (ii) collection of a water sample for physical and chemical analysis including conductivity, salinity, pH, temperature, turbidity, hardness, alkalinity, calcium, magnesium, chloride, sulfate, nitrate, nitrite, and iron. Data gaps exist in terms of what was provided to our team by DINEPA and CTE-RMPP. There are multiple ways that monitoring efforts could be further reinforced and improved.

• We commend CTE for the data that has been collected. Data that was particularly useful to this study included flow rate, chloride, conductivity, turbidity, and nitrate measurements. We recommend that, at a minimum, these parameters continue to be measured monthly.

• Data format consolidation – it appears that existing records are maintained in several different formats including paper and digital spreadsheets, and that the retrieval of data for analysis is a challenge. The most consistent and accessible records were hand-written notes. Simplicity, clarity, and accessibility are key to ensuring CTE-RMPP has the data needed to properly manage its water resources. It was our impression that the current digital data management scheme was unclear or overly complicated, which led to difficulty in locating and compiling data when it was requested. Developing a standard data architecture and recording and archiving method is recommended along with training for CTE-RMPP or DINEPA employees involved in water monitoring.

• Monthly flow measurements can be augmented and eventually made simpler by the incorporation of the staff gauge into monitoring and development of a stage-discharge curve. This would also make daily flow measurements more feasible

and allow for automatic flow monitoring using pressure transducers. An increase in monitoring frequency would allow for better understanding the complex recharge dynamics when coupled with rainfall data.

· Table 3 provides recommendations for measurement parameters and timing of sampling which is recommended. This monitoring should begin as soon as possible and be incorporated into a permanent monitoring program so that data is available for water use planning or future studies.

Parameter	Daily	Weekly	Monthly	Quarterly	Yearly	Notes
Tunnel Flow Rate			X			Select and document a standard location and methodology. Electromagnetic velocity probe or industry standard equivalent recommended.
Tunnel Flow Height (stage)	X					Existing staff gauge is difficult to read and does not indicate actual water depth. Recommend installation of new staff gauge with easy to read centimeter scale. Over time, stage can be used to estimate flow on a daily basis.
Conductivity (uS/cm)		X				Low cost conductivity/pH field probe, calibrated as required.
pH		X				
Temperature		X				
Chloride			X			Low level chloride analysis often required, suggest detection limit of 1 mg/L or lower.
Nitrate			X			CTE-RMPP lab analysis
Turbidity			X			CTE-RMPP lab analysis
E. coli			X			Simple tests such as the compartment bag test may be sufficient and more economical than a full analysis at the CTE-RMPP lab.
Hydrochemistry				X		CTE-RMPP lab analysis of Ca, Mg, Na, Cl, K, CO3, HCO3, SO4, NO2, Fe, TDS, Hardness, Alkalinity
Compilation and publication of data					X	Recommend that a short memorandum which primarily contains a table of the measured results be published online so that data is easily available. This is also a good interval to review issues with data collection and revise the program in order to reduce data gaps.

Table 3. Tunnel monitoring program recommendations.

B – Water Source Protection, Enhancement and River Monitoring

Water source protection and enhancement planning – This study provides an improved understanding of discharge dynamics and recharge areas for the tunnel which highlight interim insights useful for guiding next steps to protect and enhance it.

· Recharge protection areas can be delineated to protect critical areas of recharge and reduce sources of contamination near the tunnel.

· Land use practices in the recharge area can be mapped and reviewed to guide focused interventions, such as forestation, terracing of steep slopes, and development of exclusion zones.

· Sinkhole delineation can be performed to locate zones of concentrated recharge. Fences could be built to keep wildlife and

livestock out and to eliminate potential contamination sources.

· The ridgetop area southeast of the tunnel portal is becoming increasingly urbanized; efforts at sanitation planning and infrastructure in this area would help protect the tunnel from biological contamination.

River Froide monitoring – The Riviere Froide is likely a major component of the hydrogeological system that supplies the tunnel. Temporal and spatial data of river flow and water quality are needed to better define the relation between the Froide and Tunnel Diquini. While short-duration measurement campaigns may be incorporated into later studies, the most useful data would come from a permanent and well-defined monitoring program.

· Periodic streamflow measurement at multiple locations along the upper reaches of the Riviere Froide to locate zones of gain and loss. Although measurements ideally should be conducted weekly or monthly, quarterly measurement is a good starting interval based on seasonal flow variations.

· Measurement should include flow rate, field water quality including pH, conductivity, and temperature, and sample collection for low-level chloride analysis. It is also recommended collection of grab samples for stable isotopes of $\delta^{18}O$ and δD during high and low flow events at least bi-annually when corresponding flow and chloride data is also available.

C – Further Hydrogeological Characterization

Refinement of the tunnel recharge area – This study indicates a large uncertainty in the spatial extent of the tunnel's recharge. The improvement of the knowledge of this aspect is important to guide water source protection, land use planning, and future uses of the Riviere Froide. Due to the karst nature of the aquifer, there is likely both diffuse and concentrated recharge occurring. Potential study methods include:

· A monitoring program using stable isotopes of $\delta^{18}O$ and δD along with chloride collected over a multi-year period to record changes occurring due to both drought and hurricane-induced recharge events.

· Periodic streamflow measurement at multiple locations along the upper reaches of the Riviere Froide to locate zones of gain and loss.

· Dye tracer testing of karst dolines and the Froide River is perhaps the most definitive method for delineating the recharge area, although transit times may be prohibitive.

· Sampling of various major seeps and the fault face in the tunnel may provide insight into the spatial extent and amount of recharge.

Refinement of tunnel recharge and discharge dynamics – As previously mentioned, the tunnel system appears to be largely driven by large climatic events of 3-to7year cycles.

· A concerted and coordinated effort should be made by CTE-RMPP, DINEPA, and BME to locate any documents related to historical flow rates from the first decades after the tunnel was constructed. This will help in understanding how and if the tunnel has been affected by the land use changes and climate changes that have likely decreased the flow in other springs in the area, such as Source Diquini.

· Careful analysis of these recharge and discharge trends may also help to predict the future effects of climate change on the tunnel and major carbonate spring discharge to Port-au-Prince's water supply.

Refinement of tunnel geology and structure

· A concerted and coordinated effort should be made by CTE-RMPP, DINEPA, and

BME to locate any documents related to the tunnel design and detailed local geologic mapping.

· Geologic mapping along the tunnel adit to better understand the ways in which lithologic and structural changes affect the occurrence of groundwater flow into the tunnel. Such mapping may also be useful if future efforts to secure a reliable source of water for Port-au-Prince include the possibility of similar tunnels.

Increased rainfall monitoring and sampling

· Daily rainfall data suitable to determine rainfall intensity was not made available to this study. If such data is located, an analysis could be performed comparing rainfall intensity over periods of recorded flow rates to better understand recharge thresholds and the conditions conducive to diffuse or concentrated recharge.

· Implementation of a rainfall monitoring program that also samples rainfall for $\delta^{18}O$, δD and chloride. Potential localities for such a program include Degand, south of the tunnel, and Fermate, in the upper-eastern reaches of the Froide watershed. Such rainfall intensity measurements coupled with meteoric hydrochemistry will allow for better recharge estimates, and will be a valuable resource to all future hydrogeological studies in the Massif de la Selle.

Category	Activity	Financial Costs	Expertise Required	Equipment Required	Institutional Involvement
A	Tunnel Monitoring Program (see Table 3)	Low (annual)	Technician	Flow meter, staff gauge, pH/Conductivity probe field probe, CTE-RMPP lab, low-level chloride probe	CTE-RMPP technician and data manager
B	Water Source Protection and Enhancement Planning	Moderate (planning) High (implementation)	Hydrogeologist, sanitation planner, land use planner	Minimal	DINEPA, CTE-RMPP, MARNDR coordination, community and local leader support
	Riviere Froide Monitoring Program	Low (annual)	Hydrologist setup, Technician operation	Same as phase 1 with addition of vehicle	CTE-RMPP technician and data manager
C	Refinement of Tunnel Recharge Area	High (one-time)	Hydrologist / Hydrogeologist	Dye tracing materials and equipment, flow meter, sampling bottles	CTE-RMPP technician, DINEPA approval of dye tracing
	Refinement of Tunnel Recharge and Discharge Dynamics	Moderate or Low if sufficient monitoring has occurred	Hydrologist / Hydrogeologist	Minimal	CTE-RMPP data manager
	Refinement of Tunnel Geology and Structure	Moderate (one-time)	Geologist, geological engineer	Minimal	CTE-RMPP, BME records review
	Rainfall Monitoring and Sampling	Moderate (one-time setup) Low (annual)	Hydrologist setup, Technician operation	Two to three telemetric weather stations with simple sample collection mechanism	CTE-RMPP, MARNDR technician and support

Table 4 – Phased recommendations and resource needs.

Section 5.0 - Conclusions

This study applied discrete datasets to derive an understanding of the tunnel hydrology and hydrogeology. We believe this study is sufficient in characterizing the tunnel on an interim basis from which to inform planning and decision-making with regards to guiding the sustainability and protection of Tunnel Diquini. Disciplined monitoring and the associated temporal datasets are important to advance the understanding and characterization of the tunnel and the Massif de la Selle regional aquifer that supports it. Using the data and findings in this study, the potential exists for source protection and enhancement programs in key zones of the tunnel watershed. Additional studies could also be focused to better understand the interaction between the tunnel and the nearby Riviere Froide. If any hydraulic or significant watershed changes are proposed for the Riviere Froide, we recommend comprehensive studies to evaluate and quantify tunnel impacts.

The Massif de la Selle carbonate aquifer is arguably Haiti's most important aquifer system, as it is responsible for providing a significant proportion of water supply to Port-au-Prince from its large springs with the benefit of gravity and its rivers supply the bulk of recharge to the Plaine du Cul-de-Sac aquifer. Further characterizing and understanding the aquifer as a whole would enable future informed planning and operations to protect and enhance the important resources.

There are many lessons learned from this study and implementation of the tunnel that can help to guide future water supply exploration and water supply development elsewhere in Haiti and in other areas of the Massif de la Selle. It is our opinion that Tunnel Diquini is a favorable case study to warrant the evaluation of other tunneling opportunities in the country that take advantage of the carbonate bedrock geology that benefits from high recharge rates, and the topography that supports gravity-fed water supplies.

Limitations of Investigation

Aspects of the assessment were especially limited by the unavailability of data and resources regarding the Massif de la Selle aquifer. The lack of consistent monitoring and records of discharge, streamflow, and precipitation made it especially challenging to quantify recharge rates and size of the tunnel's aquifer. A focused and basic level of analysis and synthesis was applied throughout the report with the primary objective to provide initial insights into the tunnel dynamics and recommendations for further study.

A limited amount of historical data was available to support this analysis, and this study included a single sampling event which is just a snapshot of a dynamic system. Conclusions in this report are preliminary and presented to aid interim planning and decision-making and to guide any future study and characterization.

This assessment was performed using professional care and skill ordinarily exercised, under similar circumstances, by experienced geologists and hydrogeologists practicing in this or similar locations with very limited sources of data and resources. Changes in analysis and interpretations can and will occur with the acquisition and analysis of new data, such as monitoring reports, water quality data, and tracer and isotope data. Analysis and interpretations presented in this report must be considered fluid and subject to review and revision as additional data is compiled. Analysis and interpretations described in this report may be invalidated wholly or partially by the results of continued data collection and observations.

REFERENCES

Adamson, J.K., Jean-Baptiste, G., and Miner, W.J., 2016, Summary of groundwater resources in Haiti, in Wessel, G.R., and Greenberg, J.K., eds., Geoscience for the Public Good and Global Development: Toward a Sustainable Future: Geological Society of America Special Paper 520, p. 1–22, doi:10.1130/2016.2520(14).

BME [Bureau des Mines et de l'Energie], 1993, Notice Explicative de la Carte Géologique d'Haïti: Port-au-Prince, Bureau des Mines et de l'Energie.

BRGM [Bureau de Recherches Géologiques et Minières], 1988, La Synthèse géologique notamment dans ses parties stratigraphiques et tectoniques: Bureau des Mines et de l'Energie, Port-au-Prince, Haiti.

BRGM [Bureau de Recherches Géologiques et Minières], 1989, Étude des ressources en eau de la région de Port-au-Prince.

Butterlin J., 1960, Géologie générale et régionale de la République d'Haiti [General Regional Geology of the Republic of Haiti]: Institut des Hautes Etudes de l'Amérique Latine, 194 p.

CERCG [Centre d'Etudes et de Réalisations Cartographiques Géographiques], 1989, Carte Géologique de la République D'Haïti [Geologic map of the Republic of Haiti]: Bureau des Mines et de l'Energie, Port-au-Prince, scale 1:250,000, 1 sheet.

Cox, et al, 2011, Géologie de Port-au-Prince. 1:250,000 scale.

Döll, P., and Fiedler, K., 2008, Global-scale modeling of groundwater recharge: Hydrology and Earth Systems Sciences, no. 12, p. 863 – 885.

Gonfiantini and Simonot, 1988, Isotopic Investigation of Groundwater in the Cul-de-Sac Plain, Haiti. International Atomic Energy Agency, IAEA-SM-299/132, Pg 22.

Hijmans, R.J., S.E. Cameron, J.L. Parra, P.G. Jones and A. Jarvis, 2005. Very high resolution interpolated climate surfaces for global land areas. International Journal of Climatology 25: 1965-1978.

LGL, 2011, Actualisation du Schéma Directeur d'Alimentation en Eau Potable de la Région Métropolitaine de Port-au-Prince: PHASE 1 : Collecte des données et Analyse Diagnostic, Rapport no 1.4 Étude des ressources en eau. Pg 151, N/D: SLI 608471, LGL 211374.

Miner, W.J., and Adamson, J. (2017). Modeling the Spatial Distribution of Groundwater Recharge in Haiti using a GIS Approach, Geological Society of America 2017 Annual Meeting, Seattle, Washington, doi: 10.1130/abs/2017AM-297120.

Moliere, E., and Boisson, D., 1993, Coupes Géologiques d'Haiti, in, Notice Explicative de la Carte Géologique : Port-au-Prince, Bureau des Mines et de l'Energie.

Oxfam, 2014, Carte Geologique de Canaan, Jerusalem, Corail et Onanville (CROIX DES BOUQUETs, Haiti), Evaluation technique des menaces naturelles et vulnerabilite de la commune de Croix des Bouquets, Port-au-Prince. 1:10,000 scale.

Pubellier, M. 2000, Plate boundary readjustment in oblique convergence: Example of the Neogene of Hispaniola, Greater Antilles. Tectonics, Vol. 19, No.4, p 630-648.

Scanlon, B.R., Healy, R., and Cook, P.G., 2002, Choosing appropriate techniques for quantifying groundwater recharge: Hydrogeolology Journal, no. 10, p. 18–39.

Suez, 2013, Travaux prioritaires de renforcement de la production d'eau. Pg 178.

Taylor, G.C., and Lemoine, R.C., 1949, Ground water in the Cul-de-Sac Plain, Haiti: U.S. Geological Survey Open-File Report, 59 p.

UNDP [United Nations Development Program], 1990, Carte Hydrogéologique République d'Haiti [Hydrogeologic Map of the Republic of Haiti]: United Nations Development Program, New York, scale 1:250,000, 1 sheet.

United Nations, 1991, République d'Haïti : Programme des Nations Unies pour le Développement : Développement et Gestion des Ressources en Eau. [Government of Haiti and Organization of the United Nations, Department of Technical Cooperation for Development]: Report HAI/86/004, vol. 6.

U.S. National Aeronautics and Space Administration. Hispaniola region, Landsat 8: spectral bands 1 through 7. Product L1T.

Vacher, H.L., and Ayers, J.F., 1980, Hydrology of Small Oceanic Islands – Utility of an estimate of recharge inferred from the chloride concentration of the fresh-water lenses: Journal of Hydrology, vol. 45, p. 21–37.

Waite, H. 1960. Reconnaissance Investigations of Public Water Supplies of Port au Prince and in 12 Villages in the Department du Nord, Haiti. United States Geological Survey.

Woodring, W.P., Brown J.S., and Burbank, W.S., 1924, Geology of the Republic of Haiti. Department of Public Works, Port-au-Prince, Haiti.

World Health Organization, 2011, Guidelines for drinking-water quality, 4th edition: WHO, Geneva, Switzerland.

HYDROGEOLOGICAL INVESTIGATION OF SOURCE MARIANI

Characterization of Hydrology and Guidance for Source Monitoring and Protection

Department Ouest, Republic of Haiti

Final Report
October 2018
Revised March 2020

Note: Additional data collection and research since this study was completed warrants revisiting and updating some of the analysis and findings of this report.

Prepared for:
Inter-American Development Bank & DINEPA

Prepared by:
Northwater International and Rezodlo S.A.

Keywords
Source Mariani, Plaine du Cul-de-Sac; Groundwater; Haiti; Port au Prince; hydrogeology; water supply; Massif de la Selle

Latitude, Longitude
18.535N, 72.427W

Citation
Northwater International and Rezodlo. 2019. Hydrogeological Characterization of Source Mariani: Port-au-Prince, Haiti, Inter-American Development Bank, Technical Report, HA-T1239-P001

Original report in English.

Authors
James K. Adamson, PG
Javan Miner, PE
Pierre-Yves Rochat

Table of Contents

EXECUTIVE SUMMARY **42**

SECTION 1.0 - INTRODUCTION AND PHYSICAL SETTING **44**

SECTION 1.1 – CLIMATE AND LAND COVER 44
SECTION 1.2 – GEOLOGY 45

SECTION 2.0 - METHODS AND RESULTS **46**

SECTION 2.1 – HYDROLOGY 50
SECTION 2.2 – WATER QUALITY AND HYDROCHEMISTRY 53
SECTION 2.3 – STABLE ISOTOPE 56
SECTION 2.4 – GROUNDWATER AGE 57
SECTION 2.5 – AQUIFER STORAGE 58
SECTION 2.6 – GROUNDWATER RECHARGE 58

SECTION 3.0 - DISCUSSION **60**

SECTION 4.0 - RECOMMENDATIONS FOR CONTINUED ACTIVITIES **61**

A – STRENGTHENING ONGOING MONITORING EFFORTS 61
B – WATER SOURCE PROTECTION, ENHANCEMENT AND RIVER MONITORING 63
C – FURTHER HYDROGEOLOGICAL CHARACTERIZATION 63

SECTION 5.0 - CONCLUSIONS **65**

REFERENCES **66**

EXECUTIVE SUMMARY

Source Mariani is currently the most distal source of water that supplies the CTE-RMPP water system. It is the largest naturally flowing spring and the second largest single water source that supplies the Port-au-Prince municipal water system. When the pumping station is in operation, an average of ~19,144 m³/day spring flow can supply ~17% of total municipal production, and 24% of all spring flow supplying metropolitan Port-au-Prince region (CTE-RMPP data 2014-2018). The spring discharges from limestones that drain a portion of the Massif de La Selle carbonate aquifer system, west of the Riviere Froide and north of the Riviere Momance. The objective of this evaluation is to better understand the spring flow characteristics and the origin of the waters to guide future study of the Massif de la Selle aquifer system and to aid CTE-RMPP in water use planning, development, monitoring, and protection.

This investigation was accomplished by a combination of literature and data review, satellite and topographic imagery analysis, and field reconnaissance. A brief field mission to the spring was conducted in April 2019 which included: (i) physical and chemical sampling, (ii) stable isotope sampling, (iii) chlorofluorocarbon (CFC) and sulfur hexafluoride (SF6) sampling, and (iv) visual observation of local geology. A follow-up visit to the spring was conducted in January 2020 to verify more recent flow monitoring data received from CTE-RMPP.

Based on the study, the key results and conclusions are summarized below:

Spatial Distribution of Groundwater Recharge

1. The groundwater recharge area that contributes to the spring flow appears to be approximately 15 km² but may be as large as 34 km².

a. This uncertainty in the recharge area is due to the large effect that annual fluctuations in precipitation volume and intensity have on the recharge rates.

a. The average recharge elevation is estimated at 580 m above mean sea level with a corresponding temperature of 22.7 C. This suggests the possibility that some spring flow may originate from distal zones in the regional carbonate aquifer such as within the Riviere Momance basin.

Groundwater Budget

1. The long-term average annual recharge rate is estimated at 38% of annual precipitation. During high intensity rainfall periods, the recharge rates may approach 50%, while during normal or low precipitation periods the recharge could be approximately 15%.

2. Aquifer storage relative to the spring is estimated between 155 and 259 million m³.

3. The limestone karst aquifer that feeds the spring is well mixed and has an average groundwater age of between 21 and 35 years based on a single sampling event.

Flow Characteristics

1. Recharge to the regional aquifer appears to be largely affected by high intensity and high-volume rainfall events such as hurricanes and tropical storms. There appears to be a 3-to-7-year cycle of recharge trends partially influenced by El Niño and La Niña events.

2. Spring discharge displays mild seasonal variability with monthly average flows typically ranging between 14,500 and 25,000 m³/d with an average of 19,500 m³/d.

a. Instantaneous (daily) flows display greater variability, ranging from 7,600 to 30,700 m³/d.

b. Based on the spring catchment infrastructure as observed in 2019, total spring flow is measured from a single water meter. However, this method does not account for

overflow. As a result, some high spring flows could be underreported.

3. The spring flow is most vulnerable to extended periods of average or below average precipitation and consecutive years without high intensity rainfall periods such as tropical storms and hurricanes.

a. This recharge characteristic combined with the recent flow regression that extends from 2014 to 2019 may foster perceptions that the spring flow has been decreasing over the long-term or that acute impacts have occurred.

b. Limited historical data from between 1925 and 1933 suggests that average spring discharge remains relatively stable or perhaps has even increased due to increased precipitation intensity.

4. The cyclic and multi-annual recharge characteristics of the regional carbonate aquifer are important for water managers and planners to understand and utilize in balancing the different water sources of CTE-RMPP.

Connection to Regional Groundwater and Surface Water

1. Source Mariani flows from the regional Massif de la Selle carbonate aquifer.

a. The regional aquifer also supplies many of CTE-RMPP major springs, Tunnel Diquini, and provides base flow to river systems.

b. Monitoring is required to better understand the complex hydraulic relationships between these major outlets of the aquifer.

c. Source Mariani is the lowest elevation terrestrial outlet known for the aquifer and appears to emanate from a topographic exposure of the main aquifer lithology rather than as a contact spring. This may act to sustain flows even when higher elevation springs exhibit reduced flows.

d. Source Mariani essentially serves as a drain for the western portion of the Massif de la Selle aquifer.

2. Source Mariani does not appear to have a significant hydraulic connection to the Riviere Momance or Riviere Froide. This is supported by the isotope and tracer sampling and analysis of recharge catchment size.

Aquifer Vulnerability

1. Due to the high permeability and rapid infiltration rates typical in karst limestone environments, the spring waters have high vulnerability to contamination. This is confirmed by the elevated nitrate levels consistently measured in spring discharge.

2. Urbanization and land use changes in the hills south of the spring are considered the greatest risk to groundwater quality and flow. The lack of centralized waste management and sanitation, combined with the karst hydrogeology, significantly increases the risk of direct contamination of the aquifer waters.

a. Land use planning, zoning, and managed development of the area south of the spring in an area larger than the existing spring protection perimeter is necessary in order to protect the spring water from future water quality and flow impacts.

Conclusions and Recommendations

This study provides a preliminary basis from which to inform planning and decision-making with regards to the sustainability and protection of Source Mariani, so it continues to be an important water supply into the future. Recommendations are provided at the end of the report regarding water source protection, compilation of historical data, and monitoring the climate, flow, and water quality. Significant increases in study efficiency would be gained by combining the recommendations of this study with those of the Tunnel Diquini characterization (Northwater International and Rezodlo 2018).

SECTION 1.0 - Introduction and Physical Setting

This study is part of a coordinated effort to better understand the existing and potential water supplies that serve the metropolitan area of Port-au-Prince. Its intent is to characterize the hydrology of Source Mariani waters and better understand the origin and characteristics of its flow.

Source Mariani is currently the most distal source of water that supplies the CTE-RMPP water system. It is the largest naturally flowing spring and second largest single water source for the Port-au-Prince municipal water system. When the pumping station is in operation, Source Mariani accounts for approximately 12% of the total municipal production, and 15% of all the spring flow supplying metropolitan Port-au-Prince region (based on 2014 data). The spring discharges from limestones that drain a portion of the Massif de La Selle carbonate aquifer system, west of the Riviere Froide and north of the Riviere Momance.

The Source Mariani catchment ranges from the outlet at 24 m to over 650 m in the karst plateau north of the Riviere Momance. The spring catchment infrastructure was reportedly constructed in 1992, although recent improvements have been made to the overflow, pumping and power stations, and supply line up to the reservoir. A spring protection area approximately 4.5-hectares in size has been fenced and reforested around the spring and corridor up to the reservoir. The catchment is a broad concrete structure with block perforations to allow inflow from the colluvial deposits that transmit the groundwater to the surface.

Section 1.1 - Climate and Land Cover

Average annual rainfall ranges from 1,300 mm/year near the spring to 1,700 mm/year in the upper reaches of the Riviere Froide watershed. Based on data from the Petion-ville meteorological station (UHM, 2018), two distinct rainy seasons occur in the catchment, the first peaking in May and the second in September/October (Figure 1). Precipitation varies from year to year, with periods of intense rainfall and hurricanes spaced between periods of relative drought. These cycles appear to occur on 3-to-7-year rotations linked to El Niño and La Niña events. A slight increase in annual precipitation is apparent in data from 1980 to 2016 for the Petion-ville station (Figure 1). Recently, unusually high rainfall and intense hurricane seasons between 2007 and 2010 were followed by decreased precipitation from 2011 to 2016.

Land cover in the catchment is variable, with steeper slopes tending to be covered with scrub, and flatter areas used for subsistence agriculture and sporadic forest. Woodring (1924) described the watershed area as primarily scrub vegetation, indicating the possibility that land cover has not changed considerably in the southerly hills over the last 100 years. Given this, perhaps the hydrology of the area had adjusted to deforested conditions when spring flow measurements were first collected in the 1920s and 1930s.

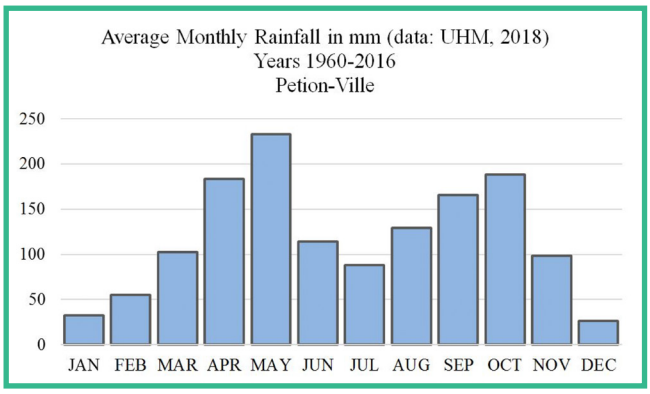

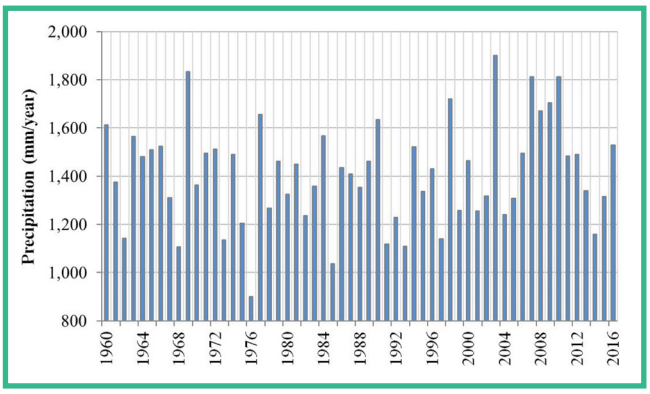

Figure 1. Average Monthly Precipitation at Petion-ville UHM Station and Annual Precipitation from 1980 to 2016.

Section 1.2 – Geology

The geology of the spring catchment is composed of carbonates that range from lower Miocene to middle Eocene age. The spring outlet is primarily surrounded to the west, south and east by weathered Eocene age marl and chalky limestone with relatively low permeability. More recent colluvial deposits cover the bedrock formations north of the spring. Several outcrops of hard limestone were observed along the south and southeastern side of the spring and are interpreted to be middle to upper Eocene age, indicating that the spring result from a topographic intersection with the piezometric surface associated with regional limestones that are hydraulically connected through faults and fractures to the recharge areas within the Massif de la Selle. Source Mariani is the lowest elevation terrestrial outlet known for the Massif de la Selle aquifer. The geologic and topographic intersection may be a key explanation for the consistently high flow rates of the spring, which serves as a 'drain' for a large portion of the aquifer.

To the south of the spring outlet, approximately 9.8 km² (65%) of the 15.2 km² catchment is composed of hard, bedded limestones of upper to middle Eocene age. Regional folding has created a triangular wedge which widens westward and is composed of detrital limestones of lower Miocene age. These limestones transgress into the marls and chalks of the upper Eocene formations (Figure 2). The southern portion of the catchment appears to be altered by a high degree of karst weathering at elevations between 400 and 600m. These karst features likely promote high infiltration and recharge rates through the upper to middle Eocene limestones into the regional carbonate aquifer.

Figure 2 displays the geology of the interpreted spring catchment and associated watersheds based on the adaptation of various sources of data (CERCG 1989, Eptisa 2015, Pubellier 2000 and Cox et al 2011).

Photos 1 and 2. Detrital limestone, chalk and marl of lower Miocene or upper Eocene age, outcrops to west and south of spring.

Photos 3 and 4. Hard micritic, well bedded limestone of middle to upper Eocene age, outcrops on southeast side of spring and in majority of catchment.

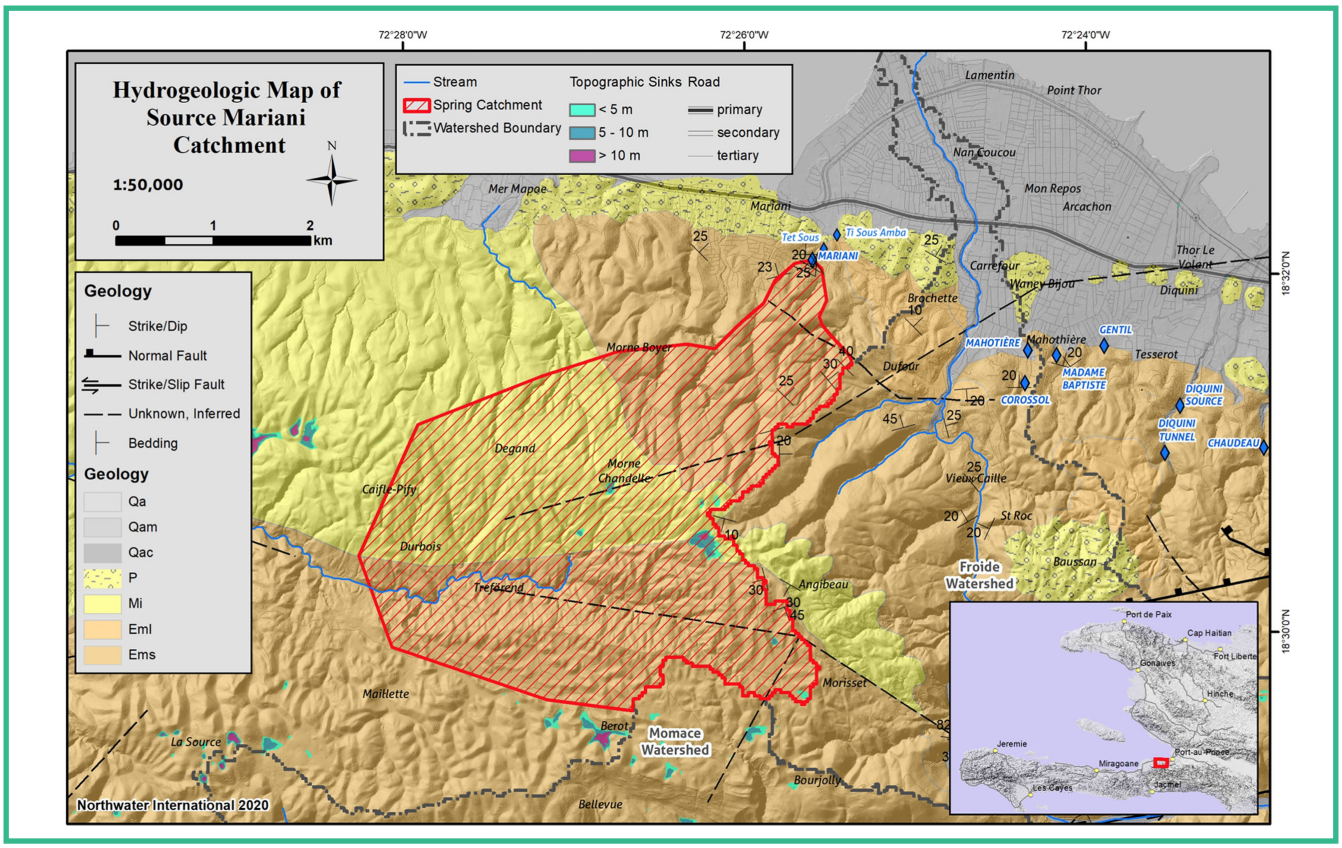

Figure 2. Geologic Map of Interpreted Spring Catchment and Associated Watersheds.

Section 2.0 - Methods and Results

Two brief field visits to the spring were conducted as a part of this study. The first was conducted on April 2, 2019 and included: i) physical and chemical sampling, ii) stable isotope sampling, iii) chlorofluorocarbon (CFC) and sulfur hexafluoride (SF6) sampling and, iv) visual observation of local geology. The second visit was conducted on January 16, 2020 and included: i) spring flow rate measurement, ii) review of CTE-RMPP flow meter readings, and iii) visits to two nearby springs. All activities at the spring were performed under the supervision of Jean Jimmy Cyndigue or Ing. Pierre Colon Geffrard of CTE-RMPP.

Most flow data for this report is derived from a totalizing flow meter between the spring and the pumping station. The reading on this meter is documented monthly by CTE-RMPP technicians. The flow meter measures all the flow diverted to the pumping station. Unfortunately, during periods of high discharge, the overflow from the spring catchment is not monitored, so high flows may not be accurately recorded. The January 16, 2020, flow measurement was taken in a canal downgradient of the pumping station that receives the flow when the pumping station is not in operation.

The field team was allowed to enter the spring catchment to visually inspect the construction and nature of the water seepage during the April 2, 2019, visit. A layer of silt and fine sand with some gravel was noted to cover most of the catchment floor. According to CTE staff, the catchment floor is cleaned twice per year. A washout portal was observed, although internal concrete dividers may limit its functionality. The overflow portal flows from the catchment into a rock and concrete-lined open channel and is diverted to surface drainage below the pumping station. Groundwater flow into the catchment is achieved via offsetting gaps in the bottom four layers of concrete block along the south and southwest corners of the catchment. Colluvial

gravel and cobble deposits were visible through the gaps, along with extensive roots that likely originated from trees surrounding the catchment. These roots are reportedly cut during the bi-annual maintenance. CTE staff noted that, after cleaning, an increase in flow occurs. However, this may reflect temporary adjustments to the hydraulic gradient due to lowering of the catchment floor after sediment removal.

Water sampling was undertaken in the spring catchment, adjacent to the gaps in the blocks where groundwater seepage occurs. A 12V sampling pump with flexible tygon tubing was used to collect low-flow samples. Samples for physical, chemical and stable isotope analysis were collected by filling laboratory prepared sample bottles. Chlorofluorocarbons (CFCs) and sulfur hexafluoride (SF6) were collected as a means to age-date the groundwater discharging from the spring. Samples for CFC-11, CFC-12 and CFC-113 were collected using the glass bottle method with copper tubing as described by USGS and the Reston chlorofluorocarbon laboratory. Samples for SF6 were collected using 1 Liter amber plastic-coated safety glass bottles with polyseal cone-lined caps, also employing methodologies developed by the USGS and University of Utah Noble Gas Lab. All sampling bottles and excess air tubes for CFCs and SF6 were provided by the Dissolved and Noble Gas Lab at the University of Utah. Samples for excess air analysis were also collected in ¼-inch copper tubes with clamps; these samples support correction of the SF6 data. Upon completion of sampling, all samples were wrapped in insulating materials and transported to the US for shipment to the respective laboratories.

Two additional springs were visited on 16 January 2020 to aid in the characterization of the local and regional hydrology. The springs are locally known as Tet Sous and Ti Sous Amba and had a combined flow of approximately 58 L/s which seep from the semi-consolidated Pliocene formations that overlie the limestone. It is possible that portions of these flows are return flows from Source Mariani.

Photo 5. Panoramic view of spring catchment.

Photo 6. Panoramic view of inside spring catchment, outlet to distribution at bottom right.

Photo 7. West outlet to pumping. station.

Photo 8. East outlet to pumping station.

Photo 9. Inside view, overflow portal to surface drainage.

Photo 10. Outside view, overflow portal to surface drainage.

Photo 11. Historical washout portal.

Photo 12. Flow in downstream canal when pump station not in operation.

Photo 13. Sampling in April 2019.

Photo 14. Totalizing flow meter measuring spring flow to pumping station.

Photo 15. Roots entering the spring catchment.

Photo 16. Clean-up in progress to remove fallen debris from slope above catchment.

Photo 17. Pumping station.

Photo 18. Overflow and drainage canals leading from catchment.

Photo 19. Source Ti Sous Amba.

Photo 20. Flow measurement, Source Tet Sous.

Photo 21. Source Tet Sous.

Section 2.1 – Hydrology

Spring flow varies based on the intensity and duration of recharge events and the transit time through the aquifer. A discontinuous flow dataset was compiled from CTE-RMPP and Eptisa (2015) spanning intermittently between October 2008 and July 2019. The data was primarily provided by Ing. Pierre Colon Geffrard of CTE-RMPP. Flow measurements were provided as average monthly flow data by CTE and as discrete measurements by Eptisa. Mr. Jean Jimmy Cyndigue of CTE-RMPP continues to record monthly flow on the totalizing flow meter between the spring and pumping station and at a meter between the pumping station and the reservoir. Some inconsistency and confusion are apparent regarding some of the historical data, as several measurements indicate the spring overflow, but not the total flow, and the current flow meter does not measure overflow events.

Seven older discrete discharge measurements were documented for the spring from 1925 to 1933 (Direction Generale des Travaux Publics, 1918 - 1938), ranging from 170 L/s to 280 L/s with an average of 217 L/s. The recent discharge data ranges from 88 L/s to 355 L/s with an average of 225 L/s. This indicates that spring discharge trends may not have varied substantially in the past ninety years. While a long-term trend of decreasing discharge is not supported by the data, a short-term trend of decreasing discharge is apparent between 2009 and 2015. Average spring discharge was 288 L/s in the 2008 – 2009 data and only 217 L/s in the 2014 – 2019 data. This recent trend is believed to be the result of adjustments to the 2007 – 2008 period, when unusually high and intense precipitation occurred (Figure 3).

Based on the available data and a previous study of nearby Tunnel Diquini (Northwater International and Rezodlo. 2018), recharge to the regional aquifer and to the spring appears to be largely affected by high intensity and high-volume rainfall events such as hurricanes and tropical storms. There appears to be a 3-to-7-year cycle of recharge trends partially

influenced by El Niño and La Niña events (figure 3). Conversely, extended periods of declining flow rates occur during drought, El Niño or normal years. Figure 3 shows discharge data from 2008 to 2019 for both Source Mariani and Tunnel Diquini, along with annual average precipitation as measured in Petion-ville. A similar trend is apparent between Source Mariani and Tunnel Diquini that parallels the annual precipitation curve, lending evidence to the hypothesis that aquifer discharge rates are highly linked to years of increased precipitation intensity and volume. The high variability in flow rates in 2014 could result from the difference between average monthly flows and instantaneous flows. The variability may also be affected by the partial capture of flow prior to catchment and pumping station rehabilitation.

Insufficient data was available to establish clear long-term trends in spring flow. The common understanding is that the spring flow rates have been decreasing through time, however, this trend is only apparent in the short term due to the above mentioned El Niño and La Niña cycles. Comparison of flow between the 1920s and 1930s and recent data suggest remarkably stable average discharge and hint at the possibility of increasing flow. Figure 4 shows average monthly discharge for the 2008 to 2019 data compared to monthly averages for the 1925 to 1933 data. Further study of these long-term and cyclic flow dynamics of Source Mariani, Tunnel Diquini and other major Port-au-Prince springs would provide valuable insights for water management and planning. It is also worth noting that a combined additional flow of 58 L/s was measured from Source Tet Sous and Source Ti Sous Amba downgradient of Source Mariani. The similarity in field water quality between these springs and Source Mariani may indicate that they are connected to the regional aquifer, or that their flow is actually recirculated waters form Source Mariani.

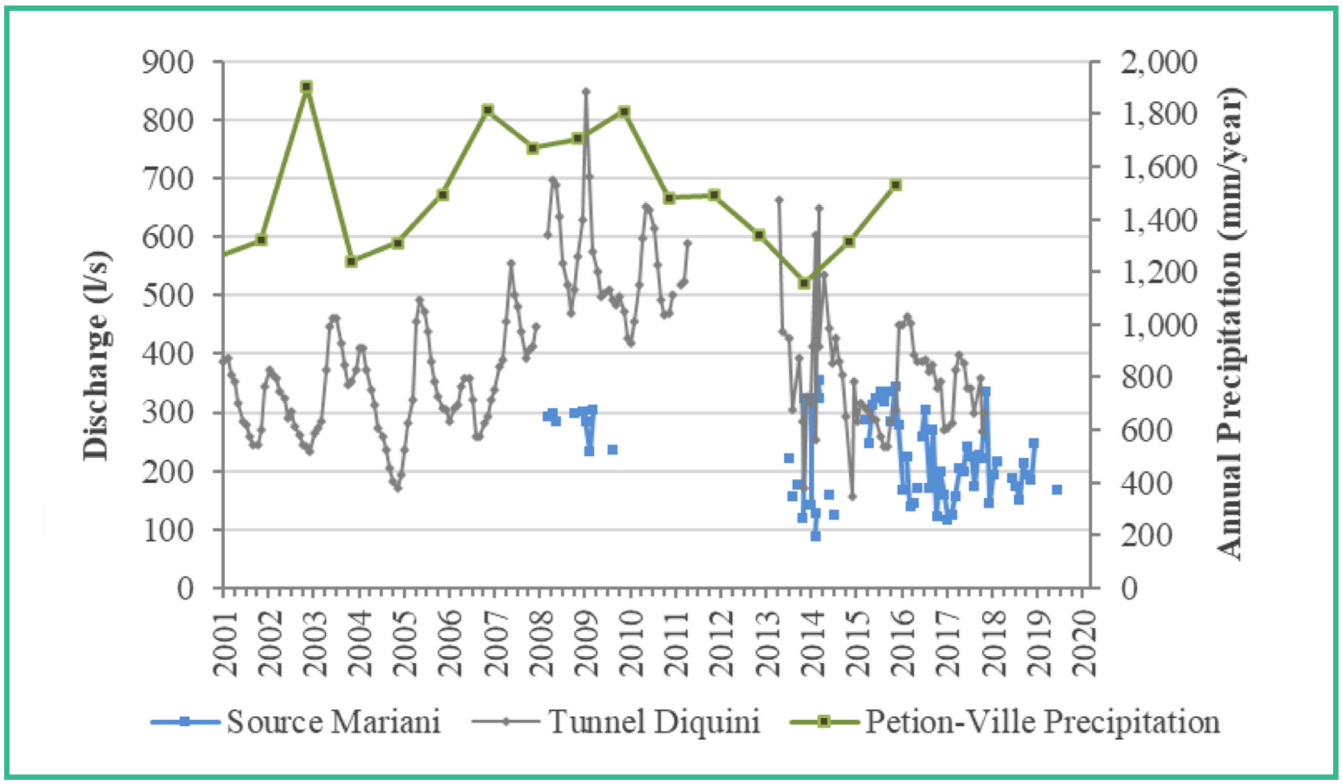

Figure 3 - Source Mariani and Tunnel Diquini flow with annual precipitation at Petion-ville Station, 2007 - 2016.

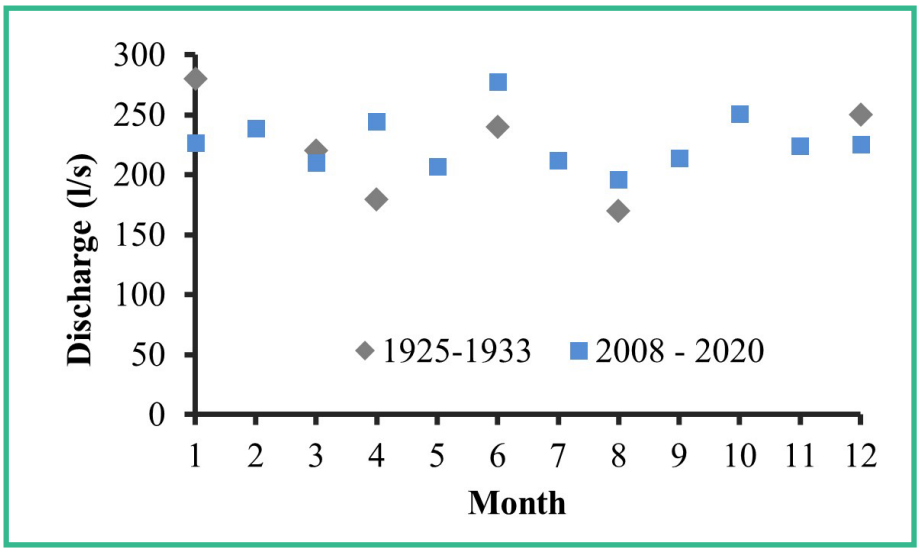

Figure 4- Source Mariani average monthly discharge, historical comparison.

Spring	Latitude (dd)	Longitude (dd)	Elevation (m)	Average Discharge (L/s)	Percent RMPP Spring Flow (%)
CARREFOUR-FEUILLES	18.52211	-72.33881	103.2	76.7	6%
CHAUDEAU	18.51719	-72.38315	125.6	47.4	3%
COROSSOL	18.52349	-72.40638	123.2	55.3	4%
DESPLUMES	18.50099	-72.28644	518.8	12.3	1%
DIQUINI SOURCE	18.52120	-72.39130	84.5	37.7	3%
DIQUINI TUNNEL	18.51680	-72.39285	136.0	432.4	31%
DOCO	18.50966	-72.25284	360.0	13.4	1%
FRERE	18.51684	-72.25465	228.8	78.0	6%
LECLERC	18.52361	-72.36055	91.1	28.2	2%
MADAME BAPTISTE	18.52604	-72.40326	77.6	68.5	5%
MAHOTIERE	18.52656	-72.40609	86.5	110.7	8%
MARIANI	18.53525	-72.42699	24.4	225	16%
METIVIER	18.50717	-72.24198	406.0	22.0	2%
MILLET	18.48277	-72.28716	906.8	16.9	1%
PLAISANCE	18.51746	-72.29767	271.5	54.3	4%
TETE DE LAU	18.50228	-72.28631	481.3	37.1	3%
TURGEAU	18.52473	-72.31933	195.4	73.3	5%

Note: for comparative purposes, only average monthly discharges provided by CTE-RMPP were used in this table; the average discharge and percentage of total for Source Mariani and Tunnel Diquini are slightly different than reported elsewhere. Most discharge data is from 2010, 2011 and 2014.

Table 1 - Springs of the Massif de la Selle used by CTE-RMPP.

Section 2.2 - Water Quality and Hydrochemistry

Source Mariani is considered to have good physical and chemical quality as a drinking water supply. Its groundwater is fairly dilute (240 mg/l total dissolved solids), and it is a $CaHCO_3$ type, which is characteristic of a limestone aquife. Nitrate was the only potential parameter of concern from the April 2019 sampling event (8.4 mg/l as NO_3). Monitoring by CTE-RMPP from 2008 to 2016 similarly reported slightly elevated nitrate concentrations with an average of 12.5 mg/l (as NO_3) which is below USEPA (10 mg/l as NO_3-N), WHO (50 mg/l as NO_3) and DINEPA (50 mg/l as NO_3) potable water guidelines (Table 2). Biological sampling and analysis was not performed as a part of this study.

The total organic carbon (TOC) measurement of 3.4 mg/l is slightly higher than the typical for groundwater, possibly indicating surficial contamination. There was also a measurable concentration of barium at 0.174 mg/l. Barium occurs in the open ocean at a concentration of 0.05 mg/l, and it is a group two element, the same as calcium. Barium substitutes for calcium during limestone formation, and when the limestone dissolves barium, it ends in the groundwater. Other trace metals were below detection limits, indicating a low likelihood of current industrial or commercial contamination.

Due to the nature of the aquifer, the spring is susceptible to surficial contamination within the recharge areas, especially near the outlet, as evidenced by the nitrate and TOC data. Further study concerning the aquifer and spring hydrology would help locate the primary recharge areas and locations where the aquifer is most vulnerable to contamination due to increased conduit flow and concentrated recharge. Table 2 provides the water quality and hydrochemistry data available from previous studies and the April 2, 2019, sampling event.

Water quality monitoring data provided by CTE-RMPP allows for analysis of several parameters on a monthly and annual basis.

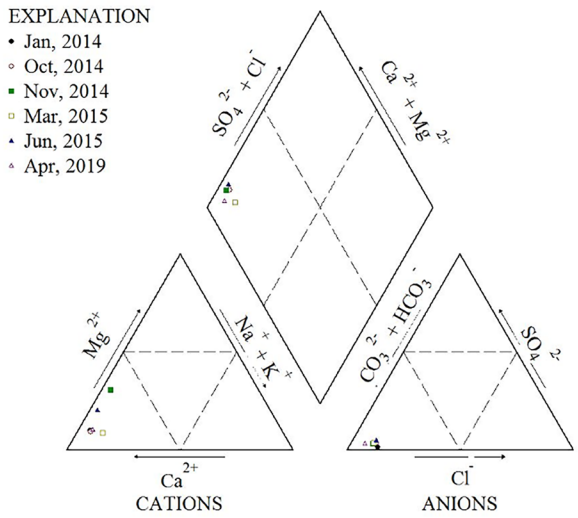

Figure 10 - Piper diagram of Source Mariani Waters.

Trends in monthly groundwater conductivity (Figure 6) and chloride (Figure 7) illustrate a several month lag-time between the onset of the rainy season (April and September) and the corresponding decrease in dissolved solids. The relatively small variation in conductivity indicates that the aquifer is generally well mixed. Seasonal variations in chloride are intriguing and may point to the variations in recharge rate throughout the year, with higher recharge rates occurring during months with high rainfall as it is typical of karst aquifers. Both conductivity and chloride show an increasing trend from the 2008-2009 data through the end of 2016, the same period during which spring discharge was generally decreasing. Plotting conductivity and chloride relative to measured spring discharge confirms this trend (Figure 8). The increased conductivity and chloride, and decreased flow, result from lower recharge and slower groundwater flow during decreased annual precipitation and rainfall intensity. This trend may be associated with the multi-year flow and recharge cycles mentioned in Section 2.1. Current conditions are likely more indicative of typical flow and water quality, whereas the 2008-2009 data is more indicative of increased recharge and flow conditions.

Conversely, both turbidity and nitrate increase with the flow rate. This result is not unexpected, since surficial contamination

occurs most during periods of high rainfall and runoff. Turbidity and nitrate do not appear to be correlated (Figure 8), possibly indicating different sources. Some of the highest turbidity measurements happened shortly after the intense 2007-2008 hurricane season, while peaks in nitrate occur more frequently as urbanization near the spring has increased. Turbidity may be in part due to aquifer hydrology and karst muds, while nitrate appears more anthropogenic in origin. Mobilization of the sediment build-up in the floor of the catchment is also likely a source of high turbidity during larger flow periods.

Parameter	Units	DINEPA Standard	WHO Guidelines	USEPA MCL	USEPA Secondary MCL	Source Mariani 18.535 -72.427			
Date Collected						23-Mar-15	29-Jun-15	6-Aug-16	2-Apr-19
Alkalinity, Total (CaCO3)	mg/l	500	--	--	--	200	200		**190**
Bicarbonate (CaCO3)	mg/l	--	--	--	--	244	244		**232**
Chloride	mg/l	250	250	--	250	17	18	18.5	**9.7**
Conductivity	umhos/cm	--	--	--	--	420	406	390	**400**
Fluoride	mg/l	2	1.5	4	--				**0.4**
Ammonia (N)	mg/l	--	--	--	--		0.12	0.03	< 0.045
Nitrite (NO2)	mg/l	3	3	1	--				**0.1**
Nitrate (NO3)	mg/l	50	50	--	--	10.6	11.1	9.7	**8.4**
Nitrate (NO3-N)	mg/l	--	--	10	--				**1.9**
pH @ 25°C	Units	--	--	--	--	7.5	7.7	7.6	**7.8**
Sulfate	mg/l	250	500	--	250	8	11	4	**5.9**
Silica (SiO2)	mg/l	--	--	--	--				**20.2**
TOC	mg/l	--	--	--	--				**3.4**
Antimony	mg/l	--	0.02	0.006	--				< 0.00037
Arsenic	mg/l	--	0.01	0.01	--				< 0.0076
Barium	mg/l	--	0.7	2	--				**0.174**
Beryllium	mg/l	--	--	0.004	--				< 0.00016
Cadmium	mg/l	--	0.003	0.005	--				< 0.00036
Calcium	mg/l	100	--	--	--	75.3	139.34	72.1	**73.2**
Chromium	mg/l	--	0.05	0.1	--		0.016	0.01	< 0.0014
Copper	mg/l	1	2	1.3	--		1.84	0.88	0.00518
Iron	mg/l	0.2	--	--	0.3	0.03	0.08	0.12	**0.052**
Lead	mg/l	0.01	0.01	0.015	--				< 0.0031
Magnesium	mg/l	100	--	--	--	4.86	22.34		**5.39**
Manganese	mg/l	--	0.5	--	0.05	0.001		0.141	**0.00404**
Potassium	mg/l	--	--	--	--	0.9	1.5	1.4	**0.796**
Silver	mg/l	--	--	--	0.1				< 0.0019
Sodium	mg/l	--	--	--	--	12.13	6.82	6.11	**5.91**
Thallium	mg/l	--	--	0.002	--				< 0.00011
Zinc	mg/l	3	--	--	5				< 0.0044
Total Hardness (CaCO3)	mg/l	300	--	--	--	188	348	180	**180**
Mercury	mg/l	--	0.0005	0.002	--				< 0.00015
Total Dissolved Solids	mg/l	600	1000	--	500		197.3	187.7	**240**

Note: 2015 and 2016 data provided by CTE-RMPP

Table 2. Hydrochemical Analyses of Source Mariani Waters.

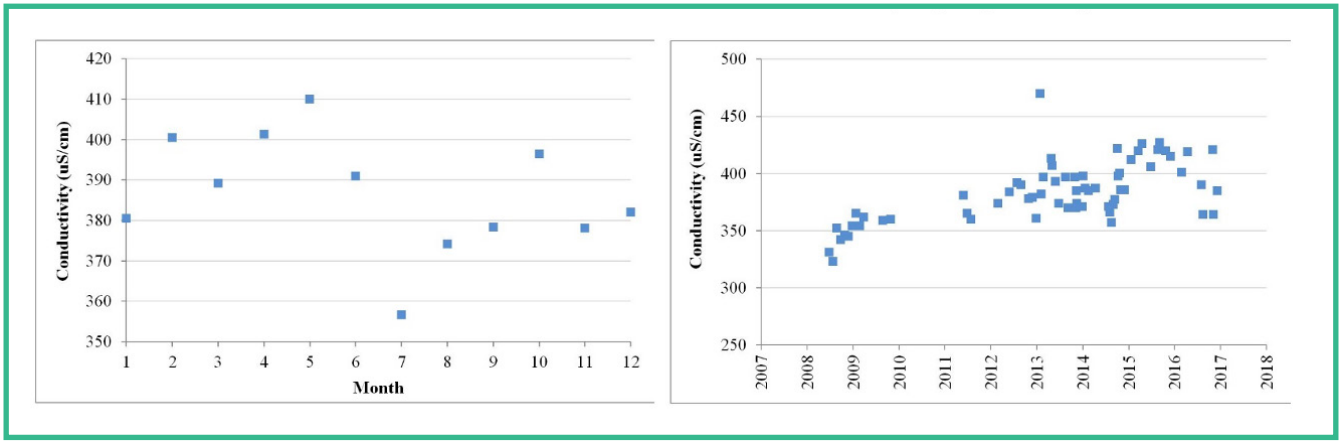

Figure 6. (left) Average monthly spring conductivity, (right) spring water conductivity time-series (data: CTE-RMPP).

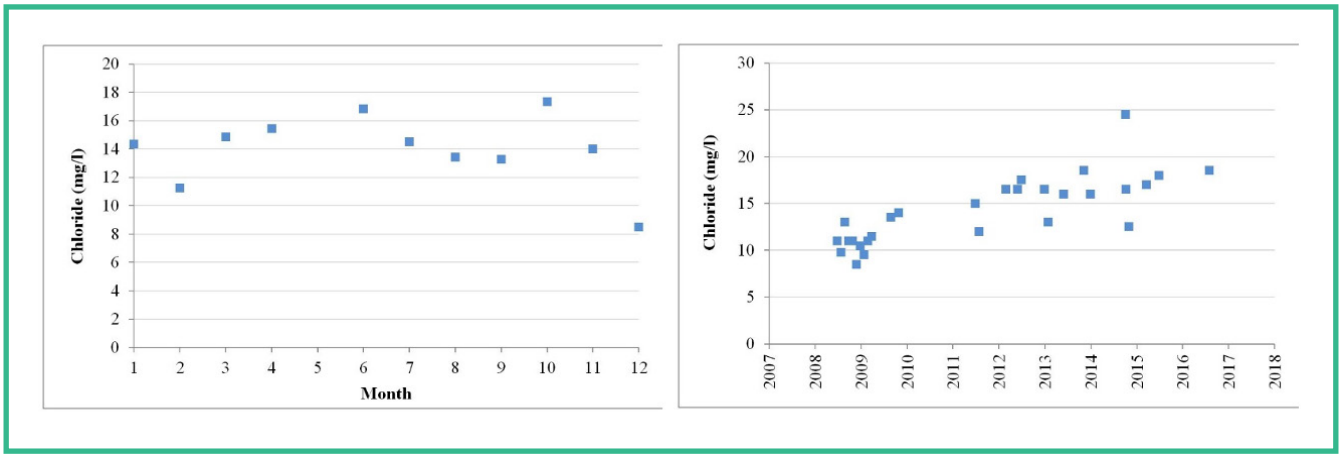

Figure 7. (left) Average monthly spring chloride, (right) spring water chloride time-series (data: CTE-RMPP).

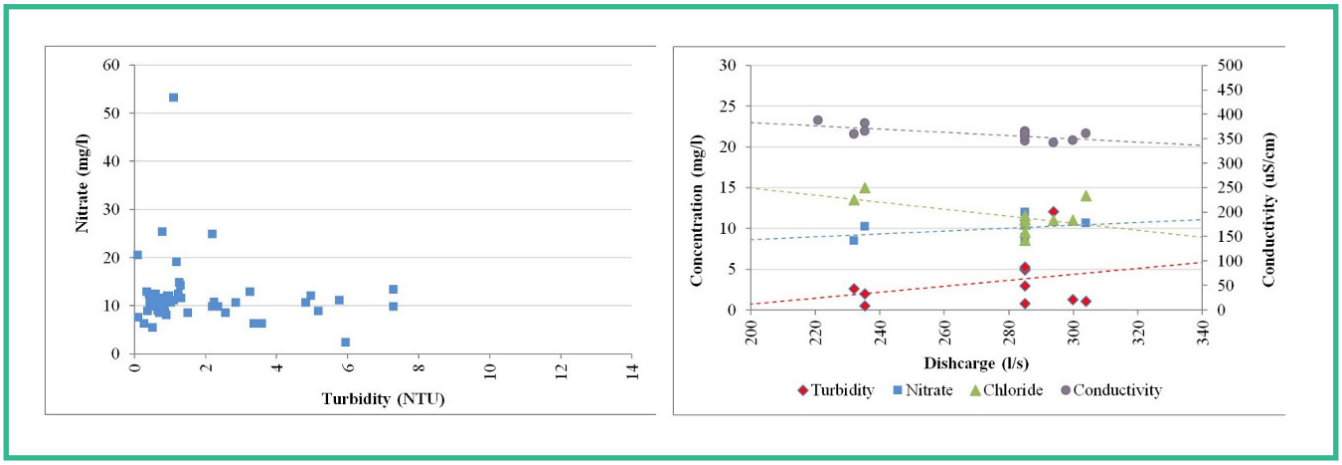

Figure 8. (left) Spring water turbidity vs. nitrate, (right) spring discharge vs conductivity, chloride, nitrate and turbidity (data: CTE-RMPP).

Section 2.3 – Stable Isotope

Stable isotopes of oxygen ($\delta^{18}O$) and hydrogen (δD) were sampled to aid in evaluating recharge dynamics. Gonfiantini and Simonot (1988) observed a linear trajectory of $\delta^{18}O$ versus elevation from samples collected south of Port-au-Prince (Figure 9). They found that there is a -0.9 per mil change for every 1,000 meters of elevation gain for water points on the plain, and estimated a slope of -1.4 per mil change for every 1,000 meters of elevation for the springs south of Port-au-Prince. This linear trajectory can be applied to Source Mariani, as it was one of the originally sampled points in 1987 and has similar characteristics to the springs in the area (Figure 10).

The stable isotope composition of the sample collected in April 2019 was $\delta^{18}O$ = -3.19 per mil and δD = -14 per mil, while Gonfiantini and Simonot (1988) measured the groundwater discharging from the spring in the 1980s and their results were $\delta^{18}O$ = -3.21 per mil and δD = -14 per mil. These results are essentially the same, since the analytical uncertainty in the measurement is ±0.1 $\delta^{18}O$, and ±1 δD. The aquifer water has essentially the same isotopic composition over the past 32 years, which implies that the aquifer is well mixed before it emerges from the spring.

Applying the $\delta^{18}O$ value to the -0.9 and -1.4 per mil/1000-meter regression slopes, the likely minimum recharge elevation is 100 meters above sea level, and the average recharge elevation is 580 m above sea level. This estimated average recharge elevation is near the high end of the elevations found within the 15.2 km² recharge catchment, suggesting the possibility that some recharge would be derived from farther distances and at higher elevations in the Massif de la Selle aquifer. This possibility is coherent with an analysis of recharge temperature based on noble gas sampling. Annual average temperatures in the catchment at 580 m elevation are in the range of 23˚ C to 25˚ C, which is slightly above the average recharge temperature calculated for the CFC and SF6 analysis of 22.7˚ C. Lower temperatures in the range of 20˚ C to 23˚ C are found south of the probable recharge catchment, in the Riviere Momance watershed. This suggests that the Source Mariani aquifer is connected to the greater Massif de la Selle aquifer that supplies base flow to the Riviere Momance and Riviere Froide. However, this does not suggest that Source Mariani receives recharge from the Riviere Momance flows, which would likely occur in a warmer recharge temperature due to warming of the surface flow. Given that both Source Mariani and Riviere Momance derive a substantial portion of base flow from the Massif de la Selle aquifer, up gradient changes to the hydrology or recharge potential may alter flow rates in both waters.

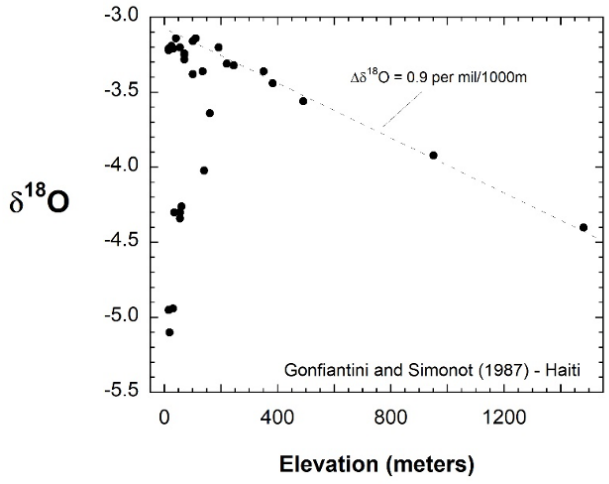

Figure 9 – Oxygen-18 versus elevation in groundwater near Plaine du Cul-de-Sac.

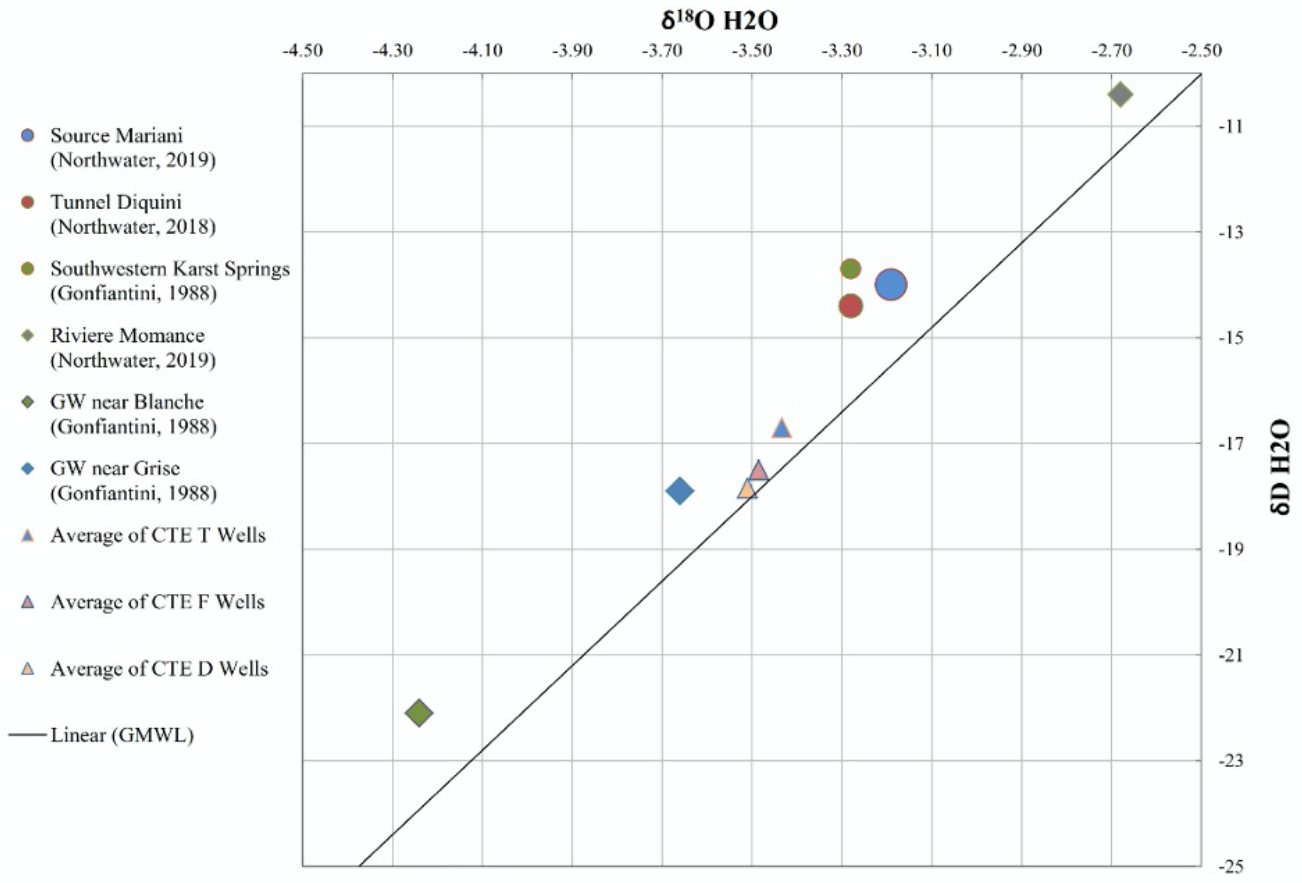

Figure 10 – Stable Isotope Data Plotted with Global Meteoric Water Line (GMWL).

Section 2.4 – Groundwater Age

Chlorofluorocarbons (CFCs) and sulfur hexafluoride (SF6) were collected as a means to age-date the groundwater. These estimates are based on CFCs and SF6 accumulating in air during the 20th century, measuring their solubility in water and extrapolating back to the atmosphere (Appendix B). Both methods require assumption or measurement of other parameters. For CFCs the primary adjustable parameter is the recharge temperature, which affects solubility of the CFCs. For SF6 the primary adjustable parameters are excess air, recharge temperature, and recharge elevation. For both analyses, the recharge temperature was set at 22.7 C based on the noble gas analysis. For SF6 the recharge elevation was set at 580 m and the excess air at 1.5 cc/l based on the laboratory results. Only CFC-113 and the SF6 results were within useable limits. The CFC calculated recharge age date was 1984, indicating the water is 35 years old. The calculated recharge date for the SF6 was 1998, indicating the water is 21 years old. It is not uncommon for these two age-dating methods to reach slightly different results (the older the water, the greater the discrepancy). Averaging these results, we can assume a groundwater age for the spring of 28 years. This result is similar to that measured for Tunnel Diquini, which also flows from the same aquifer. Further sampling of CFC's and SF6 during higher flow and lower flow events could further help illuminate the recharge dynamics of the aquifer.

Section 2.5 – Aquifer Storage

With the available data, a planning level estimate of storage in the aquifer can be made. Recognizing that the isotope data from 1988 and 2019 indicate the aquifer is well mixed, meaning dispersion is high in the aquifer porous structure, then the annual output of the spring multiplied by the age of the groundwater equates to a qualitative storage estimate. Using the calculated average annual discharge from 2008 to 2016 of 7.4 million m^3/year, this method estimates between 155 and 259 million m^3 of storage. This estimate is approximate; refinements are expected with further analysis of discharge and sampling data and tracer tests.

Section 2.6 – Groundwater Recharge

The groundwater recharge rates associated with the spring discharge were estimated using the chloride mass balance method and a custom GIS-based direct recharge model developed by Miner and Adamson (2017). Twenty-nine chloride measurements for the spring waters (Table 3) and 12 rainfall chloride samples from the Massif de la Selle (Table 4) were available for the mass balance. The average chloride values for rainfall and spring water are 5.5 mg/l and 14.4 mg/l respectively for all available years. However, the average chloride of spring water during the high flow period from 2008 through 2009 was only 11.2 mg/l, while the average for the normal flow years between 2011 and 2016 was 16.7 mg/l. Based on these ranges of spring water chloride, recharge rates may vary between 33% and 49% of annual precipitation, with an average recharge rate of 38%. This equates to 600 mm of recharge from the 1,580 mm/year of rainfall in the recharge area. The combination of the low and average recharge rate with the average annual spring discharge shows that the recharge area of the spring aquifer is likely between 12.3 and 15.2 km^2.

The GIS-based recharge model developed by Miner and Adamson was calibrated to historical average annual base flow in the Rivieres Grise, Blanche and Momance that flow from the Massif de la Selle aquifer to the south and west. Average modeled recharge in the 15 km^2 spring catchment was 15%of annual precipitation, or 240 mm/year. This is less than indicated by the chloride mass-balance. The discrepancy could be due to the lack of rainfall chloride measurements, especially in the high elevation areas, since precipitation varies greatly across the recharge area. The GIS model does not account well for the anomalous events of rainfall intensity and duration, such as during hurricanes and tropical storms. In any case, it is likely that the spatial extent of the spring recharge area ranges between 15 and 34 km^2. This range highlights the importance of additional monitoring and diagnostics to refine the understanding of the spring.

The chloride time series data allows for an analysis of potential recharge rate variations from year to year, and a comparison to actual precipitation volumes. Over a two-year period from 2007 to 2008 there were seven months with precipitation higher than 250 mm, while over a six-year period from 2009 to 2015 there were only a total of five months with precipitation over 250 mm. The latter period corresponds to a decreased flow both at Source Mariani and at Tunnel Diquini. Considering the average rainfall chloride value of 5.5 mg/l and the average spring chloride of 11.2 mg/l (2008-2009), it is possible that annual recharge rates approach 50% of annual precipitation in years of high rainfall volume and intensity. The 38% average is largely influenced by the anomalous high years and could be lower than 20% of precipitation in a typical year, as indicated by the GIS-based recharge model.

Date	Chloride (mg/l)	Date	Chloride (mg/l)
Jul-08	11.0	Mar-12	16.5
Aug-08	9.7	Jun-12	16.5
Sep-08	13.0	Jul-12	17.5
Oct-08	11.0	Jan-13	16.5
Nov-08	11.0	Feb-13	13.0
Dec-08	8.5	Jun-13	16.0
Jan-09	10.5	11/12/2013	18.5
Feb-09	9.5	Jan-14	16.0
Mar-09	11.0	10/6/2014	24.5
Apr-09	11.5	10/12/2014	16.5
Sep-09	13.5	Nov-14	12.5
Nov-09	14.0	3/23/2015	17.0
Jul-11	15.0	6/29/2015	18.0
Aug-11	12.0	8/6/2016	18.5
		4/1/2019	19.4
		Average (2008 - 2019)	14.4
		Average (2008-2009)	11.2
		Average (2011-2019)	16.7

Table 3. Groundwater Chloride Measurements for Source Mariani.

Date	Location	Zone	Chloride (mg/l)	Latitude (dd)	Longitude (dd)	Elevation (m)
10/4/2016	Laboule[1,2]	Massif de la Selle	< 1	18.495	-72.315	850
10/19/2016	Laboule[2]	Massif de la Selle	< 1	18.495	-72.315	850
10/24/2016	Laboule[2]	Massif de la Selle	< 1	18.495	-72.315	850
8/1/2018	Petionville	Massif de la Selle	7.1	18.511	-72.290	380
8/2/2018	Petionville	Massif de la Selle	13.6	18.511	-72.290	380
8/2/2018	Petionville	Massif de la Selle	9.89	18.511	-72.290	380
9/28/2018	Thomassin 36	Massif de la Selle	1.78	18.482	-72.317	1025
10/2/2018	Thomassin 36	Massif de la Selle	0.71	18.482	-72.317	1025
10/6/2018	Thomassin 36	Massif de la Selle	1.24	18.482	-72.317	1025
01/04/19	Petionville	Massif de la Selle	7.64	18.511	-72.290	380
02/04/19	Petionville	Massif de la Selle	18.1	18.511	-72.290	380
03/22/19	Petionville	Massif de la Selle	4.65	18.511	-72.290	380
		Average	5.5			

[1] Sample taken during Hurricane Matthew

[2] Assumes chloride values for Laboule and Clercine 12 are approximately 0.5 mg/l

Table 4. Rainfall Chloride in Massif de la Selle.

Section 3.0 - Discussion

Based on the study, the key results are outlined and discussed below:

Spatial Distribution of Groundwater Recharge

1. The groundwater recharge area that contributes to the spring flow appears to be approximately 15 km² but may be as large as 34 km².

a. This uncertainty in the recharge area is due to the large effect that annual fluctuations in precipitation volume and intensity have on the recharge rates.

b. The average recharge elevation is estimated at 580 m above mean sea level with a corresponding temperature of 22.7 C. This suggests the possibility that some spring flow may originate from distal zones in the regional carbonate aquifer such as within the Riviere Momance basin.

Groundwater Budget

1. The long-term average annual recharge rate is estimated at 38% of annual precipitation. During high intensity rainfall periods, the recharge rates may approach 50%, while during normal or low precipitation periods the recharge could be approximately 15%.

2. Aquifer storage relative to the spring is estimated between 155 and 259 million m³.

3. The limestone karst aquifer that feeds the spring is well mixed and has an average groundwater age of between 21 and 35 years based on a single sampling event.

Flow Characteristics

1. Recharge to the regional aquifer appears to be largely affected by high-intensity and high-volume rainfall events such as hurricanes and tropical storms. There appears to be a 3-to-7-year cycle of recharge trends partially influenced by El Niño and La Niña events.

2. Spring discharge displays mild seasonal variability with monthly average flows typically ranging between 14,500 and 25,000 m³/d with an average of 19,500 m³/d.

a. Instantaneous (daily) flows display greater variability, ranging from 7,600 to 30,700 m³/d.

b. Based on the spring catchment infrastructure as observed in 2019, total spring flow is measured from a single water meter. Since this method does not account for overflow, some high spring flows could be underreported.

3. The spring flow is most vulnerable to extended periods of average or below average precipitation and consecutive years without high intensity rainfall periods such as tropical storms and hurricanes.

a. This recharge characteristic combined with the recent flow regression that extends from 2014 to 2019 may foster perceptions that the spring flow has been decreasing over the long-term or that acute impacts have taken place.

b. Limited historical data from between 1925 and 1933 suggests that average spring discharge remains relatively stable or perhaps has even increased due to increased precipitation intensity.

4. The cyclic and multiannual recharge characteristics of the regional carbonate aquifer are important for water managers and planners to understand and utilize in balancing the different water sources of CTE-RMPP.

Connection to Regional Groundwater and Surface Water

1. Source Mariani flows from the regional Massif de la Selle carbonate aquifer.

a. The regional aquifer also supplies many of CTE-RMPP's major springs and Tunnel Diquini and provides base flow to river systems.

b. Monitoring is required to better understand the complex hydraulic relationships between these major outlets of the aquifer.

c. Source Mariani is the lowest elevation terrestrial outlet known for the aquifer. It appears to emanate from a topographic exposure of the main aquifer lithology rather than as a contact spring. This may act to sustain flows even when higher elevation springs exhibit reduced flows.

d. Source Mariani essentially serves as a drain for the western portion of the Massif de la Selle aquifer.

2. Source Mariani does not appear to have a significant hydraulic connection to the Riviere Momance or Riviere Froide. This is supported by the isotope and tracer sampling, and analysis of recharge catchment size.

Aquifer Vulnerability

1. Due to the high permeability and rapid infiltration rates typical in karst limestone environments, the spring waters have high vulnerability to contamination. This is confirmed by the elevated nitrate levels consistently measured in spring discharge.

2. Urbanization and land use changes in the hills south of the spring are considered the greatest risk to groundwater quality and flow. The lack of centralized waste management and sanitation combined with the karst hydrogeology significantly increases the risk of direct contamination of the aquifer waters.

a. Land use planning, zoning, and managed development of the area south of the spring in an area larger than the existing spring protection perimeter is necessary in order to protect the spring water from future water quality and flow impacts.

Section 4.0 - Recommendations for Continued Activities

Due to Source Mariani's importance as the second largest single water supply to Port-au-Prince, additional efforts are warranted to guide water source protection and enhancement, water use planning and future water supply development in the Massif de la Selle aquifer. Based on the findings of this study, recommendations fall into three categories that include: (i) improvements to ongoing monitoring efforts, (ii) water source protection and enhancement, and (iii) options for additional study. Future activities would be greatly aided by increased availability of temporal datasets for climate, flow, hydrochemistry, and stable isotopes. The recommendations by category, and the narrative provides supplemental detail. The recommendations provided closely parallel Tunnel Diquini's. A significant improvement in efficiency would be gained by combining these efforts.

A - Strengthening Ongoing Monitoring Efforts

Historical monitoring data collected by CTE-RMPP provided insights into the spring dynamics. It is our understanding that current monitoring efforts, when performed, include: (i) recording the portion of monthly discharge that is diverted to the pumping station, ii) recording monthly pumping volumes up to the reservoir, and (iii) periodic collection of water samples for physical and chemical analysis, often including conductivity, salinity, pH, temperature, turbidity, hardness, alkalinity, calcium, magnesium, chloride, sulfate, nitrate, nitrite, and iron. Many data gaps exist in the material provided to our team by DINEPA and CTE-RMPP. There are certainly multiple ways that could further reinforce and improve monitoring efforts.

• We commend CTE-RMPP for the data that has been collected. Data that was particularly useful to this study included: flow rate, chloride, conductivity, turbidity, and nitrate measurements. We recommend that, at a minimum, these parameters continue to be measured monthly.

• Since a comprehensive flow meter measuring spring discharge already exists, an increase in monitoring frequency would be relatively easy to implement. Daily recording of discharge at the meter between the spring and pumping station would allow for better understanding of recharge dynamics.

o It appears that an electronic data logger has been installed on the totalizing flow meter, but staff did not use this feature and did not know how to operate it. Therefore, training and implementation of a scheduled read-off from data logger is recommended, to reduce the need for manual daily recording on the meter face and reduce clerical errors.

• Spring catchment overflow is not currently measured. Construction of a method to measure overflow rates is recommended. Overflow measurements, when they occur, could be added to the pumping rate data in order to estimate total spring flow rates.

• Discharge data collection and storage should clearly delineate the flow measurement type as i) spring discharge to pumping station, ii) spring discharge overflow, iii) total spring discharge, and iv) pumped volume to reservoir.

• Table 5 provides recommendations for measurement parameters and timing of sampling. Monitoring should begin as soon as possible and be incorporated into a permanent monitoring program so that data is available for water use planning or future studies.

Parameter	Daily	Weekly	Monthly	Quarterly	Yearly	Notes
Spring discharge to pumping station	X					Either read manually from totalizing flow meter or downloaded periodically from data logger installed on meter.
Spring discharge overflow	X					Requires simple construction of weir in overflow canal and installation of staff gauge to measure water height behind weir.
Total spring discharge	X					Simple addition of discharge to pumping station and overflow discharge.
Pumped volume	X					Read manually from totalizing flow meter installed between pumping station and reservoir.
Conductivity (uS/cm)		X				Low-cost conductivity/pH field probe, calibrated as required.
pH		X				
Temperature		X				
Chloride			X			Low level chloride analysis often required, suggest detection limit of 1 mg/l or lower.
Nitrate			X			CTE-RMPP lab analysis.
Turbidity			X			CTE-RMPP lab analysis.
E. coli			X			Simple tests such as the compartment bag test may be sufficient and more economical than a full analysis at the CTE-RMPP lab.
Hydrochemistry				X		CTE-RMPP lab analysis of Ca, Mg, Na, Cl, K, CO3, HCO3, SO4, NO2, Fe, TDS, Hardness, Alkalinity.
Compilation and publication of data					X	Recommend that a short memorandum that primarily contains a table of the measured results is published online so that data is easily available. This is also a good interval to review issues with data collection and review the program to reduce data gaps.

Table 5 – Spring Monitoring Program Recommendations.

B – Water Source Protection, Enhancement and River Monitoring

Water source protection and enhancement planning – This study provides an improved understanding of discharge dynamics and recharge areas for the spring that highlights interim insights useful to guiding future steps to protect and enhance the spring.

- Recharge protection areas can be delineated to protect critical areas of recharge and reduce contamination sources near the spring.

- Land-use practices in the recharge area can be mapped and reviewed in order to guide focused interventions such as forestation, terracing of steep slopes, and development exclusion zones.

- Sinkhole delineation can be performed to locate areas of concentrated recharge. Fences to keep wildlife and livestock out could eliminate potential contamination sources.

- The area immediately south of the spring protection zone is becoming increasingly urbanized. Efforts at sanitation planning and infrastructure in that area would help protect the spring from biological contamination.

- Regular schedules for spring catchment inspection and cleaning can be implemented, perhaps quarterly. At a minimum this includes the sediment and root removal from inside the catchment and sediment removal from on top of it.

- Installation of sediment barriers within the catchment may help reduce the mobilization of sediment into the supply line.

C – Further Hydrogeological Characterization

Refinement of the spring recharge area and geology – This study indicates some uncertainty in the spatial extent of the spring recharge. Refining the knowledge of this area is important to guide water source protection, land use planning, and future water supply development. Due to the karst nature of the aquifer, there is likely both diffuse and concentrated recharge. Potential study methods include:

- A monitoring program utilizing stable isotopes $\delta^{18}O$ and δD along with chloride collected over a multi-year period to record changes happening due to both drought and hurricane-induced recharge events.

- Dye tracer testing of karst dolines and the Momance and Froide River are perhaps the most definitive methods for delineating the recharge area. Transit times, however, may be prohibitive.

- Geologic mapping of the recharge catchment to better understand the ways in which lithologic and structural changes affect the recharge, occurrence, and flow of groundwater to the spring. Such mapping would expand the coverage and detail of geological and hydrogeological mapping performed by Eptisa (2015).

- Hydrochemical, isotopic, and flow characterization of Source Ti Sous and Source Tet Sous below Source Mariani to determine their connection to the regional aquifer and relationship to Source Mariani

Refinement of spring recharge and discharge dynamics – As previously mentioned, the regional aquifer system appears to be largely driven by large climatic events on 3-to-7-year cycles.

- A coordinated effort should be made by CTE-RMPP and DINEPA to locate historical flow rates for the spring. This will aid in the understanding of how and if the spring has been affected by changes in land use changes and climate.

- Careful analysis of these recharge and discharge trends may also help predict the future effects of climate change on the major carbonate spring that discharges to Port-au-Prince's water supply.

Increased rainfall monitoring and sampling

• Daily data suitable for determining rainfall intensity within the spring catchment was not made available for this study. If such data is located or collected, an analysis could be performed comparing rainfall intensity over the periods of recorded flow rates to better understand recharge thresholds and the conditions conducive to diffuse or concentrated recharge.

• The implementation of a rainfall monitoring program that also samples rainfall for $\delta^{18}O$, δD and chloride is advisable. Potential localities for such a program include Morne Boyer, Morne Chandelle, and Berot. This would provide precipitation data at various elevations within the catchment and would be a complement to the rainfall monitoring in Degand and Fermate that has been recommended to support Tunnel Diquini characterization (Northwater International and Rezodlo, 2018). Such rainfall intensity measurements, coupled with meteoric hydrochemistry, will allow for better recharge estimates and be a valuable resource to all future hydrogeological studies in the Massif de la Selle.

Category	Activity	Financial Costs	Expertise Required	Equipment Required	Institutional Involvement
A	Spring Monitoring Program (see Table 3)	Low (annual)	Technician	pH/Conductivity field probe, CTE-RMPP lab, low-level chloride probe, installation of weir and staff gauge	CTE-RMPP technician and data manager
B	Water Source Protection and Enhancement Planning	Moderate (planning) High (implementation)	Hydrogeologist, sanitation planner, landuse planner	Minimal	DINEPA, CTE-RMPP, MARNDR coordination, community and local leader support
C	Refinement of Spring Recharge Area and Geology	High (one-time)	Hydrologist / Hydrogeologist / Geologist	Dye tracing materials and equipment, sampling bottles, geological reconnaissance equipment	CTE-RMPP technician, DINEPA approval of dye tracing
	Refinement of Spring Recharge and Discharge Dynamics	Moderate or Low if sufficient monitoring has occurred	Hydrologist / Hydrogeologist	Minimal	CTE-RMPP data manager
	Rainfall Monitoring and Sampling	Moderate (one-time setup) Low (annual)	Hydrologist setup, Technician operation	Two to three telemetric weather stations with simple sample collection mechanism	CTE-RMPP, MARNDR technician and support

Table 6. Phased recommendations and resource needs.

Section 5.0 - Conclusions

This study applied limited and discrete datasets to derive an understanding of the spring hydrology and hydrogeology. The analysis and insights of this characterization were greatly aided by previous efforts to characterize the nearby Tunnel Diquini. We believe this study is sufficient in characterizing the spring on an interim basis from which to inform planning and decision-making with regards to guiding the sustainability and protection of Source Mariani. Disciplined monitoring and the associated temporal datasets are important to advance the understanding and characterization of the spring and the Massif de la Selle regional aquifer that supports it. Using the data and findings in this study, the potential exists for source protection and enhancement programs in key zones of the spring's watershed. Additional studies could also focus on better understanding and characterizing the recharge catchment to the spring.

The Massif de la Selle carbonate aquifer is arguably Haiti's most important aquifer system, as it is responsible for providing a significant proportion of water supply to Port-au-Prince from its large springs with the benefit of gravity, and its rivers supply the bulk of recharge to the Plaine du Cul-de-Sac aquifer. Further characterizing and understanding the aquifer as a whole would foster informed planning and operations into the future to protect and enhance these important resources. The results of this study and of Tunnel Diquini's provide important insights that can be used to guide such further studies.

Limitations of Investigation

Aspects of the assessment were especially limited by the unavailability of data and resources regarding the Massif de la Selle aquifer. The lack of consistent monitoring and records of discharge and precipitation made it especially challenging to quantify recharge rates and extent of the recharge basin. A focused and basic level of analysis and synthesis was applied throughout the report with the primary objective to provide initial insights into the spring dynamics and recommendations for further study.

A limited amount of historical data was available to support this analysis, and this study included a single sampling event that is just a snapshot of a dynamic system. Conclusions in this report are preliminary and presented to aid interim planning and decision-making, and to guide any future study and characterization.

This assessment was performed using the professional care and skill ordinarily exercised, under similar circumstances, by experienced geologists and hydrogeologists practicing in this or similar locations with very limited sources of data and resources. Changes in analysis and interpretations can and will occur with the acquisition and analysis of new data, such as monitoring reports, water quality data, and tracer and isotope data. Analysis and interpretations presented in this report must be considered fluid and subject to review and revision as additional data is compiled. Analysis and interpretations described in this report may be invalidated wholly or partially by the results of continued data collection and observations.

REFERENCES

Adamson, J.K., Jean-Baptiste, G., and Miner, W.J., 2016, Summary of groundwater resources in Haiti, in Wessel, G.R., and Greenberg, J.K., eds., Geoscience for the Public Good and Global Development: Toward a Sustainable Future: Geological Society of America Special Paper 520, p. 1–22, doi:10.1130/2016.2520(14).

BME [Bureau des Mines et de l'Energie], 1993, Notice Explicative de la Carte Géologique d'Haïti: Port-au-Prince, Bureau des Mines et de l'Energie.

BRGM [Bureau de Recherches Géologiques et Minières], 1988, La Synthèse géologique notamment dans ses parties stratigraphiques et tectoniques: Bureau des Mines et de l'Energie, Port-au-Prince, Haiti.

BRGM [Bureau de Recherches Géologiques et Minières], 1989, Étude des ressources en eau de la région de Port-au-Prince.

Butterlin J., 1960, Géologie générale et régionale de la République d'Haiti [General Regional Geology of the Republic of Haiti]: Institut des Hautes Etudes de l'Amérique Latine, 194 p.

CERCG [Centre d'Etudes et de Réalisations Cartographiques Géographiques], 1989, Carte Géologique de la République D'Haïti [Geologic map of the Republic of Haiti]: Bureau des Mines et de l'Energie, Port-au-Prince, scale 1:250,000, 1 sheet.

CGIAR. (2007). Global Geospatial Potential EvapoTranspiration and Aridity Index, Methodology and Dataset Description. Available at: https://cgiarcsi.community/data/global-aridity-and-pet-database/. ARC/INFO Grid format, 30 arcs seconds.

Cox, et al, 2011, Géologie de Port-au-Prince. 1:250,000 scale.

Direction Generale des Travaux Publics [Republic of Haiti Public Works]. (1918 - 1938). Bulletin Hydrographique, Les Eaux de Surface de la Republique d'Haiti. Port-au-Prince, 16 bulletin reports in the series.

Döll, P., and Fiedler, K., 2008, Global-scale modeling of groundwater recharge: Hydrology and Earth Systems Sciences, no. 12, p. 863 – 885.

Eptisa. 2015. Réalisation d'études hydrogéologiques sur la région métropoliaine de Port-au-Prince (RMPP), Carte Géologique.

Gonfiantini and Simonot, 1989, Isotopic Investigation of Groundwater in the Cul-de-Sac Plain, Haiti. International Atomic Energy Agency, IAEA-SM-299/132, Pg 22.

Hijmans, R.J., S.E. Cameron, J.L. Parra, P.G. Jones and A. Jarvis, 2005. Very high resolution interpolated climate surfaces for global land areas. International Journal of Climatology 25: 1965-1978.

Miner, W.J., and Adamson, J. (2017). Modeling the Spatial Distribution of Groundwater Recharge in Haiti using a GIS Approach, Geological Society of America 2017 Annual Meeting, Seattle, Washington, doi: 10.1130/abs/2017AM-297120.

Moliere, E., and Boisson, D., 1993, Coupes Géologiques d'Haiti, in, Notice Explicative de la Carte Géologique : Port-au-Prince, Bureau des Mines et de l'Energie.

Northwater International and Rezodlo. 2018. Hydrogeological Characterization of Tunnel Diquini: Port-au-Prince, Haiti, Inter-American Development Bank, Technical Report, HA-T1239-P001

Oxfam, 2014, Carte Geologique de Canaan, Jerusalem, Corail et Onanville (CROIX DES BOUQUETs, Haiti), Evaluation technique des menaces naturelles et vulnerabilite de la commune de Croix des Bouquets, Port-au-Prince. 1:10,000 scale.

Polidori et al. 2014. Eleboration du Référentiel Hydrographique d'Haiti à Partir d'un MNT Aster.

Pubellier, M. 2000, Plate boundary readjustment in oblique convergence: Example of the Neogene of Hispaniola, Greater Antilles. Tectonics, Vol. 19, No.4, p 630-648.

Scanlon, B.R., Healy, R., and Cook, P.G., 2002, Choosing appropriate techniques for quantifying groundwater recharge: Hydrogeolology Journal, no. 10, p. 18–39.

Suez, 2013, Travaux prioritaires de renforcement de la production d'eau. Pg 178.

Taylor, G.C., and Lemoine, R.C., 1949, Ground water in the Cul-de-Sac Plain, Haiti: U.S. Geological Survey Open-File Report, 59 p.

UNDP [United Nations Development Program], 1990, Carte Hydrogéologique République d'Haiti [Hydrogeologic Map of the Republic of Haiti]: United Nations Development Program, New York, scale 1:250,000, 1 sheet.

United Nations, 1991, République d'Haïti: Programme des Nations Unies pour le Développement: Développement et Gestion des Ressources en Eau. [Government of Haiti and Organization of the United Nations, Department of Technical Cooperation for Development]: Report HAI/86/004, vol. 6.

U.S. National Aeronautics and Space Administration. Hispaniola region, Landsat 8: spectral bands 1 through 7. Product L1T.

Woodring, W.P., Brown J.S., and Burbank, W.S., 1924, Geology of the Republic of Haiti. Department of Public Works, Port-au-Prince, Haiti.

World Health Organization, 2011, Guidelines for drinking-water quality, 4th edition: WHO, Geneva, Switzerland.

Yeh, Hsin-Fu et al. (2014). Identifying Seasonal Groundwater Recharge Using Environmental Stable Isotopes. Water. 6, 2849-2861. Doi: 10.3390/w6102849.

Plaine du Cul-de-Sac

Groundwater Flow Model

Department Ouest, Republic of Haiti

Final Report

Prepared for:
Inter-American Development Bank & DINEPA

Prepared by:
Northwater International and Rezodlo S.A.

Table of Contents

1.0 - INTRODUCTION **69**

2.0 - CONSTRUCTION OF THE MODEL **69**

2.1 – MODEL AREA SETTING 69
2.2 – DATA 69
2.3 – METHODOLOGY 71
2.4 – EXAMPLE CROSS SECTIONS WITH HYDROSTRATIGRAPHY 76

3.0 - DEVELOPMENT OF THE NUMERICAL MODEL **76**

3.1 – GENERAL APPROACH 76
3.2 – SELECTION OF MODEL CODE 76
3.3 – ASSUMPTIONS 77
3.4 – MODEL EXTENT 77
3.5 – MODEL DISCRETIZATION 77
3.6 – SELECTION OF LAYERS 79
3.7 – BOUNDARY CONDITIONS 79
3.8 – MODEL PARAMETERIZATION 86

4.0 - MODEL CALIBRATION **86**

4.1 – GENERAL APPROACH 86
4.2 – CALIBRATION TARGETS 87
4.3– ADJUSTED PARAMETERS 89
4.4– CALIBRATION RESULTS 90

5.0 - MODEL RESULTS **91**

5.1 – GROUNDWATER FLOW 91
5.2 – GROUNDWATER BUDGET 92
5.3 – GROUNDWATER STORAGE 93

6.0 - MODEL LIMITATIONS AND SENSITIVITY **93**

7.0 - CONCLUSIONS AND CONSIDERATIONS **94**

REFERENCES **95**

1.0 - INTRODUCTION

A numerical groundwater flow model was developed to better understand the hydraulic characteristics of the Plaine du Cul-de-Sac (PCS) aquifer and support water supply development planning for the Port-au-Prince metropolitan area. The model effort was preceded by data mining and research that resulted in a borehole database that was important for the development of the model. The database is presented in a separate report (Northwater International 2018). The modeling was also supported with recent data and characterization of the aquifer (Northwater International and Rezodlo 2017).

The primary goal of the modeling exercise was to support the Haitian government in understanding: i) the sustainable and renewable quantities of groundwater available from the aquifer; ii) the complex recharge dynamics; and iii) surface water / groundwater interactions between lakes and river systems. With a regional groundwater model, the water supply development planning can be informed and potential impacts of development and climate change scenarios can be considered.

Upon completion of the hydrogeological database, the modeling process included the following:

1. Construction of the geologic and conceptual models.

2. Development of a steady-state groundwater flow model.

3. Parameterization and calibration of the groundwater flow model.

4. Presentation of results.

5. Running of model scenarios as guided by the Inter-American Development Bank (IDB).

MODFLOW 2005 code was selected for modeling the PCS aquifer. MODFLOW is the United States Geological Survey (USGS) three-dimensional finite-difference groundwater model. MODFLOW is considered an international standard for simulating and predicting groundwater conditions, and its code has been extensively tested in various environments and conditions. It is widely accepted, and the theory behind it is well documented, easy to replicate, and can be applied to realistic conditions and adapted for future developments of the model. The ViewLog software from Earthfx Inc. was applied to build the model. This software directly integrates with the borehole database for building, developing and refining the model. Groundwater Vistas Advanced, version 6 was used to run the model simulations.

2.0 - Construction of the Model

2.1 - Model Area Setting

Illustrates the geologic and physiographic setting of the study area with primary rivers, streams, canals, lakes, and the regional drainage basins that are relevant to the Plaine du Cul-de-Sac (PCS). The PCS groundwater model boundary that is the primary focus of this report is outlined in red. The main aim of this report is to document the groundwater flow modeling effort. Further details of the study area and aquifer can be found in the supporting literature.

2.2 - Data

The data used to build the model was obtained from geological and subsurface information compiled from previous reports and borehole logs from various sources that were integrated into a database (Northwater International 2018). As detailed in the database report, the reliability and integrity of datasets is variable, and professional judgement was important in terms of how to insert data into the model. Table 1 outlines primary sources of data used in the modeling process. The current conditions of the annual average precipitation rates across the Plaine were modeled using the WorldClim Version 1.4 dataset produced by Hijmans (2005). Precipitation was primarily incorporated into the model through the recharge boundary conditions. Figure 2 displays recorded annual average precipitation at the Petion-Ville Hydrometeorological Unit of Haiti (UHM) station from 1960 to 2016; the WorldClim Version 1.4 dataset is based on climate normals from 1960 to 1990. Figure 3 shows the model area and the data locations that supported its development and calibration.

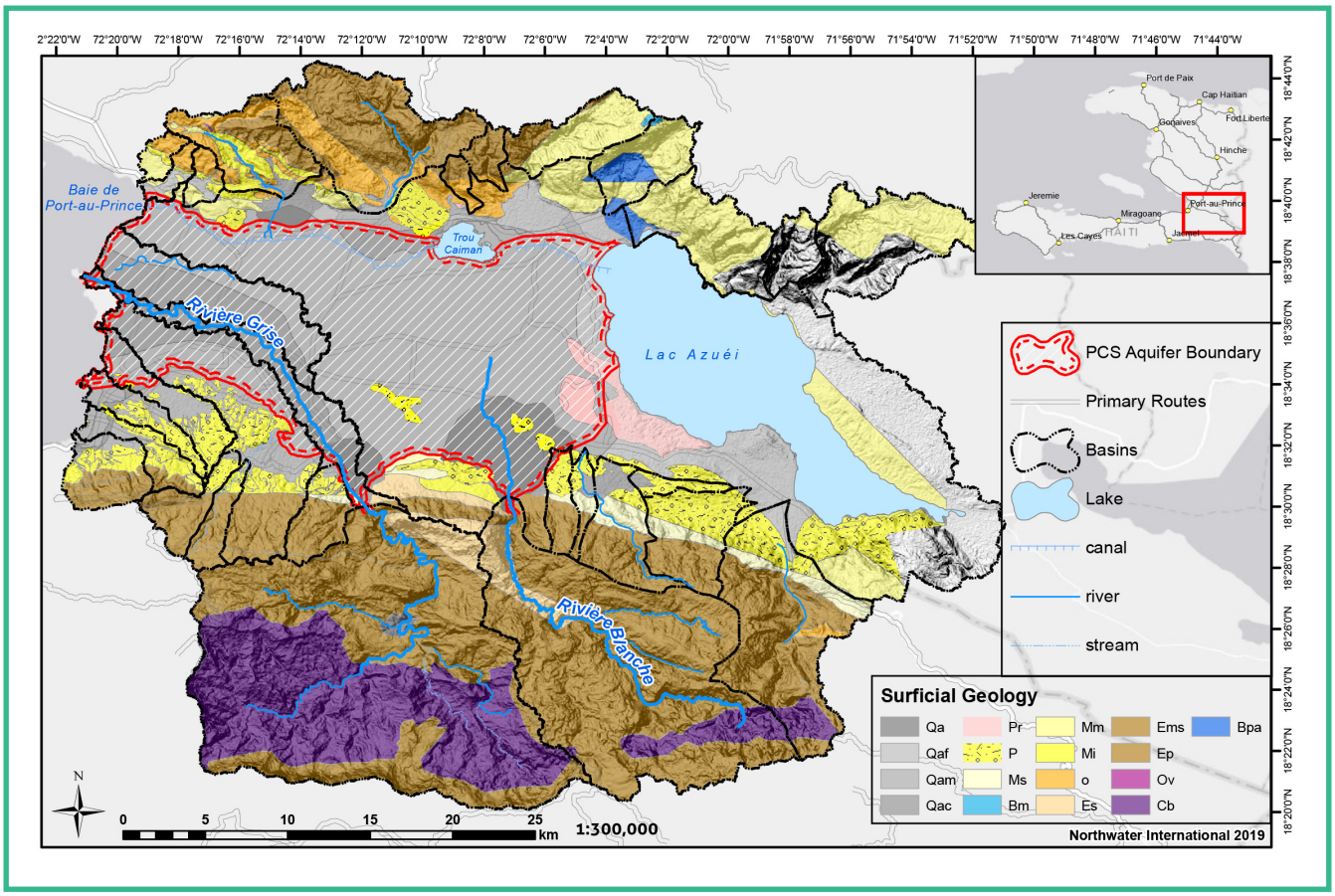

Figure 1. Geologic setting of the PCS Aquifer and the Basin.

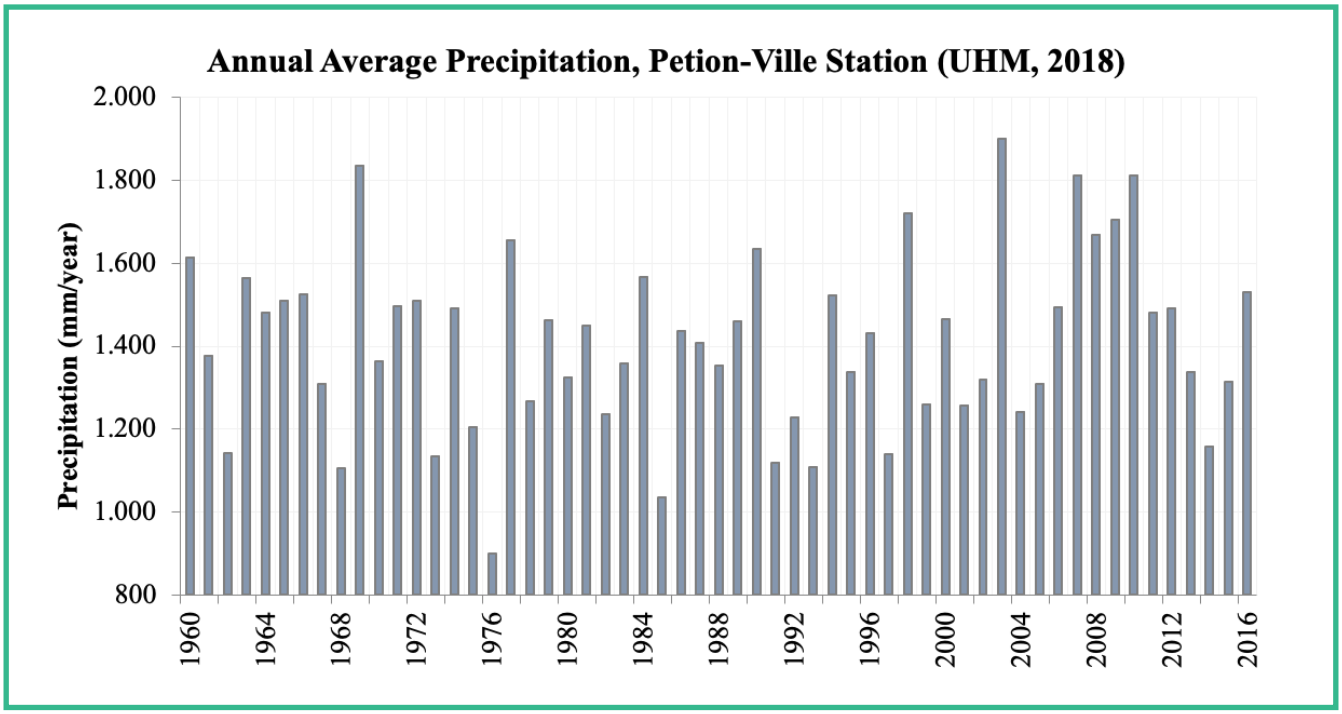

Figure 2 - Annual average precipitation at Petion-Ville Station, 1960-2016 (UHM, 2018).

Data Source	Summary
CTE-RMPP / DINEPA	2013-2014: Well inspection, testing and rehabilitation of 17 municipal wells. Drilling of 17 monitoring piezometers, with lithology and water levels. 2001 – 2017: Well lithology, well construction, pump test data, and water levels for the G wells. CTE-RMPP: Water quality monitoring data for select wells from 2006 – 2016.
Northwater International / Haiti Foratech / Geotechsol / Drilltech	72 private well drilling records that include lithology, well construction, and static water levels. Some wells have pump test data and field water quality.
Blue Ridge Missions	Drilling records for 73 wells, include lithology, well construction, static water level, and airlift yield. Drilling records for 150+ additional wells are available but do not have coordinates available. These were not entered into the database.
Haitian American Sugar Company (HASCO)	Well completion, lithology, water level, pump test records for 57 high capacity irrigation wells. Historical records provided by Foratech Environnement.
EPTISA 2016 SIGES DATABASE	Water quality data and water level measurements for several of the CTE-RMPP production wells and monitoring piezometers.
Living Water International	Locations of over 250 hand pump wells, but no data regarding well construction, lithology, or water levels.
Private Drilling Companies	Select drilling records from private drilling companies that shared data.

Table 1 - Summary of key data sources in the hydrogeological database.

2.3 - Methodology

The geologic modeling approach was based on identifying and correlating stratigraphic contacts in subsurface data (borehole logs and analyses of previous data) to produce unit surfaces across the study area. Isopach, or sediment thickness contours, were generated by subtracting adjacent surfaces.

General Approach

The first step was to gain an understanding of the various surficial geological units, as defined on the geology map, as well as their relative geometries. A stratigraphic framework was developed using the geological mapping, available literature, borehole records, and an analysis of the geomorphology of the plain.

The stratigraphic framework contains the units to be modeled, and describes their lithology and stratigraphic relationship to other units in the framework. The units in the framework are derived from those contained in the surficial geology map, which also lists their stratigraphic position and textural characteristics. Using datasets illustrated in Figure 3, Figure 4, and the reliable borehole records as the basis for the framework, ensures that the model conforms to the most accurate sources of geological information. The position of each unit in the framework is unique, that is, the order of the units in the three-dimensional model is inviolable. Each unit also has defined characteristics (e.g., silty clay with sand beds). This enables appropriate aquifer property values to be assigned to each unit.

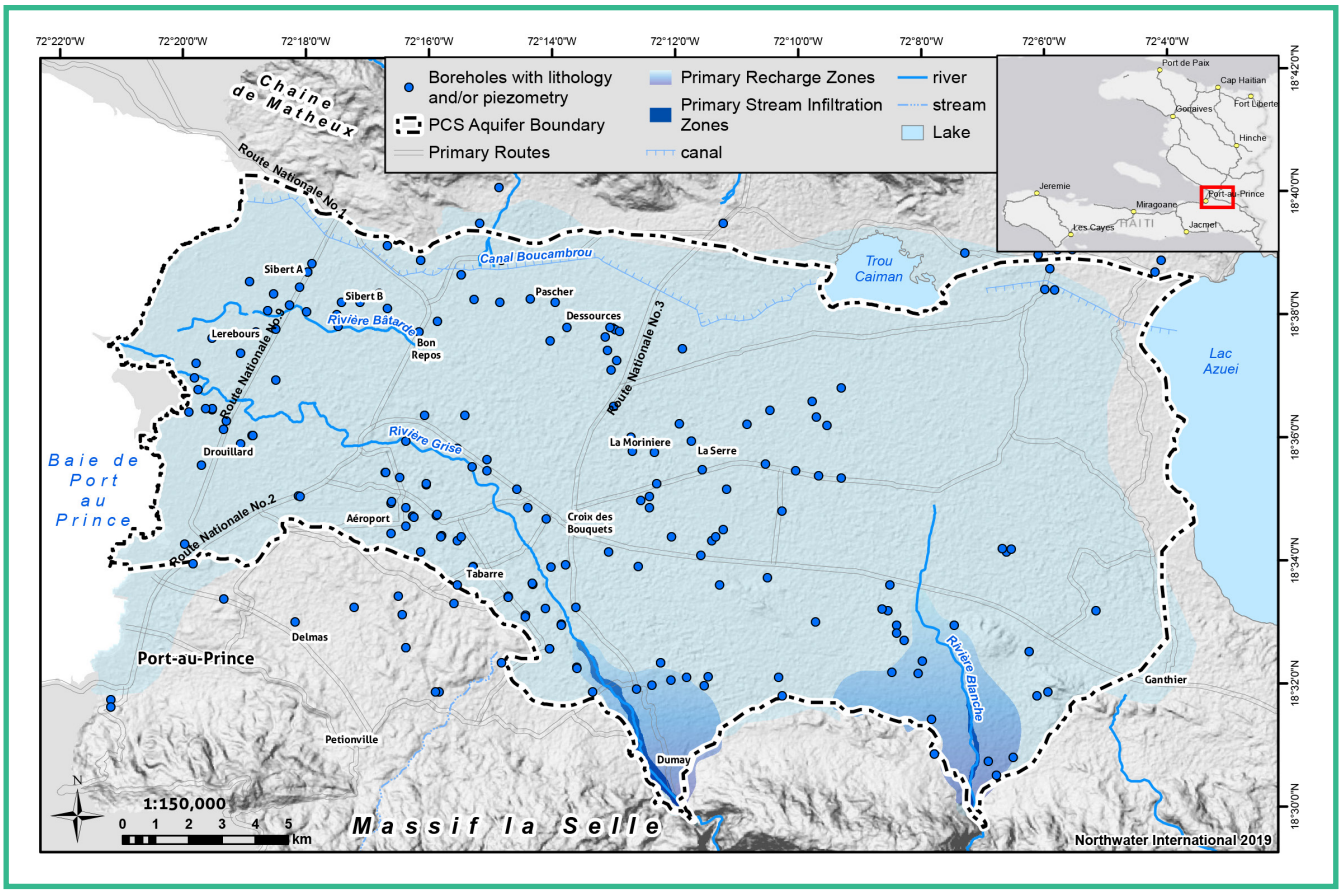

Figure 3 - Plaine du Cul-de-Sac Model Area.

Table 2 contains the simplified stratigraphic framework developed for the study area based on a review of 140 borehole lithology logs in the database. It was clear through the analysis of lithology logs that the alluvial aquifer has complex stratigraphy with dozens of layers of various strata with variable extent, thicknesses, and properties. Bulk characterization was necessary in order to develop a regional groundwater flow model for the aquifer.

Nearly all the borehole records had a layer of finer-grained soils of various thicknesses, whereas the upper layer acts as an aquitard and its texture is variable depending on its depositional setting. The soils are thicker and finer-grained further from the Riviere Grise and Riviere Blanche inlets to the plain. Beneath the soil, many borehole records indicate a silty sand aquifer unit (layer 2) that stores and yields smaller quantities of water. Many of the shallow boreholes intended for hand pumps or small-yield wells are installed in these shallower sandier aquifer units. Interestingly, many of the wells drilled by NGOs terminated upon intersecting the upper section of the more productive aquifer layers (layer 3). This provided a valuable indicator for delineating the depth to more productive aquifer layers throughout the plain. Beneath the sandier aquifer unit (layer 2), there is a prevalence of sand and gravel beds with clay interbeds that store and yield significantly more groundwater than their upper counterparts. It is from this hydrostratigraphic unit (layer 3) that a majority of the higher yielding wells produce groundwater. Since very few wells intersect the entire thickness of alluvium, a fourth layer was established beneath layer 3 to represent a few of the deeper wells and the unknown strata, to differentiate the layer and provide additional modeling and calibration flexibility. This layer was set to have the same hydraulic properties as layer 3, and the two interact as one unit for all intents and purposes.

Model Layer (from top to Bottom)	Stratigraphic Framework Unit	Surficial Geology Unit
1	Sandy silt and clay – upper layer of soil development and fine-grained strata	Quaternary Alluvium
2	Silty sand	
3	Sand and gravel with sandy clay interbeds	
4		
	Bedrock / Model Boundary	**Miocene, Oligocene, and Eocene marl, sandstone, and limestone**

Note: Stratigraphic units listed from youngest at top to oldest at bottom.

Table 2 - Generalized Framework.

Once the stratigraphic framework was developed and combined with an understanding of the geology and geometry of the various units, it was possible to start coding units and stratigraphic contacts in subsurface data. Local experience and knowledge guided the interpretation of borehole logs, and a few guidelines, as described below, helped constrain it.

The data inputs used to code sediment intervals in wells and boreholes consisted of the texture and position of sediment intervals, the geographic location of a well or borehole, and the map unit in which a well or borehole was located in, as shown on the surficial geology map.

Coded sediment intervals had to be compatible with the stratigraphic framework; in other words, the texture and position of a sediment interval from a well or borehole had to be compatible with the unit that it was coded as.

To ensure that the model conformed to the surficial geology map, the uppermost unit of each well and borehole record was coded as the same unit in which the record was located in as shown on the surficial geology map. In some borehole records, the sediment of the uppermost unit did not agree with what was expected based on the surficial geology map. In these cases, the upper few meters of sediment in such wells were coded as the unit they were located in.

Discontinuities, either due to non-deposition or erosion, in borehole records were accounted for by picking the elevation of the missing surface at the same elevation of the stratigraphically adjacent underlying (i.e., older) surface. This ensures that the complete stratigraphic sequence is captured for each borehole and that zero-thicknesses are calculated for stratigraphic units at appropriate locations and depths.

Since very few boreholes reached the bedrock, an aquifer-wide depth to bedrock analysis was performed to support the modeling and storage estimates. This was done using the delineated limits of the alluvium, the locations of boreholes that intersected bedrock, and our understanding of the structural geology of the plain.

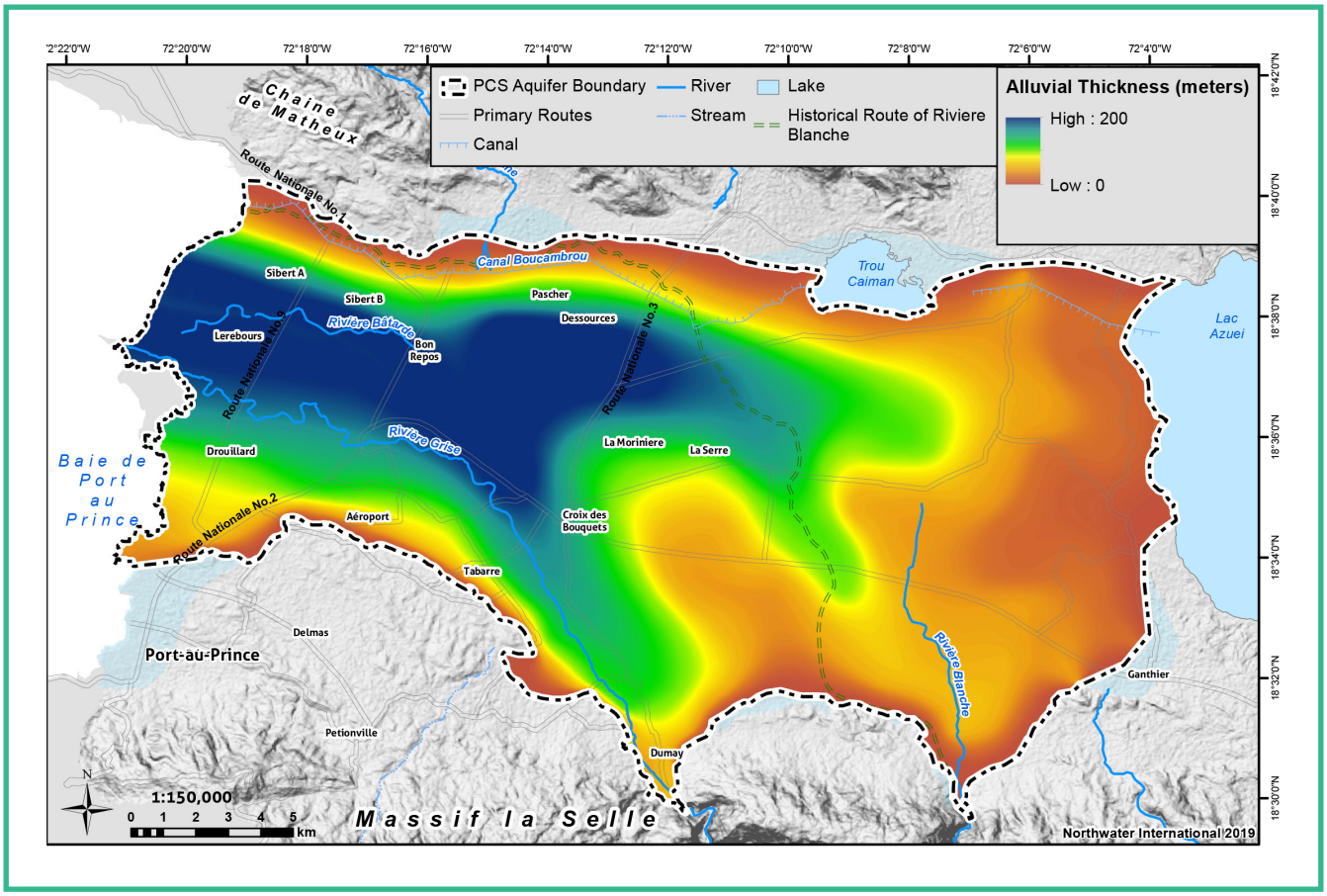

Figure 4 - Estimated Alluvial Thickness of the PCS Aquifer.

Generation of Cross Sections

The ViewLog software from Earthfx Inc. was used to generate cross-sections, pick stratigraphic contacts, and interpolate stratigraphic elevation data points to produce surfaces for each unit in the stratigraphic framework.

Two cross sections across the whole model area were first generated in areas where there was a better coverage of boreholes to compare the description of sediment intervals in higher quality records. These two cross sections are labeled A-A' and B-B' and their locations are shown in Figure 5. Most borehole records were available in the northwest between Canal Boucambrou and Riviere Batarde, and in the south around the Riviere Grise. This information was then used as a guide in interpreting well records in areas where no, or few, boreholes were located. The most notable gap in lithology data was in the eastern and northeastern portion of the aquifer which limits the hydrogeological understanding of connectivity between the aquifer and Lac Azuei, Trou Caiman and Canal Boucambrou.

Geological picking was performed along a 17x11 grid as shown in Figure 6 to generate the model layers. Layer picking using local knowledge and borehole logs extended to mapped bedrock exposures on either side of the alluvial deposits. A boundary line was drawn around the overburden deposits at the overburden/bedrock interface as displayed on the surficial geology map. This boundary was used to constrain the interpolation of unit surfaces to within the area when overburden deposits were mapped – i.e., to prevent deposits from being interpolated in areas where the bedrock is mapped at the surface. This was achieved by adding elevation control points along the boundary. At each point, the elevation of each unit in the framework was

assigned the elevation of the bedrock surface, that is, all elevation surfaces at each control point were merged. Therefore, zero-thickness values are calculated for each unit at these control points.

Cross-sections were completed by identifying and correlating stratigraphic contacts on well records and boreholes as described above. A number of cross-sections had only phantom boreholes and did not have any boreholes with logs. In such cases, adjacent completed sections with well or borehole records were used as a guideline to infer the location of stratigraphic contacts in these barren sections.

Once all cross-sections had been completed, elevation surfaces for each unit were generated by kriging stratigraphic contact elevation data points independently for each surface. Isopachs were generated by subtracting the elevation surface of a unit from its immediate underlying (i.e., stratigraphically older) neighbor.

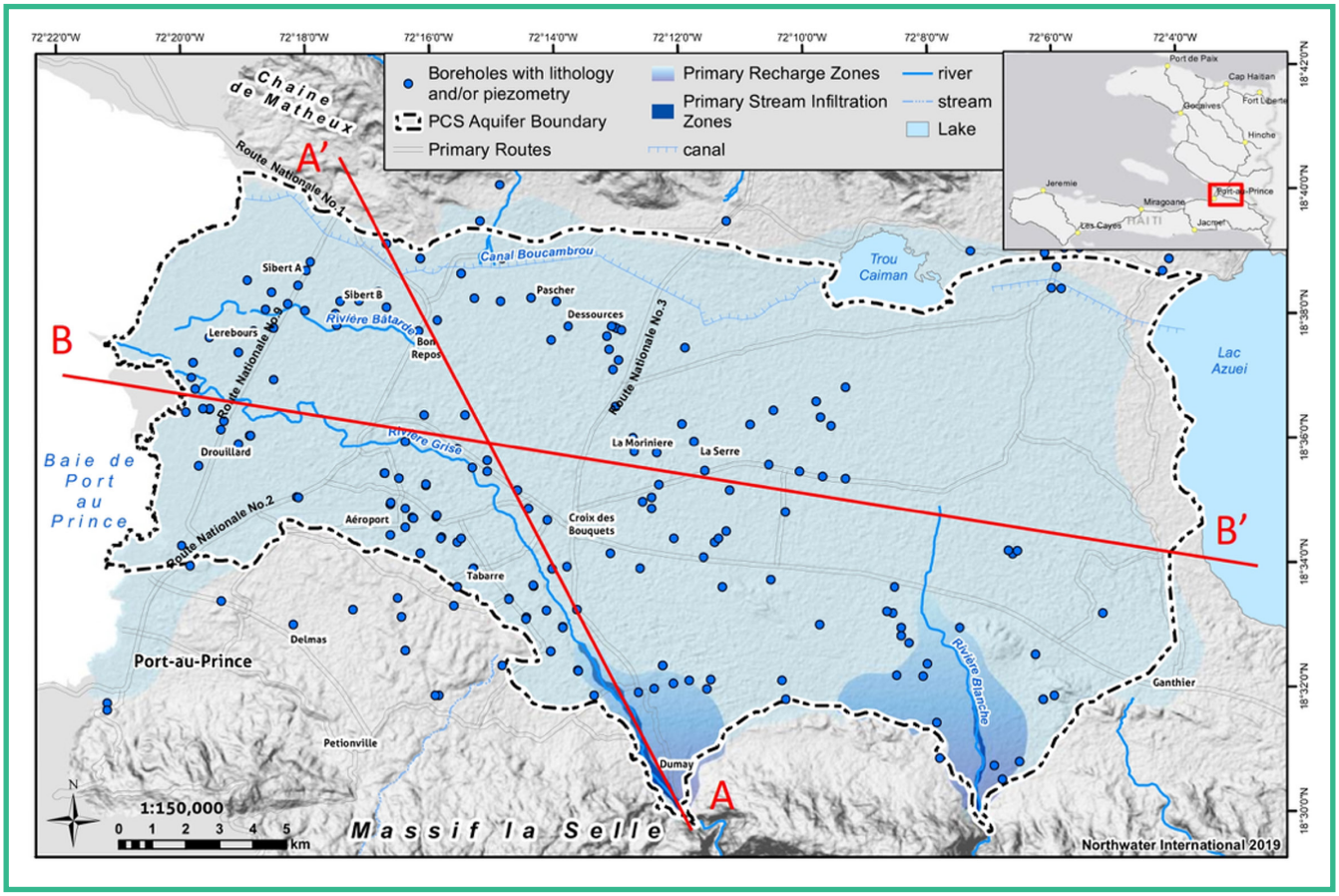

Figure 5 – Geologic cross section locations using reliable borehole logs.

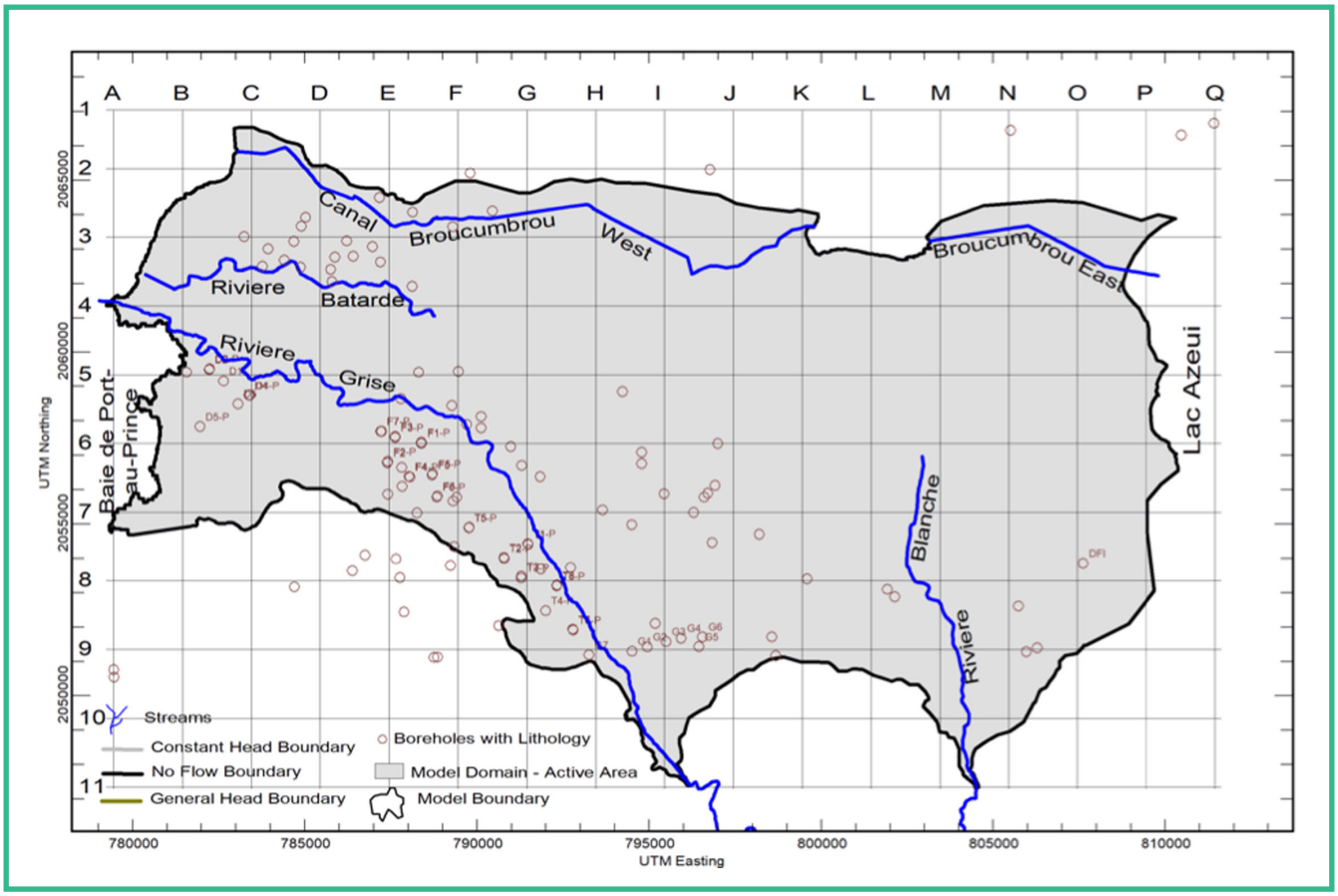

Figure 6. Grid of sections applied to build 3D model.

2.4 – Example Cross Sections with Hydrostratigraphy

Figure 7 and 8 show the four bulk hydrostratigraphic units that were defined along the two primary cross sections (Figure 20). The figures show the locations of boreholes with lithology that was within 3 km of the cross-section line.

3.0 – Development of the Numerical Model

3.1 – General Approach

A numerical model representing the prevailing hydrogeologic conditions within the study area was developed. The model is based on previous studies and the latest available data to simulate the hydrogeologic processes that are most representative of the local conditions. The model includes the overburden as described in the geologic model presented in previous sections. Pumping data were compiled from CTE-RMPP for recent years to estimate the actual pumping rate for the municipal production wells. Extraction rates for other non-municipal wells were estimated based on professional judgement and local knowledge of the aquifer and are further discussed in Section 3.7.

3.2 – Selection of Model Code

Based on the local hydrogeological setting and study objectives, the United States Geological Survey (USGS) finite-difference model MODFLOW was selected to simulate groundwater flows in the study area. MODFLOW is capable of simulating three-dimensional groundwater flows in saturated porous media. It is a widely used and well tested code that can effectively simulate both steady-state and transient groundwater flows of various degrees of complexity. The

open source, non-proprietary program has a number of different graphical interfaces available for pre and post processing. One of the main advantages of the MODFLOW code is that it maintains mass balance in each model cell, and therefore allows reliable advective particle tracking.

Earthfx ViewLog 4, ESRI ArcGIS, and Groundwater Vistas Advanced version 6 were used as pre and post processing tools. ViewLog's advanced capability of integrated borehole data management and interpretation was used to refine the local hydrostratigraphy. ViewLog can efficiently create MODFLOW input files and was used in accurately assigning stream bed elevations and water levels to the stream segments using the digital elevation model. Custom Visual Basic (VB) utilities were developed to assist in model preparation, including assigning the streams to the appropriate model layer, in order to ensure model layer continuity, assign hydraulic conductivity to each model cell based on layer pinch-out, and assign appropriate wetting factors. MS Access 2010 was used to store project data in a relational database and as an analysis and querying tool.

3.3 - Assumptions

The basic assumptions of the MODFLOW code are as follows:

1. Flow is laminar and Darcy's law is valid

2. Density of fluid is constant

3. Medium of flow is saturated

4. Principal direction of horizontal hydraulic conductivity or transmissivity is parallel to the model axes.

Flow of water under the ground is generally laminar unless large-aperture fractures or void spaces are present. The total area covered by this study is small enough to consider a constant density of water. Water level and transmissivity data of the immediate vicinity of the study area suggest that the groundwater flow patterns are mainly controlled by large scale heterogeneities in transmissivity and not by the horizontal anisotropy in the aquifers. Therefore, orientation of the model grid is insignificant for the study.

3.4 - Model Extent

The model extent is approximately 363 square kilometers and was selected to correspond to the extent of overburden in the Plaine du Cul-de-Sac. Where possible, the domain has been extended to physical boundaries. For example, the western boundary extends to the ocean, while eastern boundary extends to Lac Azuei. The plain is rimmed to the north and south by semi-consolidated or consolidated bedrock that forms a natural boundary.

3.5 - Model Discretization

In a numerical model, the conceptual model's domain is replaced by a discretized model consisting of an array of cells. The size of the cells is critical in the design of the grid. The discretization of the grid in the horizontal dimension is a function of the expected hydraulic gradient as well as the scale of data available for the model.

The horizontal extent of the model domain has been discretized with rectangular finite difference grids. Total coverage of the model grids is 629.18 km² (32.6 km X 19.3 km). A uniform grid of 100 m X 100 m has been specified in the entire area (Figure 9).

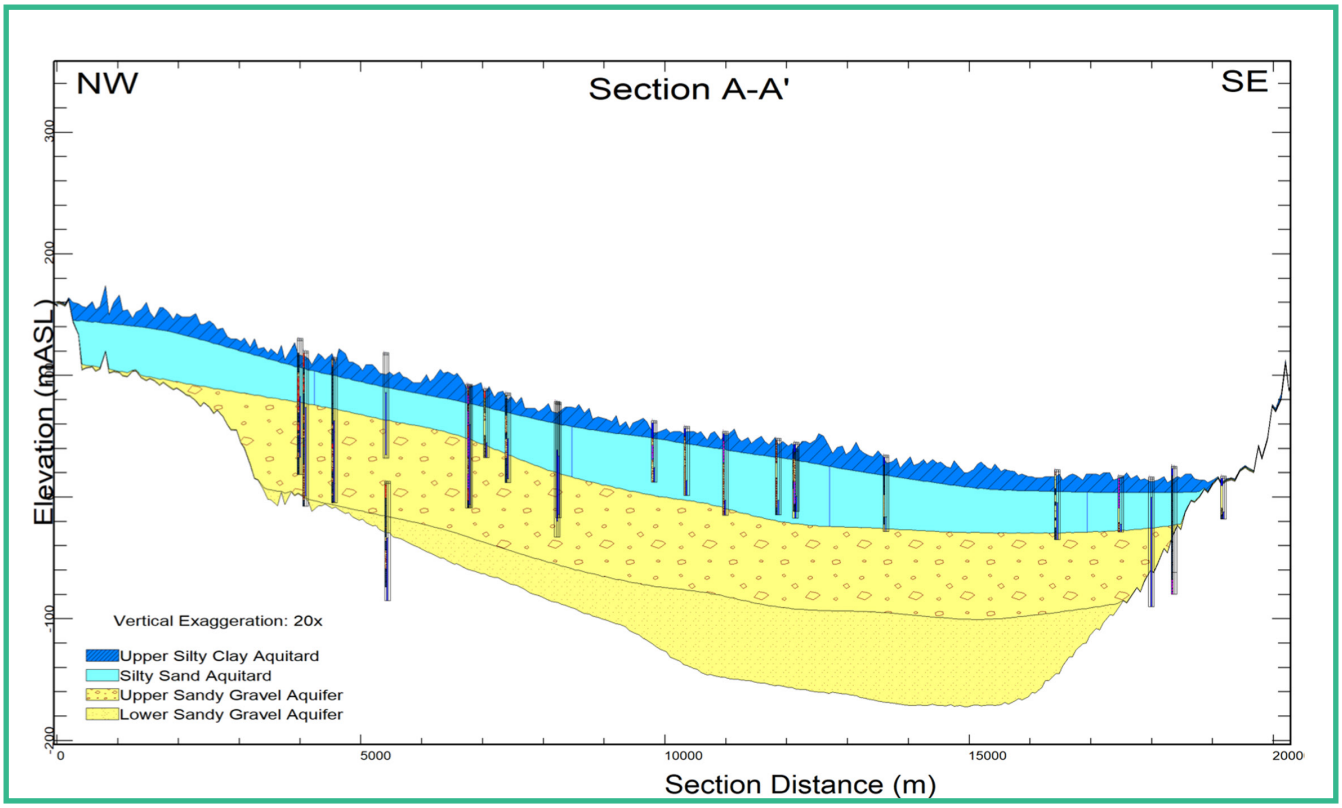

Figure 7 - Geologic section A-A' showing generalized interpreted hydrostratigraphy.

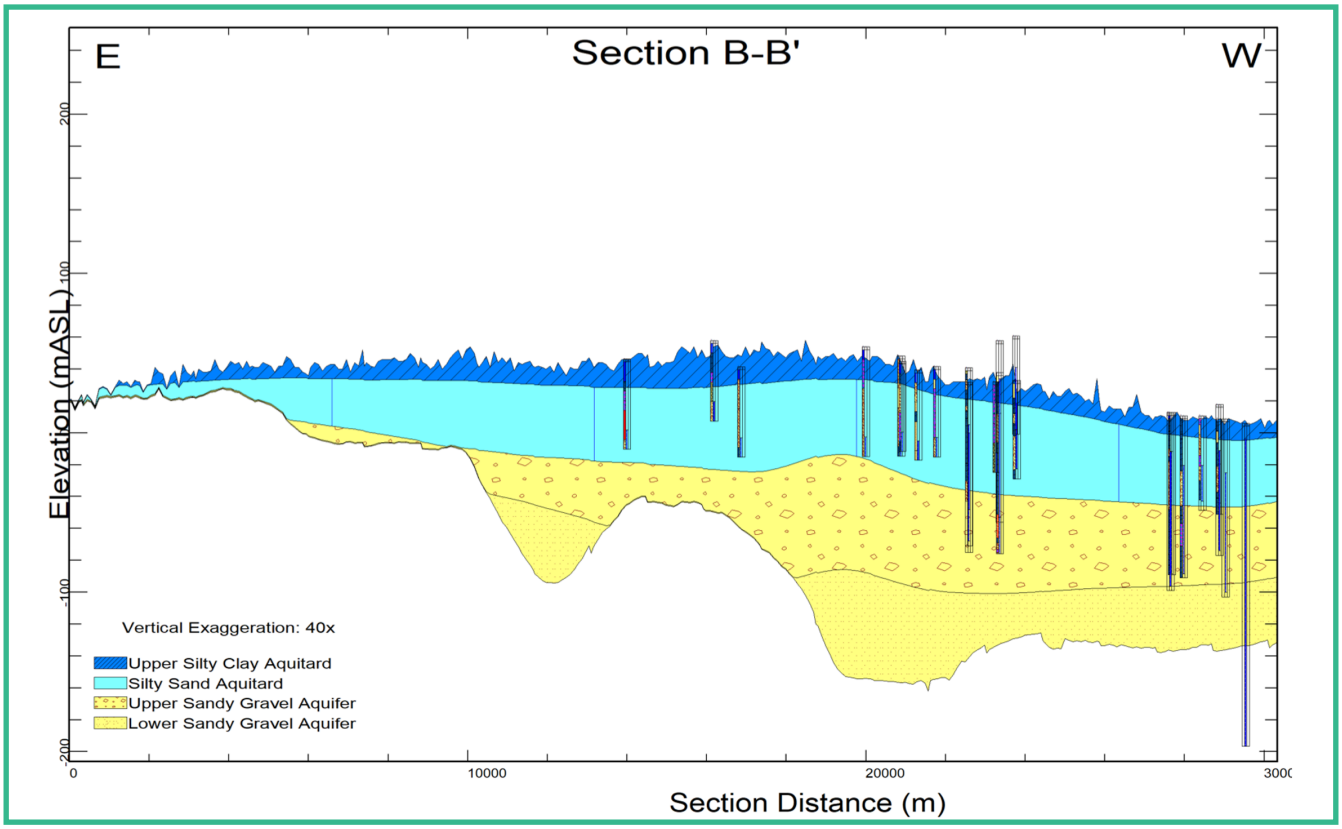

Figure 8 - Geologic section B-B' showing generalized interpreted hydrostratigraphy.

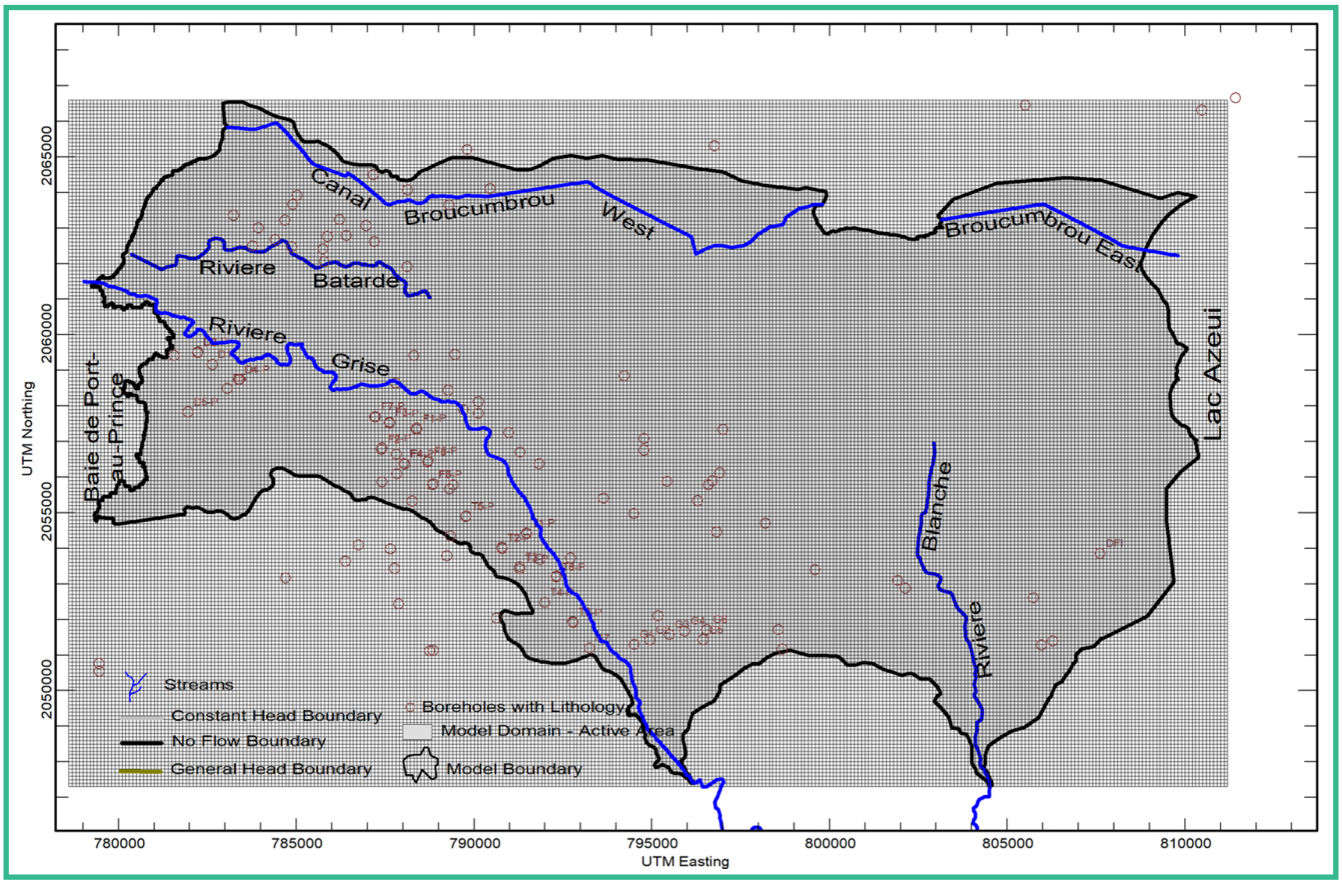

Figure 9 - Groundwater flow model domain and grid.

3.6 - Selection of Layers

Model layers were selected based on bulk hydrostratigraphic units interpreted from borehole logs, expert knowledge of the aquifer, and surficial geological maps. The hydrostratigraphic units applied in the modeling are based on the geologic model discussed in Section 2.3.

A low permeability bedrock layer has been chosen as the model bottom. In areas where individual stratigraphic units were absent from the stratigraphic sequence (e.g., discontinuities, non-conformities, pinch-outs), a minimum thickness of 0.5 m was used to ensure layer continuity across the model domain, and the hydraulic conductivity was changed to match that of the underlying unit found immediately below. These corrections were applied across the entire model domain using Viewlog's equation processing utility.

Following are the model layers from top to bottom:

- **Layer 1: Upper Silty Clay Aquitard**
- **Layer 2: Silty Sand Aquifer**
- **Layer 3: Upper Sandy Gravel Aquifer**
- **Layer 4: Lower Sandy Gravel Aquifer**

3.7 - Boundary Conditions

A number of specified heads have been assigned along the natural model boundaries. A specified head boundary reflects a situation where the water table or potentiometric surface is pre-specified in time. The model calculates the flux across this boundary assuming a pre-specified value of head at that location. A specified head boundary must be placed sufficiently far from stress points so as not to be a source of unreasonable flux.

Figure 10 shows the model boundary conditions. The following sub-sections discuss the selection of different boundary conditions.

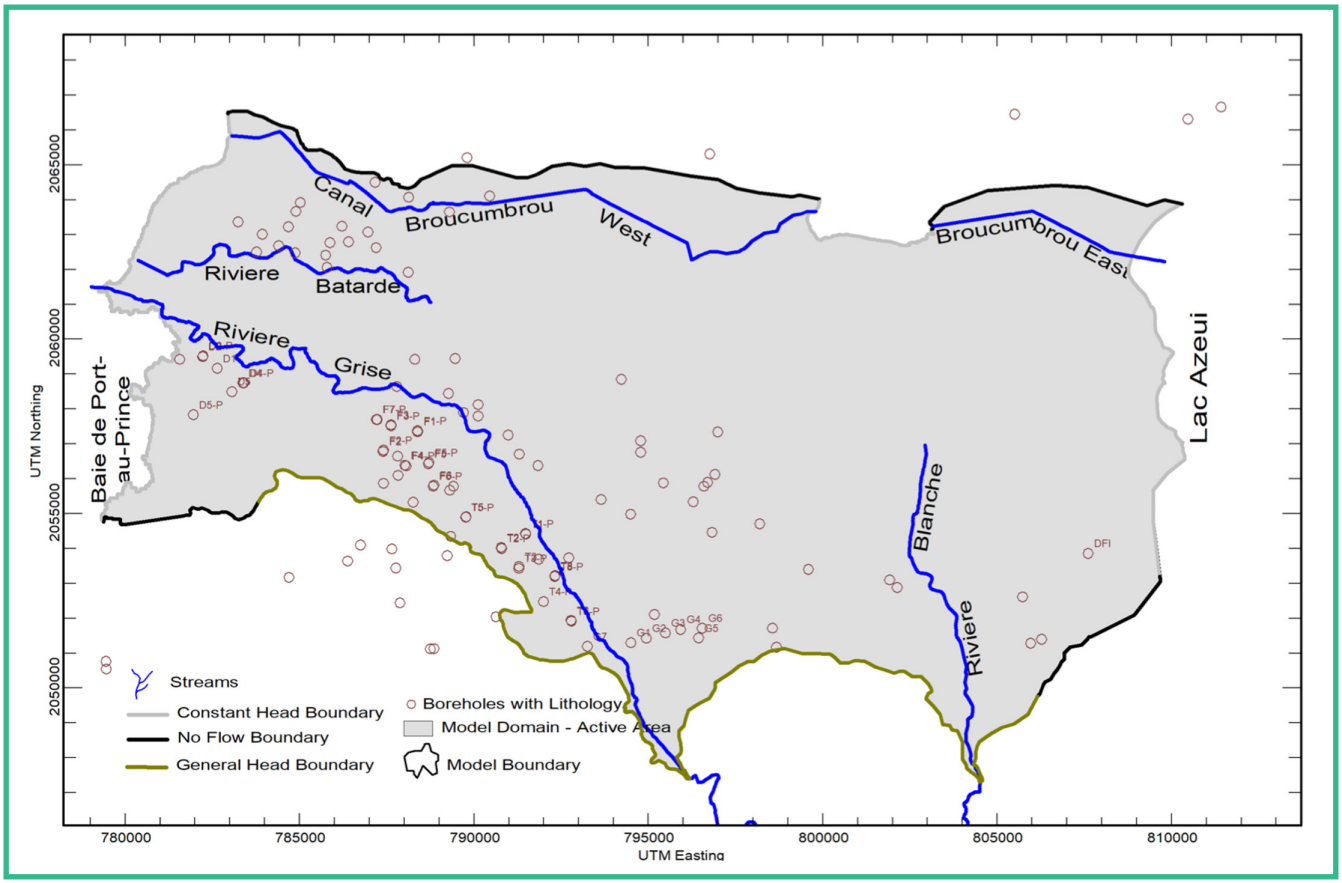

Figure 10 - Groundwater flow model boundary conditions.

3.7.1 - Lateral Boundaries

As discussed in Section 3.4, the model extent was selected to follow the delineated extent of alluvium and definitive contacts with bedrock. Ideally, the specified head boundaries are applied to large natural features with known heads, such as ocean or large lakes. Specified head boundaries have been selected along the ocean (0 masl) in the west, Lac Azuei (20 masl) in the east, and Trou Caiman (23.4 masl) in the north.

The northern boundary coincides with the overburden valley outline where the bedrock outcrops, and has been assigned no flow boundaries.

During preliminary model runs, it was determined that a general head boundary needed to be defined in the southern aquifer limit to account for subsurface groundwater flow entering the aquifer from adjacent Massif de la Selle karst limestone aquifer system. The general head boundary was assigned as shown in Figure 10 with a 0.04 gradient.

3.7.2 - Surface Boundaries

The model bottom works as a no flow/zero flux boundary while recharge has been assigned as a constant flux boundary at each uppermost active cell except surface water features.

3.7.3 - Recharge

Groundwater recharge represents the amount of water entering the top of the model and is one of the input parameters required for the numerical simulations. Richards (2007) discusses the difficulties associated with the reliable estimation of infiltration, and argues that, because of the non-linear recharge response with time, "recharge cannot be

described by a simple direct relationship to precipitation, since not all precipitation produces recharge". Rather, recharge is a component of the water budget that is typically derived from an array of measured and derived parameters.

Direct aerial recharge from precipitation was derived from country-scale modeling (Miner and Adamson, 2017). The estimates were developed with custom spatial datasets that include geologic permeability, slope, land cover/vegetation (NDVI), drainage density, and evapotranspiration. The Climate Normals (1961-1990) were applied to derive mean gridded estimates of the long-term average annual effective infiltration.

The Riviere Grise basin was one of the calibration areas for the Miner and Adamson (2017) modeling, as it was one of the few basins in Haiti with historical streamflow data to support calibration. Based on the analysis, the recharge ranges from less than 5 to over 230 mm/year across the aquifer and provides an input of approximately 15,000 m³/year into it (Figure 11). Increased recharge also occurs along the edges of the alluvial valley at bedrock contacts where surficial runoff from the mountains enters the plain. In general, recharge decreases in the lower elevations due to reduced precipitation, increased evapotranspiration, and less permeable soils.

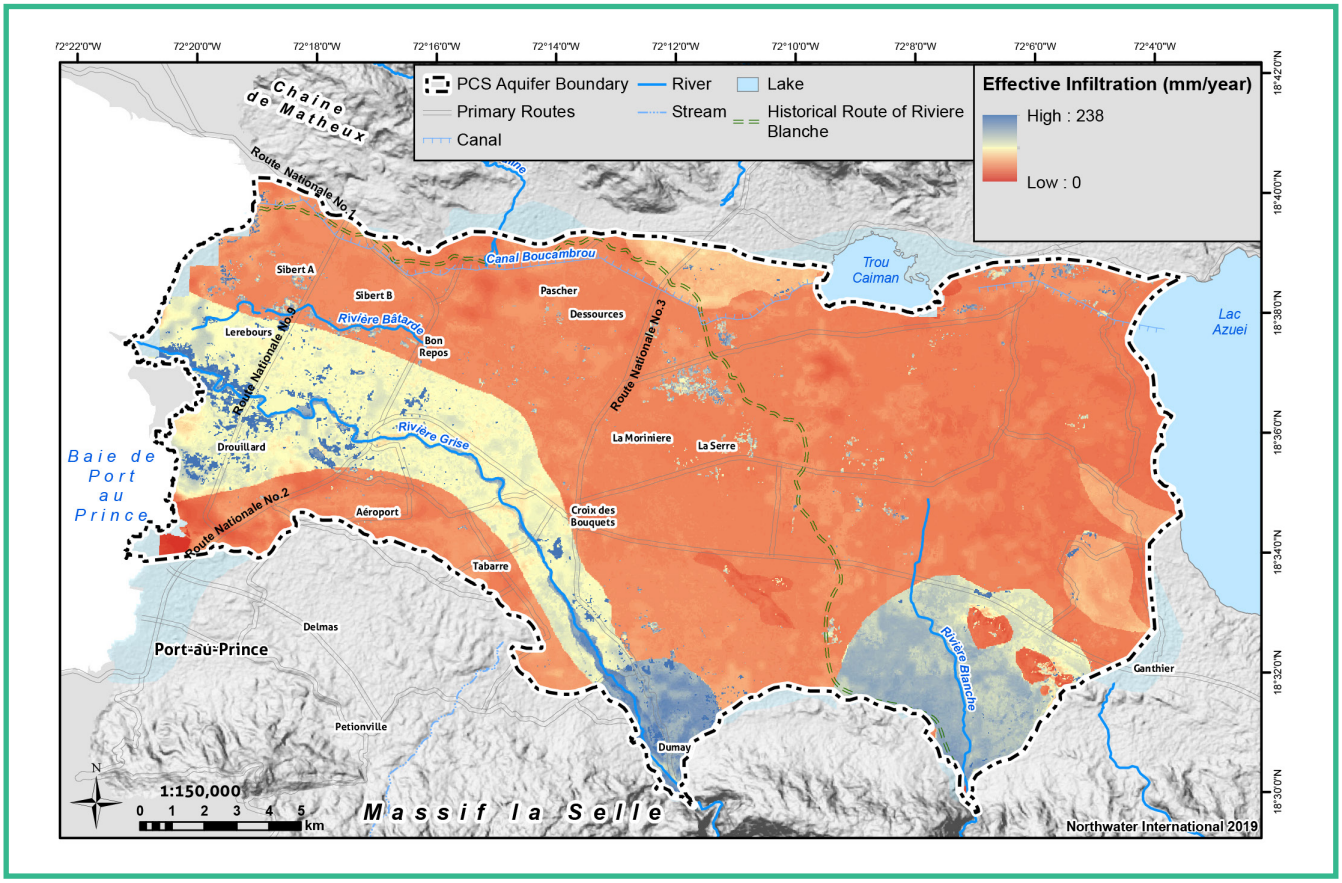

Figure 11 - Groundwater recharge by infiltration.

3.7.4 – Rivers and Streams

Streams have been defined with MODFLOW "river" and "drain" packages. The flux at a river cell can be either discharging (water exiting the model domain and entering the surface water regime) or recharging (water entering the model domain). Depending on the surrounding groundwater conditions, which are calculated by the model, the river cells will have a positive or negative flux. The flux at a drain cell can only be discharging (water exiting the model domain into the surface water regime). When the water level in the model is below the elevation of the drain cell, there is no interaction between the drain cell and the model domain, and consequently the flux is zero. Canal Boucambrou has been modelled with the drain package, while the Grise, Batarde, and Blanche rivers have been modeled with the river package.

Actual data defining the properties (such as width, bed thickness, water level, bed elevation, hydraulic conductivity of the bed materials etc.) of drains and streams are not available for every cell. However, several cross sections and field observations were made available from previous reconnaissance activities by the team. The 1.5m LIDAR elevation dataset was valuable for interpolating cross sections along the length of the streams.

3.7.5 – Pumping Wells

There are 141 pumping wells currently incorporated into the model, pumping approximately 75,000 m³/day (Figure 12 and Table 3). Pumping wells were assigned to appropriate hydrostratigraphic layers based on their actual or inferred screen elevations.

· There are 26 municipal CTE-RMPP production wells. Pumping rates were established based on recent data obtained upon request. The daily pumping rates range from 4,230 m³/day (F2) to 0 m³/day (G wells, and new Canaan well).

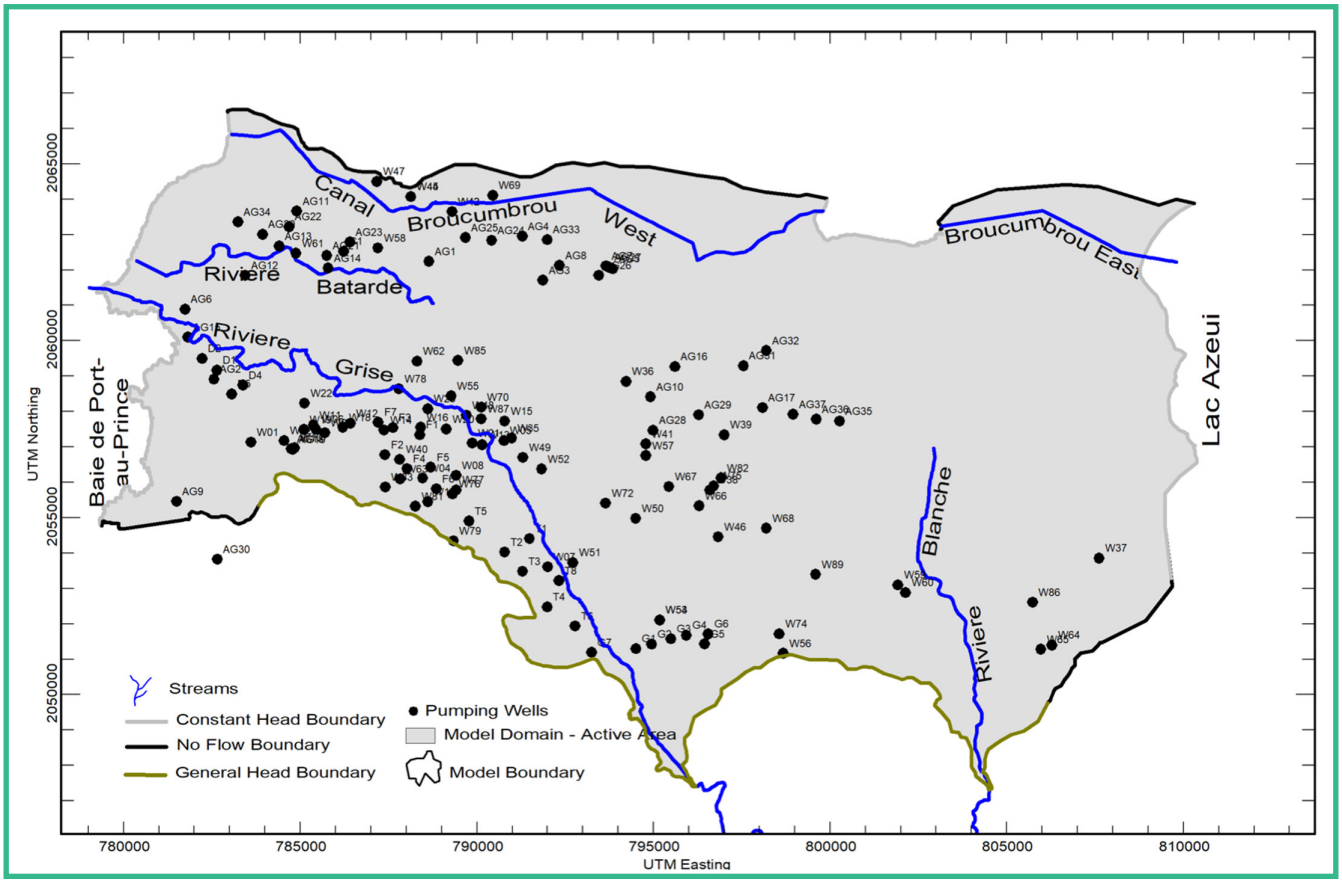

Figure 12 - Pumping Wells Incorporated into the Model.

- There was no pumping data available for agricultural wells in the plain. For the purpose of initial model runs, a pumping rate of 250 m^3/day was assigned to 37 agricultural wells spread across the plain for which borehole records were available.

- There was no pumping data available for commercial and private wells. Pumping rates were assigned based on a World Bank survey of several large capacity truck filling stations in the plain and the reported pump sizes that were installed on private wells from well records. There are 50 commercial / private wells included.

- Community wells refer to wells that are typically equipped with hand pumps or small submersible pumps; there are hundreds of such wells across the plain. We assigned a 15 m^3/day pumping rate to 27 of these wells to account for this demand in initial model runs.

Well ID	Type	UTM X	UTM Y	Elev (masl)	Total Depth (m)	Bottom Elevation (masl)	Screen Top (masl)	Screen Bot (masl)	Pump Rate (m^3/d)
AG1	Agriculture	788641	2062246	20.3	98.80	-78.5	-30.4	-75.2	-250
AG2	Agriculture	782556	2058919	8.0	89.00	-81.0	-7.5	-40.3	-250
AG3	Agriculture	791870	2061715	25.8	97.50	-71.7	19.6	-68.8	-250
AG4	Agriculture	791283	2062957	21.6	96.30	-74.7	15.5	-71.2	-250
AG5	Agriculture	793847	2062038	25.4	91.40	-66.0	3.5	-63.2	-250
AG6	Agriculture	781738	2060895	4.8	91.40	-86.6	-5.0	-81.8	-250
AG7	Agriculture	793655	2062118	24.9	156.00	-131.1	-101.1	-131.1	-250
AG8	Agriculture	792337	2062133	24.3	82.30	-58.0	5.7	-53.3	-250
AG9	Agriculture	781499	2055464	6.4	96.20	-89.8	-8.3	-41.3	-250
AG10	Agriculture	794914	2058418	44.9	193.80	-148.9	-17.5	-140.6	-250
AG11	Agriculture	784898	2063668	9.8	97.50	-87.7	6.8	-83.7	-250
AG12	Agriculture	783440	2061850	7.7	77.70	-70.0	6.7	-52.2	-250
AG13	Agriculture	784401	2062680	11.1	173.70	-162.6	-93.0	-128.4	-250
AG14	Agriculture	785787	2062056	14.6	93.00	-78.4	2.6	-59.5	-250
AG15	Agriculture	781817	2060105	7.2	50.30	-43.1	-13.6	-57.2	-250
AG16	Agriculture	795607	2059275	32.5	91.40	-58.9	14.5	-56.1	-250
AG17	Agriculture	798091	2058111	34.3	110.60	-76.3	1.5	-73.8	-250
AG18	Agriculture	784740	2056950	19.5	104.80	-85.3	-14.0	-81.6	-250
AG19	Agriculture	784784	2056937	20.0	77.40	-57.4	2.2	-53.6	-250
AG20	Agriculture	783933	2063011	8.4	201.00	-192.6	0.4	-103.6	-250
AG21	Agriculture	785752	2062410	13.6	103.50	-89.9	-5.3	-60.2	-250
AG22	Agriculture	784680	2063226	9.2	61.00	-51.8	-7.4	-44.3	-250
AG23	Agriculture	786404	2062791	13.6	149.39	-135.8	1.0	-88.1	-250
AG24	Agriculture	790413	2062840	21.0	236.20	-215.2	-25.6	-197.0	-250
AG25	Agriculture	789670	2062918	20.6	108.60	-88.0	-18.1	-77.4	-250
AG26	Agriculture	793447	2061852	26.0	152.00	-126.0	-96.0	-126.0	-250
AG27	Agriculture	793725	2062082	25.0	83.80	-58.8	-28.8	-58.8	-250
AG28	Agriculture	794988	2057476	53.7	111.20	-57.5	14.8	-43.6	-250
AG29	Agriculture	796274	2057910	43.3	102.10	-58.8	15.5	-54.6	-250
AG30	Agriculture	782648	2053828	53.9	102.10	-48.2	26.1	-44.0	-250
AG31	Agriculture	797541	2059296	29.0	121.90	-92.9	-63.3	-88.6	-250
AG32	Agriculture	798195	2059727	29.0	114.90	-85.9	-20.9	-82.7	-250
AG33	Agriculture	791988	2062862	21.8	125.00	-103.2	-73.2	-103.2	-250
AG34	Agriculture	783237	2063361	7.1	82.01	-74.9	-25.9	-71.9	-250
AG35	Agriculture	800265	2057732	42.0	102.40	-60.4	18.2	-57.4	-250
AG36	Agriculture	799607	2057785	40.4	105.20	-64.8	9.8	-60.8	-250
AG37	Agriculture	798953	2057926	37.6	111.28	-73.7	0.0	-70.0	-250
D1	Municipal	782636	2059170	9.0	57.60	-48.60	-20.32	-42.8	-250
D2	Municipal	782221	2059502	7.0	58.00	-51.00	-19.60	-43.9	-1193
D4	Municipal	783376	2058750	11.0	100.00	-89.00	-11.52	-60.5	-2890
D5	Municipal	783057	2058499	9.0	100.00	-91.00	-81.31	-88.4	-2401
F1	Municipal	788385	2057349	39.0	110.00	-71.00	5.17	-68.0	-2202
F2	Municipal	787396	2056780	37.0	83.00	-46.00	-37.58	-46.0	-4230
F3	Municipal	787619	2057552	36.0	111.80	-75.80	-70.22	-75.8	-3463
F4	Municipal	788018	2056389	41.0	45.00	-4.00	16.93	-4.0	-3296
F5	Municipal	788692	2056430	47.0	104.40	-57.40	28.66	-18.2	-4046
F6	Municipal	788848	2055817	50.0	62.00	-12.00	12.58	-7.8	-3371
F7	Municipal	787206	2057700	31.0	60.00	-29.00	18.60	-22.7	-1463
G1	Municipal	794499	2051304	118.5	121.30	-2.8	72.1	-0.4	0
G2	Municipal	794943	2051429	128.6	97.80	30.8	82.8	32.6	0
G3	Municipal	795487	2051581	127.7	110.20	17.5	84.2	23.3	0
G4	Municipal	795926	2051680	127.1	104.90	22.2	84.5	39.6	0
G5	Municipal	796442	2051437	125.3	125.70	-0.4	55.7	0.6	0
G6	Municipal	796546	2051718	121.6	130.00	-8.4	49.0	-6.1	0
G7	Municipal	793248	2051196	113.2	118.00	-4.8	45.5	-3.8	0
T1	Municipal	791481	2054411	77.0	110.00	-33.00	-8.10	-19.7	-3375
T2	Municipal	790783	2054031	74.0	100.03	-26.03	-19.76	-25.7	-2324
T3	Municipal	791290	2053485	84.0	109.00	-25.00	44.35	-23.9	-2470
T4	Municipal	791989	2052481	99.0	110.00	-11.00	60.17	7.9	-242
T5	Municipal	789772	2054908	61.0	102.00	-41.00	27.20	-39.8	-1788
T6	Municipal	792781	2051939	11.1	96.22	-85.09	-33.67	-85.1	-2916
T8	Municipal	792321	2053224	91.0	100.00	-9.00	59.73	-6.0	-1266
W01	Private	783602	2057135.4	11.4	70.0	-58.6	-16.6	-56.6	-2422
W02	Private	784539	2057182.3	16.7	70.0	-53.3	-11.3	-51.3	-4542
W03	Private	785694	2057400.9	22.7	70.0	-47.3	-5.3	-45.3	-1696
W04	Private	788462	2056123.4	45.9	70.0	-24.1	17.9	-22.1	-407
W05	Private	790764	2057183.1	52.6	70.0	-17.4	37.6	-12.4	-1817
W06	Private	785446	2057501.1	20.8	60.0	-39.2	5.8	-34.2	-814
W07	Private	792002	2053613.1	84.4	60.0	24.4	69.4	29.4	-163
W08	Private	789406	2056198.6	51.9	60.0	-8.1	36.9	-3.1	-182

Well ID	Type	UTM X	UTM Y	Elev (masl)	Total Depth (m)	Bottom Elevation (masl)	Screen Top (masl)	Screen Bot (masl)	Pump Rate (m^3/d)
W09	Private	786004	20576000	22.5	60.0	-37.5	7.5	-32.5	-569
W10	Private	784831	2056982.3	20.2	60.0	-39.8	5.2	-34.8	-569
W11	Private	785370	2057621.8	19.7	60.0	-40.3	4.7	-35.3	-2023
W12	Private	786417	2057669	26.0	60.0	-34.0	11.0	-29.0	-569
W13	Private	790143	2057062.8	50.9	60.0	-9.1	35.9	-4.1	-569
W14	Private	787369	2057477	32.0	60.0	-28.0	17.0	-23.0	-1453
W15	Private	790782	2057731	48.0	60.0	-12.0	33.0	-7.0	-2023
W16	Private	788401	2057556	37.0	60.0	-23.0	22.0	-18.0	-569
W17	Private	788604	2055455.3	50.3	60.0	-9.7	35.3	-4.7	-569
W18	Private	786206	2057556.8	24.2	60.0	-35.8	9.2	-30.8	-1453
W19	Private	785098	2057495.8	20.2	60.0	-39.8	5.2	-34.8	-569
W20	Private	789132	2057509	42.0	60.0	-18.0	27.0	-13.0	-136
W21	Private	789862	2057112	48.0	60.0	-12.0	33.0	-7.0	-136
W22	Private	785115	2058240	18.8	60.0	-41.2	3.8	-36.2	-250
W23	Private	788608	2058080	37.5	60.0	-22.5	22.5	-17.5	-388
C1	Municipal	786227	2062528.9	14.2	82.0	-67.8	1.2	-64.8	0
W35	Community	790974	2057252.8	52.2	67.1	-14.9	-2.7	-14.9	-15
W36	Community	794224	2058853.8	39.7	54.9	-15.2	-3.0	-15.2	-15
W37	Community	807614	2053859.6	58.4	54.9	3.6	15.8	3.6	-15
W38	Community	796596	2055789	64.3	54.9	9.4	21.6	9.4	-15
W39	Community	796994	2057346.2	44.6	54.9	-10.3	1.9	-10.3	-15
W40	Community	787814	2056650.7	39.6	48.8	-9.1	3.1	-9.1	-15
W41	Community	794779	2057090	56.1	48.8	7.4	19.6	7.4	-15
W42	Community	789292	2063651.8	18.7	29.0	-10.2	-4.1	-10.2	-15
W43	Community	789292	2063651.8	18.7	36.6	-17.8	-5.6	-17.8	-15
W44	Community	788124	2064077	23.7	103.7	-80.0	23.7	23.7	-15
W45	Community	788124	2064077	23.7	85.4	-61.7	23.7	23.7	-15
W46	Community	796828	2054463.4	94.6	61.0	33.6	45.8	33.6	-15
W47	Community	787167	2064505.5	15.4	33.5	-18.1	-12.0	-18.1	-15
W48	Community	789697	2057897.9	37.6	54.9	-17.2	-5.0	-17.2	-15
W49	Community	791299	2056703.9	56.3	54.9	1.4	13.6	1.4	-15
W50	Community	794495	2054980.9	83.5	48.8	34.7	46.9	34.7	-15
W51	Community	792718	2053734.9	87.4	54.9	32.6	44.8	32.6	-15
W52	Community	791833	2056379.8	61.0	48.8	12.2	24.4	12.2	-15
W53	Community	795174	2052111.3	119.2	61.0	58.2	70.4	58.2	-15
W54	Community	795174	2052111.3	119.2	61.0	58.2	70.4	58.2	-15
W55	Community	789266	2058445.1	39.8	54.9	-15.1	-2.9	-15.1	-15
W56	Community	798675	2051169	112.3	91.5	20.8	39.1	26.9	-15
W57	Community	794785	2056757.8	58.9	54.9	4.1	16.3	4.1	-15
W58	Community	787196	2062622.9	15.7	44.2	-28.5	-22.4	-28.5	-15
W59	Community	801921	2053103.5	86.4	61.0	25.4	37.6	25.4	-15
W60	Community	802135	2052885.4	92.2	54.9	37.3	49.5	37.3	-15
W61	Community	784875	2062477	12.4	45.7	-33.4	-21.2	-33.4	-15
W62	Commercial	788300	2059427.3	30.9	61.0	-30.1	-17.9	-30.1	-500
W63	Private	787823	2056097	41.4	48.8	-7.4	4.8	-7.4	-50
W64	Private	806280	2051400.7	160.2	115.9	44.3	62.6	44.3	-50
W65	Private	805965	2051284.9	130.4	54.9	75.6	87.8	75.6	-50
W66	Private	796286	2055341.1	72.4	67.1	5.3	17.5	5.3	-50
W67	Private	795432	2055881.7	68.2	64.0	4.2	14.8	4.2	-50
W68	Private	798197	2054706.4	62.8	91.5	-28.6	-16.4	-28.6	-50
W69	Private	790446	2064112.6	20.5	42.7	-22.2	-10.0	-22.2	-50
W70	Private	790116	2058125.8	43.2	54.9	-11.7	0.5	-11.7	-50
W71	Private	820631	2046429.8	139.9	97.6	42.3	54.5	42.3	-50
W72	Private	793643	2055410.8	74.0	54.9	19.1	31.3	19.1	-50
W73	Private	816627	2052013.4	23.5	68.6	-45.1	-39.0	-45.1	-50
W74	Private	798561	2051721.1	107.3	61.0	46.3	58.5	46.3	-50
W75	Private	796699	2055901.4	62.3	61.0	1.3	13.5	1.3	-50
W76	Private	789308	2055676.5	53.4	54.9	-1.5	10.7	-1.5	-50
W77	Private	789412	2055788.9	53.6	54.9	-1.3	10.9	-1.3	-50
W78	Private	787784	2058644.1	30.2	54.9	-24.7	-12.5	-24.7	-50
W79	Private	789328	2054347.6	65.8	54.9	10.9	23.1	10.9	-50
W80	Private	821151	2046992.5	85.4	79.3	6.2	85.4	85.4	-50
W81	Private	788257	2055328.2	49.7	67.1	-17.4	0.9	-11.3	-50
W82	Private	796907	2056126.3	58.6	54.9	3.8	16.0	3.8	-50
W83	Private	787404	2055869.1	42.9	67.1	-24.2	-12.0	-24.2	-50
W84	Private	821364	2046885.3	78.2	85.4	-7.1	5.1	-7.1	-50
W85	Private	789462	2059445.1	32.7	61.0	-28.3	-16.1	-28.3	-50
W86	Commercial	805732	2052610.5	92.0	73.2	18.9	31.1	18.9	-50
W87	Commercial	790121	2057793.6	46.4	61.0	-14.6	-2.4	-14.6	-50
W89	Agriculture	799591	2053399	82.7	109.8	-27.0	-2.6	-20.9	-500
W90	Commercial	820704	2048425.3	26.6	64.0	-37.5	-25.3	-37.5	-500

Table 3 - Pumping wells incorporated into the model.

3.8 – Model Parameterization

Initial hydraulic conductivity (K) values for the model were compiled from 35 pump tests throughout the aquifer (Northwater 2018) and derived from specific capacity estimates and published literature (Freeze & Cherry 1979) where necessary.

Hydraulic conductivity was adjusted as required during model calibration to improve results, as described in the following section. As previously mentioned, a general head boundary was added to the southern aquifer limits during the calibration process as hydraulic conductivity modifications were not a practical solution given the ranges of values from wells.

4.0 Model Calibration

4.1 – General Approach

Calibration is the process of adjusting the model parameters within reasonable limits to obtain a good match between the model results and the estimates derived from actual observations.

To evaluate the model calibration, the resulting heads generated from the simulations were compared to the water table measurements at different observation wells. There were 131 observation points throughout the model area in hydrogeological database (Northwater 2018). The locations of these observation wells are shown in Figure 14. The targets were assigned to appropriate model layers based on the reported or inferred screen bottom elevations. A number of targets either did not have any screen or well construction information available. In these situations, a first attempt was made to assign layers based on the bottom of the well. If the bottom elevation of the well was also not available, the target was assigned to the primary production layer of the aquifer.

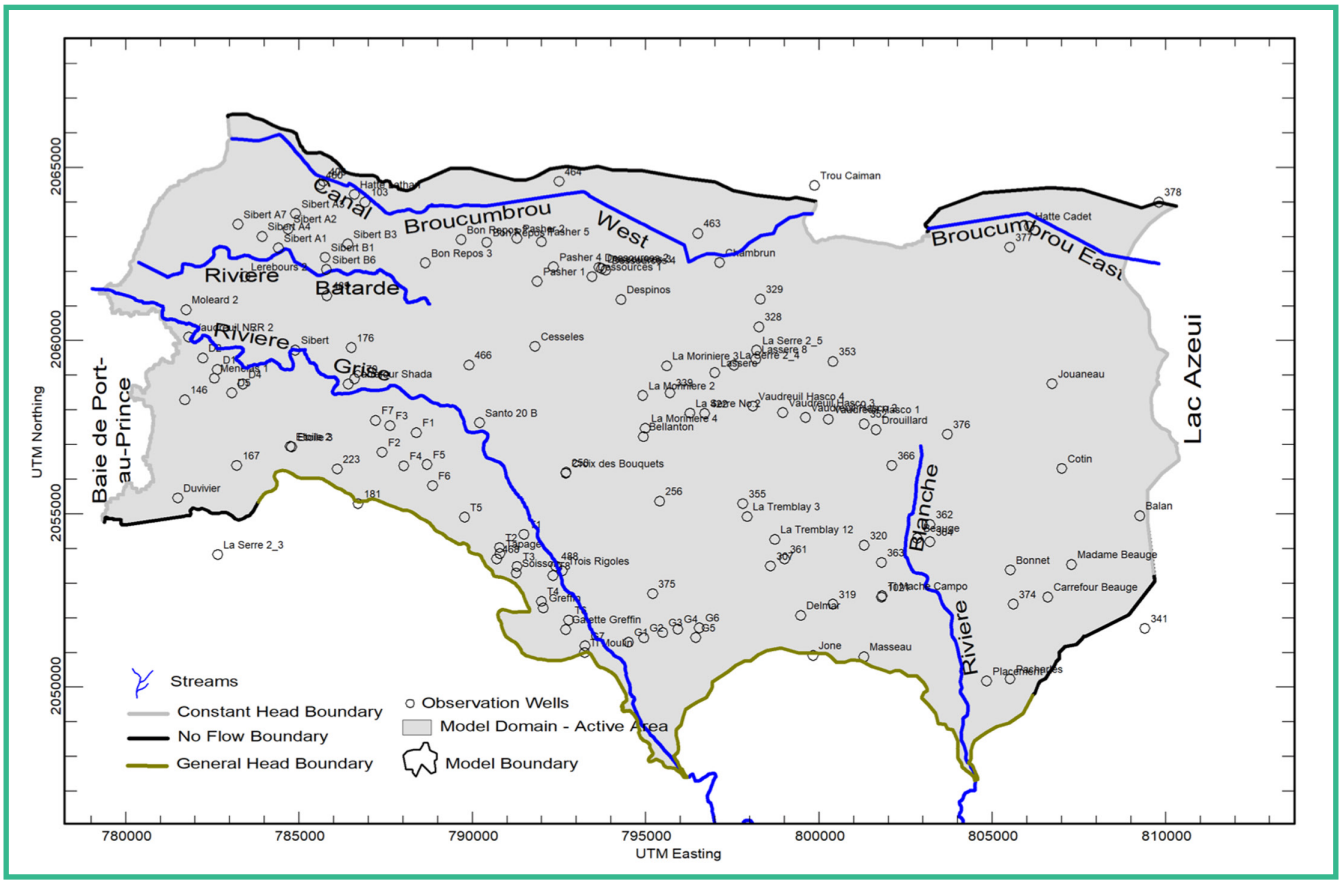

Figure 13 - Observation wells used for calibration targets.

The Root Mean Square (RMS) error is an overall measure of the differences between values predicted using a model and the observed values. The values of the residual were plotted at the location of each observation point and compared with the contoured potentiometric surface. The cumulative probability of the residuals was also plotted to monitor the relative degree to which the simulation matches the field data. While calibrating the model, groundwater flow directions, water budget, and hydraulic head gradients were compared qualitatively between simulated and measured values to verify the reasonableness of the resulting simulations.

4.2 - Calibration Targets

Figure 13 illustrate the groundwater elevation calibration targets that were assigned for the model calibration process. The elevations are based on discrete measurements of static water levels in wells from various well testing or monitoring campaigns.

Well Name	UTM X (m)	UTM Y (m)	Elev. (masl)	Well Depth (m)	Screen Top (masl)	Screen Bottom (masl)	Target Head (masl)
Bon Repos 3	788641	2062246	20.3	98.8	-30.4	-75.2	18.2
Menelas 1	782556	2058919	8	89	-7.5	-40.3	6.2
Pasher 1	791870	2061715	25.8	97.5	19.6	-68.8	25.2
Pasher 2	791283	2062957	21.6	96.3	15.5	-71.2	19.6
Dessources 4	793847	2062038	25.4	91.4	3.5	-63.2	24.5
Moleard 2	781738	2060895	4.8	91.4	-5	-81.8	4.2
Dessources 2	793655	2062118	24.9	156			23.7
Pasher 4	792337	2062133	24.3	82.3	5.7	-53.3	23.1
Duvivier	781499	2055464	6.4	96.2	-8.3	-41.3	3
La Moriniere 2	794914	2058418	44.9	193.8	-17.5	-140.6	42.8
Sibert A3	784898	2063668	9.8	97.5	6.8	-83.7	7.7
Lerebours 2	783440	2061850	7.7	77.7	6.7	-52.2	5.3
Sibert A1	784401	2062680	11.1	173.7	-93	-128.4	8.7
Sibert B6	785787	2062056	14.6	93	2.6	-59.5	10.9
Vaudreuil NRR 2	781817	2060105	7.2	50.3	-13.6	-57.2	4.8
La Moriniere 3	795607	2059275	32.5	91.4	14.5	-56.1	28.2
Vaudreuil Hasco 4	798091	2058111	34.3	110.6	1.5	-73.8	29.7
Etoile 2	784740	2056950	19.5	104.8	-14	-81.6	14.3
Etoile 3	784784	2056937	20	77.4	2.2	-53.6	14.8
Sibert A4	783933	2063011	8.4	201	0.4	-103.6	5.9
Sibert B1	785752	2062410	13.6	103.5	-5.3	-60.2	8.1
Sibert A2	784680	2063226	9.2	61	-7.4	-44.3	8.3
Sibert B3	786404	2062791	13.6	149.39	1	-88.1	10.9
Bon Repos 1	790413	2062840	21	236.2	-25.6	-197	21
Bon Repos 2	789670	2062918	20.6	108.6	-18.1	-77.4	17.7
Dessources 1	793447	2061852	26	152			26
Dessources 3	793725	2062082	25	83.8			24.9
La Moriniere 4	794988	2057476	53.7	111.2	14.8	-43.6	53.7
La Serre No.2	796274	2057910	43.3	102.1	15.5	-54.6	43.3
La Serre 2_3	782648	2053828	53.9	102.1	26.1	-44	53.9
La Serre 2_4	797541	2059296	29	121.9	-63.3	-88.6	29
La Serre 2_5	798195	2059727	29	114.9	-20.9	-82.7	28.9
Pasher 5	791988	2062862	21.8	125			21
Sibert A7	783237	2063361	7.1	82.01	-25.9	-71.9	2.2
Vaudreuil Hasco 1	800265	2057732	42	102.4	18.2	-57.4	42
Vaudreuil Hasco 2	799607	2057785	40.4	105.2	9.8	-60.8	33.5
Vaudreuil Hasco 3	798953	2057926	37.6	111.28	0	-70	37.6
D1	782636	2059170	9	57.6	-20.32	-42.8	5.5
D2	782221	2059502	7	58	-19.6	-43.9	5.7
D4	783376	2058750	11	100	-11.52	-60.5	9.2
T8	792321	2053224	91	100	59.73	-6	59.2
F5	788692	2056430	47	104.4	28.66	-18.2	40.7
T2	790783	2054031	74	100.03	-19.76	-25.7	55.8
T1	791481	2054411	77	110	-8.1	-19.7	56.3
T3	791290	2053485	84	109	44.35	-23.9	58.9
D5	783057	2058499	9	100	-81.31	-88.4	8.9
F3	787619	2057552	36	111.8	-70.22	-75.8	33.6
T5	789772	2054908	61	102	27.2	-39.8	46.3
T6	792781	2051939	11.1	96.22	-33.67	-85.1	0
F2	787396	2056780	37	83	-37.58	-46	34.2
F7	787206	2057700	31	60	18.6	-22.7	29.2
T4	791989	2052481	99	110	60.17	7.9	91.4
F1	788385	2057349	39	110	5.17	-68	38.6
F6	788848	2055817	50	62	12.58	-7.8	42.8
F4	788018	2056389	41	45	16.93	-4	37.9
G1	794499	2051304	118.5	121.3	72.1	-0.4	91.6
G2	794943	2051429	128.6	97.8	82.8	32.6	94
G3	795487	2051581	127.7	110.2	84.2	23.3	94.9
G4	795926	2051680	127.1	104.9	84.5	39.6	95.2

Well Name	UTM X (m)	UTM Y (m)	Elev. (masl)	Well Depth (m)	Screen Top (masl)	Screen Bottom (masl)	Target Head (masl)
G5	796442	2051437	125.3	125.7	55.7	0.6	81
G6	796546	2051718	121.6	130	49	-6.1	71.8
G7	793248	2051196	113.2	118	45.5	-3.8	91.1
Sibert	784890	2059729	14.9				11.13
Hatte Lathan	786595	2064221	10.3				7.4
Carrefour Shada	786418	2058752	25.3				18.5
Despinos	794282	2061187	29.4				15.8
Cesseles	791805	2059835	37.6				29.33
Santo 20 B	790207	2057636	48.1				32.29
Bellanton	794931	2057235	55.4				30.44
Croix des Bouquets	792694	2056172	64.4				32.31
Tapage	790796	2053856	75.6				64.2
Trois Rigoles	792593	2053360	83.2				78.18
Soisson	791265	2053295	83.5				80.57
Greffin	792041	2052291	96.4				92
Galette Greffin	792692	2051667	106.8				103.15
Ti Moulin	793232	2051003	118.3				115.49
Trou Caiman	799868	2064483	26.1				18.66
Chambrun	797132	2062255	25.5				21.11
Lassere 8	798175	2059472	30				28
Lassere	796991	2059080	32.1				31
La Tremblay 3	797926	2054929	58.5				40.23
La Tremblay 12	798723	2054267	82.2				49.26
Delmar	799469	2052075	94.6				81.72
Jone	799826	2050920	97.1				73.67
Drouillard	801644	2057430	43.7				29.2
Beauge	802835	2054304	73.1				61.37
Ti Mache Campo	801821	2052641	92.6				71.35
Masseau	801292	2050881	109.9				63.06
Placement	804834	2050183	160.7				104.45
Hatte Cadet	806068	2063306	25				15.4
Jouaneau	806723	2058757	33.9				28.23
Cotin	807006	2056311	42.4				36.16
Balan	809252	2054950	44.2				20.16
Madame Beauge	807284	2053544	54.1				37.24
Bonnet	805517	2053386	78.3				53.15
Carrefour Beauge	806598	2052606	64.4				62.5
Pacharles	805510	2050240	153.5				108
146	781700	2058300	3.5				2.5
167	783200	2056400	10.2				8.5
400	785700	2064600	6.1				7
460	785600	2064500	6				5
103	786900	2064000	12.2				8
489	785800	2061300	15.4				15
176	786500	2059800	20.4				18.5
466	789900	2059300	34.8				28
170	786600	2058900	25.7				21.5
223	786100	2056300	30.5				27
181	786700	2055300	48.7				30
464	792500	2064600	20.8				16.5
250	792700	2056200	63.7				32
468	790700	2053700	78.3				49
488	792400	2053500	78.9				51
463	796500	2063100	24.9				25
329	798300	2061200	30.3				26.5
328	798262	2060400	29.2				28.5
339	795700	2058500	39.4				30
422	796700	2057900	41.6				31
256	795400	2055370	75.2				35
355	797800	2055300	56.3				36
361	799000	2053700	82.2				56
307	798600	2053500	91.9				55
375	795200	2052700	113.7				71
353	800400	2059400	36.3				30
352	801300	2057600	44.1				32
376	803700	2057300	42.4				36.5
366	802100	2056400	55.2				39
362	803200	2054700	66.7				55.5
364	803200	2054200	75.3				59
320	801300	2054100	70.7				56
363	801800	2053600	79.4				58.5
1021	801800	2052600	93.8				65
319	800400	2052400	83.5				66
378	809800	2064000	24.2				23
377	805500	2062700	25.4				23.5
374	805600	2052400	98.9				58
341	809400	2051700	99.9				70

Table 4 - Model Calibration Targets.

4.3- Adjusted Parameters

The following model parameters were adjusted from their initial values to calibrate the model:

1. Hydraulic conductivity of model layers;
2. River bed conductance;
3. Stages in rivers, streams and canals.

A uniform value of 0.1 was assumed for the vertical anisotropy ratio (Kv/Kh) for all the hydraulic conductivity zones. Figure 14 shows the hydraulic conductivity zones that were established and applied to calibrate the model. These zones were selected based on the specific capacity and hydraulic conductivity data from over 45 locations in the aquifer that were available in the database, combined with a geomorphic analysis of the plain. During the calibration process, hydraulic conductivities had to be adjusted lower in many zones to achieve model calibration. This is attributed to the fact that specific capacity and pump test data were mostly available for higher capacity production wells. Table 4 presents the calibration parameters, calibrated value and their range of variation.

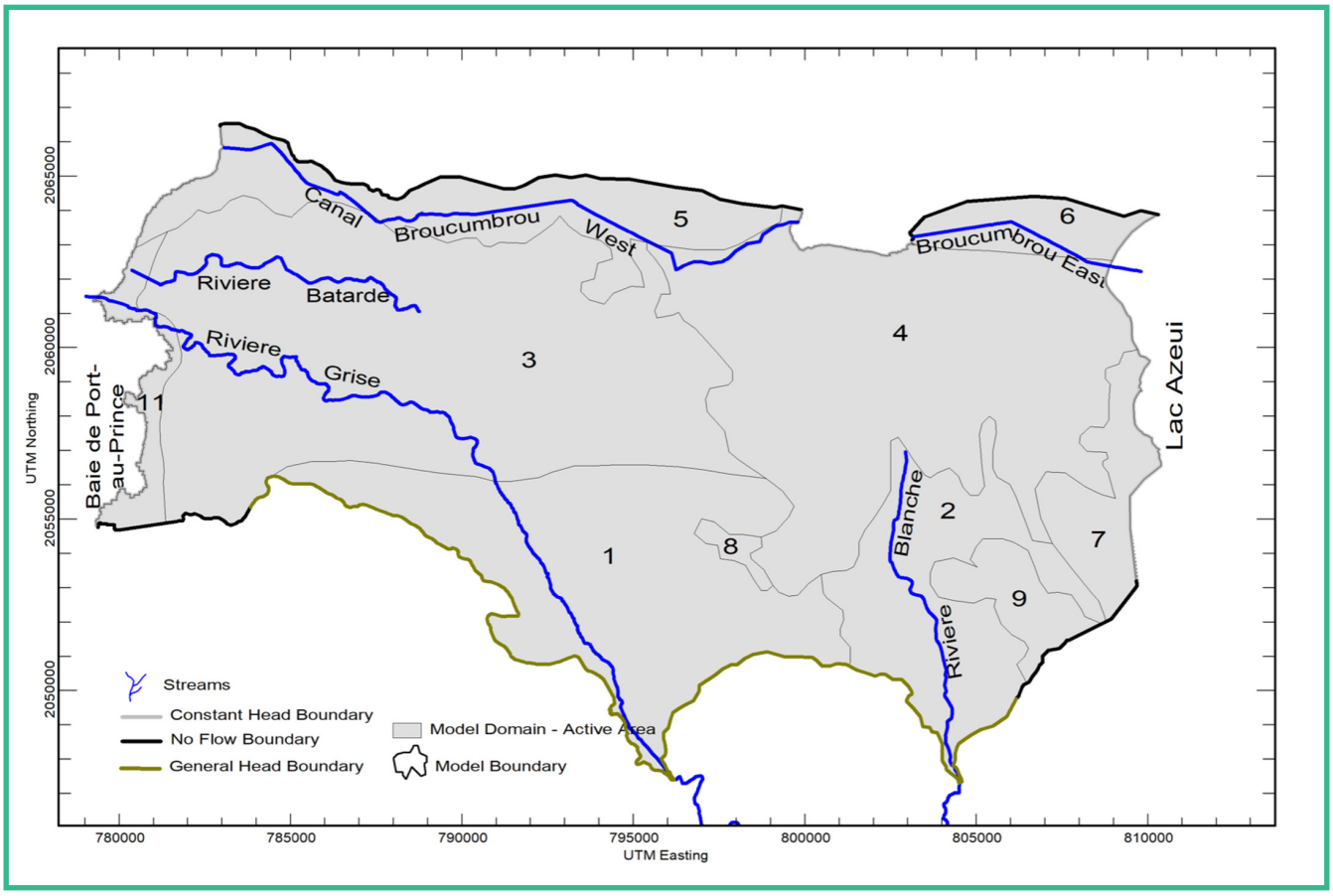

Figure 14 - Hydraulic conductivity zones developed for calibration.

Zone	Bulk Hydraulic Conductivity (m/d)			
	Layer 1	Layer 2	Layer 3	Layer 4
1		10	30	30
2		15	20	20
3		10	15	15
4		8	10	10
5		50	50	50
6		2	5	5
7		0.864	0.864	0.864
8		0.864	0.0864	0.0864
9		0.0864	0.0864	0.0864
10	0.00864			
11		10	30	30

Table 5 - Hydraulic conductivity values by zone.

4.4- Calibration Results

Figure 15 presents a scatter plot showing the goodness of fit between the observed and simulated heads. The 45° line represents the perfect match between observed and simulated heads while a random distribution of the points around the line indicates that the simulated heads are not over or under predicted across the study area. The root mean squared error (RMSE) value is 12.04 and absolute residual mean is 8.43 m. Considering a large range of observation points and the high gradient of the aquifer, the calibration obtained is very good. As a usual calibration practice, root mean squared residual (12.04 m) should be scaled by dividing it by the range of calibration points (115.5) to estimate a scaled root mean squared value that can be evaluated for the goodness of calibration. In our case, the scaled root mean squared value is 0.104 m.

The correlation coefficient between observed and model heads is 0.92. While a better calibration is represented by a correlation coefficient close to 1, Spitz and Moreno (1996) suggest that the correlation coefficient should lie between 0.7 and 1.0 for a calibrated flow model.

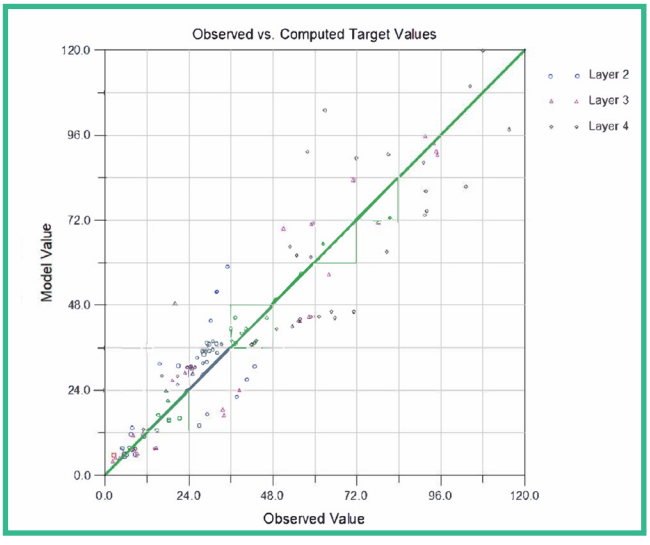

Figure 15 - Scatter Plot of Observed vs Simulated Heads.

5.0 - Model Results

5.1 - Groundwater Flow

Figure 16 shows the calibrated potentiometric surface map of the primary aquifer zone. The groundwater flow shows similar trends to what has been illustrated in previous literature. The hydraulic gradient is steepest in the southern limits of the aquifer where the Riviere Grise and Riviere Blanche enter the plain and recharge the aquifer. A groundwater divide bisects the aquifer in the east-central portion where groundwater flows either westward towards the ocean or north and eastward into Trou Caiman, Canal Boucambrou, and Lac Azuei.

Due to the limited potentiometric and lithology data, several areas have a limited level of confidence in terms of the groundwater flow model and groundwater balance:

- The eastern zone of the aquifer, between the simulated N-S oriented groundwater divide to the boundary of Lac Azuei.

- The northeastern zone of the aquifer, near the boundary with Trou Caiman, Canal Boucambrou and the bedrock contact in the northeast.

The south zone of the aquifer, where, due to bedrock underlying alluvium, it was difficult to interpret if observation wells were influenced by hydraulic heads in the bedrock units

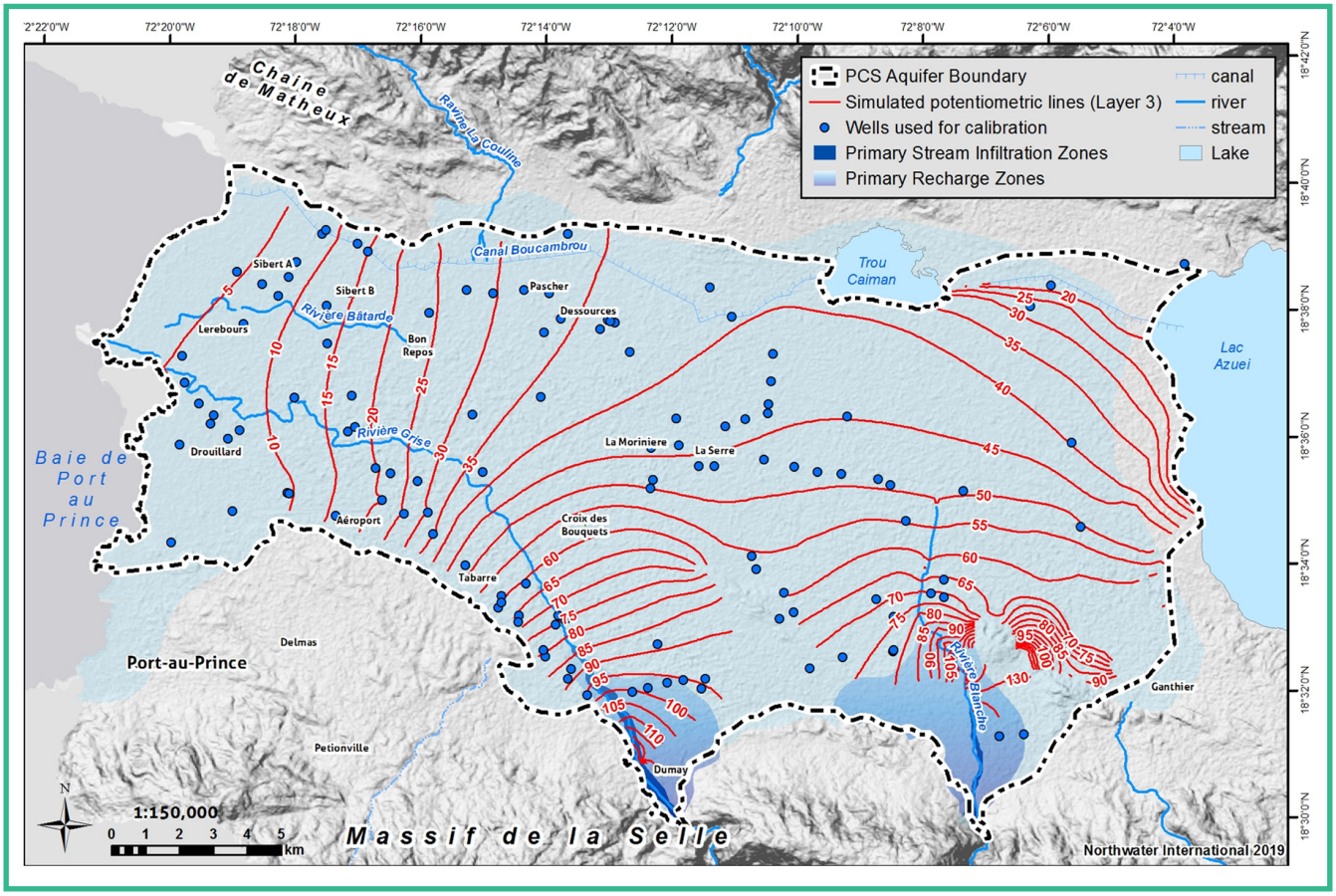

Figure 16 - Simulated heads of the calibrated model.

5.2 – Groundwater Budget

Based on the calibrated model output, the steady-state groundwater budget is presented in Table 6. The groundwater budget for the model area can be expressed by the following equation which outlines the inputs and outputs.

	MODEL RUN INITIAL	
	IN (m^3/d)	OUT (m^3/d)
Recharge (Rech)	15,200	--
Riviere Blanche (Rsw)	16,253	--
Riviere Grise (Rsw)	95,742	--
General Head (Rgh)	6,226	--
Canal Boucambrou (Dsw)	--	13,281
Riviere Batard (Rsw)	1,154	--
Lac Azuei/Etang Sumautre (Dsw)		1,838
Trou Caiman (Dsw)	--	3,890
Ocean (Dsea)	--	43,808
Pumping (ABS)	--	71,582

Table 6. Groundwater budget simulation results.

Rech+Rsw +Rsea=Dsw+Dsea+ABS

Where:

Rech
Groundwater recharge (direct infiltration).

Rsw
Groundwater recharge from stream infiltration (river leakage).

Rsea
Seawater entering aquifer (saltwater intrusion).

Dsw
Discharge to surface water bodies.

Dsea
Discharge to the sea.

ABS
Discharge via well abstraction.

Based on the steady-state model and initial model run, the following observations are noted regarding the water balance:

- Renewable recharge inputs to the aquifer are on the order of 135,000 m^3/day. If current pumping is 71,600 m^3/day, this would imply a 0.53, or 53% groundwater development ratio

- 83% of the aquifer inputs are from infiltration of the Riviere Grise and Riviere Blanche, which is consistent with historical findings

- Influx to the PCS alluvial aquifer from Massif de la Selle limestone aquifer is a moderately important input (5% of total recharge simulated in the model). This input supported calibration along the southern boundary of the aquifer

- Canal Boucambrou appears to be a drain from the PCS aquifer. This relationship needs to be further researched and monitored.

- Based on the steady state simulation and assumed pumping schemes, saltwater intrusion does not appear to be a major factor at present for the primary aquifer layer. Dry season stress periods may enhance the risk, and the shallow layer is most susceptible. The coastal area of the aquifer has few wells; further, there was limited data to calibrate the model along the coast.

- Trou Caiman appears to receive water from the PCS aquifer, at a range of 45 L/s (3,890 m^3/day) according to what is suggested by model simulation.

- Lac Azuei does not appear to receive a significant proportion of its water budget from the PCS aquifer. The model simulation suggests a range of 21 L/s (1838 m^3/day). It appears influenced by stream infiltration of the Riviere Blanche. Groundwater that discharges to the eastern portion of Canal Boucambrou may flow into Lac Azuei. This hydrological relationship between the aquifer, Lac Azuei, and Canal Boucambrou needs to be further investigated with studies and monitoring.

5.3 – Groundwater Storage

Total aquifer storage is estimated to be in the range of 6.32E+9 m³ (6.32 km³), differentiated into three different model layers (Table 7). The estimates were based on layer volumes calculated from the model and a limited dataset of PCS aquifer storage properties from pump tests. Specific yield values from published literature (Morris and Johnson, 1967) were applied.

	Silty Sand Aquifer (L2)[1]	Upper Sandy Gravel Aquifer (L3)[1,2]	Lower Sandy Gravel Aquifer (L4)[1,2]
Volume (m^3)	1.03E+10	1.12E+10	8.62E+09
Groundwater Storage (m^3)[1]	1.89E+09	2.51E+09	1.93E+09
[1] based on specific yield of 18% for L2 and 22% for L3 and L4			
[2] based on specific yield as noted above plus the specific storage based on estimates from five wells with average of 6.59E-4			

Table 7 – Groundwater storage estimates.

6.0 – Model Limitations and Sensitivity

Uncertainty is a factor in any groundwater flow model, especially for regional models in areas with limited spatial and temporal datasets. Errors associated with model inputs can be associated with factors such as errors in measurement, scale, origin, data, and calculation. Because the development of a conceptual and numerical model often relies on synthesizing and analyzing data from diverse sources and datasets, there are many opportunities for the modeling results to be affected by sources of error.

- Although the calibration process achieved the targets and resulted in a good RMSE and correlation between simulated and observed heads, the residual error is not equally distributed over the whole model area. Simulated heads had higher errors in some areas, largely due to uncertain boundary conditions and the possibility that vertical and horizontal model boundaries and modeled conditions may not correspond to the aquifer's natural physical boundaries. As previously mentioned, the eastern portion of the aquifer had limited data for building and calibrating the model.

- All the elevations' measurements are derived from the topographic surface of the 1.5m MTN LiDAR digital elevation model and then averaged to obtain values for the grid cells in the model. This factor adds a certain level of uncertainty and variability in simulated head conditions. The lack of surveyed conditions of the study area to a specific datum also introduces a source of error, as the observed heads and river dimensions are largely based on coarse granular surface elevations from the digital elevation model.

- The model was built in a regional context; the many and complex heterogeneities identified from borehole log analysis are not captured due to the goal of simulating a regional system. This may result in differences between simulated and observed conditions as more local level simulations are performed. The numerical model was developed in a manner that supports future refinement of the geological model when more localized simulations are desired.

- Error associated with the groundwater balance is always a factor in simulating flow conditions, and it is important that the model considers uncertainty. Data used for recharge

and streamflow infiltration were based on observations and calculations from past studies. The model was largely calibrated to simulate discrete measurements of groundwater elevations and to accommodate characterized recharge dynamics of the river systems. Continuous streamflow monitoring of the rivers and wells, and monitoring of chloride concentrations in groundwater, surface water, and precipitation will allow additional calibration targets and future refinements of the model.

- A brief sensitivity analysis was performed to understand the uncertainty in the calibrated model by the estimation of parameters, boundary conditions, and stressors. The purpose of such an analysis is to understand the model response when parameters are varied. Hydraulic conductivity, recharge, and riverbed parameters (stage/conductance) were the key parameters evaluated by multiplying each parameter by various multipliers. The RMSE changes for the variations indicate that the model is most sensitive to: (i) river bed and flow stage of the Riviere Grise and Riviere Blanche, and (ii) hydraulic conductivity of the defined aquifer units. The greatest sensitivity of the model appears from changes in the stage and/or riverbed conductance of the Riviere Grise.

- The modeling effort is also sensitive to the geological model, as it is a large factor in defining the surface water and groundwater connections.

- The model does not account for interflow to the aquifer from the aquifer bottom or northern limits. This is considered a conservative assumption in that if interflow does occur from these areas, recharge to the aquifer could be larger than modeled.

- The modeling is steady-state and does not accommodate either simulations of changes in storage or transient conditions during extreme climate events or stress periods.

7.0 - Conclusions and Considerations

The steady-state groundwater flow model presented serves as a good tool to support further steps of groundwater development and management in a regional context. The model is structured to support steady-state simulations of various groundwater abstraction, environmental, and climate change scenarios. Its results suggest that renewable groundwater resources are on the order of 130,000 m^3/day; these results further validate the importance of the Riviere Grise streamflow infiltration in the recharge and groundwater flow dynamics of the aquifer system.

Although a volume of borehole and well data was available to develop and calibrate the model, the quality and reliability of data is spatially variable. Further, a limited quantity of time-series or temporal data was available for river/stream stages, and water levels in wells. The development of transient and stress period models should be considered under the directive of a focused objective, and a specific data mining, research, and monitoring campaign can be done to support such transient model development and validation.

We recommend that scientific characterization be performed in the northeast, east, and southeast portions of the PCS aquifer to better understand lithology and the surface and groundwater interactions related to Lac Azuei, Canal Boucambrou, and Trou Caiman. These will support model refinement and result in a greater level of confidence for these zones of the aquifer. Especially to better understand potential impacts on surface water bodies and saltwater intrusion vulnerability of the aquifer

Saltwater intrusion risk in the coastal areas should also be further investigated with monitoring.

The importance of temporal monitoring of water levels and water quality in wells should be considered a priority to support future and advanced groundwater flow modeling and simulations. The temporal monitoring of flow and stage in the Riviere Grise, Riviere Blanche, and Canal Boucambrou is also recommended considering their importance in the dynamics of the aquifer. Well pumping/abstraction estimates and monitoring is also a large data gap that could be addressed with future activities, as current aquifer-wide abstraction was estimated based on limited data.

References

Anderson, M.P. and W.W. Woessner, 1992. Applied Groundwater Modeling, Simulation of Flow and Advective Transport, Academic Press, 381 pp.
Freeze, R.A. and Cherry, J.A., 1979, Groundwater, Prentice-Hall Inc., 29 pp.
Hijmans, R.J., S.E. Cameron, J.L. Parra, P.G. Jones and A. Jarvis, 2005. Very high resolution interpolated climate surfaces for global land areas. International Journal of Climatology 25: 1965-1978.
Miner, W.J., and Adamson, J, 2017. Modeling the Spatial Distribution of Groundwater Recharge in Haiti using a GIS Approach, Geological Society of America 2017 Annual Meeting, Seattle, Washington, doi: 10.1130/abs/2017AM-297120.
Morris, D.A. and A.I. Johnson, 1967. Summary of hydrologic and physical properties of rock and soil materials as analyzed by the Hydrologic Laboratory of the U.S. Geological Survey, U.S. Geological Survey Water-Supply Paper 1839-D, 42p.
Northwater International, 2018. Plaine du Cul-de-Sac Interim Hydrogeological Database, Version 1.0: Port-au-Prince, Haiti, Inter-American Development Bank.
Northwater International and Rezodlo, 2017. An Evaluation of the Plaine du Cul-de-Sac aquifer and its potential to serve Canaan: Port-au-Prince, Haiti, United States Agency for International Development and American Red Cross, Technical Report, cooperative agreement no. AID-521-A-15-00010, 40 p.
Richards, P.A., 2007. The Importance of Accurate Hydrogeological Conceptualization – Are we Correct?, CGS/IAH Joint Conference Proceedings, Ottawa, ON, Oct. 2007, pp. 123-130.
Spitz, K., and J. Moreno, 1996. A Practical Guide to Groundwater and Solute Transport Modeling, John Wiley & Sons, Inc., New York, NY.

REPORT APPENDICES

APPENDIX A - HYDROGEOLOGICAL INVESTIGATION OF TUNNEL DIQUINI: LABORATORY REPORTS

Analysis Reports.

First Environmental Laboratories, Inc.
IL ELAP / NELAC Accreditation # 100292
1600 Shore Road • Naperville, Illinois 60563 • Phone (630) 778-1200 • Fax (630) 778-1233

Analytical Report

Client: NORTHWATER CONSULTING
Project ID: Diquini and Cap Haitien
Sample ID: Tunel Diquini
Sample No: 18-2208-002

Date Collected: 04/15/18
Time Collected: 15:00
Date Received: 04/20/18
Date Reported: 05/11/18

Analyte	Result	R.L.	Units	Flags
Alkalinity, Total (CaCO3) **Method: 2320B 1997**				
Analysis Date: 04/27/18 10:00				
Alkalinity, Total (CaCO3)	230	5	mg/L	
Alkalinity, Bicarbonate (CaCO3) **Method: 2320B 1997**				
Analysis Date: 04/27/18 10:00				
Alkalinity, Bicarbonate (CaCO3)	< 5	5	mg/L	
Ammonia (as N) **Method: 350.1R2.0**				
Analysis Date: 05/03/18				
Ammonia (as N)	< 0.10	0.10	mg/L	
Chloride by IC **Method: 300.0**				
Analysis Date: 05/03/18				
Chloride	6.20	3.00	mg/L	N S
Conductivity **Method: 2510B 1997**				
Analysis Date: 04/27/18 9:00				
Conductivity @ 25°C	382	5	umhos/cm	
Fluoride **Method: 4500F,C 1997**				
Analysis Date: 04/30/18 11:00				
Fluoride	0.27	0.10	mg/L	
Total Hardness, as CaCO3 **Method: 2340B 1997**				
Analysis Date: 05/01/18				
Total Hardness, as CaCO3	202	5	mg/L	
Nitrite (as N) **Method: 4500NO2,B 2000**				
Analysis Date: 04/26/18 9:00				
Nitrite (as N)	< 0.01	0.01	mg/L	H
Nitrate (as N) **Method: 353.2R2.0**				
Analysis Date: 04/30/18				
Nitrate (as N)	1.95	0.10	mg/L	

First Environmental Laboratories, Inc.
IL ELAP / NELAC Accreditation # 100292
1600 Shore Road • Naperville, Illinois 60563 • Phone (630) 778-1200 • Fax (630) 778-1233

Analytical Report

Client: NORTHWATER CONSULTING
Project ID: Diquini and Cap Haitien
Sample ID: Tunel Diquini
Sample No: 18-2208-002

Date Collected: 04/15/18
Time Collected: 15:00
Date Received: 04/20/18
Date Reported: 05/11/18

Analyte	Result	R.L.	Units	Flags
Sulfate **Method: 375.2R2.0**				
Analysis Date: 04/30/18				
Sulfate	< 15	15	mg/L	
TOC **Method: 5310C 2000**				
Analysis Date: 05/03/18				
TOC	0.4	0.2	mg/L	
Total Mercury **Method: 7470A**				
Analysis Date: 04/27/18				
Mercury	< 0.0005	0.0005	mg/L	
Total Metals **Method: 6010C**		**Preparation Method 3010A**		
Analysis Date: 05/01/18		Preparation Date: 04/30/18		
Antimony	< 0.006	0.006	mg/L	
Arsenic	< 0.010	0.010	mg/L	
Barium	0.116	0.005	mg/L	
Beryllium	< 0.004	0.004	mg/L	
Cadmium	< 0.005	0.005	mg/L	
Calcium	74.4	0.5	mg/L	
Chromium	< 0.005	0.005	mg/L	
Copper	< 0.005	0.005	mg/L	
Iron	< 0.05	0.05	mg/L	

Lead	< 0.005	0.005	mg/L
Magnesium	4.1	0.5	mg/L
Manganese	< 0.005	0.005	mg/L
Potassium	< 0.5	0.5	mg/L
Silver	< 0.005	0.005	mg/L
Sodium	3.1	0.5	mg/L
Thallium	< 0.010	0.010	mg/L
Zinc	< 0.010	0.01	mg/L

Total Dissolved Solids **Method: 2540C 1997**

Analysis Date: 04/30/18 9:30

Total Dissolved Solids	214	10	mg/L

K(Henry) from Bullister et al., 2002, Deep-Sea Research, v. 49, 175-187.
In older version K(Henry) was from Wilhelm et al., 1977, Chemical Reviews, v. 77, 219-262.
Bullister et al., 2002, salting out effect was added.
Units of concentration fMol/L, fMol = 10E-15 Moles.
Busenberg and Plummer -- Revised September 2010
Worksheet Name:

Standard used for calibration.
Lab tank SF6 in N2 150 pptv
CMDL/NOAA tank Air 5.12 pptv

Lab Temperature in °C 21.0
K_{Henry} 0.0002848 Headspace Correction
Lab Pressure in mm mercury 638.0
Salinity 0.0

0.0342 26.0

Enrichment 1.00
Meters =0; feet =1 0
fMol/L=0; pg/kg =1 0

Local SF6 enrichment factor (1.00= Northern Hemisphere)
Select units of elevation
Select units of concentration

You can change:
1) Excess air in cc at STP
2) Temperature in C
3) Elevation
4) Salinity in o/oo

Samples should be collected without headspace (HS). If a HS forms, the HS volume (column "HS") is measured and a correction is applied. Since the total pressure of the HS bubble cannot be measured, the HS SF_6 concentration cannot be exactly calculated. The MAXIMUM PERCENT UNCERTAINTY in the water concentration that may be introduced by the HS bubble is given in column "AO". The uncertainty is significantly smaller in most cases.

Corrected Age Date Results

ID No.	Sample No.	Sample Name	Sampling Date (Mo/day/year)	Time	Sample Mass	Bottle Headspace in cc	Excess Air (mL)	Recharge Temperature (C)	Elevation meters	Salinity in (o/oo) parts per thousand	Uncorrected SF6 (pptv) partial pressure	fMol/Kg	Piston flow model SF6 recharge year	Piston flow model SF6 recharge age	SF6 FemtoMol/kg With HS corr.	Excess air cc/kg at STP	Calculated SF6 (pptv) partial pressure	Piston flow model SF6 recharge year	Piston flow model SF6 recharge age, years	Sample Name	Maximum % headspace uncertainty	Comments
											0.00	0.00	1952.0	-52.0	0.00	0	0.00	1952.0	-52.0		#DIV/0!	0
											0.00	0.00	1952.0	-52.0	0.00	0	0.00	1952.0	-52.0		#DIV/0!	0
											0.00	0.00	1952.0	-52.0	0.00	0	0.00	1952.0	-52.0		#DIV/0!	0
SF6-060118-08		17-1100 - Tunnel			0.76	0.00	2.0	26.00	600		4.24	0.90	1998.5	-98.5	0.90	2	2.99	1992.5	-92.5	17-1100 - Tunnel	0.00	0
											0.00	0.00	1952.0	-52.0	0.00	0	0.00	1952.0	-52.0		#DIV/0!	0
											0.00	0.00	1952.0	-52.0	0.00	0	0.00	1952.0	-52.0		#DIV/0!	0
SF6-060118-12		17-1100 - Tunnel			0.76	0.00	2.0	26.00	600		4.15	0.88	1998.0	-98.0	0.88	2	2.92	1992.5	-92.5	17-1100 - Tunnel	0.00	0

SAMPLE ID	CFC-11 (pmoles/kg)	CFC-12 (pmoles/kg)	CFC-113 (pmoles/kg)	Salinity (‰)	Recharge Elev. (m)	Recharge Temp (C)	Comments	Pwater	Elev. correction	KRT_11	KRT_12	KRT_113	eq. air conc_11 (ppt)	eq. air conc_12 (ppt)	eq. air conc_113 (ppt)	CFC-11 Rech. year	CFC-12 Rech. year	CFC-113 Rech. year
17-1100	2.13328782	1.237491322	0.114884435	0	500	25		0.0312	0.91088	0.01044	0.00292	0.00298	224.407	464.698	42.28851	1986	1988	1984.5
17-1100	2.143946117	1.291954792	0.131666169	0	500	25		0.0312	0.91088	0.01044	0.00292	0.00298	225.528	485.15	48.4658	1986	1989	1985.5
17-1100	2.113995722	1.268698722	0.126896695	0	500	25		0.0312	0.91088	0.01044	0.00292	0.00298	222.377	476.417	46.71017	1985.5	1989	1985.5
17-1100	4.003506609	1.164597057	0.120602682	0	500	25	This sample was different from the rest	0.0312	0.91088	0.01044	0.00292	0.00298	421.141	437.325	44.39337	Cont.	1987	1985

ISOTECH
ISOTECH LABORATORIES INC

ANALYSIS REPORT

Lab #:	663361	Job #:	38243	IS-90371	Co. Job#:
Sample Name:	Tunnel Diquini				Co. Lab#:
Company:	Northwater Consulting				
API/Well:					
Container:	125ml bottle				
Field/Site Name:	18009				
Location:	Tunnel Diquini				
Formation/Depth:					
Sampling Point:					
Date Sampled:	4/15/2018 15:00	Date Received:	5/09/2018	Date Reported:	5/16/2018

δD of water	----------	-14.4 ‰ relative to VSMOW
$\delta^{18}O$ of water	----------	-3.28 ‰ relative to VSMOW

Tritium content of water	----------	na
$\delta^{13}C$ of DIC	----------	na
^{14}C content of DIC	----------	na
$\delta^{15}N$ of nitrate	----------	na
$\delta^{18}O$ of nitrate	----------	na
$\delta^{34}S$ of sulfate	----------	na
$\delta^{18}O$ of sulfate	----------	na
Vacuum Distilled? *	----------	No

Remarks:

nd = not detected. na = not analyzed.
*Indicates if vacuum distillation was utilized for hydrogen and oxygen isotopic analysis of water

APPENDIX B - HYDROGEOLOGICAL INVESTIGATION OF TUNNEL DIQUINI: CFC AND SF6 METHODOLOGIES

Chlorofluorocarbons (CFCs)

Chlorofluorocarbon (CFC) compounds have been synthesized on an industrial scale since 1931. They have primarily been used as refrigerants and aerosol can propellants, but also as foam blowing agents, solvents, and in insulation. Production reached its peak during the 1970s and 1980s before it was recognized that CFCs contribute to the destruction of the Earth's ozone. Production was subsequently banned in the 1990s as part of a global agreement. Three principal CFC compounds were used during the 20th century: trichlorofluoromethane, dichlorodifluoromethane, and trichlorotrifluoroethane, whose trade names are CFC-11, CFC-12, and CFC-113, respectively. The CFCs production and release to the atmosphere have been measured and reconstructed back to 1940 (McCarthy et al., 1977; Gamlen et al., 1986; Wisegarver and Gammon, 1988; Fisher and Midgley, 1993; Fraser et al., 1996).

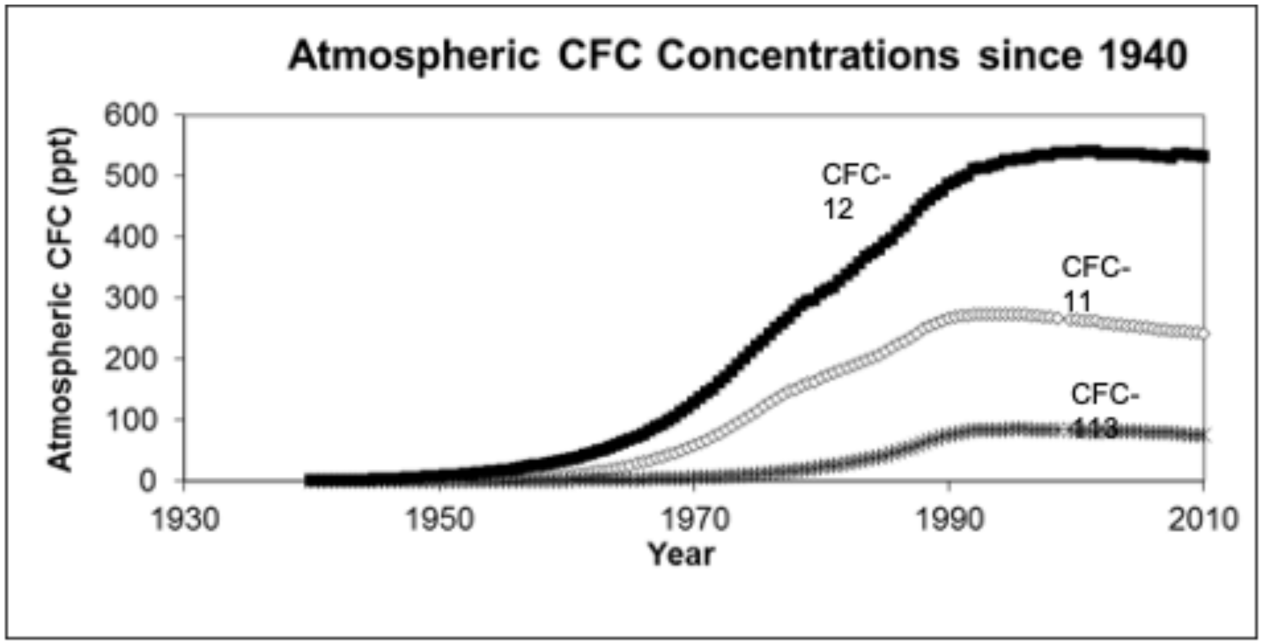

The basis for age-dating with dissolved CFC measurements in groundwater is based on comparing the measured values to those of the atmospheric concentrations at the time of recharge. This is accomplished by recognizing that the dissolved concentration Ci is

$$C_i = K_H p_i$$

where KH is the Henry's constant and pi is the partial pressure of the CFC in air. The concentration is related back to atmospheric concentration through pi

$$p_i = x_i(P - p_{H2O})$$

where xi is the dry air mole fraction of the CFC, P is the atmospheric pressure and pH2O is the water vapor pressure. Henry constants have been carefully measured for the three CFCs of interest and solubility determined as a function of temperature and salinity. A number of comparative age-dating

studies have shown the reliability of the CFC approach (Busenberg and Plummer, 1992; Busenberg and Plummer, 1993; Ekwurzel et al., 1994; Cook and Solomon, 1997).

Sulfur Hexafluoride SF_6

SF_6 is used as electrical insulator in high-voltage switches and transformers. It is also used as a blanket gas in the production of magnesium metal. Production of SF_6 began in 1953, and ever since SF_6 is building up concentration the atmosphere. SF_6 has a lower solubility in water compared to the CFCs at 30 ppm. Solubility of SF_6 is temperature and salinity dependent. Solubility is also dependent on elevation and on any excess air in the water. Excess air origin is originated by from rapid recharge that traps air in the vadose zone and carries that air into the saturated zone where it solubilizes. If trapped in pockets of air formed in the aquifer space, SF_6 will readily partition into that trapped air because its low solubility. The basis of using SF_6 as an age dating tool relies on Henry's constant of SF_6 with respect to water. The Henry's constant for SF_6 is 0.00024 mols/kg-bar. The measured concentration in groundwater can be compared to the atmospheric concentration through the use of its Henry's constant, resulting in an age date. There are natural sources of SF_6 associated hot springs and fumaroles. Sometimes these sources can interfere with age dating of groundwater.

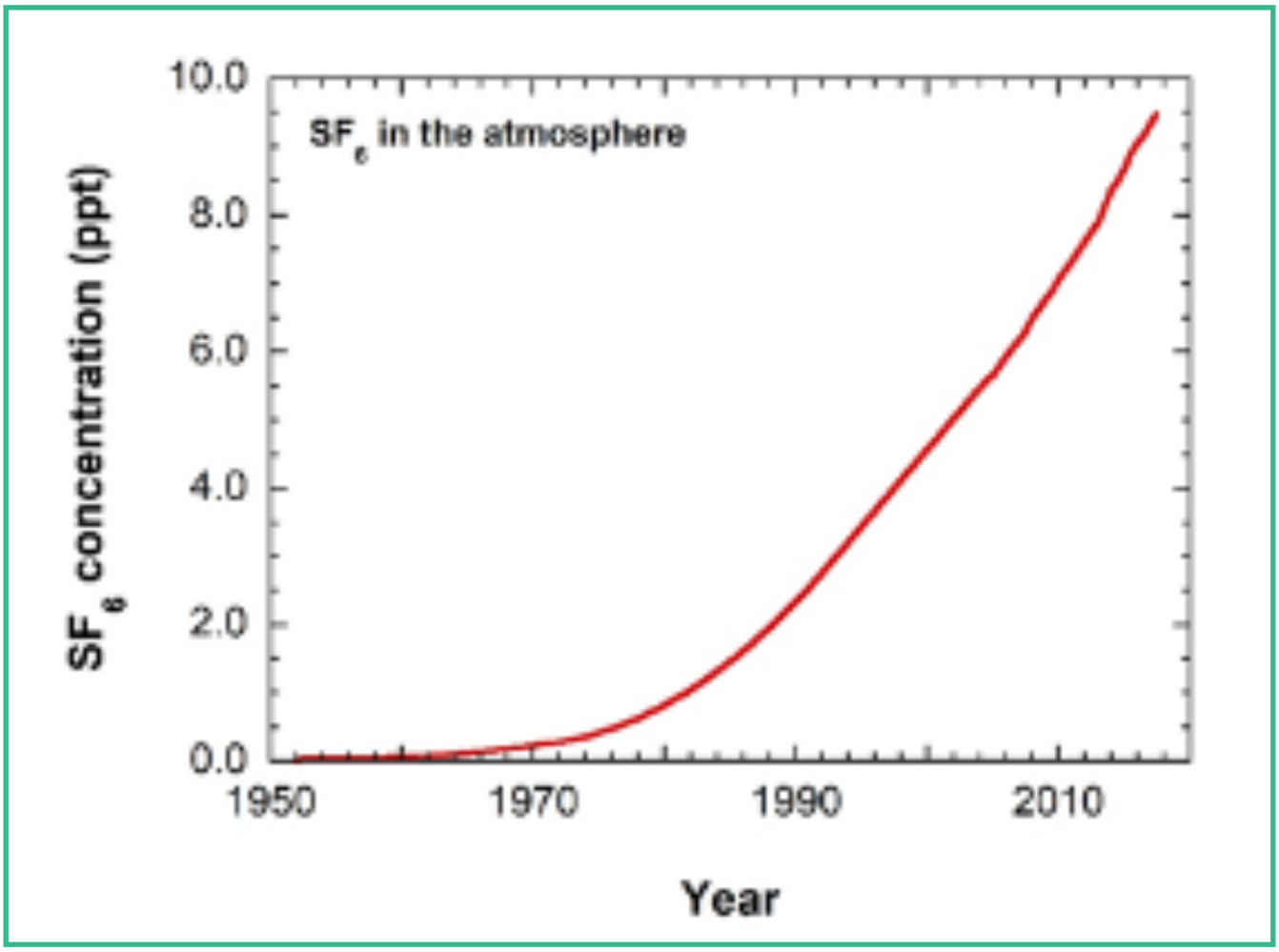

APPENDIX C - HYDROGEOLOGICAL INVESTIGATION OF TUNNEL DIQUINI: COMPILED DATASETS

Compiled Discharge Data for Tunnel Diquini, Source Diquini and Riviere Froide

Water Point Name	Date	Stage (cm)	Flow (cfs)	Flow (gpm)	Flow (L/s)	Flow (m3/h)	Flow (m3/d)	Data Source
Tunnel Diquini	6/2018		10.1	4,740	300	1,080	25,920	CTE-RMPP
Tunnel Diquini	5/2018		9.0	4,213	267	960	23,040	CTE-RMPP
Tunnel Diquini	4/15/2018	15.5 cm	12.7	5,687	359	1,292	31,004	Northwater, 2018
Tunnel Diquini	3/2018		10.1	4,740	300	1,080	25,920	CTE-RMPP
Tunnel Diquini	2/2018		11.6	5,412	343	1,233	29,592	CTE-RMPP
Tunnel Diquini	1/2018		11.6	5,412	343	1,233	29,592	CTE-RMPP
Tunnel Diquini	12/2017		13.0	6,074	384.4	1,384	33,213	CTE-RMPP
Tunnel Diquini	11/2017		13.4	6,276	397.2	1,430	34,320	CTE-RMPP
Tunnel Diquini	10/2017		12.5	5,870	371.5	1,337	32,098	CTE-RMPP
Tunnel Diquini	9/2017		9.5	4,446	281.4	1,013	24,312	CTE-RMPP
Tunnel Diquini	8/2017		9.2	4,303	272.3	980	23,528	CTE-RMPP
Tunnel Diquini	7/2017		9.1	4,264	269.9	972	23,317	CTE-RMPP
Tunnel Diquini	6/2017		11.9	5,569	352.5	1,269	30,454	CTE-RMPP
Tunnel Diquini	5/2017		11.5	5,390	341.1	1,228	29,472	CTE-RMPP
Tunnel Diquini	4/2017		12.9	6,023	381.2	1,372	32,934	CTE-RMPP
Tunnel Diquini	3/2017		12.5	5,828	368.9	1,328	31,872	CTE-RMPP
Tunnel Diquini	2/2017		13.2	6,166	390.3	1,405	33,719	CTE-RMPP
Tunnel Diquini	1/2017		13.0	6,094	385.7	1,388	33,323	CTE-RMPP
Tunnel Diquini	12/2016		13.0	6,094	385.7	1,388	33,323	CTE-RMPP
Tunnel Diquini	11/2016		13.5	6,297	398.5	1,435	34,433	CTE-RMPP
Tunnel Diquini	10/2016		15.2	7,135	451.6	1,626	39,019	CTE-RMPP
Tunnel Diquini	9/2016		15.7	7,344	464.8	1,673	40,162	CTE-RMPP
Tunnel Diquini	8/2016		15.2	7,123	450.8	1,623	38,951	CTE-RMPP
Tunnel Diquini	7/2016		15.2	7,123	450.8	1,623	38,949	CTE-RMPP
Tunnel Diquini	6/2016		10.3	4,821	305.1	1,098	26,364	CTE-RMPP
Tunnel Diquini	5/2016		9.6	4,514	285.7	1,028	24,684	CTE-RMPP
Tunnel Diquini	4/2016		8.1	3,810	241.2	868	20,837	CTE-RMPP
Tunnel Diquini	3/2016		8.1	3,812	241.2	868	20,843	CTE-RMPP
Tunnel Diquini	2/2016		8.7	4,091	258.9	932	22,371	CTE-RMPP
Tunnel Diquini	1/2016		9.7	4,552	288.1	1,037	24,890	CTE-RMPP
Tunnel Diquini	12/2015		9.8	4,572	289.4	1,042	25,000	CTE-RMPP
Tunnel Diquini	11/2015		10.2	4,755	300.9	1,083	26,000	CTE-RMPP
Tunnel Diquini	10/2015		10.3	4,837	306.2	1,102	26,452	CTE-RMPP
Tunnel Diquini	9/2015		10.7	4,998	316.3	1,139	27,329	CTE-RMPP
Tunnel Diquini	8/2015		9.6	4,514	285.7	1,028	24,684	CTE-RMPP
Tunnel Diquini	7/2015		11.9	5,590	353.8	1,274	30,570	CTE-RMPP

Water Point Name	Date	Stage (cm)	Flow (cfs)	Flow (gpm)	Flow (L/s)	Flow (m3/h)	Flow (m3/d)	Data Source
Tunnel Diquini	6/25/2015		5.3	2,477	157	564	13,548	EPTISA (2016)
Tunnel Diquini	5/2015		9.9	4,647	294.1	1,059	25,412	CTE-RMPP
Tunnel Diquini	4/2015		12.3	5,757	364.4	1,312	31,483	CTE-RMPP
Tunnel Diquini	3/2015		13.0	6,098	386.0	1,390	33,348	CTE-RMPP
Tunnel Diquini	2/2015		14.4	6,760	427.8	1,540	36,966	CTE-RMPP
Tunnel Diquini	1/16/2015		13.0	6,067	384	1,382	33,178	EPTISA (2016)
Tunnel Diquini	12/12/2014		15.0	7,031	445	1,602	38,448	EPTISA (2016)
Tunnel Diquini	11/5/2014		18.1	8,451	535	1,926	46,215	EPTISA (2016)
Tunnel Diquini	10/2014		13.9	6,496	411	1,480	35,521	CTE-RMPP
Tunnel Diquini	9/25/2014		21.9	10,264	650	2,339	56,125	EPTISA (2016)
Tunnel Diquini	9/2014		8.6	4,014	254	915	21,948	CTE-RMPP
Tunnel Diquini	8/29/2014		20.4	9,548	604	2,175	52,210	EPTISA (2016)
Tunnel Diquini	8/2014		13.9	6,496	411	1,480	35,521	CTE-RMPP
Tunnel Diquini	7/22/2014		10.7	5,000	316	1,139	27,341	EPTISA (2016)
Tunnel Diquini	6/30/2014		11.1	5,176	328	1,179	28,306	EPTISA (2016)
Tunnel Diquini	6/2014		5.8	2,706	171	617	14,796	CTE-RMPP
Tunnel Diquini	5/20/2014		9.6	4,505	285	1,026	24,633	EPTISA (2016)
Tunnel Diquini	4/11/2014		13.2	6,182	391	1,409	33,804	EPTISA (2016)
Tunnel Diquini	2/27/2014		10.2	4,795	304	1,093	26,222	EPTISA (2016)
Tunnel Diquini	1/27/2014		14.4	6,747	427	1,537	36,893	EPTISA (2016)
Tunnel Diquini	12/10/2013		14.8	6,905	437	1,573	37,757	EPTISA (2016)
Tunnel Diquini	11/14/2013		22.4	10,475	663	2,387	57,283	EPTISA (2016)
Tunnel Diquini	10/2013							
Tunnel Diquini	9/2013							
Tunnel Diquini	8/2013							
Tunnel Diquini	7/2013							
Tunnel Diquini	6/2013							
Tunnel Diquini	5/2013							
Tunnel Diquini	4/2013							
Tunnel Diquini	3/2013							
Tunnel Diquini	2/2013							
Tunnel Diquini	1/2013							
Tunnel Diquini	12/2012							
Tunnel Diquini	11/2012							
Tunnel Diquini	10/2012							

Water Point Name	Date	Stage (cm)	Flow (cfs)	Flow (gpm)	Flow (L/s)	Flow (m3/h)	Flow (m3/d)	Data Source
Tunnel Diquini	9/2012							
Tunnel Diquini	8/2012							
Tunnel Diquini	7/2012							
Tunnel Diquini	6/2012							
Tunnel Diquini	5/2012							
Tunnel Diquini	4/2012							
Tunnel Diquini	3/2012							
Tunnel Diquini	2/2012							
Tunnel Diquini	1/2012							
Tunnel Diquini	12/2011							
Tunnel Diquini	11/2011		19.9	9,298	589	2,119	50,846	CTE-RMPP
Tunnel Diquini	10/2011		17.7	8,279	524	1,886	45,274	CTE-RMPP
Tunnel Diquini	9/2011		17.4	8,162	517	1,860	44,634	CTE-RMPP
Tunnel Diquini	8/2011							
Tunnel Diquini	7/2011		16.9	7,919	501	1,804	43,304	CTE-RMPP
Tunnel Diquini	6/2011		15.9	7,431	470	1,693	40,634	CTE-RMPP
Tunnel Diquini	5/2011		15.8	7,379	467	1,681	40,349	CTE-RMPP
Tunnel Diquini	4/2011		16.6	7,785	493	1,774	42,569	CTE-RMPP
Tunnel Diquini	3/2011		18.6	8,703	551	1,983	47,589	CTE-RMPP
Tunnel Diquini	2/2011		20.7	9,692	613	2,208	52,998	CTE-RMPP
Tunnel Diquini	1/2011		21.8	10,204	646	2,325	55,797	CTE-RMPP
Tunnel Diquini	12/2010		22.0	10,291	651	2,345	56,272	CTE-RMPP
Tunnel Diquini	11/2010		20.2	9,453	598	2,154	51,693	CTE-RMPP
Tunnel Diquini	10/2010		17.5	8,194	519	1,867	44,807	CTE-RMPP
Tunnel Diquini	9/2010		15.4	7,187	455	1,638	39,303	CTE-RMPP
Tunnel Diquini	8/2010		14.1	6,591	417	1,502	36,040	CTE-RMPP
Tunnel Diquini	7/2010		14.4	6,749	427	1,538	36,904	CTE-RMPP
Tunnel Diquini	6/2010		16.0	7,468	473	1,702	40,836	CTE-RMPP
Tunnel Diquini	5/2010		16.8	7,873	498	1,794	43,051	CTE-RMPP
Tunnel Diquini	4/2010		16.3	7,647	484	1,742	41,818	CTE-RMPP
Tunnel Diquini	3/2010		16.6	7,785	493	1,774	42,569	CTE-RMPP
Tunnel Diquini	2/2010		17.2	8,031	508	1,830	43,917	CTE-RMPP
Tunnel Diquini	1/2010		17.0	7,975	505	1,817	43,612	CTE-RMPP
Tunnel Diquini	12/2009		16.8	7,873	498	1,794	43,050	CTE-RMPP
Tunnel Diquini	11/2009		18.2	8,530	540	1,944	46,647	CTE-RMPP
Tunnel Diquini	10/2009		19.4	9,095	576	2,072	49,736	CTE-RMPP
Tunnel Diquini	9/2009		23.8	11,123	704	2,534	60,826	CTE-RMPP

Water Point Name	Date	Stage (cm)	Flow (cfs)	Flow (gpm)	Flow (L/s)	Flow (m3/h)	Flow (m3/d)	Data Source
Tunnel Diquini	8/2009		28.6	13,398	848	3,053	73,265	CTE-RMPP
Tunnel Diquini	7/2009		21.2	9,921	628	2,260	54,250	CTE-RMPP
Tunnel Diquini	6/2009		19.1	8,957	567	2,041	48,981	CTE-RMPP
Tunnel Diquini	5/2009		17.2	8,031	508	1,830	43,917	CTE-RMPP
Tunnel Diquini	4/2009		15.9	7,423	470	1,691	40,592	CTE-RMPP
Tunnel Diquini	3/2009		17.5	8,177	518	1,863	44,715	CTE-RMPP
Tunnel Diquini	2/2009		18.8	8,785	556	2,002	48,038	CTE-RMPP
Tunnel Diquini	1/2009		21.4	10,017	634	2,282	54,778	CTE-RMPP
Tunnel Diquini	12/2008		23.2	10,875	688	2,478	59,468	CTE-RMPP
Tunnel Diquini	11/2008		23.6	11,037	699	2,515	60,352	CTE-RMPP
Tunnel Diquini	10/2008		20.3	9,512	602	2,167	52,017	CTE-RMPP
Tunnel Diquini	9/2008							
Tunnel Diquini	8/2008							
Tunnel Diquini	7/2008		15.1	7,059	447	1,608	38,604	CTE-RMPP
Tunnel Diquini	6/2008		14.0	6,536	414	1,489	35,744	CTE-RMPP
Tunnel Diquini	5/2008		13.7	6,426	407	1,464	35,139	CTE-RMPP
Tunnel Diquini	4/2008		13.2	6,198	392	1,412	33,895	CTE-RMPP
Tunnel Diquini	3/2008		14.8	6,922	438	1,577	37,852	CTE-RMPP
Tunnel Diquini	2/2008		16.2	7,592	481	1,730	41,515	CTE-RMPP
Tunnel Diquini	1/2008		16.9	7,921	501	1,805	43,312	CTE-RMPP
Tunnel Diquini	12/2007		18.7	8,758	554	1,995	47,892	CTE-RMPP
Tunnel Diquini	11/2007		15.4	7,184	455	1,637	39,286	CTE-RMPP
Tunnel Diquini	10/2007		13.2	6,167	390	1,405	33,722	CTE-RMPP
Tunnel Diquini	9/2007		12.8	5,987	379	1,364	32,737	CTE-RMPP
Tunnel Diquini	8/2007		11.4	5,355	339	1,220	29,281	CTE-RMPP
Tunnel Diquini	7/2007		10.9	5,097	323	1,161	27,873	CTE-RMPP
Tunnel Diquini	6/2007		9.9	4,622	293	1,053	25,272	CTE-RMPP
Tunnel Diquini	5/2007		9.5	4,468	283	1,018	24,434	CTE-RMPP
Tunnel Diquini	4/2007		8.8	4,095	259	933	22,395	CTE-RMPP
Tunnel Diquini	3/2007		8.7	4,081	258	930	22,317	CTE-RMPP
Tunnel Diquini	2/2007		10.8	5,059	320	1,153	27,665	CTE-RMPP
Tunnel Diquini	1/2007		12.1	5,680	360	1,294	31,061	CTE-RMPP
Tunnel Diquini	12/2006		12.1	5,680	360	1,294	31,061	CTE-RMPP
Tunnel Diquini	11/2006		11.6	5,434	344	1,238	29,713	CTE-RMPP
Tunnel Diquini	10/2006		10.6	4,945	313	1,127	27,043	CTE-RMPP
Tunnel Diquini	9/2006		10.4	4,873	308	1,110	26,646	CTE-RMPP
Tunnel Diquini	8/2006		9.6	4,504	285	1,026	24,628	CTE-RMPP

Water Point Name	Date	Stage (cm)	Flow (cfs)	Flow (gpm)	Flow (L/s)	Flow (m3/h)	Flow (m3/d)	Data Source
Tunnel Diquini	7/2006		10.2	4,787	303	1,091	26,179	CTE-RMPP
Tunnel Diquini	6/2006		10.4	4,873	308	1,110	26,646	CTE-RMPP
Tunnel Diquini	5/2006		11.0	5,167	327	1,177	28,253	CTE-RMPP
Tunnel Diquini	4/2006		12.0	5,593	354	1,274	30,586	CTE-RMPP
Tunnel Diquini	3/2006		13.0	6,099	386	1,390	33,350	CTE-RMPP
Tunnel Diquini	2/2006		14.8	6,935	439	1,580	37,921	CTE-RMPP
Tunnel Diquini	1/2006		15.9	7,442	471	1,696	40,694	CTE-RMPP
Tunnel Diquini	12/2005		16.6	7,774	492	1,771	42,509	CTE-RMPP
Tunnel Diquini	11/2005		15.4	7,203	456	1,641	39,390	CTE-RMPP
Tunnel Diquini	10/2005		10.9	5,100	323	1,162	27,890	CTE-RMPP
Tunnel Diquini	9/2005		9.5	4,442	281	1,012	24,293	CTE-RMPP
Tunnel Diquini	8/2005		7.9	3,713	235	846	20,304	CTE-RMPP
Tunnel Diquini	7/2005		6.5	3,054	193	696	16,699	CTE-RMPP
Tunnel Diquini	6/2005		5.8	2,692	170	613	14,723	CTE-RMPP
Tunnel Diquini	5/2005		6.1	2,870	182	654	15,695	CTE-RMPP
Tunnel Diquini	4/2005		6.9	3,231	205	736	17,669	CTE-RMPP
Tunnel Diquini	3/2005		7.9	3,713	235	846	20,304	CTE-RMPP
Tunnel Diquini	2/2005		8.8	4,103	260	935	22,438	CTE-RMPP
Tunnel Diquini	1/2005		9.2	4,299	272	980	23,509	CTE-RMPP
Tunnel Diquini	12/2004		10.5	4,922	312	1,121	26,914	CTE-RMPP
Tunnel Diquini	11/2004		11.4	5,354	339	1,220	29,277	CTE-RMPP
Tunnel Diquini	10/2004		12.6	5,905	374	1,346	32,292	CTE-RMPP
Tunnel Diquini	9/2004		13.8	6,480	410	1,476	35,436	CTE-RMPP
Tunnel Diquini	8/2004		13.8	6,474	410	1,475	35,402	CTE-RMPP
Tunnel Diquini	7/2004		12.6	5,905	374	1,346	32,292	CTE-RMPP
Tunnel Diquini	6/2004		11.9	5,570	353	1,269	30,460	CTE-RMPP
Tunnel Diquini	5/2004		11.7	5,461	346	1,244	29,864	CTE-RMPP
Tunnel Diquini	4/2004		12.9	6,017	381	1,371	32,905	CTE-RMPP
Tunnel Diquini	3/2004		14.1	6,591	417	1,502	36,042	CTE-RMPP
Tunnel Diquini	2/2004		15.6	7,300	462	1,663	39,917	CTE-RMPP
Tunnel Diquini	1/2004		15.5	7,274	460	1,657	39,775	CTE-RMPP
Tunnel Diquini	12/2003		15.1	7,059	447	1,608	38,604	CTE-RMPP
Tunnel Diquini	11/2003		12.6	5,882	372	1,340	32,162	CTE-RMPP
Tunnel Diquini	10/2003		9.6	4,504	285	1,026	24,628	CTE-RMPP
Tunnel Diquini	9/2003		9.2	4,299	272	980	23,509	CTE-RMPP
Tunnel Diquini	8/2003		9.0	4,198	266	957	22,956	CTE-RMPP
Tunnel Diquini	7/2003		7.9	3,705	235	844	20,261	CTE-RMPP

Water Point Name	Date	Stage (cm)	Flow (cfs)	Flow (gpm)	Flow (L/s)	Flow (m3/h)	Flow (m3/d)	Data Source
Tunnel Diquini	6/2003		8.2	3,826	242	872	20,921	CTE-RMPP
Tunnel Diquini	5/2003		8.2	3,855	244	878	21,082	CTE-RMPP
Tunnel Diquini	4/2003		8.8	4,134	262	942	22,606	CTE-RMPP
Tunnel Diquini	3/2003		9.3	4,349	275	991	23,784	CTE-RMPP
Tunnel Diquini	2/2003		10.2	4,764	302	1,085	26,050	CTE-RMPP
Tunnel Diquini	1/2003		9.8	4,603	291	1,049	25,173	CTE-RMPP
Tunnel Diquini	12/2002		11.0	5,130	325	1,169	28,055	CTE-RMPP
Tunnel Diquini	11/2002		11.3	5,301	336	1,208	28,990	CTE-RMPP
Tunnel Diquini	10/2002		12.1	5,680	360	1,294	31,061	CTE-RMPP
Tunnel Diquini	9/2002		12.3	5,748	364	1,310	31,432	CTE-RMPP
Tunnel Diquini	8/2002		12.6	5,878	372	1,339	32,141	CTE-RMPP
Tunnel Diquini	7/2002		11.7	5,459	345	1,244	29,851	CTE-RMPP
Tunnel Diquini	6/2002		9.1	4,258	270	970	23,285	CTE-RMPP
Tunnel Diquini	5/2002		8.3	3,868	245	881	21,151	CTE-RMPP
Tunnel Diquini	4/2002		8.3	3,877	245	883	21,203	CTE-RMPP
Tunnel Diquini	3/2002		8.8	4,108	260	936	22,464	CTE-RMPP
Tunnel Diquini	2/2002		9.4	4,413	279	1,005	24,132	CTE-RMPP
Tunnel Diquini	1/2002		9.6	4,508	285	1,027	24,650	CTE-RMPP
Tunnel Diquini	12/2001		10.6	4,974	315	1,133	27,199	CTE-RMPP
Tunnel Diquini	11/2001		11.9	5,577	353	1,271	30,499	CTE-RMPP
Tunnel Diquini	10/2001		12.3	5,767	365	1,314	31,536	CTE-RMPP
Tunnel Diquini	9/2001		13.2	6,189	392	1,410	33,843	CTE-RMPP
Tunnel Diquini	8/2001		13.1	6,116	387	1,394	33,445	CTE-RMPP
Tunnel Diquini	7/2001		12.5	5,840	370	1,331	31,933	CTE-RMPP
Tunnel Diquini	6/2001		11.9	5,574	353	1,270	30,482	CTE-RMPP
Tunnel Diquini	5/2001		11.5	5,399	342	1,230	29,523	CTE-RMPP
Tunnel Diquini	4/2001		10.8	5,040	319	1,148	27,562	CTE-RMPP
Tunnel Diquini	3/2001		11.4	5,356	339	1,220	29,290	CTE-RMPP
Tunnel Diquini	2/2001		12.0	5,593	354	1,274	30,586	CTE-RMPP
Tunnel Diquini	1/2001		14.4	6,749	427	1,538	36,905	CTE-RMPP
Tunnel Diquini	12/2000							
Tunnel Diquini	11/2000							
Tunnel Diquini	10/2000							
Tunnel Diquini	9/2000		10.2	4,764	302	1,085	26,050	CTE-RMPP
Tunnel Diquini	8/2000		10.1	4,712	298	1,074	25,764	CTE-RMPP
Tunnel Diquini	7/2000		10.2	4,764	302	1,085	26,050	CTE-RMPP
Tunnel Diquini	6/2000		10.6	4,974	315	1,133	27,199	CTE-RMPP

Water Point Name	Date	Stage (cm)	Flow (cfs)	Flow (gpm)	Flow (L/s)	Flow (m3/h)	Flow (m3/d)	Data Source
Tunnel Diquini	5/2000		11.6	5,408	342	1,232	29,575	CTE-RMPP
Tunnel Diquini	4/2000		12.9	6,017	381	1,371	32,901	CTE-RMPP
Tunnel Diquini	3/2000		13.2	6,187	392	1,410	33,834	CTE-RMPP
Tunnel Diquini	2/2000		13.2	6,187	392	1,410	33,834	CTE-RMPP
Tunnel Diquini	1/2000		14.1	6,590	417	1,502	36,037	CTE-RMPP
Tunnel Diquini	12/1999		14.0	6,548	414	1,492	35,804	CTE-RMPP
Tunnel Diquini	11/1999		15.0	6,999	443	1,595	38,275	CTE-RMPP
Tunnel Diquini	10/1999		14.7	6,882	436	1,568	37,636	CTE-RMPP
Tunnel Diquini	9/1999		14.7	6,870	435	1,565	37,567	CTE-RMPP
Tunnel Diquini	8/1999		13.8	6,475	410	1,475	35,407	CTE-RMPP
Tunnel Diquini	7/1999		13.8	6,475	410	1,475	35,407	CTE-RMPP
Tunnel Diquini	6/1999		12.4	5,792	367	1,320	31,674	CTE-RMPP
Tunnel Diquini	5/1999		13.2	6,187	392	1,410	33,834	CTE-RMPP
Tunnel Diquini	4/1999		14.1	6,590	417	1,502	36,037	CTE-RMPP
Tunnel Diquini	3/1999		15.0	7,017	444	1,599	38,370	CTE-RMPP
Tunnel Diquini	2/1999		15.7	7,331	464	1,670	40,090	CTE-RMPP
Tunnel Diquini	1/1999		16.5	7,723	489	1,760	42,232	CTE-RMPP
Tunnel Diquini	12/1998		15.9	7,443	471	1,696	40,703	CTE-RMPP
Tunnel Diquini	11/1998		13.5	6,301	399	1,436	34,456	CTE-RMPP
Tunnel Diquini	10/1998		12.7	5,961	377	1,358	32,599	CTE-RMPP
Tunnel Diquini	9/1998		9.1	4,252	269	969	23,250	CTE-RMPP
Tunnel Diquini	8/1998		7.8	3,656	231	833	19,993	CTE-RMPP
Tunnel Diquini	7/1998		7.0	3,267	207	744	17,868	CTE-RMPP
Tunnel Diquini	6/1998		6.9	3,231	205	736	17,669	CTE-RMPP
Tunnel Diquini	5/1998		6.9	3,231	205	736	17,669	CTE-RMPP
Tunnel Diquini	4/1998		7.1	3,305	209	753	18,075	CTE-RMPP
Tunnel Diquini	3/1998		7.1	3,342	212	761	18,274	CTE-RMPP
Tunnel Diquini	2/1998		7.5	3,512	222	800	19,207	CTE-RMPP
Tunnel Diquini	1/1998		7.8	3,656	231	833	19,993	CTE-RMPP
Tunnel Diquini	12/1997		8.1	3,801	241	866	20,788	CTE-RMPP
Tunnel Diquini	11/1997		8.7	4,078	258	929	22,300	CTE-RMPP
Tunnel Diquini	10/1997		9.0	4,198	266	957	22,956	CTE-RMPP
Tunnel Diquini	9/1997		9.2	4,318	273	984	23,613	CTE-RMPP
Tunnel Diquini	8/1997		10.1	4,732	300	1,078	25,877	CTE-RMPP
Tunnel Diquini	7/1997		9.8	4,566	289	1,040	24,970	CTE-RMPP
Tunnel Diquini	6/1997		9.4	4,400	279	1,003	24,062	CTE-RMPP
Tunnel Diquini	5/1997		10.3	4,816	305	1,097	26,335	CTE-RMPP

Water Point Name	Date	Stage (cm)	Flow (cfs)	Flow (gpm)	Flow (L/s)	Flow (m3/h)	Flow (m3/d)	Data Source
Tunnel Diquini	4/1997		10.7	4,986	316	1,136	27,268	CTE-RMPP
Tunnel Diquini	3/1997		11.2	5,242	332	1,194	28,668	CTE-RMPP
Tunnel Diquini	2/1997		11.2	5,242	332	1,194	28,668	CTE-RMPP
Tunnel Diquini	1/1997		11.4	5,329	337	1,214	29,143	CTE-RMPP
Tunnel Diquini	12/1996		11.3	5,285	335	1,204	28,901	CTE-RMPP
Tunnel Diquini	11/1996		10.9	5,113	324	1,165	27,959	CTE-RMPP
Tunnel Diquini	10/1996		10.9	5,113	324	1,165	27,959	CTE-RMPP
Tunnel Diquini	9/1996		10.9	5,113	324	1,165	27,959	CTE-RMPP
Tunnel Diquini	8/1996		11.2	5,242	332	1,194	28,668	CTE-RMPP
Tunnel Diquini	7/1996		10.3	4,816	305	1,097	26,335	CTE-RMPP
Tunnel Diquini	6/1996		9.0	4,201	266	957	22,974	CTE-RMPP
Tunnel Diquini	5/1996		8.6	4,004	253	912	21,894	CTE-RMPP
Tunnel Diquini	4/1996		8.7	4,084	259	931	22,334	CTE-RMPP
Tunnel Diquini	3/1996		10.3	4,817	305	1,098	26,343	CTE-RMPP
Tunnel Diquini	2/1996		10.3	4,816	305	1,097	26,335	CTE-RMPP
Tunnel Diquini	1/1996		10.3	4,817	305	1,098	26,343	CTE-RMPP
Tunnel Diquini	12/1995		13.1	6,130	388	1,397	33,523	CTE-RMPP
Tunnel Diquini	11/1995		13.2	6,187	392	1,410	33,834	CTE-RMPP
Tunnel Diquini	10/1995		13.3	6,220	394	1,417	34,016	CTE-RMPP
Tunnel Diquini	9/1995		13.1	6,130	388	1,397	33,523	CTE-RMPP
Tunnel Diquini	8/1995		13.3	6,246	395	1,423	34,154	CTE-RMPP
Tunnel Diquini	7/1995		13.6	6,360	403	1,449	34,776	CTE-RMPP
Tunnel Diquini	6/1995		14.6	6,852	434	1,561	37,472	CTE-RMPP
Tunnel Diquini	5/1995		15.1	7,059	447	1,608	38,604	CTE-RMPP
Tunnel Diquini	4/1995		16.1	7,540	477	1,718	41,230	CTE-RMPP
Tunnel Diquini	3/1995		14.1	6,611	418	1,506	36,150	CTE-RMPP
Tunnel Diquini	2/1995		16.1	7,540	477	1,718	41,230	CTE-RMPP
Tunnel Diquini	1/1995		13.6	6,358	402	1,449	34,767	CTE-RMPP
Tunnel Diquini	12/1994		11.2	5,242	332	1,194	28,668	CTE-RMPP
Tunnel Diquini	11/1994		8.5	3,999	253	911	21,868	CTE-RMPP
Tunnel Diquini	10/1994		8.9	4,176	264	951	22,836	CTE-RMPP
Tunnel Diquini	9/1994		9.3	4,366	276	995	23,872	CTE-RMPP
Tunnel Diquini	8/1994		7.5	3,512	222	800	19,207	CTE-RMPP
Tunnel Diquini	7/1994		7.5	3,512	222	800	19,207	CTE-RMPP
Tunnel Diquini	6/1994		7.6	3,539	224	806	19,354	CTE-RMPP
Tunnel Diquini	5/1994		8.5	3,999	253	911	21,868	CTE-RMPP
Tunnel Diquini	4/1994		8.1	3,801	241	866	20,788	CTE-RMPP

Water Point Name	Date	Stage (cm)	Flow (cfs)	Flow (gpm)	Flow (L/s)	Flow (m3/h)	Flow (m3/d)	Data Source
Tunnel Diquini	3/1994		9.4	4,400	279	1,003	24,062	CTE-RMPP
Tunnel Diquini	2/1994		8.1	3,801	241	866	20,788	CTE-RMPP
Tunnel Diquini	1/1994		7.7	3,609	228	822	19,734	CTE-RMPP
Tunnel Diquini	12/1993		7.7	3,609	228	822	19,734	CTE-RMPP
Tunnel Diquini	11/1993		10.7	5,028	318	1,146	27,492	CTE-RMPP
Tunnel Diquini	10/1993		7.7	3,609	228	822	19,734	CTE-RMPP
Tunnel Diquini	9/1993		10.7	5,028	318	1,146	27,492	CTE-RMPP
Tunnel Diquini	8/1993		7.7	3,609	228	822	19,734	CTE-RMPP
Tunnel Diquini	7/1993		8.5	3,999	253	911	21,868	CTE-RMPP
Tunnel Diquini	6/1993		8.5	3,999	253	911	21,868	CTE-RMPP
Tunnel Diquini	5/1993		8.4	3,939	249	897	21,540	CTE-RMPP
Tunnel Diquini	4/1993		8.9	4,151	263	946	22,697	CTE-RMPP
Tunnel Diquini	3/1993		9.4	4,400	279	1,003	24,062	CTE-RMPP
Tunnel Diquini	2/1993		9.4	4,400	279	1,003	24,062	CTE-RMPP
Tunnel Diquini	1/1993		9.0	4,198	266	957	22,956	CTE-RMPP
Tunnel Diquini	12/1992		9.0	4,198	266	957	22,956	CTE-RMPP
Tunnel Diquini	11/1992		8.5	3,999	253	911	21,868	CTE-RMPP
Tunnel Diquini	10/1992		7.2	3,373	214	769	18,446	CTE-RMPP
Tunnel Diquini	9/1992		6.5	3,048	193	694	16,667	CTE-RMPP
Tunnel Diquini	8/1992		6.5	3,048	193	694	16,667	CTE-RMPP
Tunnel Diquini	7/1992		6.6	3,089	196	704	16,891	CTE-RMPP
Tunnel Diquini	6/1992		5.4	2,520	160	574	13,781	CTE-RMPP
Tunnel Diquini	5/1992		7.0	3,288	208	749	17,980	CTE-RMPP
Tunnel Diquini	4/1992		7.0	3,288	208	749	17,980	CTE-RMPP
Tunnel Diquini	3/1992		7.0	3,288	208	749	17,980	CTE-RMPP
Tunnel Diquini	2/1992		7.1	3,304	209	753	18,066	CTE-RMPP
Tunnel Diquini	1/1992		7.5	3,497	221	797	19,120	CTE-RMPP
Tunnel Diquini	12/1991		7.1	3,304	209	753	18,066	CTE-RMPP
Tunnel Diquini	11/1991		10.6	4,941	313	1,126	27,017	CTE-RMPP
Tunnel Diquini	10/1991		10.6	4,941	313	1,126	27,017	CTE-RMPP
Tunnel Diquini	9/1991		10.6	4,941	313	1,126	27,017	CTE-RMPP
Tunnel Diquini	8/1991		10.6	4,941	313	1,126	27,017	CTE-RMPP
Tunnel Diquini	7/1991		9.6	4,470	283	1,018	24,443	CTE-RMPP
Tunnel Diquini	6/1991		9.4	4,407	279	1,004	24,097	CTE-RMPP
Tunnel Diquini	5/1991		10.3	4,816	305	1,097	26,335	CTE-RMPP
Tunnel Diquini	4/1991		10.3	4,816	305	1,097	26,335	CTE-RMPP
Tunnel Diquini	3/1991		10.3	4,816	305	1,097	26,335	CTE-RMPP

Water Point Name	Date	Stage (cm)	Flow (cfs)	Flow (gpm)	Flow (L/s)	Flow (m3/h)	Flow (m3/d)	Data Source
Tunnel Diquini	2/1991							CTE-RMPP
Tunnel Diquini	1/1991							CTE-RMPP
Tunnel Diquini	12/1990		11.2	5,242	332	1,194	28,668	CTE-RMPP
Tunnel Diquini	11/1990		9.9	4,610	292	1,050	25,212	CTE-RMPP
Tunnel Diquini	10/1990		9.1	4,280	271	975	23,406	CTE-RMPP
Tunnel Diquini	9/1990		10.3	4,816	305	1,097	26,335	CTE-RMPP
Tunnel Diquini	8/1990		10.3	4,816	305	1,097	26,335	CTE-RMPP
Tunnel Diquini	7/1990		10.3	4,816	305	1,097	26,335	CTE-RMPP
Tunnel Diquini	6/1990		10.3	4,816	305	1,097	26,335	CTE-RMPP
Tunnel Diquini	5/1990		12.1	5,680	360	1,294	31,061	CTE-RMPP
Tunnel Diquini	4/1990		12.1	5,680	360	1,294	31,061	CTE-RMPP
Tunnel Diquini	3/1990		12.1	5,680	360	1,294	31,061	CTE-RMPP
Tunnel Diquini	2/1990		14.1	6,590	417	1,502	36,037	CTE-RMPP
Tunnel Diquini	1/1990		13.6	6,385	404	1,455	34,914	CTE-RMPP
Tunnel Diquini	12/1989		14.1	6,590	417	1,502	36,037	CTE-RMPP
Tunnel Diquini	11/1989		14.1	6,590	417	1,502	36,037	CTE-RMPP
Tunnel Diquini	10/1989		9.8	4,609	292	1,050	25,203	CTE-RMPP
Tunnel Diquini	9/1989		9.4	4,400	279	1,003	24,062	CTE-RMPP
Tunnel Diquini	8/1989		8.8	4,099	259	934	22,412	CTE-RMPP
Tunnel Diquini	7/1989		8.5	3,999	253	911	21,868	CTE-RMPP
Tunnel Diquini	6/1989		8.5	3,999	253	911	21,868	CTE-RMPP
Tunnel Diquini	5/1989		8.8	4,099	259	934	22,412	CTE-RMPP
Tunnel Diquini	4/1989		9.1	4,249	269	968	23,233	CTE-RMPP
Tunnel Diquini	3/1989		9.4	4,400	279	1,003	24,062	CTE-RMPP
Tunnel Diquini	2/1989		9.4	4,400	279	1,003	24,062	CTE-RMPP
Tunnel Diquini	1/1989		9.0	4,200	266	957	22,965	CTE-RMPP
Tunnel Diquini	12/1988		9.2	4,306	273	981	23,544	CTE-RMPP
Tunnel Diquini	11/1988		9.4	4,400	279	1,003	24,062	CTE-RMPP
Tunnel Diquini	10/1988		8.5	3,999	253	911	21,868	CTE-RMPP
Tunnel Diquini	9/1988		8.5	3,999	253	911	21,868	CTE-RMPP
Tunnel Diquini	8/1988		8.3	3,880	246	884	21,220	CTE-RMPP
Tunnel Diquini	7/1988		7.9	3,707	235	845	20,269	CTE-RMPP
Tunnel Diquini	6/1988		7.3	3,418	216	779	18,688	CTE-RMPP
Tunnel Diquini	5/1988		7.6	3,561	225	811	19,475	CTE-RMPP
Tunnel Diquini	4/1988		8.4	3,948	250	900	21,591	CTE-RMPP
Tunnel Diquini	3/1988		8.6	4,040	256	921	22,092	CTE-RMPP
Tunnel Diquini	2/1988		8.5	3,961	251	903	21,660	CTE-RMPP

Water Point Name	Date	Stage (cm)	Flow (cfs)	Flow (gpm)	Flow (L/s)	Flow (m3/h)	Flow (m3/d)	Data Source
Tunnel Diquini	1/1988		8.6	4,040	256	921	22,092	CTE-RMPP
Tunnel Diquini	12/1987		8.3	3,885	246	885	21,246	CTE-RMPP
Tunnel Diquini	11/1987		6.4	2,988	189	681	16,338	CTE-RMPP
Tunnel Diquini	10/1987		6.4	3,004	190	684	16,425	CTE-RMPP
Tunnel Diquini	9/1987		6.1	2,868	182	653	15,682	CTE-RMPP
Tunnel Diquini	8/1987		5.5	2,577	163	587	14,092	CTE-RMPP
Tunnel Diquini	7/1987		4.3	2,027	128	462	11,085	CTE-RMPP
Tunnel Diquini	6/1987		4.3	2,027	128	462	11,085	CTE-RMPP
Tunnel Diquini	5/1987		4.5	2,106	133	480	11,517	CTE-RMPP
Tunnel Diquini	4/1987		5.4	2,522	160	575	13,789	CTE-RMPP
Tunnel Diquini	3/1987		5.3	2,462	156	561	13,461	CTE-RMPP
Tunnel Diquini	2/1987		5.3	2,492	158	568	13,625	CTE-RMPP
Tunnel Diquini	1/1987		6.0	2,823	179	643	15,440	CTE-RMPP
Tunnel Diquini	12/1986		6.4	3,013	191	687	16,476	CTE-RMPP
Tunnel Diquini	11/1986		6.9	3,231	205	736	17,669	CTE-RMPP
Tunnel Diquini	10/1986		6.9	3,231	205	736	17,669	CTE-RMPP
Tunnel Diquini	9/1986		7.5	3,533	224	805	19,319	CTE-RMPP
Tunnel Diquini	8/1986		7.7	3,609	228	822	19,734	CTE-RMPP
Tunnel Diquini	7/1986		7.6	3,561	225	811	19,475	CTE-RMPP
Tunnel Diquini	6/1986		6.5	3,048	193	694	16,667	CTE-RMPP
Tunnel Diquini	5/1986		7.0	3,264	207	744	17,850	CTE-RMPP
Tunnel Diquini	4/1986		7.1	3,324	210	757	18,179	CTE-RMPP
Tunnel Diquini	3/1986		7.3	3,418	216	779	18,688	CTE-RMPP
Tunnel Diquini	2/1986		7.7	3,609	228	822	19,734	CTE-RMPP
Tunnel Diquini	1/1986		7.7	3,609	228	822	19,734	CTE-RMPP
Tunnel Diquini	12/1985		8.2	3,854	244	878	21,073	CTE-RMPP
Tunnel Diquini	11/1985		8.5	3,999	253	911	21,868	CTE-RMPP
Tunnel Diquini	10/1985		8.5	3,999	253	911	21,868	CTE-RMPP
Tunnel Diquini	9/1985		9.8	4,607	292	1,050	25,194	CTE-RMPP
Tunnel Diquini	8/1985		10.7	4,985	316	1,136	27,259	CTE-RMPP
Tunnel Diquini	7/1985		13.1	6,130	388	1,397	33,523	CTE-RMPP
Tunnel Diquini	6/1985		13.0	6,074	384	1,384	33,212	CTE-RMPP
Tunnel Diquini	5/1985		12.1	5,656	358	1,289	30,931	CTE-RMPP
Tunnel Diquini	4/1985		12.1	5,680	360	1,294	31,061	CTE-RMPP
Tunnel Diquini	3/1985		12.0	5,606	355	1,277	30,655	CTE-RMPP
Tunnel Diquini	2/1985		11.3	5,268	333	1,200	28,806	CTE-RMPP
Tunnel Diquini	1/1985		15.3	7,178	454	1,635	39,252	CTE-RMPP

Water Point Name	Date	Stage (cm)	Flow (cfs)	Flow (gpm)	Flow (L/s)	Flow (m3/h)	Flow (m3/d)	Data Source
Tunnel Diquini	12/1984		15.3	7,178	454	1,635	39,252	CTE-RMPP
Tunnel Diquini	11/1984		15.1	7,044	446	1,605	38,517	CTE-RMPP
Tunnel Diquini	10/1984		16.4	7,672	486	1,748	41,956	CTE-RMPP
Tunnel Diquini	9/1984		15.3	7,148	452	1,629	39,087	CTE-RMPP
Tunnel Diquini	8/1984		14.3	6,696	424	1,526	36,616	CTE-RMPP
Tunnel Diquini	7/1984		12.7	5,957	377	1,357	32,573	CTE-RMPP
Tunnel Diquini	6/1984		9.1	4,257	269	970	23,276	CTE-RMPP
Tunnel Diquini	5/1984		6.9	3,247	206	740	17,755	CTE-RMPP
Tunnel Diquini	4/1984		7.3	3,406	216	776	18,628	CTE-RMPP
Tunnel Diquini	3/1984		7.8	3,647	231	831	19,941	CTE-RMPP
Tunnel Diquini	2/1984		7.8	3,647	231	831	19,941	CTE-RMPP
Tunnel Diquini	1/1984		8.2	3,844	243	876	21,021	CTE-RMPP
Tunnel Diquini	12/1983		8.0	3,745	237	853	20,477	CTE-RMPP
Tunnel Diquini	11/1983		8.0	3,765	238	858	20,589	CTE-RMPP
Tunnel Diquini	10/1983		6.9	3,252	206	741	17,781	CTE-RMPP
Tunnel Diquini	9/1983		6.0	2,805	178	639	15,336	CTE-RMPP
Tunnel Diquini	8/1983		6.0	2,805	178	639	15,336	CTE-RMPP
Tunnel Diquini	7/1983		6.0	2,812	178	641	15,379	CTE-RMPP
Tunnel Diquini	6/1983		6.5	3,040	192	693	16,623	CTE-RMPP
Tunnel Diquini	5/1983		7.3	3,410	216	777	18,645	CTE-RMPP
Tunnel Diquini	4/1983		7.8	3,634	230	828	19,872	CTE-RMPP
Tunnel Diquini	3/1983		7.8	3,634	230	828	19,872	CTE-RMPP
Tunnel Diquini	2/1983		9.9	4,636	293	1,056	25,350	CTE-RMPP
Tunnel Diquini	1/1983		12.5	5,846	370	1,332	31,968	CTE-RMPP
Tunnel Diquini	12/1982		10.8	5,056	320	1,152	27,648	CTE-RMPP
Tunnel Diquini	11/1982		10.8	5,056	320	1,152	27,648	CTE-RMPP
Tunnel Diquini	10/1982		10.8	5,056	320	1,152	27,648	CTE-RMPP
Tunnel Diquini	9/1982		12.7	5,961	377	1,358	32,599	CTE-RMPP
Tunnel Diquini	8/1982		12.7	5,961	377	1,358	32,599	CTE-RMPP
Tunnel Diquini	7/1982		14.8	6,913	438	1,575	37,800	CTE-RMPP
Tunnel Diquini	6/1982		14.8	6,913	438	1,575	37,800	CTE-RMPP
Tunnel Diquini	5/1982		18.7	8,769	555	1,998	47,952	CTE-RMPP
Tunnel Diquini	4/1982		18.0	8,404	532	1,915	45,956	CTE-RMPP
Tunnel Diquini	3/1982		14.8	6,913	438	1,575	37,800	CTE-RMPP
Tunnel Diquini	2/1982		14.8	6,913	438	1,575	37,800	CTE-RMPP
Tunnel Diquini	1/1982		14.8	6,913	438	1,575	37,800	CTE-RMPP
Tunnel Diquini	12/1981		14.8	6,913	438	1,575	37,800	CTE-RMPP

Water Point Name	Date	Stage (cm)	Flow (cfs)	Flow (gpm)	Flow (L/s)	Flow (m3/h)	Flow (m3/d)	Data Source
Tunnel Diquini	11/1981		15.5	7,246	459	1,651	39,623	CTE-RMPP
Tunnel Diquini	10/1981		16.9	7,892	500	1,798	43,157	CTE-RMPP
Tunnel Diquini	9/1981		14.8	6,913	438	1,575	37,800	CTE-RMPP
Tunnel Diquini	8/1981		14.8	6,913	438	1,575	37,800	CTE-RMPP
Tunnel Diquini	7/1981		14.8	6,913	438	1,575	37,800	CTE-RMPP
Tunnel Diquini	6/1981		14.8	6,913	438	1,575	37,800	CTE-RMPP
Tunnel Diquini	5/1981		16.9	7,892	500	1,798	43,157	CTE-RMPP
Tunnel Diquini	4/1981		13.7	6,431	407	1,465	35,165	CTE-RMPP
Tunnel Diquini	3/1981		13.7	6,431	407	1,465	35,165	CTE-RMPP
Tunnel Diquini	2/1981		13.7	6,431	407	1,465	35,165	CTE-RMPP
Tunnel Diquini	1/1981		13.7	6,431	407	1,465	35,165	CTE-RMPP
Tunnel Diquini	12/1980		12.7	5,961	377	1,358	32,599	CTE-RMPP
Tunnel Diquini	11/1980		14.8	6,913	438	1,575	37,800	CTE-RMPP
Tunnel Diquini	10/1980		12.7	5,961	377	1,358	32,599	CTE-RMPP
Tunnel Diquini	8/1959		7.3	3,427	217	781	18,740	Waite (1960)
Riviere Froide	6/9/1927		33.1	15,484	980	3,528	84,672	Hydrographic Bulletins
Riviere Froide	5/27/1928		16.5	7,742	490	1,764	42,336	Hydrographic Bulletins
Riviere Froide	8/18/1928		12.8	6,004	380	1,368	32,832	Hydrographic Bulletins
Riviere Froide	3/4/1929		12.2	5,688	360	1,296	31,104	Hydrographic Bulletins
Riviere Froide	6/27/1929		14.5	6,794	430	1,548	37,152	Hydrographic Bulletins
Riviere Froide	1/10/1930		11.5	5,372	340	1,224	29,376	Hydrographic Bulletins
Riviere Froide	4/22/1930		12.8	6,004	380	1,368	32,832	Hydrographic Bulletins
Riviere Froide	8/23/1930		12.5	5,846	370	1,332	31,968	Hydrographic Bulletins
Riviere Froide	6/26/1931		60.4	28,282	1,790	6,444	154,656	Hydrographic Bulletins
Source Diquini	4/6/1926		1.6	761	48	173	4,162	Hydrographic Bulletins
Source Diquini	11/11/1926		2.3	1,062	67	242	5,806	Hydrographic Bulletins
Source Diquini	2/16/1927		2.4	1,110	70	253	6,068	Hydrographic Bulletins
Source Diquini	2/4/1938		1.4	632	40	144	3,456	Hydrographic Bulletins
Source Diquini	2/7/1923		2.7	1,285	81	293	7,025	Hydrographic Bulletins

Water Point Name	Date	Stage (cm)	Flow (cfs)	Flow (gpm)	Flow (L/s)	Flow (m3/h)	Flow (m3/d)	Data Source
Source Diquini	7/4/1923		2.4	1,125	71	256	6,152	Hydrographic Bulletins
Source Diquini	12/12/1923		2.5	1,160	73	264	6,342	Hydrographic Bulletins
Source Diquini	4/13/1924		1.8	854	54	195	4,671	Hydrographic Bulletins
Source Diquini	11/14/2013		1.0	448	28	102	2,449	EPTISA (2016)
Source Diquini	1/27/2014		0.8	373	24	85	2,040	EPTISA (2016)
Source Diquini	2/27/2014		0.7	332	21	76	1,814	EPTISA (2016)
Source Diquini	4/11/2014		1.8	846	54	193	4,628	EPTISA (2016)
Source Diquini	6/30/2014		1.6	728	46	166	3,980	EPTISA (2016)
Source Diquini	7/22/2014		1.6	755	48	172	4,126	EPTISA (2016)
Source Diquini	8/1959		1.0	485	31	111	2,652	Waite (1960)

Compiled Water Quality Data for Tunnel Diquini and Source Diquini

Water Point Name	Date	pH	Temperature C	Conductivity (µS/cm)	Turbidity (NTU)	Chloride (mg/L)	Nitrate (mg/L as NO3)	Data Source
Tunnel Diquini	6/25/2015	7.5	24.7	641				EPTISA (2016)
Tunnel Diquini	1/16/2015	7.2	23.6	367				EPTISA (2016)
Tunnel Diquini	12/12/2014	7.1	24	381				EPTISA (2016)
Tunnel Diquini	11/5/2014							EPTISA (2016)
Tunnel Diquini	9/25/2014	7.3	25	413				EPTISA (2016)
Tunnel Diquini	8/29/2014		24	390				EPTISA (2016)
Tunnel Diquini	7/22/2014	7.9	25	415				EPTISA (2016)
Tunnel Diquini	6/30/2014		25	394				EPTISA (2016)
Tunnel Diquini	5/20/2014	8.4	25	402				EPTISA (2016)
Tunnel Diquini	4/11/2014	8.7	24	413				EPTISA (2016)
Tunnel Diquini	2/27/2014	7.4	25	407				EPTISA (2016)
Tunnel Diquini	1/27/2014	8.2	24	408				EPTISA (2016)
Tunnel Diquini	11/14/2013	7.9	24	413				EPTISA (2016)
Tunnel Diquini	7/9/2013	7.7	26	387	0.22		7.53	CTE-RMPP
Tunnel Diquini	6/3/2013	7.9	26.2	390	0.37		10.18	CTE-RMPP
Tunnel Diquini	5/7/2013	7.41	28	396	0.23		11.07	CTE-RMPP
Tunnel Diquini	4/17/2013	7.6	25.4	391	0.54		10.62	CTE-RMPP
Tunnel Diquini	3/6/2013	8	24.8	395	0.29	12	10.18	CTE-RMPP
Tunnel Diquini	2/4/2013	7.8	25.1	398	0.25		14.61	CTE-RMPP
Tunnel Diquini	1/9/2013	7.37	24.9	393	0.28			CTE-RMPP
Tunnel Diquini	12/19/2012							CTE-RMPP
Tunnel Diquini	11/19/2012	7.5	24.8	397	0.15		13.72	CTE-RMPP
Tunnel Diquini	10/23/2012	7.4	23.7	393	0.16		11.95	CTE-RMPP
Tunnel Diquini	9/19/2012	7.7	30.1	393	0.14		14.61	CTE-RMPP
Tunnel Diquini	8/14/2012	7.5	25	393	0.12		12.4	CTE-RMPP
Tunnel Diquini	7/3/2012	7.5	24.4	393	0.12		9.3	CTE-RMPP
Tunnel Diquini	6/12/2012	7.3	26.3	397	0.33	16.74	6.64	CTE-RMPP
Tunnel Diquini	5/8/2012	7.49	28.8	397	0.14		8.85	CTE-RMPP
Tunnel Diquini	4/16/2012	7.37	25.3	384	0.18		11.95	CTE-RMPP

Water Point Name	Date	pH	Temperature C	Conductivity (µS/cm)	Turbidity (NTU)	Chloride (mg/L)	Nitrate (mg/L as NO3)	Data Source
Tunnel Diquini	3/13/2012							CTE-RMPP
Tunnel Diquini	2/13/2012	7.65		368	0.13		9.74	CTE-RMPP
Tunnel Diquini	1/9/2012	7.48	24.5	376	0.2	10.49	9.74	CTE-RMPP
Tunnel Diquini	12/5/2011	7.24	24.9	388	0.25		8.85	CTE-RMPP
Tunnel Diquini	11/12/2011							CTE-RMPP
Tunnel Diquini	10/12/2011	7.48	28.3	378	0.32		8.85	CTE-RMPP
Tunnel Diquini	9/13/2011	7.09	25.1	381			6.2	CTE-RMPP
Tunnel Diquini	8/17/2011	7.25	25.7	386	0.14	10.49	10.62	CTE-RMPP
Tunnel Diquini	7/22/2011	7.31	24.6	388	0.15	10.24	8.41	CTE-RMPP
Tunnel Diquini	6/12/2011							CTE-RMPP
Tunnel Diquini	5/12/2011							CTE-RMPP
Tunnel Diquini	4/12/2011							CTE-RMPP
Tunnel Diquini	3/12/2011							CTE-RMPP
Tunnel Diquini	2/12/2011							CTE-RMPP
Tunnel Diquini	1/12/2011							CTE-RMPP
Tunnel Diquini	12/12/2010							CTE-RMPP
Tunnel Diquini	11/12/2010	7.72	25.1	381	0.34	7.99	7.31	CTE-RMPP
Tunnel Diquini	10/2010							CTE-RMPP
Tunnel Diquini	9/2010							CTE-RMPP
Tunnel Diquini	8/2010							CTE-RMPP
Tunnel Diquini	7/2010							CTE-RMPP
Tunnel Diquini	6/2010							CTE-RMPP
Tunnel Diquini	5/2010	7.08	25.2	383	0.16		7.53	CTE-RMPP
Tunnel Diquini	4/2010	6.79	26.2	387	0.37		9.3	CTE-RMPP
Tunnel Diquini	3/2010							CTE-RMPP
Tunnel Diquini	2/2010							CTE-RMPP
Tunnel Diquini	1/2010							CTE-RMPP
Tunnel Diquini	12/2009							CTE-RMPP
Tunnel Diquini	11/2009	7.3	24.3	390	0.22	8.49	10.18	CTE-RMPP
Tunnel Diquini	10/2009	7.07	24.6	393	0.19	8.99	11.07	CTE-RMPP
Tunnel Diquini	9/2009	6.86	23.9	383	0.35	13.49	7.52	CTE-RMPP
Tunnel Diquini	8/2009							CTE-RMPP
Tunnel Diquini	7/2009							CTE-RMPP
Tunnel Diquini	6/2009	6.9		379	0.16	8.99	11.51	CTE-RMPP
Tunnel Diquini	5/2009	7.04		384	0.26	10	13.24	CTE-RMPP
Tunnel Diquini	4/2009	7.38		391	0.17	10.5	10.62	CTE-RMPP

Water Point Name	Date	pH	Temperature C	Conductivity (µS/cm)	Turbidity (NTU)	Chloride (mg/L)	Nitrate (mg/L as NO3)	Data Source
Tunnel Diquini	3/2009	7.32		394	0.15	8.5	9.3	CTE-RMPP
Tunnel Diquini	2/2009	7.24		389	0.2	6.48	11.07	CTE-RMPP
Tunnel Diquini	1/2009	7.36		385	0.27	5.99	8.41	CTE-RMPP
Tunnel Diquini	12/2008	7.23		389	0.2	8.49	8.41	CTE-RMPP
Tunnel Diquini	11/2008	6.7		389	0.3	6.49	10.18	CTE-RMPP
Tunnel Diquini	10/2008	7.2		382		5.99		CTE-RMPP
Tunnel Diquini	9/2008	7.24		392		6.49		CTE-RMPP
Tunnel Diquini	8/2008			369		8.49		CTE-RMPP
Tunnel Diquini	7/2008			372		3.99		CTE-RMPP
Tunnel Diquini	6/2008			376		7.99		CTE-RMPP
Tunnel Diquini	5/2008			381		9.74		CTE-RMPP
Tunnel Diquini	4/2008			378		7.52		CTE-RMPP
Tunnel Diquini	3/2008	7.63		375		7.99		CTE-RMPP
Tunnel Diquini	2/2008	7.42		390		8.49		CTE-RMPP
Tunnel Diquini	1/2008	7.3		396	0.16	5.16		CTE-RMPP
Tunnel Diquini	12/2007	7.37		375		6.13		CTE-RMPP
Tunnel Diquini	11/2007							CTE-RMPP
Tunnel Diquini	10/2007	7.82		383		8.21		CTE-RMPP
Tunnel Diquini	9/2007	7.51		381		8.49		CTE-RMPP
Tunnel Diquini	8/2007							CTE-RMPP
Tunnel Diquini	7/2007	7.42		390	0.16	10.26		CTE-RMPP
Tunnel Diquini	6/2007	7.52		383	0.2	10.23		CTE-RMPP
Tunnel Diquini	5/2007	7.46		388	0.24	15.36		CTE-RMPP
Tunnel Diquini	4/2007							CTE-RMPP
Tunnel Diquini	3/2007	7.63		384	0.2	9.26		CTE-RMPP
Tunnel Diquini	2/2007	7.43		386	0.19	8.72		CTE-RMPP
Tunnel Diquini	1/2007	7.37		386	0.2	8.7		CTE-RMPP
Tunnel Diquini	12/2006	7.45		385	0.13	6.26		CTE-RMPP
Tunnel Diquini	11/2006							CTE-RMPP
Tunnel Diquini	10/2006	7.29		390	0.15	8.54		CTE-RMPP
Tunnel Diquini	9/2006	7.42		385	0.12	6.24		CTE-RMPP
Tunnel Diquini	8/2006	7.36		386	0.16	20.4		CTE-RMPP
Tunnel Diquini	7/2006	7.35		381	0.16	9.76		CTE-RMPP
Source Diquini	1/16/2015	7.4	24.6	439				EPTISA (2016)
Source Diquini	8/29/2014		29	449				EPTISA (2016)

Water Point Name	Date	pH	Temperature C	Conductivity (µS/cm)	Turbidity (NTU)	Chloride (mg/L)	Nitrate (mg/L as NO3)	Data Source
Source Diquini	7/22/2014	7.5	25	457				EPTISA (2016)
Source Diquini	5/20/2014	8.2		458				EPTISA (2016)
Source Diquini	4/11/2014	8.2	25	464				EPTISA (2016)
Source Diquini	2/27/2014	7.6	28	422				EPTISA (2016)
Source Diquini	1/27/2014	8.8	24	458				EPTISA (2016)
Source Diquini	11/14/2013	7.8	24	465				EPTISA (2016)
Source Diquini	7/9/2013	7.6	26.4	447	2.41		8.41	CTE-RMPP
Source Diquini	6/3/2013	7.6	26	441	2.23		12.84	CTE-RMPP
Source Diquini	5/7/2013	7.3	26.2	437	0.95	16.99	12.4	CTE-RMPP
Source Diquini	4/17/2013	7.6	25.7	441	2.08		11.95	CTE-RMPP
Source Diquini	3/6/2013	7.7	25.2	443	1.21		16.38	CTE-RMPP
Source Diquini	2/4/2013	7.6	24.9	446	1.87		12.76	CTE-RMPP
Source Diquini	1/9/2013	6.86	26.2	479	1.59	14.5	11.07	CTE-RMPP
Source Diquini	12/19/2012							CTE-RMPP
Source Diquini	11/19/2012	7.4	24.8	440	1.37	12	14.17	CTE-RMPP
Source Diquini	10/23/2012	7.3	25.5	435	1.15		12.4	CTE-RMPP
Source Diquini	9/19/2012	7.6	24.7	433	1.86		11.95	CTE-RMPP
Source Diquini	8/14/2012	7.5	25.3	436	1.64		12.84	CTE-RMPP
Source Diquini	7/3/2012	7.3	25.2	440	0.45		13.72	CTE-RMPP
Source Diquini	6/12/2012	7.3	27.6	440	0.95		7.53	CTE-RMPP
Source Diquini	5/8/2012	7.36	25.6	434	2.04	15.75	11.51	CTE-RMPP
Source Diquini	4/16/2012	7.19	25.6	420	0.62		10.18	CTE-RMPP
Source Diquini	3/13/2012							CTE-RMPP
Source Diquini	2/13/2012	7.65	24.7	405	0.8		9.74	CTE-RMPP
Source Diquini	1/9/2012	7.25	26	408	1.14	8.99	11.07	CTE-RMPP
Source Diquini	12/5/2011	7.27	25.9	421	0.87	12.99	10.62	CTE-RMPP
Source Diquini	11/12/2011							CTE-RMPP
Source Diquini	10/19/2011	7.45	27.4	413	0.62		8.41	CTE-RMPP
Source Diquini	9/13/2011	7.17	25.7	421	1.88		8.41	CTE-RMPP
Source Diquini	8/31/2011	7.27	24.6	418	1.52	12.99	10.18	CTE-RMPP

APPENDIX D – HYDROGEOLOGICAL INVESTIGATION OF SOURCE MARIANI: LABORATORY REPORTS

Analysis Reports

www.encolabs.com

SAMPLE DETECTION SUMMARY

Client ID: Source Mariani **Lab ID:** CC06218-01

Analyte	Results	Flag	MDL	PQL	Units	Method	Notes
Barium - Total	0.174		0.00110	0.0100	mg/L	EPA 200.7	
Calcium - Total	73.2		0.0390	0.100	mg/L	EPA 200.7	
Calcium Hardness	180		0.018	0.0	mg/L	SM 2340B-2011	
Chloride	9.7		1.9	5.0	mg/L	SM 4500Cl E-2011	
Copper - Total	0.00518	J	0.00160	0.0100	mg/L	EPA 200.7	
Fluoride	0.40		0.0097	0.20	mg/L	EPA 300.0	Q-01
Iron - Total	0.0520		0.0220	0.0500	mg/L	EPA 200.7	
Magnesium - Total	5.39		0.0290	0.100	mg/L	EPA 200.7	
Manganese - Total	0.00404	J	0.00150	0.0100	mg/L	EPA 200.7	
Nitrate as N	1.9		0.041	0.10	mg/L	EPA 353.2	
Nitrate/Nitrite as N	1.9		0.041	0.10	mg/L	EPA 353.2	
Nitrite as N	0.031	J	0.017	0.10	mg/L	EPA 353.2	Q-02
pH	7.8		1.0	1.0	pH	SM 4500H+B-2011	Q-01
Potassium - Total	0.796		0.150	0.500	mg/L	EPA 200.7	
Silica (SiO2) - Total	20.2		0.0270	0.214	mg/L	EPA 200.7	
Sodium - Total	5.91		0.400	0.500	mg/L	EPA 200.7	
Specific Conductance (EC) at 25 Deg C	400		1.0	1.0	umhos/cm	SM 2510B-2011	
Sulfate as SO4	5.9		2.9	5.0	mg/L	EPA 300.0	Q-01
Temperature for pH (deg. C)	20				pH	SM 4500H+B-2011	Q-01
Total Alkalinity as CaCO3	190		14	15	mg/L	EPA 310.2	Q-02
Total Dissolved Solids	240		50	50	mg/L	SM 2540C-2011	Q-02
Total Organic Carbon	3.4		0.34	1.0	mg/L	SM 5310B-2011	

www.encolabs.com

ANALYTICAL RESULTS

Description: Source Mariani **Lab Sample ID:** CC06218-01 **Received:** 04/19/19 11:00

Matrix: Surface Water **Sampled:** 04/02/19 13:00 **Work Order:** CC06218

Project: Source Mariani **Sampled By:** Javan Miner/Maxwell Pierril

Metals by EPA 200 Series Methods

^ - ENCO Cary certified analyte [NC 591]

Analyte [CAS Number]	Results	Flag	Units	DF	MDL	PQL	Batch	Method	Analyzed	By	Notes
Antimony [7440-36-0]^	0.00037	U	mg/L	1	0.00037	0.00100	9D22019	EPA 200.8	04/26/19 11:32	CMK	
Arsenic [7440-38-2]^	0.00760	U	mg/L	1	0.00760	0.0100	9D25010	EPA 200.7	04/27/19 11:16	JDH	
Barium [7440-39-3]^	**0.174**		mg/L	1	0.00110	0.0100	9D25010	EPA 200.7	04/27/19 11:16	JDH	
Beryllium [7440-41-7]^	0.000160	U	mg/L	1	0.000160	0.00100	9D25010	EPA 200.7	04/27/19 11:16	JDH	
Cadmium [7440-43-9]^	0.000360	U	mg/L	1	0.000360	0.00100	9D25010	EPA 200.7	04/27/19 11:16	JDH	
Calcium [7440-70-2]^	**73.2**		mg/L	1	0.0390	0.100	9D25010	EPA 200.7	04/27/19 11:16	JDH	
Chromium [7440-47-3]^	0.00140	U	mg/L	1	0.00140	0.0100	9D25010	EPA 200.7	04/27/19 11:16	JDH	
Copper [7440-50-8]^	**0.00518**	J	mg/L	1	0.00160	0.0100	9D25010	EPA 200.7	04/27/19 11:16	JDH	
Iron [7439-89-6]^	**0.0520**		mg/L	1	0.0220	0.0500	9D25010	EPA 200.7	04/27/19 11:16	JDH	
Lead [7439-92-1]^	0.00310	U	mg/L	1	0.00310	0.0100	9D25010	EPA 200.7	04/27/19 11:16	JDH	
Magnesium [7439-95-4]^	**5.39**		mg/L	1	0.0290	0.100	9D25010	EPA 200.7	04/27/19 11:16	JDH	
Manganese [7439-96-5]^	**0.00404**	J	mg/L	1	0.00150	0.0100	9D25010	EPA 200.7	04/27/19 11:16	JDH	
Mercury [7439-97-6]^	0.000150	U	mg/L	1	0.000150	0.000200	9D25029	EPA 245.1	04/26/19 12:09	RLF	
Potassium [7440-09-7]^	**0.796**		mg/L	1	0.150	0.500	9D25010	EPA 200.7	04/27/19 11:16	JDH	

Silica (SiO2) [763-18-69]^	**20.2**		mg/L	1	0.0270	0.214	9D25010	EPA 200.7	04/27/19 11:16	JDH
Silver [7440-22-4]^	0.00190	U	mg/L	1	0.00190	0.0100	9D25010	EPA 200.7	04/27/19 11:16	JDH
Sodium [7440-23-5]^	**5.91**		mg/L	1	0.400	0.500	9D25010	EPA 200.7	04/27/19 11:16	JDH
Thallium [7440-28-0]^	0.000110	U	mg/L	1	0.000110	0.00100	9D22019	EPA 200.8	04/26/19 11:32	CMK
Zinc [7440-66-6]^	0.00440	U	mg/L	1	0.00440	0.0100	9D25010	EPA 200.7	04/27/19 11:16	JDH

Classical Chemistry Parameters

^ - ENCO Cary certified analyte [NC 591]

Analyte [CAS Number]	Results	Flag	Units	DF	MDL	PQL	Batch	Method	Analyzed	By	Notes
Ammonia as N [7664-41-7]^	0.045	U	mg/L	1	0.045	0.10	9E07011	EPA 350.1	05/07/19 13:55	MKS	Q-01
Calcium Hardness	**180**		mg/L	1	0.018	0.0	9D25010	SM 2340B-2011	04/27/19 11:16	JDH	
Chloride [16887-00-6]^	**9.7**		mg/L	1	1.9	5.0	9D29019	SM 4500Cl E-2011	04/29/19 13:59	MKS	
Fluoride [16984-48-8]^	**0.40**		mg/L	1	0.0097	0.20	9E06020	EPA 300.0	05/07/19 04:28	MKS	Q-01
Nitrate as N [14797-55-8]	**1.9**		mg/L	1	0.041	0.10	[CALC]	EPA 353.2	04/30/19 13:18	MKS	
Nitrate/Nitrite as N^	**1.9**		mg/L	1	0.041	0.10	9D30028	EPA 353.2	04/30/19 13:18	MKS	
Nitrite as N [14797-65-0]^	**0.031**	J	mg/L	1	0.017	0.10	9D19013	EPA 353.2	04/20/19 10:21	MKS	Q-02
pH^	**7.8**		pH	1	1.0	1.0	9D26010	SM 4500H+B-2011	04/26/19 12:57	ASC	Q-01
Specific Conductance (EC) at 25 Deg C^	**400**		umhos/cm	1	1.0	1.0	9D23033	SM 2510B-2011	04/23/19 15:24	JOC	
Sulfate as SO4 [14808-79-8]^	**5.9**		mg/L	1	2.9	5.0	9E06020	EPA 300.0	05/07/19 04:28	MKS	Q-01
Temperature for pH (deg. C)	**20**		pH	1			9D26010	SM 4500H+B-2011	04/26/19 12:57	ASC	Q-01
Total Alkalinity as CaCO3 [471-34-1]^	**190**		mg/L	1	14	15	9D29018	EPA 310.2	04/29/19 14:31	MKS	Q-02
Total Dissolved Solids^	**240**		mg/L	1	50	50	9D20004	SM 2540C-2011	04/22/19 11:28	JOC	Q-02

Classical Chemistry Parameters

^ - ENCO Orlando certified analyte [NC 424]

Analyte [CAS Number]	Results	Flag	Units	DF	MDL	PQL	Batch	Method	Analyzed	By	Notes
Total Organic Carbon^	**3.4**		mg/L	1	0.34	1.0	9D23024	SM 5310B-2011	04/24/19 15:53	S1R	

www.encolabs.com

FLAGS/NOTES AND DEFINITIONS

B The analyte was detected in the associated method blank.

D The sample was analyzed at dilution.

J The reported value is between the laboratory method detection limit (MDL) and the laboratory method reporting limit (MRL), adjusted for actual sample preparation data and moisture content, where applicable.

U The analyte was analyzed for but not detected to the level shown, adjusted for actual sample preparation data and moisture content, where applicable.

E The concentration indicated for this analyte is an estimated value above the calibration range of the instrument. This value is considered an estimate.

MRL Method Reporting Limit. The MRL is roughly equivalent to the practical quantitation limit (PQL) and is based on the low point of the calibration curve, when applicable, sample preparation factor, dilution factor, and, in the case of soil samples, moisture content.

PQL PQL: Practical Quantitation Limit. The PQL presented is the laboratory MRL.

N The analysis indicates the presence of an analyte for which there is presumptive evidence (85% or greater confidence) to make a "tentative identification".

P Greater than 25% concentration difference was observed between the primary and secondary GC column. The lower concentration is reported.

[CALC]	Calculated analyte - MDL/MRL reported to the highest reporting limit of the component analyses.
J-06	The associated laboratory control sample exhibited low bias; the reported result should be considered to be a minimum estimate.
Q-01	Analysis performed outside of method - specified holding time.
Q-02	Sample received outside of method - specified holding time.
QM-07	The spike recovery was outside acceptance limits for the MS and/or MSD. The batch was accepted based on acceptable LCS recovery.
QM-08	Post-digestion spike did not meet method requirements due to confirmed matrix effects (dilution test).

ISOTECH®
ISOTECH LABORATORIES INC

ANALYSIS REPORT

Lab #: 715541 Job #: 41344 IS-90371 Co. Job#:
Sample Name: Source Mariani Co. Lab#:
Company: Northwater Consulting
API/Well:
Container: 125ml bottle
Field/Site Name: Source Mariani Characterization
Location: Mariani, Haiti
Formation/Depth:
Sampling Point:
Date Sampled: 4/02/2019 13:00 Date Received: 4/16/2019 Date Reported: 4/29/2019

δD of water	----------	-14.0 ‰ relative to VSMOW
$\delta^{18}O$ of water	----------	-3.19 ‰ relative to VSMOW
Tritium content of water	----------	na

$\delta^{13}C$ of DIC	----------	na
^{14}C content of DIC	----------	na
$\delta^{15}N$ of nitrate	----------	na
$\delta^{18}O$ of nitrate	----------	na
$\delta^{34}S$ of sulfate	----------	na
$\delta^{18}O$ of sulfate	----------	na
Vacuum Distilled? *	----------	No

Remarks:

nd = not detected. na = not analyzed.
*Indicates if vacuum distillation was utilized for hydrogen and oxygen isotopic analysis of water

APPENDIX E - HYDROGEOLOGICAL INVESTIGATION OF SOURCE MARIANI: CFC AND SF6 METHODOLOGIES

Chlorofluorocarbons (CFCs)

Chlorofluorocarbon (CFC) compounds have been synthesized on an industrial scale since 1931. They have primarily been used as refrigerants and aerosol can propellants, but also as foam blowing agents, solvents, and in insulation. Production reached its peak during the 1970s and 1980s before it was recognized that CFCs contribute to destruction of the Earth's ozone. Production was subsequently banned in the 1990s as part of a global agreement. Three principal CFC compounds were used during the 20th century: trichlorofluoromethane, dichlorodifluoromethane, and trichlorotrifluoroethane, whose trade names are CFC-11, CFC-12, and CFC-113, respectively The CFCs production and release to the atmosphere have been measured and reconstructed back to 1940 (McCarthy et al., 1977; Gamlen et al., 1986; Wisegarver and Gammon, 1988; Fisher and Midgley, 1993; Fraser et al., 1996).

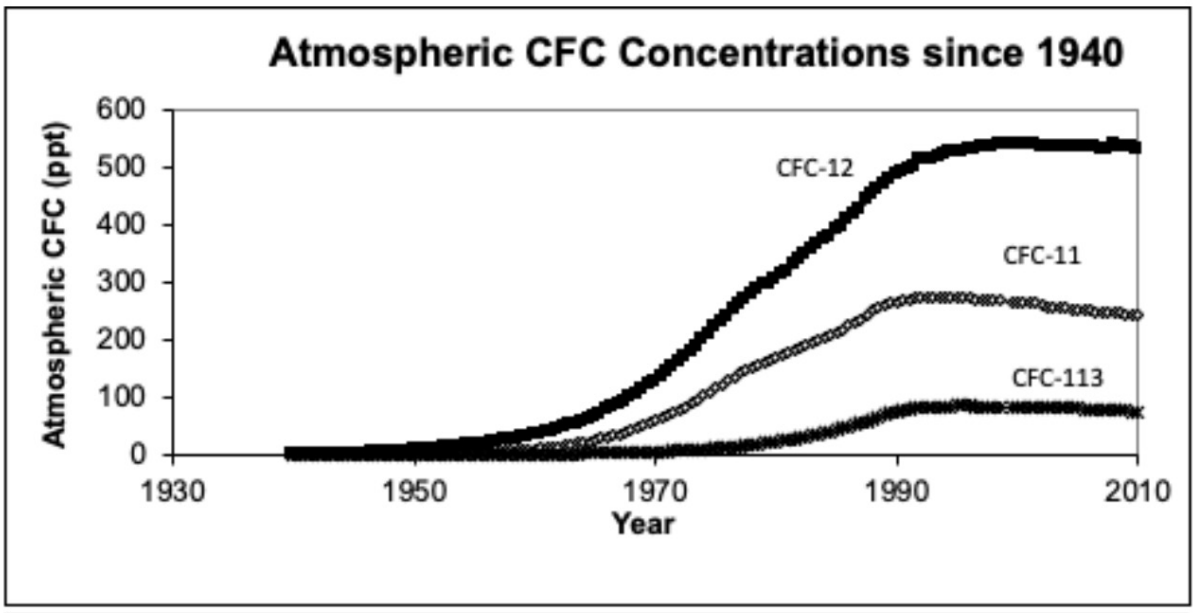

Atmospheric concentration of three principal CFCs produced since 1940 based on annual measurements from approximately 1980 to present and reconstructed based on release rates prior to 1980. Source: University of Utah Noble Gas Lab.

The basis for age-dating with dissolved CFC measurements in groundwater is based on comparing the measured values to those of the atmospheric concentrations at the time of recharge. This is accomplished by recognizing that the dissolved concentration Ci is

$$C_i = K_H p_i$$

where KH is the Henry's constant and pi is the partial pressure of the CFC in air. The concentration is related back to atmospheric concentration through pi

$$p_i = x_i(P - p_{H2O})$$

where xi is the dry air mole fraction of the CFC, P is the atmospheric pressure and pH2O is the water vapor pressure. Henry constants have been carefully measured for the three CFCs of interest and solubility determined as a function of temperature and salinity. A number of comparative age-dating studies have shown the reliability of the CFC approach (Busenberg and Plummer, 1992; Busenberg and Plummer, 1993; Ekwurzel et al., 1994; Cook and Solomon, 1997).

Sulfur Hexafluoride SF_6

SF_6 is used as electrical insulator in high voltage switches and transformers. It is also used as a blanket gas in the production of magnesium metal. Production of SF_6 began in 1953, and ever since SF_6 has been building up concentration the atmosphere. SF_6 has lower solubility in water compared to the CFCs at 30 ppm. Its solubility is dependent on temperature, salinity, elevation, and any excess air in the water. Excess air origin is originated by rapid recharge that traps air in the vadose zone and carries that air into the saturated zone where it solubilizes. If trapped in pockets of air form in the aquifer space, SF_6 will readily partition into that trapped air due to its low solubility. The basis of using SF_6 as an age dating tool relies on Henry's constant of SF_6 with respect water. The Henry's constant for SF_6 is 0.00024 mols/kg-bar. The measured concentration in groundwater can be compared to the atmospheric concentration through the use of its Henry's constant, resulting in an age date. There are natural sources of SF_6 associated with hot springs and fumaroles. Sometimes these sources can interfere with age dating of groundwater.

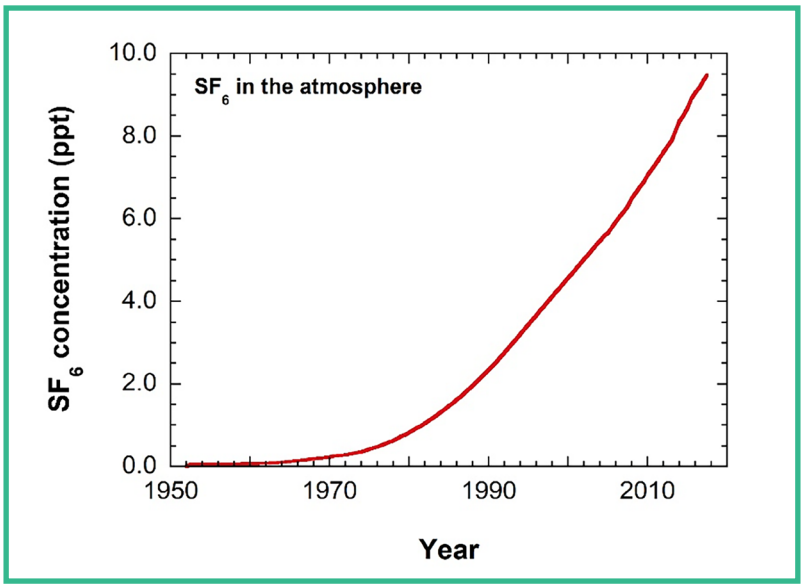

APPENDIX F – HYDROGEOLOGICAL INVESTIGATION OF SOURCE MARIANI: COMPILED DATASETS.

Compiled Discharge Data for Source Mariani

Date	Total Flow	Overflow	Type	Data Source
	L/s	L/s		
2-Apr-25	179		Instantaneous	Hydrographic Bulletins
8-Dec-27	250		Instantaneous	Hydrographic Bulletins
10-Jan-30	280		Instantaneous	Hydrographic Bulletins
22-Apr-30	180		Instantaneous	Hydrographic Bulletins
23-Aug-30	170		Instantaneous	Hydrographic Bulletins
26-Jun-31	240		Instantaneous	Hydrographic Bulletins
7-Mar-33	220		Instantaneous	Hydrographic Bulletins
Oct-02		51	Overflow?	CTE-RMPP
Nov-02		39	Overflow?	CTE-RMPP
Dec-02		33	Overflow?	CTE-RMPP
Jan-03		9	Overflow?	CTE-RMPP
Feb-03		9	Overflow?	CTE-RMPP
Mar-03		28	Overflow?	CTE-RMPP
Apr-03		7	Overflow?	CTE-RMPP
Oct-08	294		Monthly Average	CTE-RMPP
Nov-08	300		Monthly Average	CTE-RMPP
Dec-08	285		Monthly Average	CTE-RMPP
Jan-09	285		Monthly Average	CTE-RMPP
Feb-09	285		Monthly Average	CTE-RMPP
Mar-09	285		Monthly Average	CTE-RMPP
Apr-09	285		Monthly Average	CTE-RMPP
May-09	300		Monthly Average	CTE-RMPP
Jun-09	300		Monthly Average	CTE-RMPP
Jul-09	302		Monthly Average	CTE-RMPP
Aug-09	285		Monthly Average	CTE-RMPP
Sep-09	232		Monthly Average	CTE-RMPP
Oct-09	304		Monthly Average	CTE-RMPP
Nov-09	304		Monthly Average	CTE-RMPP
Dec-09	304		Monthly Average	CTE-RMPP
Jan-10	304		Monthly Average	CTE-RMPP
Feb-10	304		Monthly Average	CTE-RMPP
Mar-10	236		Monthly Average	CTE-RMPP
Apr-10	236		Monthly Average	CTE-RMPP
May-10	236		Monthly Average	CTE-RMPP
Jun-10	236		Monthly Average	CTE-RMPP
Jul-10	236		Monthly Average	CTE-RMPP

Date	Total Flow	Overflow	Type	Data Source
	L/s	L/s		
Aug-10	236		Monthly Average	CTE-RMPP
Sep-10	236		Monthly Average	CTE-RMPP
Oct-10	236		Monthly Average	CTE-RMPP
Nov-10	236		Monthly Average	CTE-RMPP
Dec-10	236		Monthly Average	CTE-RMPP
Jan-11	236		Monthly Average	CTE-RMPP
Feb-11	236		Monthly Average	CTE-RMPP
Mar-11	236		Monthly Average	CTE-RMPP
Apr-11	236		Monthly Average	CTE-RMPP
May-11	236		Monthly Average	CTE-RMPP
Jun-11	236		Monthly Average	CTE-RMPP
Jul-11	236		Monthly Average	CTE-RMPP
Sep-11	236		Monthly Average	CTE-RMPP
Oct-11	236		Monthly Average	CTE-RMPP
Nov-11	236		Monthly Average	CTE-RMPP
1/24/2014	221		Instantaneous	Eptisa
2/21/2014	155		Instantaneous	Eptisa
4/8/2014	178		Instantaneous	Eptisa
5/19/2014	121		Instantaneous	Eptisa
Jun-14	325		Monthly Average	CTE-RMPP
7/22/2014	142		Instantaneous	Eptisa
Aug-14	324		Monthly Average	CTE-RMPP
8/29/2014	88		Instantaneous	Eptisa
Sep-14	128		Monthly Average	CTE-RMPP
9/25/2014	355		Instantaneous	Eptisa
Oct-14	324		Monthly Average	CTE-RMPP
12/11/2014	159		Instantaneous	Eptisa
1/27/2015	126		Monthly Average	Eptisa
Oct-15	288		Monthly Average	CTE-RMPP
Nov-15	247		Monthly Average	CTE-RMPP
Dec-15	313		Monthly Average	CTE-RMPP
Jan-16	324		Monthly Average	CTE-RMPP
Feb-16	336		Monthly Average	CTE-RMPP
Mar-16	319		Monthly Average	CTE-RMPP
Apr-16	335		Monthly Average	CTE-RMPP
May-16	283		Monthly Average	CTE-RMPP

Date	Total Flow	Overflow	Type	Data Source
	L/s	L/s		
Jun-16	346		Monthly Average	CTE-RMPP
Jul-16	280		Monthly Average	CTE-RMPP
Aug-16	169		Monthly Average	CTE-RMPP
Sep-16	225		Monthly Average	CTE-RMPP
Oct-16	139		Monthly Average	CTE-RMPP
Nov-16	144		Monthly Average	CTE-RMPP
Dec-16	170		Monthly Average	CTE-RMPP
Jan-17	259		Monthly Average	CTE-RMPP
Feb-17	304		Monthly Average	CTE-RMPP
Mar-17	172		Monthly Average	CTE-RMPP
Apr-17	269		Monthly Average	CTE-RMPP
May-17	121		Monthly Average	CTE-RMPP
Jun-17	200		Monthly Average	CTE-RMPP
Jul-17	159		Monthly Average	CTE-RMPP
Aug-17	116		Monthly Average	CTE-RMPP
Sep-17	126		Monthly Average	CTE-RMPP
Oct-17	155		Monthly Average	CTE-RMPP
Nov-17	205		Monthly Average	CTE-RMPP
Dec-17	199		Monthly Average	CTE-RMPP
Jan-18	240		Monthly Average	CTE-RMPP
Feb-18	225		Monthly Average	CTE-RMPP
Mar-18	172		Monthly Average	CTE-RMPP
Apr-18	228		Monthly Average	CTE-RMPP
May-18	223		Monthly Average	CTE-RMPP
Jun-18	335		Monthly Average	CTE-RMPP
Jul-18	144		Monthly Average	CTE-RMPP
Aug-18	192		Monthly Average	CTE-RMPP
Sep-18	216		Monthly Average	CTE-RMPP
Jan-19	189		Monthly Average	CTE-RMPP
Feb-19	174		Monthly Average	CTE-RMPP
Mar-19	150		Monthly Average	CTE-RMPP
Apr-19	213		Monthly Average	CTE-RMPP
May-19	193		Monthly Average	CTE-RMPP
Jun-19	184		Monthly Average	CTE-RMPP
Jul-19	246		Monthly Average	CTE-RMPP
Jan-20	168		Instantaneous	Northwater/Rezodlo

Compiled water quality data for source Mariani.

Date	pH	Température (°C)	CE (µS/cm)	TDS (mg/l)	Salinité	Turbidité (NTU)	Couleur vraie (U pt/Co)	Alcalinité totale (mg/l)	Bicarbonates (mg/l CaCO3)	Carbonates (mg/l CaCO3)	Dureté totale (mg/l CaCo3)	Dureté calcique (mg/l CaCo3)	Dureté magnésium (mg/l CaCO3)	Ammonium (mg/l NH4)	Arsenic (µg/l As)	Calcium (mg/l Ca)	Chlore libre (mg/l Cl2)	Chlore total (mg/l Cl2)	Chlorures (mg/l Cl)	Chrome hexavalent (mg/l Cr)	Cuivre (mg/l Cu)	Fer (mg/l Fe)	Magnésium (mg/l Mg)
Jul-08			331	159	0.1				152		184	152	32			61			11.0				9.2
Aug-08			323	155	0.1				144		156	138	18			55			9.7				5.2
Sep-08	7.38		352	170	0.1				161		190	150	40			60			13.0				11.5
Oct-08	7.99		342	165	0.1	12.0			164		168	152	16			61			11.0				4.6
Nov-08	7.45		346	187	0.1	1.2			146		176	148	28			59			11.0				6.8
Dec-08	7.40		345	166	0.1	0.7			172		176	160	16			64			8.5				3.9
Jan-09	7.51		354	171	0.1	5.0			156		184	160	24			64			10.5				5.8
Feb-09	7.35		365	176	0.1	4.8			162		172	168	4		0	67			9.5			0.07	1.0
Mar-09	7.41		354	170	0.1	2.9			158		180	168	12			67			11.0				2.9
Apr-09	7.26		362	174	0.1	5.2			164		188	168	20			67			11.5				4.9
May-09																							
Jun-09																							
Jul-09																							
Aug-09																							
Sep-09	7.24		359	173	0.1	2.6			156		179	154	25			62			13.5				6.1
Oct-09																							
Nov-09	7.33		360	174	0.1	1.0			156		176	168	8			67			14.0			0.03	1.9
Dec-09																							
Jan-10																							
Feb-10																							
Mar-10																							
Apr-10																							
May-10																							
Jun-10																							
Jul-10																							
Aug-10																							
Sep-10																							
Oct-10																							
Nov-10																							
Dec-10																							
Jan-11																							
Feb-11																							
Mar-11																							
Apr-11																							

Date	pH	Température (°C)	CE (µS/cm)	TDS (mg/l)	Salinité	Turbidité (NTU)	Couleur vraie (U pt/Co)	Alcalinité totale (mg/l)	Bicarbonates (mg/l CaCO3)	Carbonates (mg/l CaCO3)	Dureté totale (mg/l CaCo3)	Dureté calcique (mg/l CaCo3)	Dureté magnésium (mg/l CaCo3)	Ammonium (mg/l NH4)	Arsenic (µg/l As)	Calcium (mg/l Ca)	Chlore libre (mg/l Cl2)	Chlore total (mg/l Cl2)	Chlorures (mg/l Cl)	Chrome hexavalent (mg/l Cr)	Cuivre (mg/l Cu)	Fer (mg/l Fe)	Magnésium (mg/l Mg)
May-11																							
Jun-11	7.46	26.1	381	183	0.2	1.9																	
Jul-11	7.35	24.9	365	175	0.2	0.4		164			200	172	28			69			15.0			0.02	6.8
Aug-11	7.32	25.2	360	173	0.2	0.4		164			188	176	12			70			12.0			0.03	2.9
Sep-11																							
Oct-11																							
Nov-11																							
Dec-11																							
Jan-12																							
Feb-12																							
Mar-12	7.42	26.5	374			0.1		186			204	180							16.5			0.08	
Apr-12																							
May-12																							
Jun-12	7.36	24.4	384			2.2		188			194	45				18			16.5	0.006	0.18	0.15	36.2
Jul-12	7.80	25.6				3.3		178			196	166				66			17.5			0.08	7.3
Aug-12	7.20	26.5	392			1.3																0.07	
Sep-12	7.60	25.7	390			1.0																0.14	
Oct-12																							
Nov-12	8.00	25.6	378			0.4																0.12	
Dec-12	7.80	25.5	379			0.1																0.16	
Jan-13	7.90	25.1	361			0.7		170			192	172	20			69			16.5			0.08	4.9
Feb-13	7.48	25.4	470			1.3		186			204	188	16			75			13.0			0.06	8.9
Mar-13	8.00	25.1	397			1.2								0.12									
Apr-13	7.80	25.3				3.0																	
May-13	7.80	27.5	413																			0.20	
5/8/2013	7.46	26.2	407			0.7																0.24	
Jun-13	7.90	27.2	393			5.8		176			200	176	24	0.00	0	70			16.0	0.002	0.06	0.08	5.8
Jul-13	7.80	27.5	374			6.0								0.00								0.32	
2/10/2013	8.10	23.9	382											0.00			2.2	2.2				0.16	
Aug-13																							
8/21/2013	7.80	27.2	397			1.2								0.00			1.4	1.4				0.06	
Sep-13																							
9/9/2013	7.90	27.8	370			2.4								0.05			0.2	0.3				0.06	
Oct-13																							
Nov-13	8.30	26.0	397																				
11/12/2013	8.00	26.9	370			1.1	25	170			184	172		0.01		69	1.0	1.0	18.5			0.02	2.9
11/14/2013	8.40	25.0	385																				

Date	pH	Température (°C)	CE (µS/cm)	TDS (mg/l)	Salinité	Turbidité (NTU)	Couleur vraie (U pt/Co)	Alcalinité totale (mg/l)	Bicarbonates (mg/l CaCO3)	Carbonates (mg/l CaCO3)	Dureté totale (mg/l CaCo3)	Dureté calcique (mg/l CaCo3)	Dureté magnésium (mg/l CaCo3)	Ammonium (mg/l NH4)	Arsenic (µg/l As)	Calcium (mg/l Ca)	Chlore libre (mg/l Cl2)	Chlore total (mg/l Cl2)	Chlorures (mg/l Cl)	Chrome hexavalent (mg/l Cr)	Cuivre (mg/l Cu)	Fer (mg/l Fe)	Magnésium (mg/l Mg)
11/20/2013	8.00	27.8	374			0.5								0.05			0.5	0.6				0.09	
11/22/2013																							
Dec-13																							
Jan-14	7.41		371			0.5			180	0						69			16.0				4.9
1/8/2014	7.50	25.0	398																				
1/24/2014	8.30	27.0	387																				
2/17/2014	7.50	25.4	385			0.9								0.16			0.0	0.0				0.02	
2/21/2014																							
Mar-14																							
Apr-14																							
4/8/2014																							
4/11/2014	7.90	25.3	387			1.0								0.00			0.6	0.7				0.09	
4/15/2014	7.60	25.5	387			0.9								0.00			0.0	0.0				0.14	
May-14																							
5/19/2014																							
Jun-14																							
Jul-14																							
7/22/2014																							
Aug-14																							
8/1/2014	8.00	26.6	371			0.4								0.00			0.8	0.7				0.06	
8/7/2014	7.50	27.3	366			0.9								0.00			0.0	0.0				0.07	
8/20/2014	7.50	25.8	357			1.5								0.08			0.0	0.1				0.13	
8/29/2014																							
Sep-14																							
9/1/2014	8.00	26.6	373			0.4								0.00			0.7	0.8				0.06	
9/17/2014	7.40	25.9	377			0.9								2.19			0.0	0.0				0.03	
9/25/2014																							
Oct-14																							
10/6/2014	8.20	27.7	422	200		2.2	22	236			200	144		0.00	0	58	2.2	2.2	24.5	0.020	0.54	0.10	
10/12/2014	7.30	25.3	398				14	178	178	0		180		0.00		72	0.0	0.0	16.5			0.02	4.9
10/27/2014	8.20	25.8	400											0.00			2.2	2.2				0.04	
Nov-14	8.10	25.6	386	185		1.3			184	0				0.00		55			12.5				15.5
11/4/2014																							
Dec-14																							
12/5/2014	7.60	25.3	386			1.1	2							0.02			0.0	0.0				0.02	
12/11/2014																							
1/26/2015	7.53	24.8	412			0.5								0.00			0.0	0.1				0.08	

Date	pH	Température (°C)	CE (µS/cm)	TDS (mg/l)	Salinité	Turbidité (NTU)	Couleur vraie (U pt/Co)	Alcalinité totale (mg/l)	Bicarbonates (mg/l CaCO3)	Carbonates (mg/l CaCO3)	Dureté totale (mg/l CaCo3)	Dureté calcique (mg/l CaCo3)	Dureté magnésium (mg/l CaCo3)	Ammonium (mg/l NH4)	Arsenic (µg/l As)	Calcium (mg/l Ca)	Chlore libre (mg/l Cl2)	Chlore total (mg/l Cl2)	Chlorures (mg/l Cl)	Chrome hexavalent (mg/l Cr)	Cuivre (mg/l Cu)	Fer (mg/l Fe)	Magnésium (mg/l Mg)
1/27/2015																							
Feb-15																							
Mar-15																							
3/23/2015	7.50	24.5	420			0.9	8	200	200	0	208	188		0.00		75	0.0	0.1	17.0			0.03	4.9
Apr-15																							
4/21/2015	7.40	26.0	426			0.6								0.00			0.1	0.1				0.05	
May-15																							
Jun-15																							
6/29/2015	7.70	24.8	406	197		0.6	7	200				348		0.12	0	139	0.0	0.0	18.0	0.016	1.84	0.08	22.3
Jul-15																							
Aug-15																							
8/24/2015	7.40	26.5	421			0.5								0.03			0.0	0.1				0.06	
Sep-15																							
9/9/2015	7.40	27.0	427			0.9								0.00			0.1	0.1				0.05	
Oct-15																							
10/26/2015	7.00	24.8	420			0.5								0.00			0.0	0.0				0.07	
Nov-15																							
Dec-15																							
12/5/2015	7.73	27.2	415			0.6								0.00			0.1	0.1				0.05	
Jan-16																							
Feb-16																							
Mar-16																							
3/2/2016	7.00	21.6	401			3.4								0.00			0.0	0.0				0.01	
Apr-16																							
4/19/2016	7.40	25.1	419			3.6								0.03			0.1	0.1				0.08	
May-16																							
Jun-16																							
Jul-16																							
Aug-16																							
8/6/2016	7.60	26.0	390	188		7.3	56					180		0.03	0	72	0.1	0.2	18.5	0.010	0.88	0.12	
8/16/2016	7.40	23.0	364			2.3								0.00			0.0	0.1				0.02	5.8
Sep-16																							
Oct-16																							
Nov-16																							
11/5/2016	7.40	25.0	421			0.3		180						0.00			0.1	0.1				0.23	
11/8/2016	7.30	24.0	364			7.3								0.04			0.0	0.1				0.05	
Dec-16																							

Date	pH	Température (°C)	CE (µS/cm)	TDS (mg/l)	Salinité	Turbidité (NTU)	Couleur vraie (U pt/Co)	Alcalinité totale (mg/l)	Bicarbonates (mg/l CaCO3)	Carbonates (mg/l CaCO3)	Dureté totale (mg/l CaCo3)	Dureté calcique (mg/l CaCo3)	Dureté magnésium (mg/l CaCo3)	Ammonium (mg/l NH4)	Arsenic (µg/l As)	Calcium (mg/l Ca)	Chlore libre (mg/l Cl2)	Chlore total (mg/l Cl2)	Chlorures (mg/l Cl)	Chrome hexavalent (mg/l Cr)	Cuivre (mg/l Cu)	Fer (mg/l Fe)	Magnésium (mg/l Mg)
12/7/2016	7.80	29.0	385			0.8											2.2	2.2				0.02	
Jan-17																							
Feb-17																							
Mar-17																							
Apr-17																							
May-17																							
Jun-17																							
Jul-17																							
Aug-17																							
Sep-17																							
Oct-17																							
Nov-17																							
Dec-17																							
Jan-18																							
Feb-18																							
Mar-18																							
Apr-18																							
May-18																							
Jun-18																							
Jul-18																							
Aug-18																							
Sep-18																							
Oct-18																							
Nov-18																							
Dec-18																							
Jan-19																							
Feb-19																							
Mar-19																							
Apr-19	7.20	25.1	427																19.4				
May-19																							

APPENDIX G - PLAINE DU CUL-DE-SAC: GROUNDWATER FLOW MODEL SCENARIOS

The regional steady-state groundwater flow model developed for the Plaine du Cul-de-Sac aquifer allowed for simulations of groundwater flow and for an understanding of the aquifer's groundwater budget. Using this base model, model scenarios were provided by the IDB, and included three groundwater management alternatives with eight climate change scenarios.

It is important to note that decreases and increases of groundwater flow presented and discussed are not relative to the complete water balance of each of the individual hydrological systems, but only the change in proportion to the PCS aquifer. For example, a 5% decrease in flow to Canal Boucambrou does not indicate that the canal flow will be 5% lower, but only that the groundwater contribution is 5% lower. Quantifying the water budget of the surface water systems is important to better understand the potential impact of the reduced groundwater inputs.

Groundwater Flow Model Scenarios

Based on the IDB-led analysis of 36 climate change models and associated projections, four unique climate change scenarios were selected to be incorporated into the groundwater model runs. Each climate change scenario included a change in annual precipitation, temperature, and streamflow.

To complement the climate change scenarios, three different groundwater management alternatives were simulated:

1. Base: Current situation of groundwater abstraction/pumping as in the base model. This results in pumping approximately 70,000 m3/day from the aquifer

2. Alternative 1: DINEPA CTE-Wells P1, and G1 – G7 are commissioned to pump approximately 32,000 m3/day. Currently these wells exist but are not in service. This results in pumping over 100,000 m3/day from the aquifer

3. Alternative 2: DINEPA CTE drills 12 new production wells (G8 – G19), with an additional production of 45,000 m3/day. This results in pumping of over 140,000 m3/day from the aquifer

Groundwater flow model scenarios

	Climate Change	Groundwater Management
E2	Optimistic Climate Change Scenario • 7.8% increase in precipitation • 1° C increase in temperature • 1.2% increase in streamflow	E2 Base: Climate change with baseline model
		E2 Alt1: Climate change with increase of groundwater pumping by 1.5X
		E2 Alt2: Climate change with increase of groundwater pumping by 2X
E4	Central Climate Change Scenario • 0.2% increase in precipitation • 1.5° C increase in temperature • 4.7% decrease in streamflow	E4 Base: Climate change with baseline model
		E4 Alt1: Climate change with increase of groundwater pumping by 1.5X
		E4 Alt2: Climate change with increase of groundwater pumping by 2X
E6	Central-Pessimistic Climate Change Scenario • 9.6% decrease in precipitation • 2.1° C increase in temperature • 10% decrease in streamflow	E6 Base: Climate change with baseline model
		E6 Alt1: Climate change with increase of groundwater pumping by 1.5X
		E6 Alt2: Climate change with increase of groundwater pumping by 2X
E8	Pessimistic Climate Change Scenario • 25% decrease in precipitation • 2.9° C increase in temperature • 24% decrease in streamflow	E8 Base: Climate change with baseline model
		E8 Alt1: Climate change with increase of groundwater pumping by 1.5X
		E8 Alt2: Climate change with increase of groundwater pumping by 2X

Driving global climate change models considered for climate change projections.

Driving global climate models (GCM)	Historical Control scenario CTL (1960 - 1990)	Projections CMIP5 / Time period: 2050			
		RCP2.5	RCP4.5	RCP6.0	RCP8.5
bcc_csm1_1_m	X	X	X	X	X
bcc_csm1_1	X	X	X	X	X
csiro_mk3_6_0	X	X	X	X	X
fio_esm_rcp	X	X	X	X	X
gfdl_cm3	X	X	X	X	X
gfdl_esm2m	X	X	X	X	X
giss_e2_r	X	X	X	X	X
miroc_esm_che	X	X	X	X	X
miroc_esm	X	X	X	X	X

Groundwater Management Alternatives

Groundwater flow model output is presented to visualize the potentiometric surface of the two groundwater management alternatives compared to the base model. ¡Error! No se encuentra el origen de la referencia. following table includes the groundwater budget results from simulating the management alternatives.

Results of groundwater management alternatives compared to base model.

			No Climate Change Component					
			Increase Pumping By 1.45X			Increase Pumping By 2X		
	MODEL RUN BASELINE		Base-Alt1			Base-Alt2		
	IN (m3/d)	OUT (m3/d)	IN (m3/d)	OUT (m3/d)	% Change	IN (m3/d)	OUT (m3/d)	% Change
Recharge (Rech)	15.200	--	15.200	--	0%	15.200		0%
Riviere Blanche (Rsw)	16.253	--	16.653	--	2%	17.717		9%
Riviere Grise (Rsw)	95.742	--	113.734	--	19%	139.369		46%
General Head (Rgh)	6.226	--	6.287	--	1%	6.326		2%
Canal Boucambrou (Dsw)	--	13.281	--	12.812	-4%		12.238	-8%
Riviere Batard (Rsw)	1.154	--	1.494	--	30%	1.736		50%
Lac Azuei/Etang Sumautre (Dsw)	--	1.838	--	1.819	-1%		1.779	-3%
Trou Caiman (Dsw)	--	3.890	--	3.804	-2%		3.610	-7%
Ocean (Dsea)	--	43.808	--	41.018	-6%		39.171	-11%
Pumping (ABS)	--	71.582	--	103.582	45%		144.832	102%

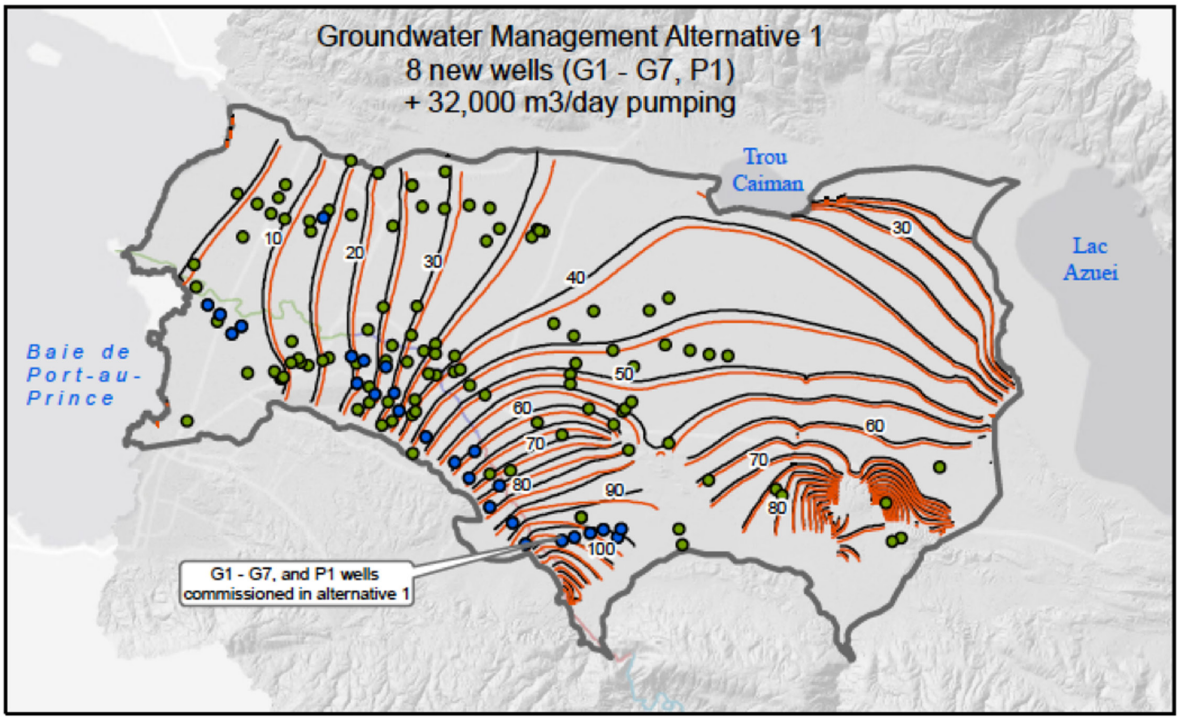

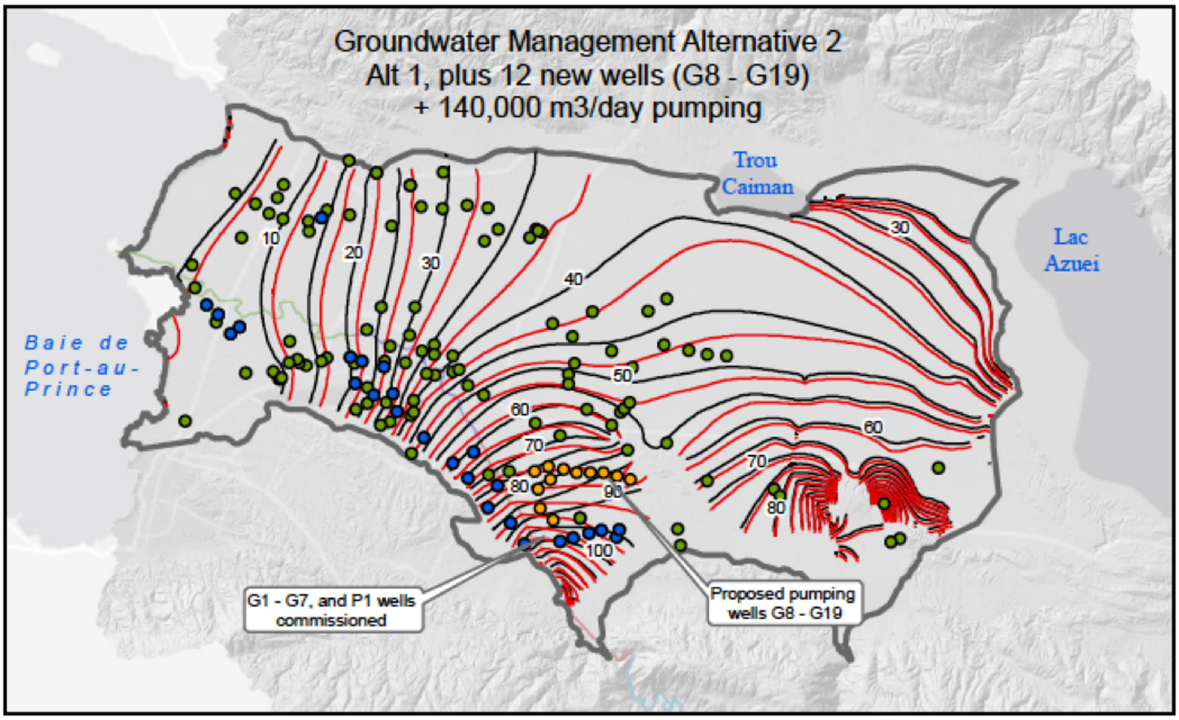

Explanation

- CTE-RMPP Pumping Wells
- Other Pumping Wells in Model
- Baseline Model Potentiometric Surface (m-asl)
- Proposed CTE-RMPP Wells (G8 to G19)
- Approxiate Aquifer
- Groundwater Management Alternatives: Potentiometric Surface (m-asl)

ALTERNATIVE 1

Alternative 1 includes the commissioning of eight existing wells that are not currently active to pump approximately 32,000 m3/day. The wells include P1, and G1-G7, all of which are in the southern portion of the aquifer near to the Riviere Grise. This alternative results in a 50% increase of groundwater pumping from the base model. A summary of the model results follows:

- The additional pumping creates an oblong cone of depression of an approximate 1.5 km radius in the G-well area. The cone of depression extends more northerly than southerly due to the steep groundwater gradient. Based on the simulation, the potentiometric surface drawdown in the cone of depression averages 1.5m and reaches up to 8 m

- Diffuse impacts to the potentiometric surface are simulated, and direct drawdown from pumping dissipates approximately 4 km down from the well field. The overall aquifer system experiences a slight decrease in water levels as it reaches a new equilibrium with the new pumping condition

- The groundwater budget indicates that that the increase in pumping is offset by an increase of river infiltration from Riviere Grise into the aquifer due to the increased hydraulic gradient between the river and the potentiometric surface of the aquifer. Based on the model simulation, Riviere Grise infiltration to the aquifer could increase up to 19% under scenario 1. Small decreases of flow into the ocean (6%) and surface water bodies (1 to 4%) were simulated

ALTERNATIVE 2

Alternative 2 includes the subsequent addition of 12 new production wells (G8 – G19), adding 45,000 m3/day of additional pumping. When combined with alternative 1, this results in pumping approximately 140,000 m3/day from the aquifer. The alternative results in a 100% increase in groundwater pumping from the base model, and a summary of the model results are as follows:

- The combined pumping of the G8 - G19 wells combined with G1 – G7 and P1 create a larger cone of depression with extends down-gradient (north) approximately 4.5 km and up-gradient (south) by half that distance due to the groundwater gradient. Based on the simulation, the potentiometric surface drawdown averages 3 m and is over 15 m (perhaps more) along the aquifer boundary associated with the outcrop area to the east of the well field

- Diffuse impacts to the aquifer under this alternative are more significant than alternative 1. The potentiometric surface of the aquifer lowers by an average of 1.5 to 2.0 m, ranging from 15 m in the area of the G wells to minimal in the eastern portion of the aquifer

- The water budget illustrates that the increase in pumping is offset by the increase of river infiltration from upper and middle Riviere Grise into the aquifer. This is caused by the increased hydraulic gradient between the river and the potentiometric surface due to drawdown, both related to the cone of depression and the diffuse regional lowering of the potentiometric surface. Based on the model simulation, the Riviere Grise infiltration to the aquifer could increase by over 40% under Alternative 2. This simulation also indicates an 8% decrease of groundwater flow to Canal Boucambrou, a 7% decrease in groundwater flow to Trou Caiman, and 3% decrease in groundwater flow to Lac Azuei.

- The vulnerability to localized seawater intrusion slightly increases in the coastal areas due to the regional lowering of water tables, although the simulation, as run for this study, does not suggest a regional occurrence of seawater intrusion. Adding pumping wells near the coast in the PCS aquifer should always be proceeded with due diligence and caution.

Climate Change Scenario Results

OPTIMISTIC CLIMATE CHANGE SCENARIO

The optimistic climate change scenario included a 7.8% increase in precipitation, 1°C increase in temperature, and a 1.2% increase in the Riviere Grise streamflow. The results of the climate change simulation and groundwater management alternatives are presented below.

This climate change scenario under current groundwater management conditions results in an increased recharge, with corresponding increases of groundwater flow to the canal, lakes, and ocean. Riviere Batarde infiltrates less into the aquifer due to the higher water tables. The optimistic climate change conditions mitigate impacts to the groundwater budget when simulating the pumping alternatives. Under Alternative 2, the increased pumping is predominantly offset by increased river infiltration. Groundwater flow to Trou Caiman and Canal Boucambrou in the two management alternatives decreases by 3% and 5%, respectively. Groundwater flow to Lac Azuei does not appear to be reduced from baseline conditions in these scenarios.

Optimistic climate change scenario results.

			Optimistic Climate Change Scenarios [+7.8% precip; + 1° C]								
			Baseline CC			Increase Pumping By 1.45X			Increase Pumping By 2X		
	MODEL RUN BASELINE		E2-Base			E2-Alt1			E2-Alt2		
	IN (m3/d)	OUT (m3/d)	IN (m3/d)	OUT (m3/d)	% Change	IN (m3/d)	OUT (m3/d)	% Change	IN (m3/d)	OUT (m3/d)	% Change
Recharge (Rech)	15.200	–	16.385	–	8%	16.385		8%	16.385		8%
Riviere Blanche (Rsw)	16.253	–	16.412	–	1%	16.871		4%	17.588		8%
Riviere Grise (Rsw)	95.742	–	96.969	–	1%	124.822		30%	162.202		69%
General Head (Rgh)	6.226	–	6.096	–	-2%	6.157		-1%	6.196		0%
Canal Boucambrou (Dsw)	–	13.281	–	13.732	3%		13.275	0,0%		12.683	-5%
Riviere Batard (Rsw)	1.154	–	965	–	-16%	1.305		13%	1.542		34%
Lac Azuei/Etang Sumautre (Dsw)	–	1.838	–	1.900	3%		1.878	2%		1.832	0%
Trou Caiman (Dsw)	–	3.890	–	4.037	4%		3.952	2%		3.762	-3%
Ocean (Dsea)	–	43.808	–	45.190	3%		42.410	-3%		40.613	-7%
Pumping (ABS)	–	71.582	–	71.582	0%		103.582	45%		144.832	102%

CENTRAL CLIMATE CHANGE SCENARIO

The central climate change scenario included a 0.2% increase in precipitation, 1.5°C increase in temperature, and a 4.7% decrease in the Riviere Grise streamflow. The results of the climate change simulation and groundwater management alternatives are presented below.
This climate change scenario under current groundwater management conditions results in a slightly diminished recharge from river infiltration, with corresponding decreases of groundwater flow to the canal, lakes, and ocean. The central climate change conditions (mostly 4.7% decrease in the Riviere Grise streamflow) magnify impacts to the groundwater budget when simulating the pumping alternatives. Under both alternatives, the increased pumping is predominately offset by increased river infiltration. Groundwater flow to Trou Caiman decreases by 10% and 15% in the two pumping alternatives, respectively and flow to Lac Azuei decreases by 9% and 11%, respectively. This scenario starts to expose the importance and sensitivity of the model to the Riviere Grise concerning its role in driving the recharge and groundwater flow of the aquifer.

Central climate change scenario results.

			Central Climate Change Scenarios [+0.2% precip; + 1.5° C]								
			Baseline CC			Increase Pumping By 1.45X			Increase Pumping By 2X		
	MODEL RUN BASELINE		E4-Base			E4-Alt1			E4-Alt2		
	IN (m3/d)	OUT (m3/d)	IN (m3/d)	OUT (m3/d)	% Change	IN (m3/d)	OUT (m3/d)	% Change	IN (m3/d)	OUT (m3/d)	% Change
Recharge (Rech)	15.200	--	15.200	--	0%	15.200		0%	15.199		0%
Riviere Blanche (Rsw)	16.253	--	15.600	--	-4%	16.152		-1%	16.951		4%
Riviere Grise (Rsw)	95.742	--	91.116	--	-5%	119.298		25%	153.080		60%
General Head (Rgh)	6.226	--	6.526	--	5%	6.587		6%	6.620		6%
Canal Boucambrou (Dsw)	--	13.281	--	12.367	-7%		11.954	-10,0%		11.450	-14%
Riviere Batard (Rsw)	1.154	--	1.541	--	34%	1.871		62%	2.080		80%
Lac Azuei/Etang Sumautre (Dsw)	--	1.838	--	1.705	-7%		1.669	-9%		1.634	-11%
Trou Caiman (Dsw)	--	3.890	--	3.572	-8%		3.487	-10%		3.314	-15%
Ocean (Dsea)	--	43.808	--	40.909	-7%		38.163	-13%		36.538	-17%
Pumping (ABS)	--	71.582	--	71.582	0%		103.582	45%		141.082	97%

CENTRAL - PESSIMISTIC CLIMATE CHANGE SCENARIO

The central-pessimistic climate change scenario included a 9.6% decrease in precipitation, 2.1°C increase in temperature, and a 10% decrease in the Riviere Grise streamflow. The results of the climate change simulation and groundwater management alternatives are presented below.

This climate change scenario under current groundwater management conditions results in a significant decrease in recharge from both river infiltration and aerial recharge, with corresponding decreases of groundwater flow to the canal, lakes, and ocean. Without any increases in groundwater pumping, groundwater flow to Trou Caiman and Lac Azuei decreases by 18%. The impacts of the central-pessimistic climate change scenario to surface water bodies are on the same order of magnitude as the 2X groundwater pumping alternative under a more central climate change condition. The increased pumping under both groundwater management alternatives results in significant increases in river infiltration, partially offsetting the abstraction. Climate change conditions are responsible for a larger proportion of the impacts to the groundwater budget than increased pumping. In the pumping alternatives, groundwater flow to Trou Caiman decreases by 20% and 25%, respectively, and groundwater flow to Lac Azuei declines by 20% and 22%, respectively. The importance of the Riviere Grise is even more apparent based on these simulations, since they show that decreased river flows can significantly affect the groundwater budget and water tables of the aquifer. The groundwater modeling does not simulate the Riviere Grise becoming completely dry, which becomes more of a seasonal possibility in these climate change conditions.

Seawater intrusion vulnerability starts to increase in the coastal areas due to the regional lowering of water tables, although the simulations did not indicate its occurrence. Regionally, a positive flux is maintained from the aquifer to the ocean, and no flux from the ocean to the aquifer.

Central - pessimistic climate change scenario results.

			Central-Pessimistic Climate Change Scenarios [-9.6% precip; + 2.1° C]								
			Baseline CC			Increase Pumping By 1.45X			Increase Pumping By 2X		
	MODEL RUN BASELINE		E6-Base			E6-Alt1			E6-Alt2		
	IN (m3/d)	OUT (m3/d)	IN (m3/d)	OUT (m3/d)	% Change	IN (m3/d)	OUT (m3/d)	% Change	IN (m3/d)	OUT (m3/d)	% Change
Recharge (Rech)	15.200	--	13.739	--	-10%	13.738		-10%	13.737		-10%
Riviere Blanche (Rsw)	16.253	--	14.518	--	-11%	14.822		-9%	15.876		-2%
Riviere Grise (Rsw)	95.742	--	88.359	--	-8%	116.454		22%	150.304		57%
General Head (Rgh)	6.226	--	6.719	--	8%	6.797		9%	6.893		11%
Canal Boucambrou (Dsw)	--	13.281	--	11.347	-15%		10.998	-17%		10.481	-21%
Riviere Batard (Rsw)	1.154	--	2.008	--	74%	2.312		100%	2.519		118%
Lac Azuei/Etang Sumautre (Dsw)	--	1.838	--	1.505	-18%		1.475	-20%		1.429	-22%
Trou Caiman (Dsw)	--	3.890	--	3.195	-18%		3.114	-20%		2.924	-25%
Ocean (Dsea)	--	43.808	--	37.573	-14%		34.949	-20%		33.277	-24%
Pumping (ABS)	--	71.582	--	71.582	0%		103.582	45%		141.082	97%

PESSIMISTIC CLIMATE CHANGE SCENARIO

The pessimistic climate change scenario included a 25% decrease in precipitation, 2.9°C increase in temperature, and a 24% decrease in the Riviere Grise streamflow. The results of the climate chance simulation and groundwater management alternatives are presented below.

The model became unstable with this scenario, as it was departing from its original calibration and could not converge with the 24% decrease in streamflow. We applied the maximum possible flow reduction while keeping the model stable, which was in the range of 18%.

This climate change scenario under current groundwater management conditions results in a decrease in recharge from both river infiltration and aerial recharge, with corresponding decreases of groundwater flow to the canal, lakes, and ocean. Without any increases in groundwater pumping, groundwater flow to Trou Caiman and Lac Azuei decreases by 27% and 32%, respectively. The increased pumping under both groundwater management alternatives results in significant increases in river infiltration, partially offsetting the abstraction. Climate change conditions are responsible for a larger proportion of the impacts to the groundwater budget than increased pumping. In the pumping alternatives, groundwater flow to Trou Caiman decreases by 29% and 38%, respectively, and groundwater flow to Lac Azuei declines by 34% and 37%, respectively. The importance of the Riviere Grise is apparent based on these simulations, since they show that decreased river flows can significantly affect the groundwater budget. The groundwater modeling did not simulate the Riviere Grise becoming completely dry, which becomes more of a possibility in these climate change conditions.

Seawater intrusion vulnerability is higher in the coastal areas due to the regional lowering of water tables, and there is a 17% to 31% change in flux between the aquifer and ocean. Regionally, a positive flux is maintained from the aquifer to the ocean, and no flux from the ocean to the aquifer.

Pessimistic climate change scenario results.

			Pessimistic Climate Change Scenarios [-25% precip; + 2.9° C]								
			Baseline CC			Increase Pumping By 1.45X			Increase Pumping By 2X		
	MODEL RUN BASELINE		E8-Base			E8-Alt1			E8-Alt2		
	IN (m3/d)	OUT (m3/d)	IN (m3/d)	OUT (m3/d)	% Change	IN (m3/d)	OUT (m3/d)	% Change	IN (m3/d)	OUT (m3/d)	% Change
Recharge (Rech)	15.200	--	11.391	--	-25%	11.390		-25%	11.262		-26%
Riviere Blanche (Rsw)	16.253	--	12.236	--	-25%	12.740		-22%	7.152		-56%
Riviere Grise (Rsw)	95.742	--	90.298	--	-6%	117.761		23%	149.678		56%
General Head (Rgh)	6.226	--	6.746	--	8%	6.974		12%	7.369		18%
Canal Boucambrou (Dsw)	--	13.281	--	10.599	-20%		10.179	-23%		9.203	-31%
Riviere Batard (Rsw)	1.154	--	2.160	--	87%	2.491		116%	2.902		152%
Lac Azuei/Etang Sumautre (Dsw)	--	1.838	--	1.248	-32%		1.216	-34%		1.150	-37%
Trou Caiman (Dsw)	--	3.890	--	2.851	-27%		2.743	-29%		2.396	-38%
Ocean (Dsea)	--	43.808	--	36.453	-17%		33.583	-23%		30.168	-31%
Pumping (ABS)	--	71.582	--	71.582	0%		103.582	45%		141.082	97%

Considerations Regarding Model Scenarios

The model scenarios suggest that impacts to the aquifer should be anticipated from both the climate change and groundwater management alternatives. The potential impacts range from minimal to more significant, especially when the pessimistic climate change scenario with more significant groundwater pumping is considered. The results presented can be considered a planning tool at the regional level to help inform groundwater development and management practices that balance potential impacts with economic and public health benefits. The scenarios also help guide what studies, modeling and other activities should be considered and prioritized in the future to facilitate improved integrated management of the groundwater resources.

Several observations regarding the model scenario results are outlined below:

1. Drawdown / cone of depression area in the zone of the G-wells from groundwater management alternatives may affect other nearby wells and create a stronger gradient between the Riviere Grise and the aquifer that may result in increased flow from the river into the aquifer. Impacts are magnified under pessimistic climate change scenarios, especially regarding decreases in the flow of the Riviere Grise

2. Scenarios result in a diffuse effect on the water balance of the aquifer due to the regional adjustment (lowering) of water tables. This effect ranges from small to potentially more significant depending on the climate change scenario and groundwater management alternatives

3. The regional lowering of water tables resulting from climate change and groundwater management alternatives reduces the groundwater flow to surface water systems (Ocean, Trou Caiman, Lac Azuei, Canal Boucambrou). These effects range from small to potentially more significant depending on the climate change scenario. Quantifying the water budget of the surface water systems is important to better understand the potential impact of the reduced groundwater inputs.

4. The pessimistic climate change scenarios appear to have a greater regional impact on the aquifer than the groundwater management alternatives. The groundwater budget and regional water tables are most sensitive to changes in the Riviere Grise flow.

5. The Riviere Grise is a critical component of the aquifer, and so its ability to sustain groundwater abstraction and flows to surface water bodies. The recharge from the river drives the hydraulic gradient, replenishes the aquifer when there is pumping or climate change stress, and mitigates saltwater intrusion risk in coastal areas.

6. Based on the evaluation of scenarios, the feasibility of the proposed well field of G8 – G19 may warrant further evaluation in terms of well interference and the potential impacts to the Riviere Grise and the aquifer. An abstraction rate and number of wells should that considers the results and potential impacts presented should be planned. Exploration and groundwater development could be considered in less developed areas of the aquifer, perhaps the area recharged by the Riviere Blanche infiltration.

Should hydrologic projections of the Riviere Grise result in sustained periods of flow below 1,500 L/s, transient or stress period modeling should be considered to evaluate the implications of this condition. If the Riviere Grise.

7. does not flow for significant periods of time, this would affect the dynamics of the aquifer in a significant way. The pumping conditions in the two groundwater management alternatives are largely offset in the groundwater budget by an increase in river infiltration. The Riviere Grise diversions upstream of the primary recharge areas may also reduce the stage and water available to infiltrate into the aquifer and mitigate the increased pumping.


IDB
Inter-American
Development Bank